

NORTHWESTERN UNIVERSITY

Studies in Natural Product Synthesis:

Towards (1) Tambromycin and (2) the Solamin Stereoisomers

A DISSERTATION

SUBMITTED TO THE GRADUATE SCHOOL

IN PARTIAL FULFILLMENT OF THE REQUIREMENTS

for the degree

DOCTOR OF PHILOSOPHY

Field of Chemistry

By

Jennifer Rote

EVANSTON, ILLINOIS

June 2020

© Copyright by Jennifer Rote 2020

All Rights Reserved

ABSTRACT

Studies in Natural Product Total Synthesis:

Towards (1) Tambromycin and (2) the Solamin Stereoisomers

Jennifer Rote

Total synthesis of natural products provides an avenue for investigation of complex chemical scaffolds, not only delivering access to biologically impactful molecules but also lending a deeper understanding of their inherent chemical reactivity. Expansion of reaction methodology, optimization of biological activity, and absolute structural confirmation can all be accomplished via the targeted total synthesis of natural products.

The solamin stereoisomers are a family of bioactive natural products whose stereocomplex structures have been the focus of many total synthesis efforts. This work outlines a novel and stereodivergent approach towards the solamin stereoisomers, featuring an application of a “traceless” Petasis methodology developed previously by the Thomson and Schaus groups for the construction of chiral allene intermediates. In this enantio- and diastereoselective method, allenols are constructed that are capable of undergoing intramolecular cyclization reactions, ultimately providing stereodefined 2,5-dihydrofuran cores as precursors to the solamin stereoisomers. The outlined application of this transformation towards the solamin stereoisomers both expands the scope of the reaction methodology and provides an yet-unreported, modular approach towards these sought-after natural product targets.

Tambromycin, a novel peptide natural product with modest biological activity, was discovered via a targeted natural product discovery approach termed metabologenomics. Given the unique structural characteristics and bioactivity of tambromycin, the total synthesis of this compound was targeted featuring an application of C–H functionalization, as well as

stereocontrolled amination. Access to the natural product has thus led to an avenue for further investigation into its bioactivity, with structure–activity relationship and target–identification studies both possible.

Prof. Regan J. Thomson
Research Advisor

ACKNOWLEDGMENTS

I would first and foremost like to thank my advisor, Regan. The kindness you showed by accepting me into your group completely changed the landscape of my time at Northwestern – I will forever be grateful for having had you as an advocate, and the confidence you showed in my potential as a chemist is one of the key reasons I continued in the program. Allowing me to pursue an internship during my time in your group again showed me how uniquely supportive and kind you are as an advisor. It's been inspiring to learn from you and to observe your creative eye towards synthesis, and I hope to have absorbed even a small amount of your brilliance towards chemistry. Finally, it's been wonderful getting to know you as a person – your down-to-earth, principled, and humorous personality has been a refreshing contrast to the many difficulties I encountered along my path. I've always been proud to be a member of your group, and I hope that in my future steps, I'll represent the type of scientist, and person, that you mentor towards success.

I would like to thank my committee members, Prof. Julia Kalow and Prof. Karl Scheidt, as their careful advice and support has helped me to grow and develop a well-rounded scientific point of view. I would also like to thank my undergraduate research advisor, Dr. Peterson – without her encouragement and attention, I would not have continued to pursue my career in chemistry.

To members of the Thomson lab past and present, my journey through graduate school would not have been nearly as enjoyable without your energy, humor, and care for one another. To Marvin and Emily – I joined the lab in admiration of you both, and I have been so grateful to count you as friends and coworkers throughout my time here. To Wan Cheng, I am so fortunate to have had the opportunity to mentor you for almost four years, and having you as a partner in research was so important to lift my spirits during challenging moments. To Ariana, it's so difficult to summarize working and living side-by-side together for five years – I'll miss having you as a

constant support, a commute buddy, and a best friend. I'm so glad that we were able to share this experience together in such a unique way.

I would also like to thank all of the wonderful friends I've made during my time at Northwestern. To the lunch crew, our daily lunches were a necessary ritual to get through all of grad school's challenges, and even in our last few months, seeing all of your faces virtually each day has been a warm reminder of normalcy and friendship. To Shaunna, Becky, Zack, and Ariana, thank you all for being such fun, caring, and lovely friends. Almost every memory I've made here has been with you all, and I know that anytime I reflect on the process of graduate school in the future, it will be inseparably mixed with the relationships and wonderful experiences we've all had together. You all have supported me through so many difficult times, and I never imagined that I would gain so many lifelong friends during these five years.

I am certain that I wouldn't have made it to the end of this process without the unwavering support and love from my family. To my parents, your words of encouragement and validation meant so much to me in high and low moments alike, and I'm forever grateful that you both have established such a loving home that I can return to whenever I'm going through a difficult time. To Morgan, the admiration I've had for you our whole lives has been one of the biggest factors encouraging me to continue achieving. Thank you for being such a strong, inspiring, and loving best friend. I share a huge part of this accomplishment with the three of you.

LIST OF ABBREVIATIONS

AA	amino acid
Ac	acetyl
acac	acetyl acetate
ACAD	acyl-CoA dehydrogenase
ACG	Annonaceous acetogenin
ACL	amino-caprolactam
ATM	azatrimethylenemethane
ACN	acetonitrile
9-BBN	9-borabicyclo(3.3.1)nonane
BGC	biosynthetic gene cluster
BINOL	1,1'-bi-2-naphthol
Bn	benzyl
Boc	di- <i>tert</i> -butyl dicarbonate
BPin	bis(pinacolato)diboron
Bu or <i>n</i> Bu	butyl
Cbz	carboxybenzyl
cod	1,4-cyclooctadiene
Cp	cyclopentadienyl
CSA	camphorsulfonic acid
CSO	camphorsulfonic oxaziridine
CuAAC	copper-catalyzed azide-alkyne cycloaddition
DA	Diels-Alder

DBU	1,8-diazabicyclo(5.4.0)undec-7-ene
DCM	dichloromethane
DIBAL	diisobutylaluminum hydride
DKP	diketopiperazine
DMAP	4-dimethylaminopyridine
DMF	dimethylformamide
DMP	Dess-Martin periodinane
DMSO	dimethyl sulfoxide
DNFNB	1,5-difluoro-2,4-dinitrobenzene
dr	diastereomeric ratio
EDC	1-ethyl-3-(3-dimethylaminopropyl)carbodiimide
EDTA	ethylenediaminetetraacetic acid
ee	enantiomeric excess
Et	ethyl
EtOAc	ethyl acetate
eq	equivalent
EWG	electron withdrawing group
Fau	faulknamycin
FDNP	1-fluoro-2,4-dinitrophenyl
Fmo	fluorenylmethoxycarbonyl
HATU	1-hydroxy-7-azabenzotriazole
HMPA	hexamethylphosphoramide
HRMS	high-resolution mass spectrometry

IMDAO	intramolecular Diels-Alder oxazole
IMPK	intramolecular Pauson-Khand
<i>i</i> Pr	isopropyl
IR	infrared
<i>J</i>	coupling constant
KHMDS	potassium hexamethyldisilazane
LCMS	liquid chromatography-mass spectrometry
LDA	lithium diisopropylamide
LiHMDS	lithium bis(trimethylsilyl) amide
LRMS	low-resolution mass spectrometry
<i>m</i> CPBA	<i>meta</i> -chloroperoxybenzoic acid
Me	methyl
MEMCl	2-methoxyethoxymethyl chloride
MeOH	methanol
MFSDA	methyl fluorosulfonyl difluoroacetate
MOM	methoxymethyl
Ms	methanesulfonyl
MS	mass spectrometry
NaHMDS	sodium bis(trimethylsilyl)amide
NBS	<i>N</i> -bromosuccinimide
NBSH	2-nitrobenzenesulfonylhydrazide
<i>n</i> BuLi	<i>n</i> -butyllithium
NMP	<i>N</i> -methylpyrrolidine

NMR	nuclear magnetic resonance
NOE	nuclear Overhauser effect
NP	natural product
NRPS	non-ribosomal peptide synthetase
OAc	acetate
<i>OiPrBPin</i>	2-isopropoxy-4,4,5-tetramethyl-1,3,2-dioxaborolane
PAL	photoaffinity label
Ph	phenyl
Phen	phenanthroline
PheOH	phenylalanine
Pr or <i>nPr</i>	propyl
<i>pTsOH</i>	<i>p</i> -toluene sulfonic acid
SAM	<i>S</i> -adenosyl methionine
SAR	structure-activity relationship
<i>sBuLi</i>	<i>sec</i> -butyllithium
SEM	3,8-bis[2-(trimethylsilyl)ethoxy]
TBAF	tetra- <i>n</i> -butylammonium fluoride
TBS	<i>tert</i> -butyldimethylsilyl
<i>tBu</i>	<i>tert</i> -butyl
TEMPO	(2,2,6,6-tetramethylpiperidin-1-yl)oxyl
Tf	(trifluoromethyl)sulfonyl
TFA	trifluoroacetic acid
THF	tetrahydrofuran

TIPS	<i>N</i> -triisopropyl silane
TMM	trimethylenemethane
TMS	trimethylsilyl
TPAP	tetrapropylammonium perruthenate
Troc	2,2,2-trichloroethoxycarbonyl chloride
Ts	toluenesulfonyl

TABLE OF CONTENTS

Chapter 1. Recent Advances in Intramolecular Allene Cyclization Reactions for Total Synthesis of Natural Products.....	23
1.1 Introduction.....	24
1.2 Allene cycloaddition reactions in total synthesis of natural products.....	25
1.2.1 Total synthesis of carbazomadurin A and B.....	25
1.2.2 Formal synthesis of (–)-vindoline.....	26
1.2.3 Total synthesis of ent-[3]-ladderanol.....	28
1.2.4 Total synthesis of (–)-cajanusine.....	30
1.3 Radical-mediated allene cyclizations towards natural product total synthesis.....	30
1.3.1 Total synthesis of meloscine.....	30
1.3.2 Formal synthesis of bicyclomycin.....	32
1.3.3 Total synthesis of waihoensene.....	34
1.4 Metal-mediated allene cyclizations towards total synthesis.....	35
1.4.1 Total synthesis of (–)-cycloclavine.....	35
1.4.2 Total synthesis of enigmazole A.....	37
1.4.3 Formal synthesis of (+)-cis-3-methyl-4-decanolide.....	39
1.4.4 Total synthesis of avenoal.....	39
1.4.5 Total synthesis of curcusones I and J.....	41
1.4.6 Total synthesis of (–)-perforanoid A.....	42

1.4.7 Total synthesis of marinoquinoline A.....	13 44
1.5 Conclusions.....	45
Chapter 2. Total Synthesis of the Solamin Stereoisomers via a “Traceless” Petasis Reaction.....	46
2.1 Introduction.....	47
2.2 Discovery and structural elucidation of the solamin stereoisomers.....	48
2.3 Biological activity of the solamin stereoisomers.....	49
2.4 Biosynthesis of the solamin stereoisomers.....	50
2.5 Previous syntheses of the solamin stereoisomers.....	51
2.5.1 Total syntheses of trans-solamin.....	51
2.5.1.1 Total synthesis of trans-solamin by Sinha, et al.....	51
2.5.1.2 Total synthesis of trans-solamin by Makabe, et al.....	53
2.5.1.3 Total synthesis of trans-solamin by Trost, et al.....	54
2.5.2 Total syntheses of cis-solamin A and B.....	56
2.5.2.1 Total synthesis of cis-solamin A by Brown, et al.....	56
2.5.2.2 Total synthesis of cis-solamin A by Makabe, et al.....	57
2.5.2.3 Total synthesis of cis-solamin A by Stark, et al.....	58
2.5.2.4 Total synthesis of cis-solamin A and cis-solamin B by Akaji, et al.....	59
2.6 This work: Application of a “traceless” Petasis reaction for solamin total synthesis.....	61
2.6.1 Petasis borono–Mannich reaction.....	61

	14
2.6.2 “Traceless” Petasis reaction inspired by Myer’s allene synthesis.	63
2.7 Synthesis of the solamin stereoisomers.	66
2.7.1 Retrosynthesis.	66
2.7.2 Stereodivergent method to access the solamin stereoisomers.	67
2.7.3 Enantioselective traceless Petasis reaction with D-mannitol-derived alkynyl boronates.	68
2.7.3.1 Synthesis of D-mannitol-derived alkynyl boronates.	68
2.7.3.2 Synthesis of (CF ₃) ₄ -BINOL.	69
2.7.3.3 Traceless Petasis reaction with mannitol-derived alkynyl boronates.	70
2.7.4 Enantioselective traceless Petasis reaction with O-benzyl alkynyl boronates.	72
2.7.4.1 Synthesis of O-benzyl alkynyl boronates.	72
2.7.4.2 Traceless Petasis reaction with O-benzyl alkynyl boronates.	73
2.7.5 Enantioselective traceless Petasis reaction with allyl boronates.	74
2.7.5.1 Synthesis of allyl boronates for traceless Petasis reaction Path B.	74
2.7.5.2 Synthesis of (R)-(Ph) ₂ -BINOL.	75
2.7.5.3 Traceless Petasis reaction with allyl boronates.	76
2.8 Modified route towards allenol intermediate.	77
2.8.1 Lewis-acid catalyzed traceless Petasis reaction towards diastereomeric allenols.	77
2.8.1.1 Synthesis of an alkynyl trifluoroborate salt and La(OTf) ₃ -cat. Petasis reaction.	77
2.8.1.2 Beyond the traceless Petasis reaction: Synthesis of the solamin stereoisomers.	79
2.9 Future directions.	81

2.9.1 Route towards completing the total synthesis of the solamin stereoisomers.	15 81
2.10 Conclusions.	82
2.11 Experimental Section.	82
2.11.1 General information.	82
2.11.2 Synthesis of boronates for enantioselective Petasis reactions.	83
2.11.2.1 Synthesis of D-Mannitol derived alkynyl boronates.	83
2.11.2.2 Synthesis of O-Benzyl alkynyl boronates.	88
2.11.2.3 Synthesis of MEM-ether allyl boronates.	90
2.11.3 Synthesis of sulfonyl hydrazides.	92
2.11.4 Synthesis BINOL catalysts for enantioselective Petasis reaction.	92
2.11.4.1 Synthesis of (S)-(CF ₃) ₃ -BINOL.	92
2.11.4.2 Synthesis of (R)-Ph ₂ -BINOL for enantioselective Petasis reaction.	96
2.11.5 Synthesis of La(OTf) ₃ -derived allenols and advanced cis-solamin B intermediates.	98
Chapter 3. Total Synthesis of Tambromycin Enabled by Indole C–H Functionalization...	102
3.1 Introduction.	103
3.1.1 Metabologenomic-driven discovery of novel NPs.	103
3.2 Tambromycin – Discovery, structural elucidation, and biosynthesis.	105
3.2.1 Discovery of tambromycin via metabologenomics.	105
3.2.2 Tambromycin structural elucidation and related compounds.	105

	16
3.2.3 Determining the biosynthetic pathway of tambromycin.....	107
3.2.3.1 NRPS-produced NPs.....	107
3.2.3.2 NRPS assembly of tambromycin – Incorporation of four nonproteinogenic AAs.	107
3.3 Total synthesis of tambromycin.....	109
3.3.1 Retrosynthesis	109
3.3.2 Accessing the indole-oxazoline fragment of tambromycin.	110
3.3.2.1 Tambromycin indole substitution and connectivity: Related NP structures.....	110
3.3.2.2 Synthetic strategy to access the 1,3,4,6-substituted indole fragment of tambromycin.	112
3.3.2.3 Synthesis of tambromycin indole-oxazoline fragment III-6.	116
3.3.3 Accessing the tambroline fragment of tambromycin.....	119
3.3.3.1 Tambroline biosynthesis and related modified lysine-containing NPs.....	119
3.3.3.2 Tambroline biosynthesis and stereochemical assignment.	122
3.3.3.3 Direct electrophilic azidation to access tambroline stereochemistry.	124
3.3.3.4 Synthesis of tambroline dipeptide fragment III-86.....	125
3.3.4 Final steps towards tambromycin total synthesis.....	126
3.4 Conclusions and outlooks	128
3.4.1 Biosynthetic-inspired total synthesis of tambromycin by Renata and coworkers.	128
3.4.2 Future directions.	129
3.4.3 Conclusions.....	131

3.5 Experimental Section	17
3.5.1 General information.	132
3.5.2 Synthesis of indole-oxazoline fragment.....	133
3.5.3 Synthesis of tambroline dipeptide.....	139
3.5.4 Final coupling and deprotection.....	143
References	147
Chapter 1.....	147
Chapter 2.....	151
Chapter 3.....	156
Appendix 1. Synthesis of Diastereomeric β-Hydroxy Phenylalanine Residues for Structural Elucidation of Faulknamycin.	165
A1.1 Introduction.....	166
A1.1.1 Development of synthetic standards for natural product (NP) structural elucidation.	166
A1.1.2 Marfey's analysis for stereochemical assignment of amino acid residues.	166
A1.2 Faulknamycin discovery and structural assignment of non-proteinogenic AAs.	168
A1.3 Diastereoselective synthesis of β -PheOH stereoisomers.	169
A1.3.1 Synthesis of β -PheOH isomers via stereoselective aminohydroxylation.	170
A1.4 Marfey's analysis of faulknamycin using β -PheOH synthetic standards.	176
A1.5 Experimental Section	178
A1.5.1 General information.	178

	18
A1.5.2 Reported spectra for β -hydroxyphenylalanine standards.....	178
A1.5.3 Synthesis of (2R, 3S) and (2R, 3R) β -PheOH standard.....	179
Appendix 2. Supplementary Data	187
A2.1 Supplementary Data.....	188
A2.1.1 NMR comparison of tambromycin III-1 to isolated natural material.....	188
A2.1.2 Marfey's analysis of tambroline stereoisomers.....	189
A2.1.3 Stereodivergent route to the solamin stereoisomers.....	190
References	191
Appendix 1.....	191
Appendix 2.....	19

LIST OF FIGURES

Figure 1.1 Allene cumulated π -bond system.	24
Figure 2.1 Structures of ACG NPs.	47
Figure 2.2 Solamin stereoisomers.	49
Figure 3.1 Structure of tambromycin and related compounds.....	106
Figure 3.2 Biosynthetic pathway for tambromycin.	108
Figure 3.3 Natural products structurally related to the indole-oxazoline core.....	111
Figure 3.4 Modified lysine-containing NPs.	120
Figure 3.5 Aminocaprolactam-containing NPs.	121
Figure 3.6 Proposed tambromycin SAR analogues.....	130
Figure 3.7 Proposed tambromycin-based proteomics probe.....	131
Figure A1.1 Peptide NP faulknamycin with unknown β -PheOH stereochemistry.....	168
Figure A1.2 β -PheOH stereoisomers.....	169
Figure A1.3 CSOs for stereoselective oxidation.....	172
Figure A1.4 LC-MS traces of Marfey's analysis for diastereomeric standards and Fau unknown (provided by Hudson Tryon).....	176
Figure A1.5 Final structural assignment for faulknamycin.....	177
Figure A2.1 Marfey's analysis for tambroline diastereomers.....	189

LIST OF SCHEMES

Scheme 1.1 Total synthesis of carbazomadurin A and B.	26
Scheme 1.2 Formal synthesis of (–)-vindoline.	27
Scheme 1.3 Total synthesis of <i>ent</i> -[3]-ladderanol.	29
Scheme 1.4 Total synthesis of (–)-cajanusine.....	30
Scheme 1.5 Total synthesis of meloscine.	32
Scheme 1.6 Formal synthesis of bicyclomycin.....	33
Scheme 1.7 Total synthesis of waihoesene.	35
Scheme 1.8 Total synthesis of (–)-cycloclavine.	36
Scheme 1.9 Total synthesis of enigmazole A.	38
Scheme 1.10 Formal synthesis of (+)- <i>cis</i> -3-methyl-4-decanolide.	39
Scheme 1.11 Total synthesis of avenoal.	40
Scheme 1.12 Total synthesis of curcusone I and J.....	42
Scheme 1.13 Total synthesis of (–)-perforanoid A.	43
Scheme 1.14 Total synthesis of marinoquinoline A.	45
Scheme 2.1 Putative biosynthetic pathway towards the solamin stereoisomers.	50
Scheme 2.2 Total synthesis of <i>trans</i> -solamin by Sinha, et al.	52
Scheme 2.3 Total synthesis of <i>trans</i> -solamin by Makabe, et al.....	53
Scheme 2.4 Total synthesis of <i>trans</i> -solamin by Trost, et al.	55
Scheme 2.5 Total synthesis of <i>cis</i> -solamin A by Brown, et al.	56
Scheme 2.6 Total synthesis of <i>cis</i> -solamin A by Makabe, et al.	57
Scheme 2.7 Total synthesis of <i>cis</i> -solamin A by Stark, et al.	58
Scheme 2.8 Total synthesis of <i>cis</i> -solamin A and B by Akaji, et al.	60

	21
Scheme 2.9 General path towards THF-core from chiral allenol.	61
Scheme 2.10 Petasis borono-Mannich reaction development and stereocontrol.	62
Scheme 2.11 Myer's allene synthesis and traceless Petasis reaction development.	64
Scheme 2.12 Possible disconnections for the traceless Petasis reaction.	65
Scheme 2.13 Retrosynthesis towards <i>cis</i> -solamin A.	66
Scheme 2.14 Divergent synthesis of the solamin stereoisomers.	67
Scheme 2.15 Synthesis of D-mannitol-derived alkynyl boronates.	68
Scheme 2.16 Synthesis of (<i>S</i>)-(CF ₃) ₃ -BINOL.	70
Scheme 2.17 Enantioselective traceless Petasis reaction with mannitol-derived alkynyl boronates.	71
Scheme 2.18 Synthesis of <i>O</i> -benzyl alkynyl boronates.	73
Scheme 2.19 Enantioselective traceless Petasis reaction with <i>O</i> -alkynyl boronates.	74
Scheme 2.20 Synthesis of allyl boronates.	74
Scheme 2.21 Synthesis of (<i>R</i>)-(Ph) ₂ -BINOL.	76
Scheme 2.22 Enantioselective traceless Petasis reaction with allyl boronates.	77
Scheme 2.23 One-pot synthesis of diastereomeric allenols.	78
Scheme 2.24 Stereochemical model of La(OTf) ₃ -cat. traceless Petasis reaction.	80
Scheme 2.25 Synthesis of THF intermediate II-149. Asterisk denotes putative stereochemistry.	80
Scheme 2.26 Final route towards <i>cis</i> -solamin B. Asterisk denotes putative stereochemistry.	81
Scheme 3.1 Retrosynthetic analysis of tambromycin.	109
Scheme 3.2 Hino, et al. route to regioisomeric mixture of substituted indole products.	112
Scheme 3.3 Retrosynthesis by Baran, et al. to access fumitremorgin A and verruculogen.	113
Scheme 3.4 Movassaghi, et al. route to C7-substituted indoles via Ir-cat. borylation.	114

	22
Scheme 3.5 Indole functionalization directed by <i>N</i> -TIPS protecting group.	115
Scheme 3.6 Baran, et al. route towards regioselective indole C6-functionalization.....	116
Scheme 3.7 Our synthesis of indole-oxazoline fragment III-6.	117
Scheme 3.8 Stable isotope feeding experiments to determine tambroline biosynthetic precursor	122
Scheme 3.9 Synthesis of stereodefined tambroline isomers.	123
Scheme 3.10 Stereospecific synthesis of α -N ₃ carboxylic acids.	124
Scheme 3.11 Our synthesis of tambroline dipeptide III-86.....	126
Scheme 3.12 Final coupling and deprotection for tambromycin total synthesis.	127
Scheme 3.13 Renata, et al. route towards tambroline dipeptide.	129
Scheme A1.1 Chiral derivatizing reagent FDNP-L-Ala-NH ₂ , or Marfey's reagent.....	167
Scheme A1.2 Routes explored for synthesis of β -PheOH standards.	170
Scheme A1.3 Representative route towards all four β -PheOH stereoisomers.....	171
Scheme A1.4 Synthesis of (+)(2 <i>R</i> , 8 <i>aS</i>)-CSO.	172
Scheme A1.5 Synthesis of (2 <i>R</i> , 3 <i>S</i>) (or (2 <i>S</i> , 3 <i>R</i>) enantiomer) via route A.	173
Scheme A1.6 Synthesis of (2 <i>R</i> , 3 <i>R</i>) (or (2 <i>S</i> , 3 <i>S</i>) enantiomer) via route B.	175
Scheme A2.1 Stereodivergent pathway to all solamin stereoisomers.	190

Chapter 1

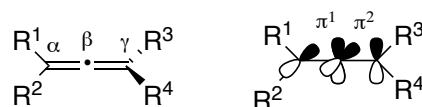
Recent Advances in Intramolecular Allene Cyclization Reactions
for Total Synthesis of Natural Products

1 Chapter 1

1.1 Introduction.

Since the first synthesis of an allene by Burton and Pechman in 1887,¹ significant progress has been made towards studying and understanding this unique chemical scaffold. Allenes are the simplest cumulenes, with two contiguous C=C bonds located in mutually perpendicular planes providing intrinsic axial chirality (Figure 1.1).^{2, 3} Allenes are more reactive than both alkene and alkyne analogues, and their increased substituent loading ability, less-hindered linear structure, and intrinsic axial chirality allows for complex reactions to proceed with stereocontrol at multiple stereocenters.

Figure 1.1 Allene cumulated π -bond system.

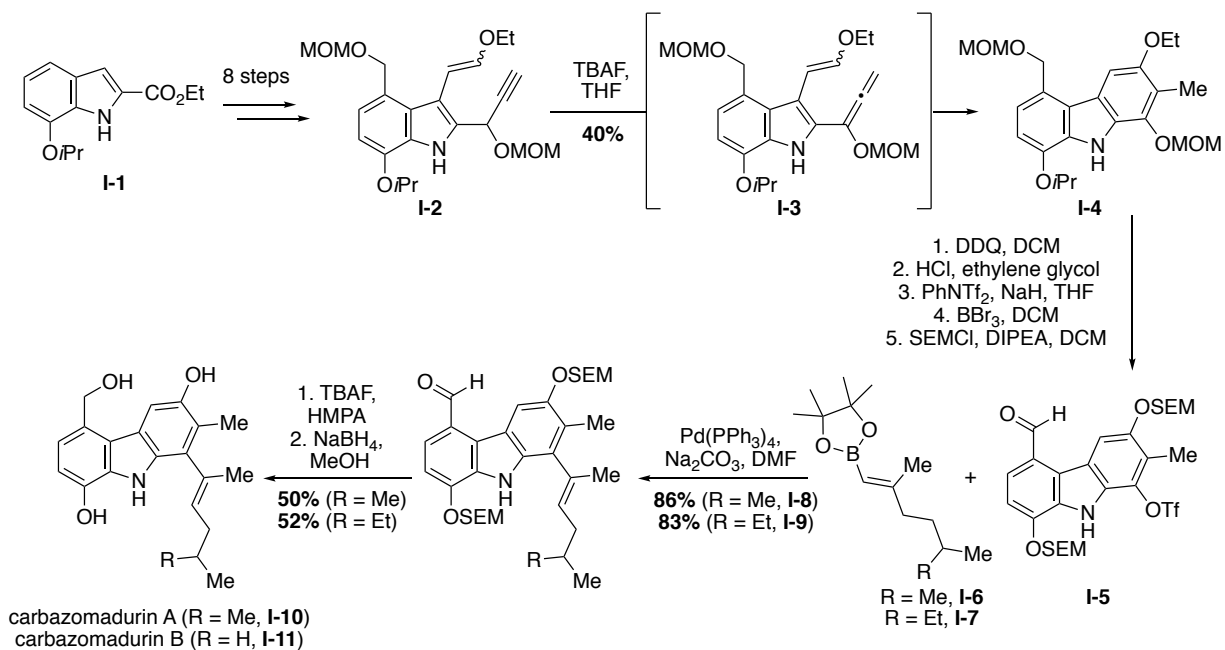


Exploration of allene reactivity has led to the development of methods for cycloaddition reactions, transition metal-catalyzed cycloadditions, transition metal-promoted cyclizations, and acid-catalyzed rearrangements of allene intermediates.² Allenes are of particular value in total syntheses, where the unique patterns of reactivity can be leveraged to rapidly access complex natural product scaffolds. While there is a breadth of literature outlining allene intermediates en route to total syntheses,³⁻⁵ this review chapter will specifically highlight recent total syntheses that utilize intramolecular allene cyclization reactions. A variety of cyclization and cycloisomerization reactions are summarized herein, emphasizing the versatility of the allene scaffold in accessing complex cyclic natural products. Chapter 2 will subsequently discuss the Thomson lab's application of a chiral allene cyclization reaction towards the total synthesis of the solamin stereoisomers.

1.2 Allene cycloaddition reactions in total synthesis of natural products.

1.2.1 Total synthesis of carbazomadurin A and B.

In 2013, Hibino and coworkers published a synthesis of the carbazole alkaloids carbazomadurin A and (*S*)-(+)-carbazomadurin B via an allene-mediated 6π -electrocyclization of propargyl ether **I-2** (Scheme 1.1).⁶ Allenyl-indole intermediates like **I-3** undergo thermal cyclization much more rapidly than corresponding bis-vinylindole precursors, and thus this type of transformation can provide efficient access to a variety of polysubstituted heterocyclic scaffolds. Thermal allene electrocyclizations have been applied by the Hibino group en route to several polysubstituted carbazole alkaloids.⁷⁻⁹ Towards carbazomadurin A and B, protected propargyl indole **I-2**, prepared in 8 steps from known ethyl-7-alkoxyindole-2-carboxylate **I-1**, was subjected to an allene-mediated thermal electrocyclic reaction using tetra-*n*-butylammonium fluoride (TBAF) in tetrahydrofuran (THF). This *in situ* generation of a reactive allene species, followed by spontaneous electrocyclization, provided desired carbazole **I-4** in 40% yield within 1 hr.¹⁰ To complete the total synthesis, compound **I-4** was then converted to 3,8-bis[2-(trimethylsilyl)ethoxy]methyl acetal (3,8-bis(OSEM))-carbazole **I-5** in five steps. Cross-coupling between **I-5** and pinacol borates **I-6** and **I-7** (prepared from commercially available 5-methyl-1-hexyne and (*S*)-(+)-5-methyl-1-heptyne, respectively) in the presence of Na_2CO_3 and $\text{Pd}(\text{PPh}_3)_4$ gave the corresponding 1-alkenyl carbazoles **I-8** and **I-9** in 86% and 83% yield, respectively. Cleavage of the SEM protecting group by using TBAF in hexamethylphosphoramide (HMPA), followed by reduction with NaBH_4 in methanol (MeOH) provided carbazomadurin A (**I-10**) and (*S*)-(+)-carbozomadurin B (**I-11**) in 50% and 52% yield over two steps.

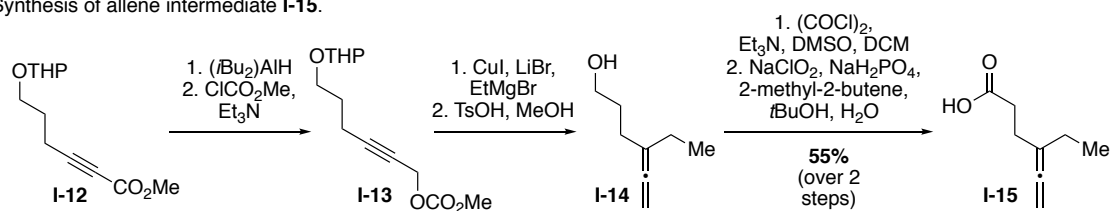
Scheme 1.1 Total synthesis of carbazomadurin A and B.

1.2.2 Formal synthesis of (–)-vindoline.

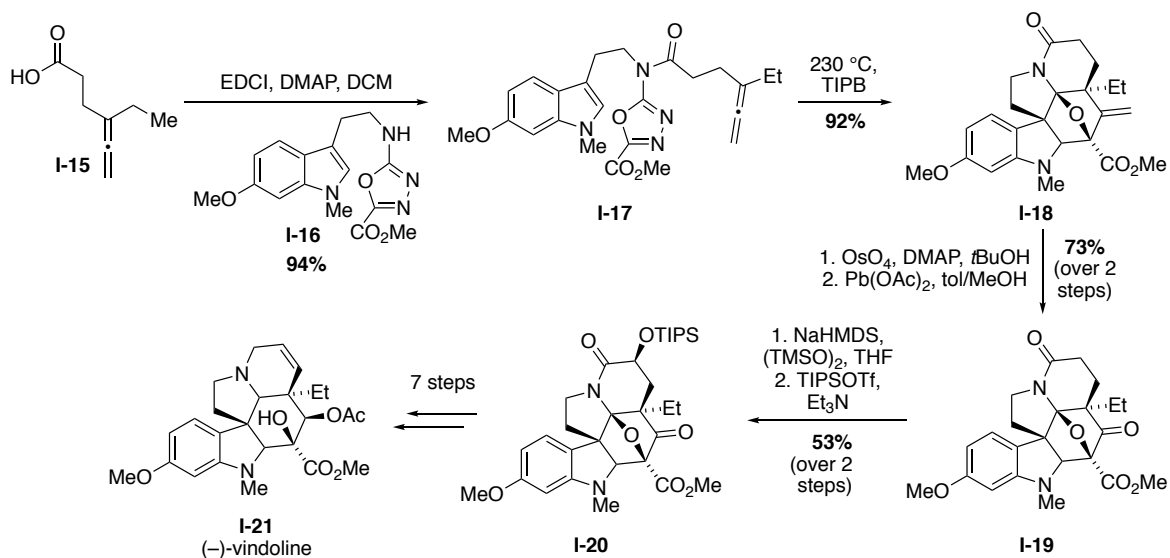
In 2015, the Boger group published a formal synthesis of (–)-vindoline via a tandem intramolecular [4+2]/[3+2] cycloaddition cascade initiated by an allene dienophile (Scheme 1.2).¹¹ In previous work to access (–)vindoline, Boger and coworkers discovered that the requisite [4+2]/[3+2] cascade suffered from lack of stereocontrol and a slow rate for the [3+2] cycloaddition when using traditional alkenyl dienophiles.^{12, 13} Instead, using an allenyl dienophile was predicted to improve reaction rate and stereoselectivity. In this work, the key allenyl cycloaddition precursor **I-17** was accessed via a 1-ethyl-3-(3-dimethylaminopropyl)carbodiimide (EDC)-mediated peptide coupling between allene **I-15** (prepared from alkyne **I-12**, Scheme 1.2a) and 1,3,4-oxadiazole **I-16** (94% yield, Scheme 1.2b). An initial Diels-Alder reaction between the electron deficient 1,3,4-oxadiazole **I-17** and the tethered allene provided a cycloadduct **I-22** that underwent loss of N₂, forming an intermediate cross-conjugated 1,3-dipole (**I-23**, Scheme 1.2c). Carbonyl ylide **I-23**

Scheme 1.2 Formal synthesis of (-)-vindoline.

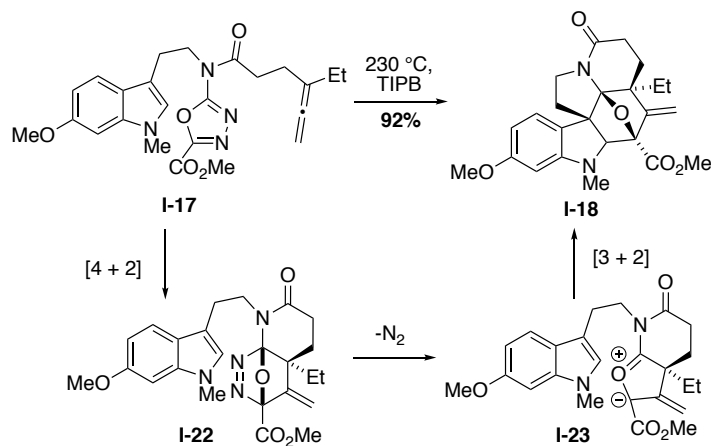
a. Synthesis of allene intermediate **I-15**.



b. Formal synthesis of (-)-vindoline from intermediate **I-15**.



c. Mechanism of [4+2]/[3+2] cycloaddition cascade.



then participated in a [3+2] dipolar cycloaddition, with regioselectivity controlled by the tether position and the complementary polarity of the reacting partners, and diastereoselectivity controlled by preference of the dipolarophile to face away from the newly formed six-membered ring. Oxidation of the exocyclic double bond was accomplished by treating intermediate **I-18** with 2:1 4-dimethylaminopyridine (DMAP):OsO₄, and subsequent oxidative cleavage of the diol using Pb(OAc)₄ in toluene/MeOH gave access to compound **I-19**. Finally, α -hydroxylation was accomplished by forming the lactam enolate with sodium bis(trimethylsilyl)amide (NaHMDS) and treating with trimethylsilyl anhydride (TMSO)₂. *In situ* protection with triisopropylsilyl trifluoromethanesulfonate (TIPSOTf) and triethylamine (Et₃N) provided silyl ether **I-20**. (–)-Vindoline (**I-21**) was accessible in seven additional steps from intermediate **I-20**, following a protocol published previously by Boger and coworkers towards the total synthesis of this molecule.¹⁴

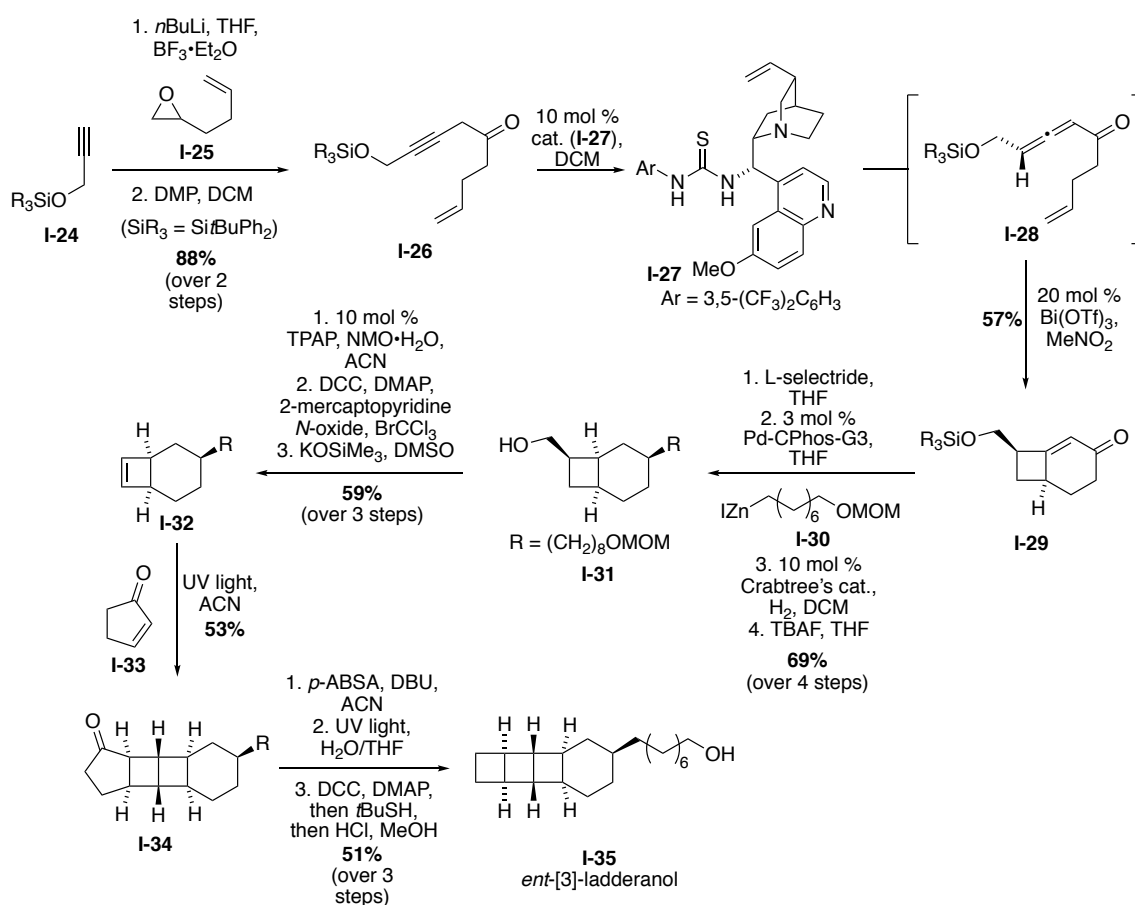
1.2.3 Total synthesis of *ent*-[3]-ladderanol.

In 2017, Brown and coworkers published the total synthesis of *ent*-[3]-ladderanol using an intramolecular [2+2] cycloaddition of an allenic ketone to access a [4.2.0]-bicycle precursor to the natural product (Scheme **1.3**).¹⁵ This marked the first example of chirality transfer in a [2+2] allenic ketone cycloaddition, and this route branched from the Brown group's previous work towards enantioselective synthesis of allenates via enantioselective isomerization of β , γ -alkynyl esters.¹⁶

¹⁷ Towards *ent*-[3]-ladderanol, addition of the lithium acetylide of **I-24** into epoxide **I-25**, followed by Dess-Martin periodinane (DMP) oxidation provided β , γ -alkynyl ketone **I-26**. Enantioselective isomerization of β , γ -alkynyl ketone **I-26** into the requisite [2+2] cycloaddition precursor **I-28** was promoted by thiourea catalyst **I-27**, providing transient allenic ketone **I-28** in 57% yield and 94:6

er. Direct addition of nitromethane ($\text{Me}(\text{NO}_2)$) and $\text{Bi}(\text{OTf})_3$ to the reaction mixture promoted the [2+2] cycloaddition reaction to form [4.2.0]-bicycle intermediate **I-29** with complete chirality transfer. According to their model for chirality transfer, the alkene tether most likely approached the allene distal to the larger $-\text{CH}_2\text{OSiR}_3$ group, and its perpendicular alignment relative to the allene resulted in the observed stereochemical outcome. To complete their synthesis, [4.2.0]-bicycle **I-29** underwent stereoselective 1,4-reduction with L-selectride, Negishi cross-coupling with zinc reagent **I-30**, stereoselective hydrogenation from the convex face with Crabtree's catalyst, and TBAF deprotection to provide intermediate **I-31**. Oxidation of the free alcohol in compound **I-31** with 10 mol % tetrapropylammonium perruthenate (TPAP) was followed by decarboxylation in the presence of BrCCl_3 . Subsequent treatment with potassium trimethyl cyanoate

Scheme 1.3 Total synthesis of *ent*-[3]-ladderanol.

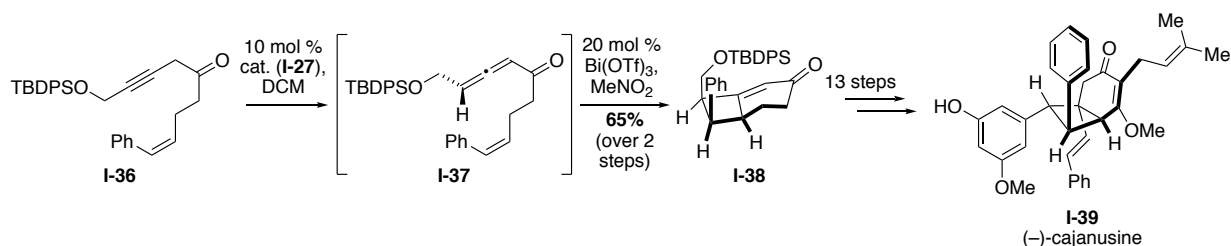


(KOSiMe₃) provided cyclobutene **I-32**, which then underwent a [2+2] cycloaddition with cyclopentenone **I-33** to yield compound **I-34**. A final Wolff rearrangement, decarboxylation, and methoxymethyl ether (MOM)-group deprotection yielded *ent*-[3]-ladderanol (**I-35**) in 51% yield over three steps.

1.2.4 Total synthesis of (–)-cajanusine.

In 2020, Brown and coworkers applied their method of stereoselective [2+2] cycloaddition of an allenic ketone (see Section 1.2.3) to accomplish the total synthesis of (–)-cajanusine (Scheme 1.4).¹⁸ β , γ -Alkynyl ketone **I-36**, prepared in five steps from 3,4-dihydropyran, was subjected to enantioselective isomerization upon treatment with urea catalyst **I-27** to form transient allenic ketone **I-37**. Addition of Bi(OTf)₃ promoted the key stereoselective [2+2] cycloaddition, yielding [4.2.0]-bicyclooctane **I-38** in 65% yield over two steps. Thirteen additional steps, including stereoselective conjugate addition and a key radical cross-coupling with a redox active ester, provided the natural product (–)-cajanusine (**I-39**).

Scheme 1.4 Total synthesis of (–)-cajanusine.



1.3 Radical-mediated allene cyclizations towards natural product total synthesis.

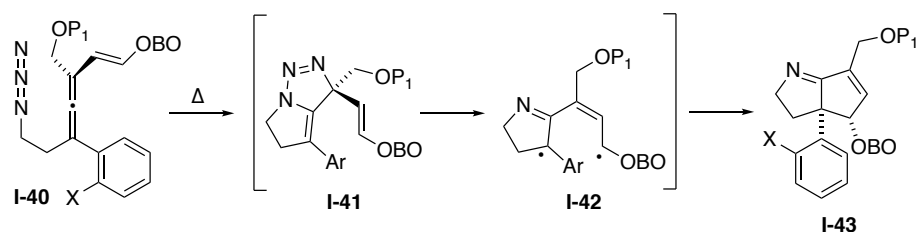
1.3.1 Total synthesis of meloscine.

In 2013, Feldman and coworkers published the total synthesis of meloscine utilizing an allenyl azide cyclization to access the azabicyclo[3.3.0]octane core (Scheme 1.5).¹⁹ This method

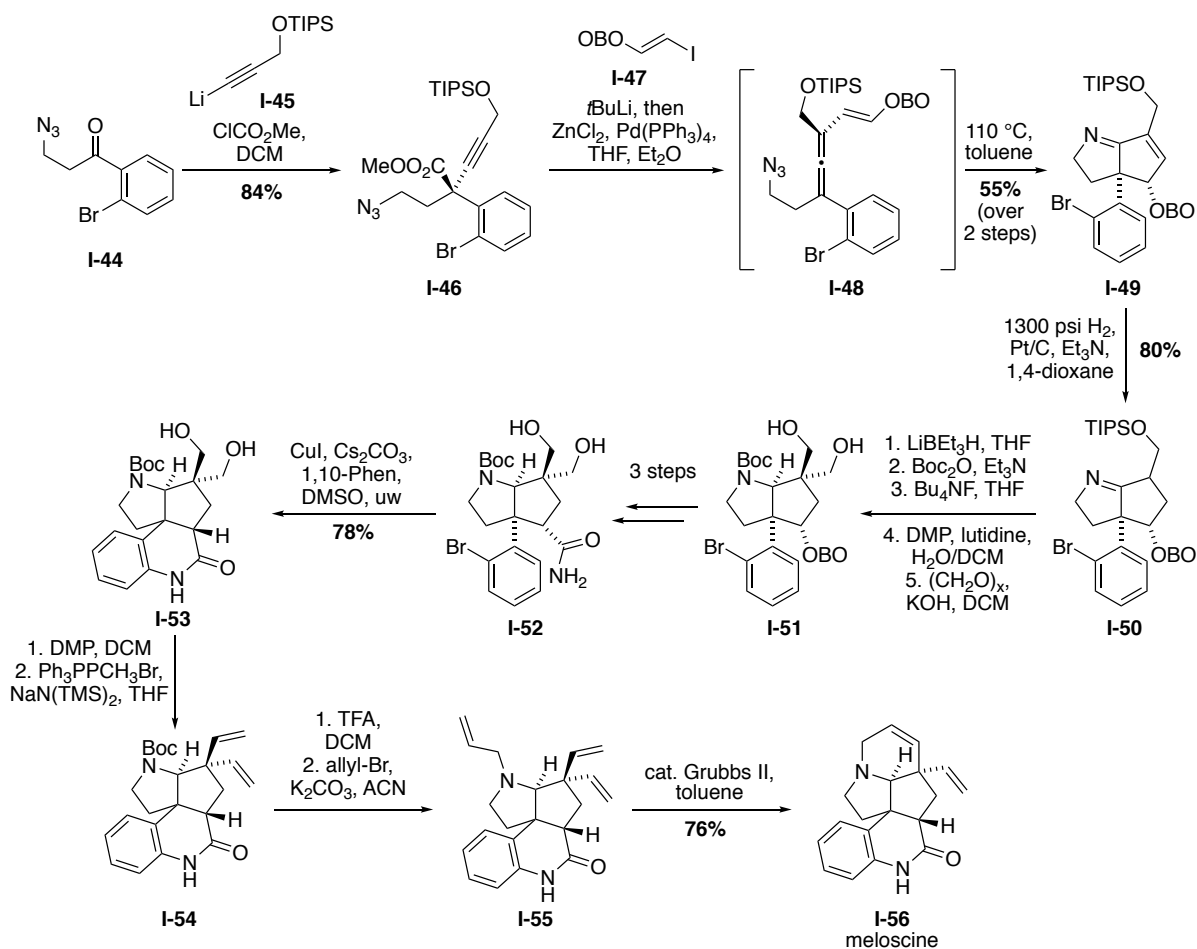
of intramolecular cyclization relies on diradical combination of an azatrimethylenemethane (ATTM) diyl intermediate (**I-42**), formed following the strain-driven release of N₂ from an allene/azide [2+3] dipolar cycloaddition intermediate (**I-41**) (Scheme 1.5a). The diyl species undergoes formal electrocyclization via a conrotatory pathway, giving rise to the desired bicycle stereoisomer. Towards meloscine, allenyl azide **I-48** was prepared beginning from benzoyl derivative **I-44** which underwent acetylide addition and acetylation of the primary alcohol, yielding the activated propargyl system **I-46**. Intermediate **I-46** was then vinylated using Vermeer's Zn/Pd based protocol,²⁰ providing allenyl azide **I-48**. This unstable key intermediate was immediately heated in toluene at 110 °C to initiate the thermal cascade sequence, forming azabicyclo[3.3.0]octane **I-49** in 55% yield. Alkene hydrogenation using high pressure and Pt/C provided intermediate **I-50**, which was converted into the C20 quaternary diol **I-51** through a series of protecting group manipulations and oxidations. A three-step procedure was followed to functionalize intermediate **I-51** along the C/D core periphery, leading to primary amide **I-52** from which the remaining ring system could be constructed. Lactam **I-53** was formed via a transition metal-mediated amidation between the 1° amide nitrogen and the aryl bromide in compound **I-52**, using modified aza-Ullman coupling conditions to provide compound **I-53** in 78% yield. Oxidation and Wittig bis-methylenation provided compound **I-54**, which underwent di-*tert*-butyl dicarbonate (Boc) removal and *N*-allylation to form triene **I-55**. A final Grubbs-mediated ring-closing metathesis provided meloscine (**I-56**) in 60% yield.

Scheme 1.5 Total synthesis of meloscine.

a. Mechanism of allenyl azide cyclization.



b. Total synthesis of meloscine.

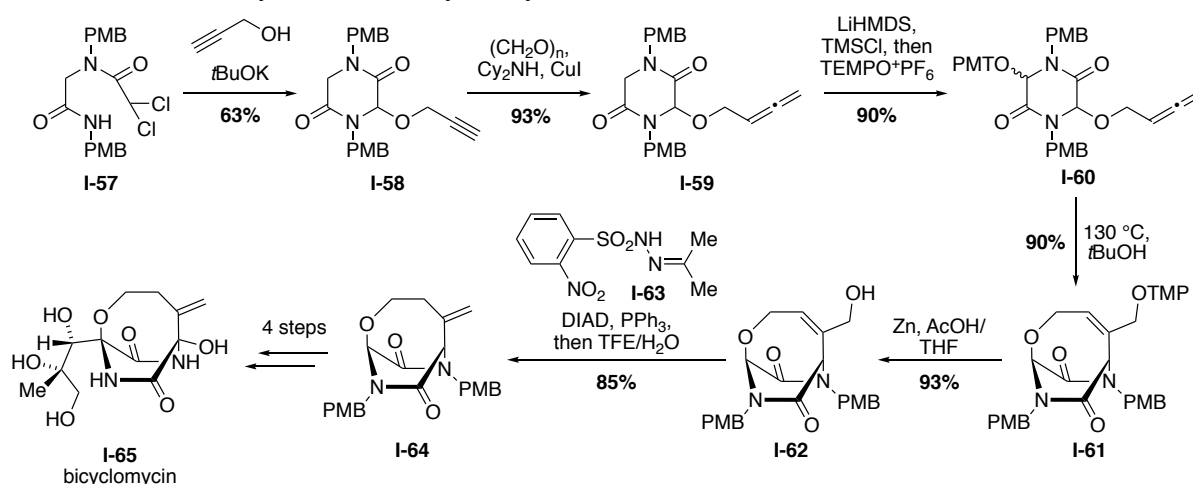


1.3.2 Formal synthesis of bicyclomycin.

In 2015, Jahn and coworkers published a formal synthesis of the antibiotic bicyclomycin via radical cycloisomerization of a diketopiperazine (DKP) derivative with a pendant allene unit (Scheme 1.6).²¹ Although radical cyclizations have been applied to a variety of alkaloid

syntheses,²²⁻²⁷ the inherently short lifetime of a DKP-precursor radical has limited the application of radical cyclization to these compounds. The Jahn group thus developed a method of intramolecular radical cyclization that relied on the persistent radical effect, wherein two radical species, one persistent and one transient, undergo selective cross-coupling. A novel allene radical acceptor alkoxyamine **I-60** was designed to incorporate both a stabilized, transient DKP radical and a persistent (2,2,6,6-tetramethylpiperidin-1-yl)oxyl (TEMPO) radical species, to induce a 6-*endo-trig* radical cyclization reaction. Towards bicyclomycin, allene intermediate **I-60** was constructed beginning from known dichloroacetamide **I-57**, which underwent oxidative cyclization under basic conditions to provide compound **I-58** in 63% yield. Crabbe homologation, followed by enolate oxygenation under internal quench conditions, provided the key allene radical acceptor **I-60**. Radical cycloisomerization took place upon heating allene **I-60** to 130 °C in *tert*-butanol (*t*BuOH) to provide desired bridged DKP **I-61** in 90% yield. The formal synthesis was completed following reductive removal of the tetramethylpiperidiny unit with zinc in acetic acid, and a reductive transposition of the internal double bond to the *exo* position via conditions developed by Movassaghi and Ahmad to furnish **I-64**.²⁸ Compound **I-64** was previously converted into bicyclomycin (**I-65**) via a four-step procedure established by Williams and coworkers.^{29, 30}

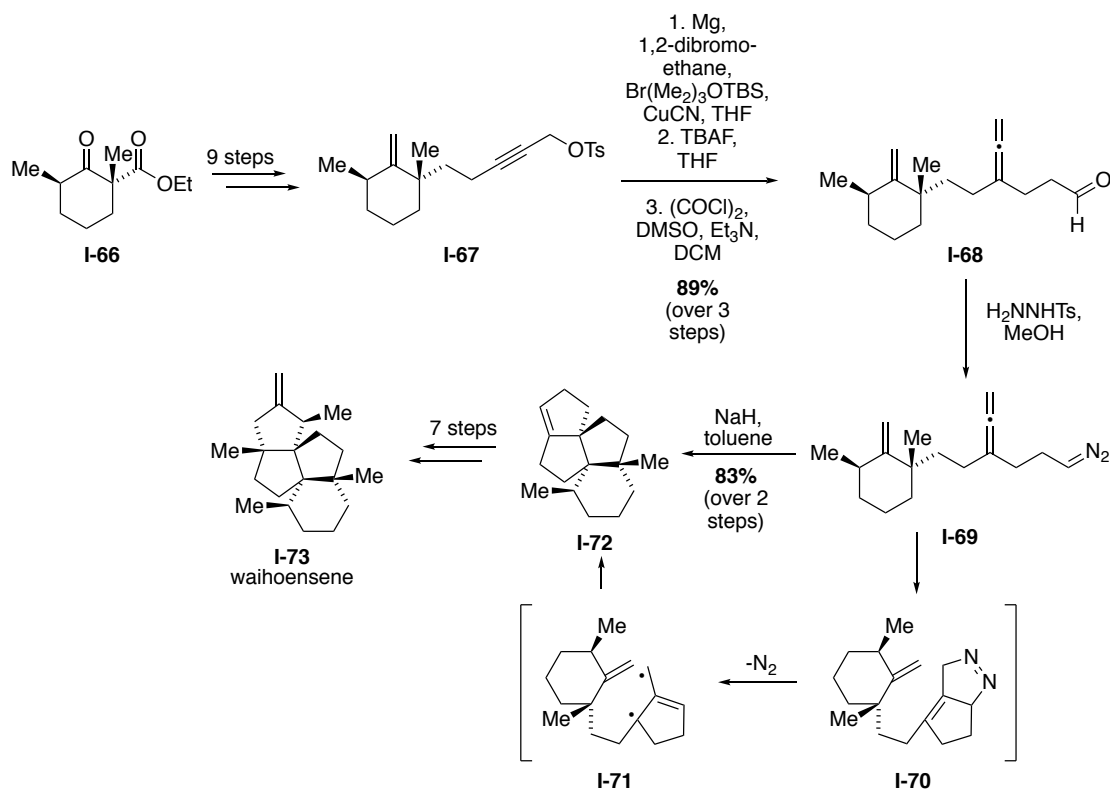
Scheme 1.6 Formal synthesis of bicyclomycin.



1.3.3 Total synthesis of waihoensene.

In 2017, the Lee group published the total synthesis of waihoensene via cycloaddition of trimethylenemethane (TMM) diyls, generated from N₂ extrusion of tetrahydropyrazole **I-70** formed by a [2+3] cycloaddition of a diazo and allene intermediate (Scheme 1.7, see Section 1.3.1 for similar diyl electrocyclizations).³¹ Their tandem cycloaddition substrate was designed to contain a six-membered ring, so that the tetracyclic skeleton of waihoensene could be constructed in one-pot. The Lee group has applied this method of allenyl diazo-generated diyl electrocyclizations to the total synthesis of many polyquinanes, including pentalene,³² panaginsene,³³ and (–)-crinipellin A.³⁴ Towards waihoensene, allenyl intermediate **I-68** was accessed beginning from racemic keto-ester **I-66**, which was converted into activated propargylic alcohol **I-67** following a nine step procedure. A copper-catalyzed SN₂ reaction with the Grignard reagent generated from 3-bromopropoxy-*tert*-butyldimethylsilane, followed by silyl deprotection with TBAF and Swern oxidation, afforded allenyl intermediate **I-68**. A terminal diazo group was installed using NH₂NNHTs, and intermediate **I-69** was then subjected to NaH in toluene to induce the key cycloaddition transformation. A [2+3] cycloaddition between diazo and allenyl pendant arms in **I-69** afforded a tetrahydropyrazole intermediate (**I-70**), which then formed the TMM diyl species **I-71** upon loss of N₂. A second [2+3] reaction between the terminal olefin and the TMM diyl provided triquinine **I-72** in 83% yield over 2 steps. A final seven step sequence involving oxidation, elimination, and methylations provided the natural product waihoensene (**I-73**).

Scheme 1.7 Total synthesis of waihoesene.



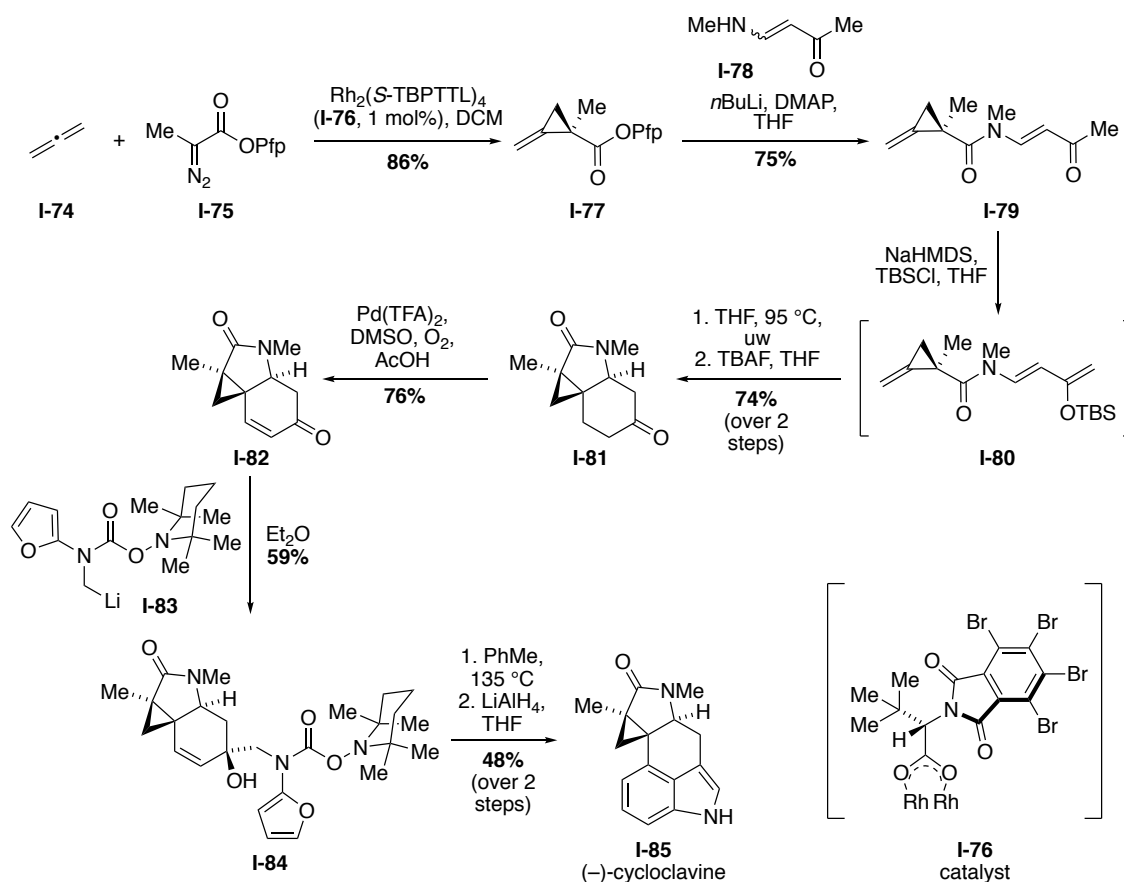
1.4 Metal-mediated allene cyclizations towards total synthesis.

1.4.1 Total synthesis of (-)-cycloclavine.

In 2016, Wipf and coworkers published the total synthesis of (-)-cycloclavine via an asymmetric cyclopropanation of allene **I-74** with a diazopropanoate **I-75**, mediated by a rhodium catalyst (Scheme 1.8).^{35, 36} Little is known about the fundamental behavior of unsubstituted allene in transition-metal catalyzed cyclopropanations, making the desired enantioselective cyclopropanation of allene particularly uncertain. Additionally, allene is known to be highly volatile and prone to oligomerization when in the presence of metals, and diazopropanoates are

known to readily undergo β -hydride elimination. However, the Wipf group accomplished an unprecedented intermolecular carbenoid cyclopropanation between allene (**I-74**) and pentafluoryl diazopropanoate **I-75** using 1 mol% dirhodium catalyst **I-76** (86% yield, 87:13 e.r.). Enantioinduction depended on the steric hindrance introduced by the diazopropanoate ester **I-75**. The key cyclopropanated product **I-77** was condensed onto vinylogous amide **I-78**, and treatment with NaHMDS following by enolate trapping with *tert*-butyldimethylsilyl chloride (TBSCl) afforded amino siloxy diene **I-80**. Upon microwave irradiation at 95 °C, intermediate **I-80** underwent an *anti*-selective intramolecular [4+2] cycloaddition with the pendant methylenecyclopropane. The crude enol ether was subjected to TBAF cleavage to afford intermediate **I-81**. Pd(DMSO)₂(TFA)₂-catalyzed dehydrogenation of ketone **I-81**, and subsequent

Scheme 1.8 Total synthesis of (-)-cycloclavine.



1,2-addition of a TEMPO carbamate afforded tertiary alcohol species **I-84**. An intramolecular Diels-Alder furan cycloaddition reaction in toluene at 135 °C resulted in cyclization/aromatization as well as thermolysis of the TEMPO carbamate protecting group, and a final LiAlH₄ reduction of the lactam provided (–)-cycloclavine (**I-85**).

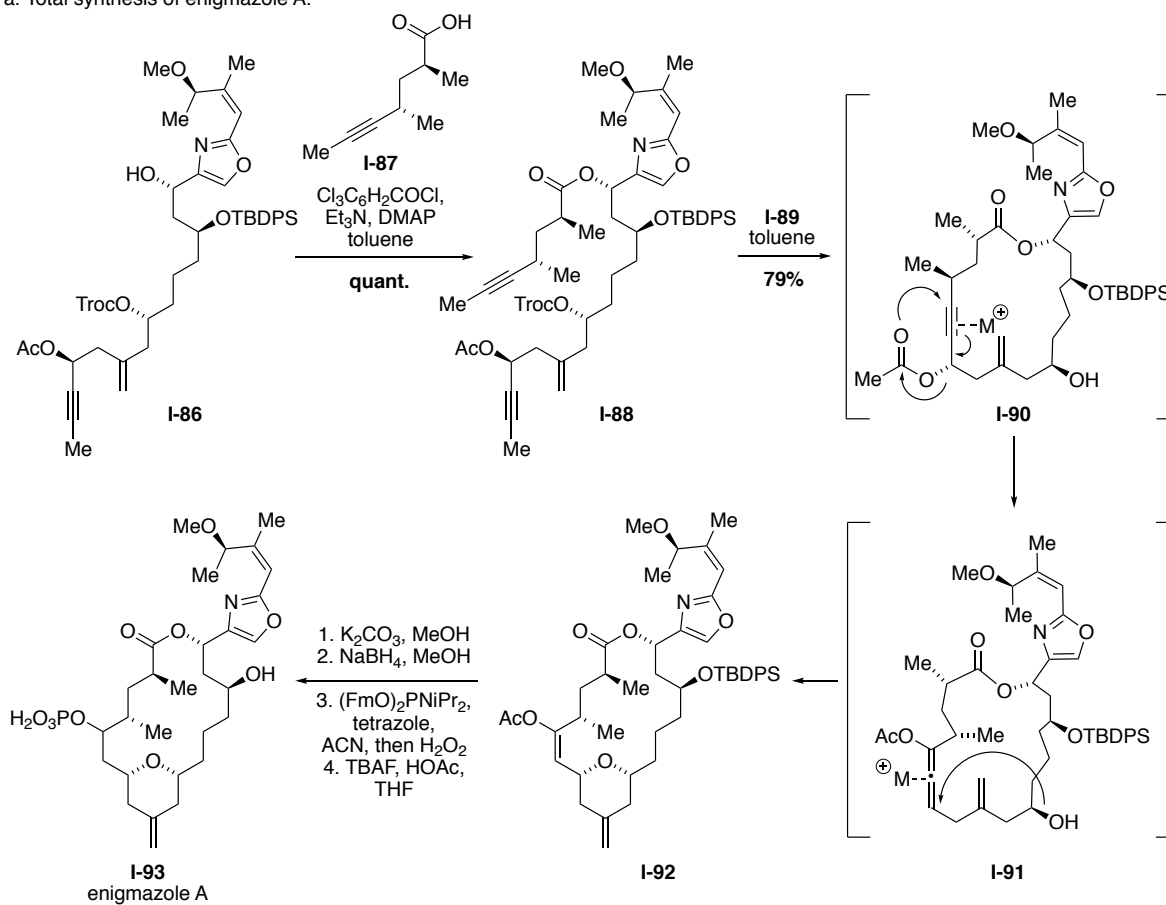
1.4.2 Total synthesis of *enigmazole A*.

In 2016, Fürstner and coworkers published the total synthesis of *enigmazole A* via a transient allenyl acetate intermediate formed by a gold-catalyzed [3,3] sigmatropic rearrangement of a propargylic acetate species (Scheme 1.9).³⁷ Previous investigations into the feasibility of this type of transformation revealed that the Au(I) activation of an alkynyl precursor would result in an allenolate intermediate following a [1,3]-shift, and the formed allenolate would then coordinate with the Au(I) catalyst to undergo nucleophilic attack and ultimately form a 2,5-dihydrofuran motif.³⁸ Here, precursor to the transannular cascade reaction, **I-88**, was prepared via esterification between alkynyl acid **I-87** and oxazole **I-86**, followed by ring-closing alkyne metathesis and ultrasound-accelerated 2,2,2-trichloroethoxycarbonyl chloride (Troc)-protecting group cleavage. Treatment of propargyl acetate **I-88** with chiral gold catalyst **I-89** induced the key [3,3] sigmatropic rearrangement, forming transient allene **I-91** that underwent a transannular hydroalkoxylation to access compound **I-92**. The success of this cyclization cascade hinged on the [3,3] sigmatropic rearrangement proceeding more rapidly than the attack of the C11–OH onto the resulting allenyl acetate species. Furthermore, the ether formed at the allenyl position distal to the acetoxy (OAc) group, ensuring that a six-membered ring product formed as opposed to an eight-membered ring. Elaboration of the *cis*-disubstituted THF ring compound **I-92** proceeded via methanolysis of the acetate, ketone reduction using NaBH₄, installation of a fluorenylmethoxycarbonyl (FmO)-protected phosphate group, and a final global deprotection of

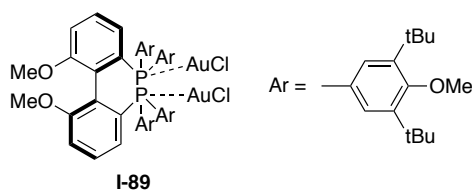
both the FmO and silyl ether protecting groups using TBAF/acetic acid (HOAc) to yield enigmazole A (**I-93**).

Scheme 1.9 Total synthesis of enigmazole A.

a. Total synthesis of enigmazole A.



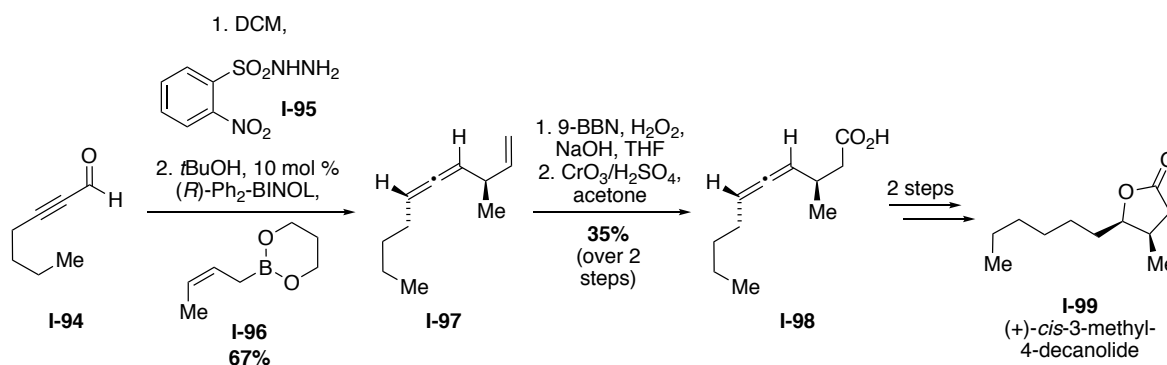
b. Structure of gold catalyst **I-89**.



1.4.3 Formal synthesis of (+)-*cis*-3-methyl-4-decanolide.

In 2017, Thomson, Schaus, and coworkers published a formal synthesis of (+)-*cis*-3-methyl-4-decanolide, featuring the stereoselective construction of chiral allene intermediate **I-97** via a “traceless” Petasis reaction (Scheme 1.10, see Chapter 2 for a detailed discussion of this transformation).³⁹ Treating alkynyl aldehyde **I-94** with 2-nitrobenzenesulfonylhydrazide (NBSH) (**I-95**), followed by addition of allyl boronate **I-96** in the presence of a chiral 1,1'-bi-2-naphthol (BINOL) catalyst afforded chiral allene **I-97**, with a 98:2 er and 20:1 dr. Hydroboration-oxidation using 9-borabicyclo(3.3.1)nonane (9-BBN), and subsequent Jone's oxidation yielded carboxylate intermediate **I-98**. Carboxylic acid **I-98** was previously converted into (+)-*cis*-3-methyl-4-decanolide (**I-99**) by the Ma group,⁴⁰ utilizing a key Cs₂CO₃-catalyzed stereoselective iodolactonization reaction. This electrophilic *anti* cyclization proceeded with complete axial chirality transfer to provide the natural product in 66% yield over two steps.

Scheme 1.10 Formal synthesis of (+)-*cis*-3-methyl-4-decanolide.

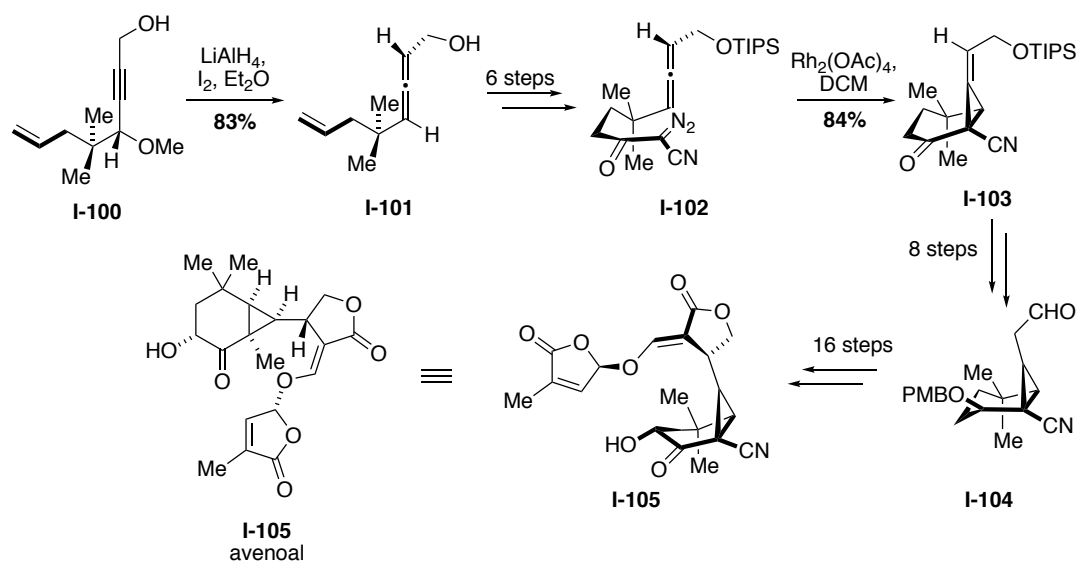


1.4.4 Total synthesis of avenoal.

In 2017, Takemoto and coworkers published the total synthesis of avenoal via a rhodium-catalyzed intramolecular allene cyclopropanation to access key *cis*-alkyldenecyclopropane **I-103** (Scheme 1.11).⁴¹ This marks the first report of stereoselective allene cyclopropanation to form a

six-membered carbocycle. Allenyl precursor **I-102** was accessed from alkyne **I-100**, beginning with a LiAlH_4 -mediated hydroalumination followed by introduction of I_2 to form allene **I-101**. Six additional steps furnished α -diazo- β -ketonitrile cycloaddition precursor **I-102**. Intramolecular allene cyclopropanation proceeded smoothly upon treatment with rhodium(II) acetate ($\text{Rh}_2(\text{OAc})_4$), and the desired alkylidenecyclopropane **I-103** was obtained in 84% yield. Electrophilicity of the Rh-carbene contributed to the exceptionally high conversion, while approach of the Rh species from the less-hindered allene face ensured formation of only the *E* isomer. Intermediate **I-103** was elaborated into all-cis-substituted cyclopropane intermediate **I-104** in eight steps, and the final structure of avenoal (**I-105**) was accessed following an additional sixteen transformations.

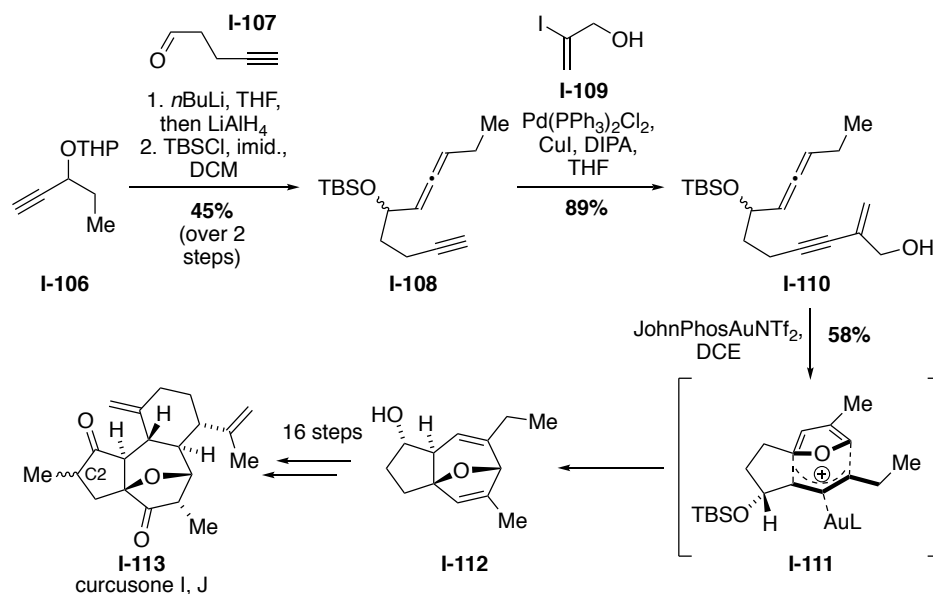
Scheme 1.11 Total synthesis of avenoal.



1.4.5 Total synthesis of curcusones I and J.

In 2017, Dai and coworkers published the total synthesis of stereoisomers curcusone I and J using a tandem gold-catalyzed furan formation and furan-allene [4+3] cycloaddition to access the 5,7-fused ring system in **I-112** (Scheme **1.12**).⁴² The Dai group previously developed this combinatorial cycloaddition cascade, wherein Au-catalyst-activation of an enyne promotes cyclization to a hydrofuran, which then isomerizes to a furan that undergoes [4+3] cycloaddition with an Au-activated allene.⁴³ Optimization of the gold catalysis system ensured that the alkyne was activated first (in the presence of a reactive allene), and that the furan formation and [4+3] cycloaddition occurred prior to any other unwanted cycloisomerization reactions.⁴³ Towards, curcusones I and J, key enyne intermediate **I-110** was accessed beginning from known alkynes **I-106** and **I-107**. Addition of the lithium acetylide of **I-106** to aldehyde **I-107**, followed by LiAlH₄ reduction and TBS protection afforded allene **I-108**. Sonogashira cross-coupling between allene **I-108** and vinyl iodide **I-109** provided the tandem cyclization precursor **I-110**. Utilizing a JohnPhos gold-catalyst system, enyne alcohol **I-110** underwent a *5-endo-dig* cyclization to form a dihydrofuran intermediate, which then isomerized to a furan ring that underwent the key Au-cat. [4+3] cycloaddition via the transition state **I-111**. The stereochemical outcome of the [4+3] addition was controlled by the TBS-protected 2° alcohol, which oriented itself away from the bulky Au-complex. Tricyclic product **I-112** was then converted into either curcusone I or J (**I-113**) (epimeric at the C2 position) in an additional sixteen steps.

Scheme 1.12 Total synthesis of curcusone I and J.

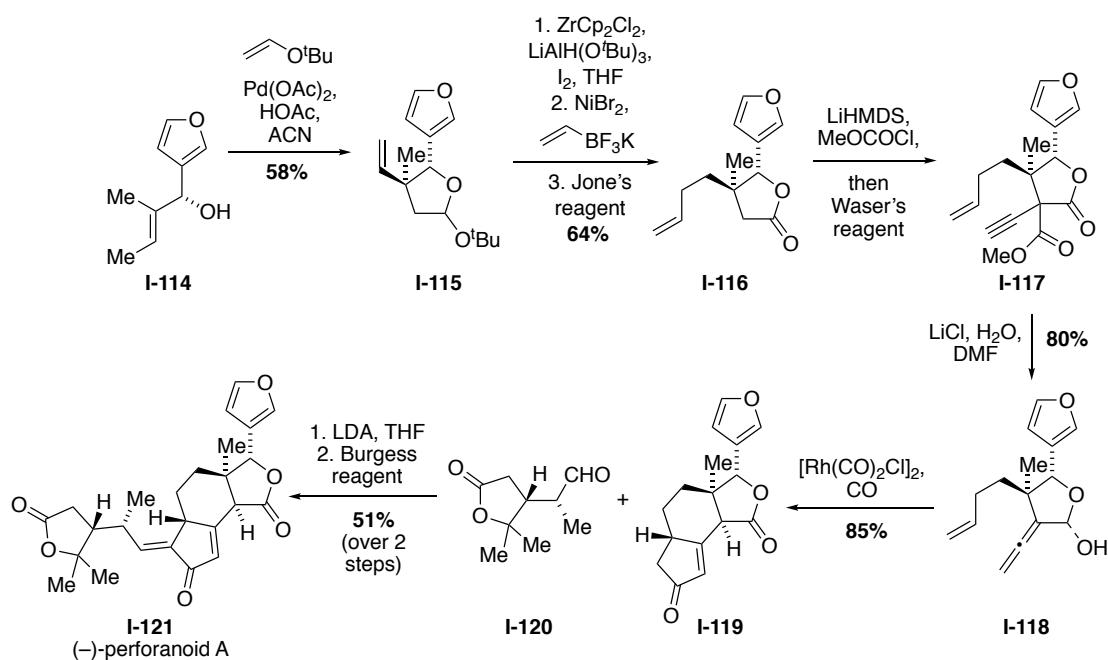


1.4.6 Total synthesis of (–)-perforanoid A.

In 2017, Yang and coworkers published the total synthesis of (–)-perforanoid A via an intramolecular Pauson-Khand (IMPK) reaction between an allene and alkene (Scheme 1.13).⁴⁴ This [2+2+1] IMPK variant relied on the cycloaddition between an alkene π -bond, a distal allene π -bond, and CO – the feasibility of this type of allenene IMPK was first exhibited by the Mukai group in 2006.⁴⁵ Preferential selectivity at the terminal bond of the allene in IMPK reactions is controlled by tuning the reaction conditions, with Rh(I) specifically promoting the regiocontrolled formation of target cyclic products.⁴⁶ Here, the IMPK allenene precursor **I-118** was accessed beginning from compound **I-114**, which underwent a palladium-catalyzed Oshima-Utimoto reaction with allylic alcohol to form furan **I-115**. Sequential iodination, metal-catalyzed cross-coupling, and Jone's oxidation provided compound **I-116**, which then underwent treatment with lithium bis(trimethylsilyl) amide (LiHMDS) and methyl carbonochloridate, followed by

acetylation using Waser's reagent to access enyne **I-117**. Enyne **I-117** was converted into allenene IMPK precursor **I-118** following treatment with LiCl in H₂O/dimethylformamide (DMF). Using a modified procedure developed by Mukai and coworkers⁴⁵ for Pauson-Khand reactions of allenenes, intermediate **I-118** was treated with [Rh(CO)₂Cl]₂ to access the IMPK product **I-119** in 68% yield. To complete the total synthesis of (–)-perforanoid A, enone **I-119** was treated with lithium diisopropylamide (LDA) and compound **I-120** (prepared in 8 steps from 5-methyl-2-furanone) to afford an aldol product that underwent a final dehydration using Burgess reagent to access (–)-perforanoid A (**I-121**) in 51% yield over 2 steps.

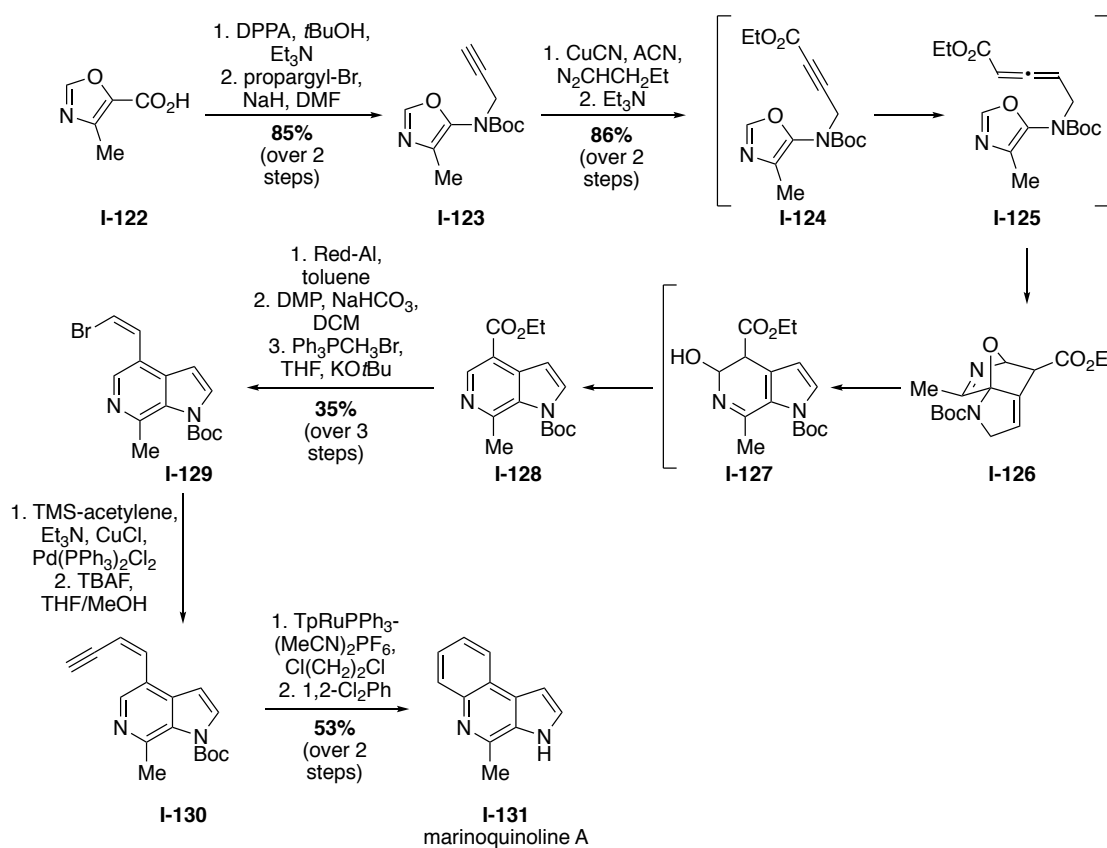
Scheme 1.13 Total synthesis of (–)-perforanoid A.



1.4.7 Total synthesis of marinoquinoline A.

In 2020, Wipf and coworkers accessed marinoquinoline A via a Cu-catalyzed intramolecular Diels-Alder oxazole (IMDAO) cycloaddition into an allenolate, exhibiting the first application of this Diels-Alder (DA) variant to access a 6-azaindole scaffold (Scheme 1.14).⁴⁷ The Wipf group previously developed an intramolecular DA furan cycloaddition reaction, and in this expansion of their methodology, a disubstituted allenyl oxazole undergoes a [4+2] reaction proceeding through a bridged bicyclic intermediate (**I-126**) followed by a partially eliminated pyrrole (**I-127**) to ultimately access the desired 6-azaindole **I-128**. To construct the key allenolate intermediate **I-125**, oxazole **I-122** was first converted into alkynyl species **I-123** via a Curtius rearrangement and subsequent *N*-alkylation with propargyl bromide. Copper-catalyzed C–H bond insertion into the terminal alkyne provided transient ethyl ester intermediate **I-124**, which then isomerized to the desired allenolate **I-125** and underwent a spontaneous IMDAO to afford 6-azaindole **I-128**. To complete the synthesis, a reduction/oxidation/Wittig series was carried out to convert 6-azaindole **I-128** into intermediate **I-129**, which then underwent Sonogashira coupling with trimethylsilyl (TMS)-acetylene and a TBAF-mediated desilylation to afford precursor **I-130**. A final ruthenium catalyzed benzannulation and Boc-deprotection provided marinoquinoline A (**I-131**) in 53% yield over two steps.

Scheme 1.14 Total synthesis of marinoquinoline A.



1.5 Conclusions.

Allenes are highly reactive and versatile chemical scaffolds, and their propensity undergo a diverse set of reactions makes these structures particularly useful in constructing complex natural products. This review has highlighted the use of intramolecular allene cyclization reactions towards recent total syntheses, with a variety of cycloaddition/cycloisomerization transformations summarized. Chapter 2 will thus discuss the Thomson lab's application of a stereocontrolled allene cyclization reaction en route to the natural product solamin.

Chapter 2

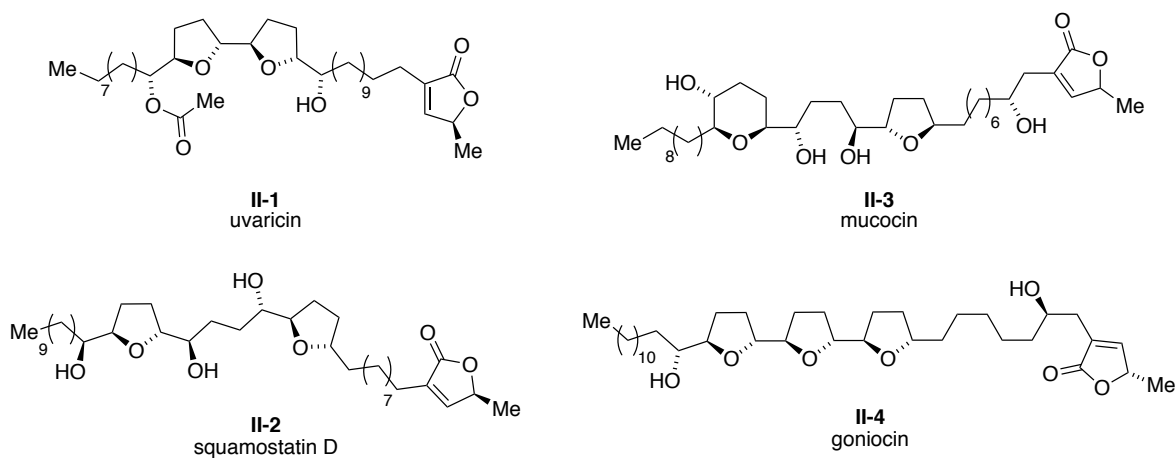
Total Synthesis of the Solamin Stereoisomers
via a “Traceless” Petasis Reaction

2 Chapter 2

2.1 Introduction.

The Annonaceous acetogenins (ACGs) are a class of natural products (NPs) isolated from tropical and sub-tropical *Annonaceae* shrubs,¹ with over 400 acetogenins isolated since the seminal discovery of uvaricin (**II-1**) in 1982.² ACGs are characterized by a C35 or C37 fatty acid skeleton, a stereodefined tetrahydrofuran (THF) core, terminal γ -lactone group, and oxygenated moieties (e.g. hydroxyls, ketones, epoxides, tetrahydropyrans, etc.) installed along the aliphatic backbone. ACGs are classified based on the number of THF rings incorporated into their structure, and ACG NPs with mono-THF, adjacent bis-THF, non-adjacent bis-THF, and tri-THF moieties have all been identified (Figure 2.1).^{1, 3-11} Of particular interest are the solamin stereoisomers (Figure 2.2), a family of mono-THF ACGs isolated from the seeds of *Annona muricata*.^{4,12-14} These compounds exhibit potent anticancer activity,^{15,16} and thus gaining access to their stereocomplex structures has become an attractive goal for many total syntheses.

Figure 2.1 Structures of ACG NPs.



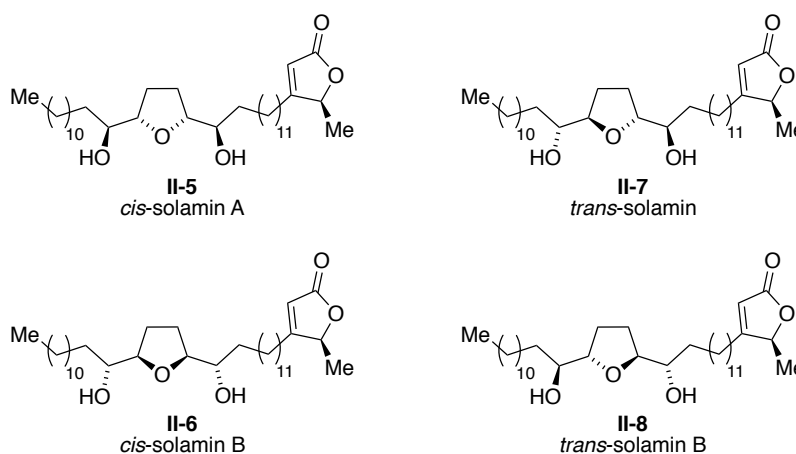
This chapter outlines efforts towards the enantioselective total syntheses of the solamin stereoisomers, utilizing methodology developed by the Thomson and Schaus groups for constructing chiral allenols.¹⁷⁻²⁰ In this method, a “traceless” Petasis reaction is used to access chiral allenes that are capable of undergoing intramolecular cyclization reactions to provide stereodefined 2,5-dihydrofuran solamin precursors (for a detailed review on recent intramolecular allene cyclizations in total syntheses, see Chapter 1). Current progress towards the total synthesis of *cis*-solamin A and B will be discussed, including a revised strategy towards accessing the NPs. Future directions will also be outlined, with an emphasis on route optimization and alternative applications of chiral allenols towards the solamin stereoisomers.

2.2 Discovery and structural elucidation of the solamin stereoisomers.

Solamin was first discovered in 1991 by the Cortes group from the seeds of *Annona muricata*.¹² Structural elucidation identified natural “solamin” as a C35 α, α -dihydroxylated mono-THF compound, with an α, β -unsaturated methyl γ -lactone moiety appended at the end of a fatty carbon chain. The stereochemical configuration about the THF core was not assigned at the time of discovery, but was later confirmed as the *threo-trans-threo* structure **II-7** shown in Figure 2.2.²¹ Natural *threo-trans-threo* solamin is henceforth referred to as *trans*-solamin. In 1998, Gleye and coworkers outlined the discovery of naturally isolated “*cis*-solamin,” a member of the solamin family with a *threo-cis-threo* relationship about the THF core.¹³ The structure of “*cis*-solamin” was further characterized in an account published by the Brown group in 2006, following the discovery that naturally isolated “*cis*-solamin” in fact contained a tetra-epimeric mixture of diastereomeric compounds **II-5** and **II-6**, termed *cis*-solamin A and *cis*-solamin B, respectively.¹⁴ Thus, current literature on the solamin stereoisomers refers to the three structures – *trans*-solamin

(**II-7**), *cis*-solamin A (**II-5**), and *cis*-solamin B (**II-6**) – shown in Figure 2.2. To our knowledge, the diastereomeric partner to *trans*-solamin, herein coined *trans*-solamin B (**II-8**), has not been observed or isolated naturally.

Figure 2.2 Solamin stereoisomers.



2.3 Biological activity of the solamin stereoisomers.

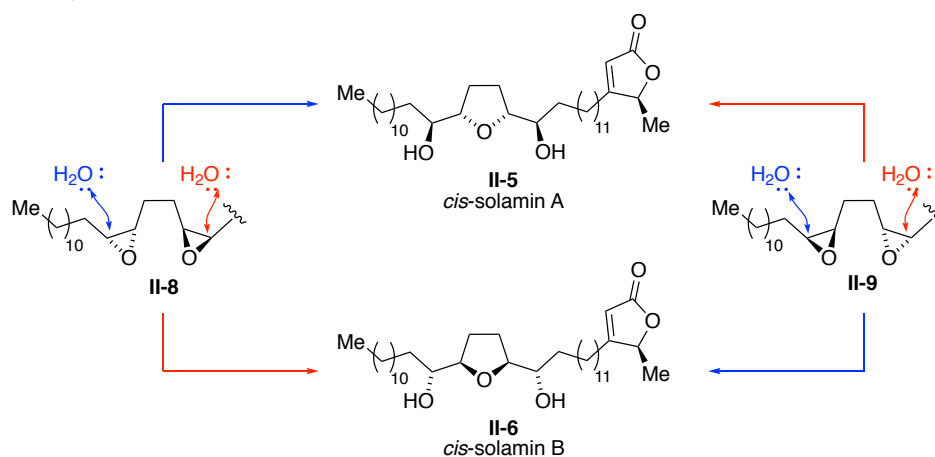
All isolated members of the solamin family exhibit cytotoxicity against mitochondrial complex I, the largest complex in the mitochondrial electron transport chain and the main gate of energy production in the cell.¹⁵ Complex I plays an essential role in biosynthesis and redox during cell growth, and it is thus believed that inhibition of mitochondrial complex I can control proliferation and metastasis of cancer cells.²² Cytotoxicity screening for the solamin stereoisomers against several tumor cell lines have revealed inhibitory potentials of 3.9 nM,¹⁵ 2.2 nM, and 2.1 nM¹⁶ for *trans*-, *cis*-A, and *cis*-B solamin respectively. Structure–activity relationship studies have suggested that the hydroxyl groups along the aliphatic backbone of the solamin stereoisomers are responsible for much of their observed cytotoxicity.¹⁵ Given their nanomolar levels of inhibition, the solamin stereoisomers have become popular targets for total syntheses aimed at improving access to these compounds.

2.4 Biosynthesis of the solamin stereoisomers.

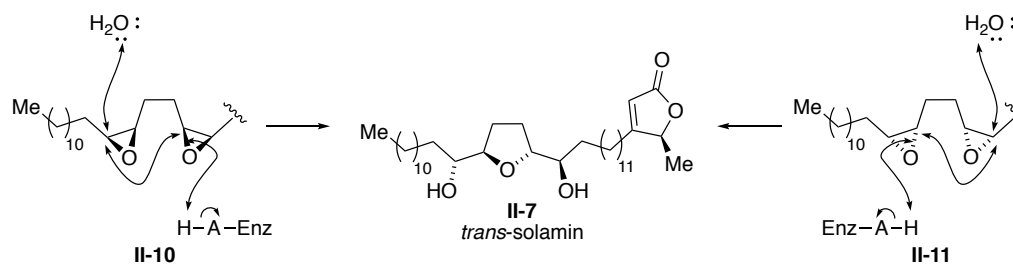
The solamin stereoisomers are believed to share a common biosynthetic pathway, each branching from an enzyme-catalyzed cyclohydration of a bis-epoxide diepomuricanin stereoisomer (Scheme 2.1).¹⁴ The putative precursor of the diepomuricanin isomers, 1,5-diene muricadienin, is postulated to undergo epoxidation to form four possible diepoxide intermediates (**II-8**, **II-9**, **II-10**, and **II-11**).²³ Subsequent activation of either epoxide in the pseudo-*C*₂-symmetrical anti-diepomuricanin A2 core (**II-8** or **II-9**) would lead to either *cis*-A (**II-5**) or *cis*-B (**II-6**) solamin. Alternatively, a similar cyclization of the pseudo-*meso* syn-diepomuricanin A1 core (**II-10** or **II-11**) would lead to *trans*-solamin (**II-7**).¹⁴

Scheme 2.1 Putative biosynthetic pathway towards the solamin stereoisomers.

a. Proposed biosynthesis of *cis*-solamin A and B.



b. Proposed biosynthesis of *trans*-solamin.



2.5 Previous syntheses of the solamin stereoisomers.

Since the first reported synthesis in 1993 by Sinha and coworkers,¹⁰ many total syntheses on the solamin stereoisomers have been published, featuring convergent, linear, and biomimetic strategies that incorporate a variety of asymmetric reactions (Sharpless asymmetric epoxidation/dihydroxylation, diastereoselective Williamson etherification, etc) to access these stereocomplex molecules.^{1, 7, 8, 24} Unfortunately, the literature on these molecules is complicated by initial misnomers of the solamin stereoisomers at the time of their discoveries (see Section 2.2 for a more detailed account of discovery). *Trans*-solamin, discovered in 1991,¹² was simply referred to as “solamin” until the discovery of natural “*cis*-solamin” in 1998¹³ indicated that multiple stereoisomers of this NP existed. Furthermore, it was found by the Brown group in 2006¹⁴ that natural “*cis*-solamin” in fact contained a mixture of *cis*-solamin A and B. Because of these misidentifications, total syntheses published between 1993 and 2006 often mistakenly refer to the target generally as “solamin” or “*cis*-solamin,” when in fact a more specific stereoisomer is being accessed. In the following sections, distinction will be made between the nominal solamin stereoisomer being targeted and the actual molecule, whether *trans*-, *cis*-A, or *cis*-B, as indicated by the absolute stereochemistry reported by the author. Work published from 2006 forward reliably reports the correct stereoisomer name/structure pairing.

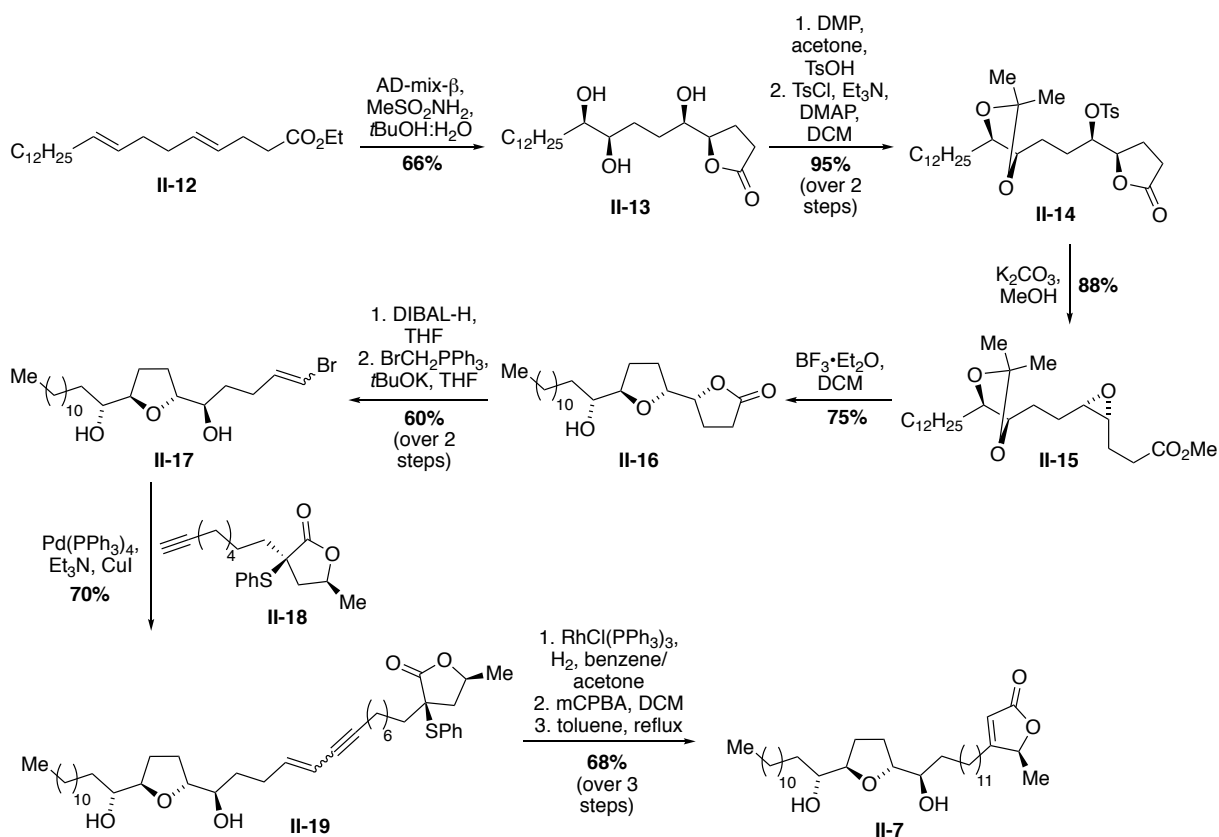
2.5.1 Total syntheses of *trans*-solamin.

2.5.1.1 Total synthesis of *trans*-solamin by Sinha, et al.

The Sinha group published the first total synthesis of *trans*-solamin in 1993 (although here referred to as “solamin”) utilizing a Sharpless asymmetric dihydroxylation strategy to construct the key *threo-trans-threo* relationship about the THF core (Scheme 2.2).¹⁰ They envisioned first

converting appropriately substituted (*E, E*)-1,5-diene **II-12** into the requisite *threo, threo* tetraol **II-13**, and then using a strategy of double inversion for two of the four stereocenters in order to access the appropriate configuration about the THF ring. Diene **II-12** was treated with commercially available AD-mix- β to afford lactone **II-13**, which was then protected as the acetonide and converted into tosylate **II-14**. Formation of epoxide **II-14** following treatment with K_2CO_3 was followed by an acid-catalyzed acetonide deprotection with $BF_3 \cdot Et_2O$ simultaneously opened the epoxide and induced lactonization, providing substituted THF **II-16** with the desired *threo-trans-threo* conformation. To complete the synthesis, compound **II-16** was reduced and subjected to a Wittig reaction to access bromoalkene **II-17**, which then underwent Pd-catalyzed cross-coupling to provide enyne **II-19**. Hydrogenation with Wilkinson's catalyst, *meta*-

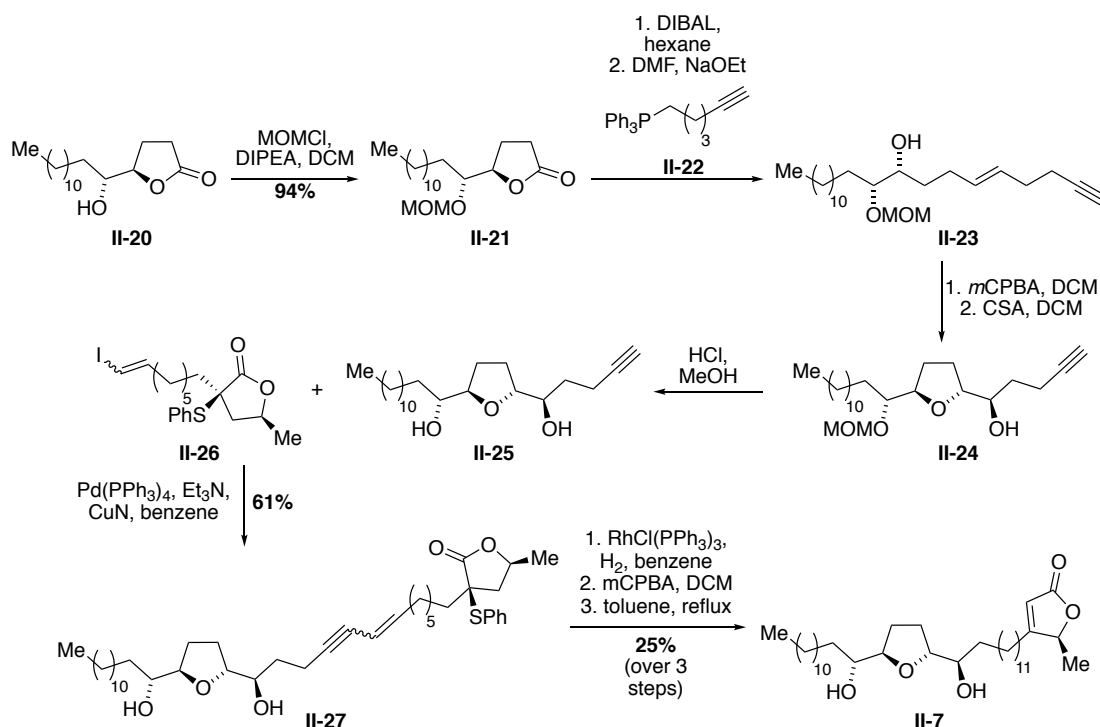
Scheme 2.2 Total synthesis of *trans*-solamin by Sinha, et al.



chloroperoxybenzoic acid- (*m*CPBA) mediated oxidation to the sulfoxide, and a thermal elimination to yield *trans*-solamin (**II-7**) as the final product.

2.5.1.2 Total synthesis of *trans*-solamin by Makabe, et al.

The Makabe group published a total synthesis of *trans*-solamin in 1994 (again, referred to as “solamin” in the original publication), beginning from solamin biosynthetic precursor (–)-muricatacin (Scheme 2.3).²⁵ Makabe and coworkers previously published a method to access (–)-muricatacin (**II-20**) in an enantiopure fashion.²⁶ The methoxymethyl ether- (MOM) protected muricatacin **II-21** was reduced with diisobutylaluminum hydride (DIBAL), and the subsequent hemiacetal was subjected to a Wittig reaction with alkyne **II-22** to form acyclic compound **II-23**. Epoxidation with *m*CPBA, followed by an acid-catalyzed cyclization with camphor sulfonic acid (CSA) provided access to the THF intermediate **II-24**. The MOM-protecting group was then removed with HCl/MeOH to give **II-25**. Finally, **II-25** was coupled with **II-26** using a Suzuki–Miyaura cross-coupling reaction (Pd(PPh₃)₄, Et₃N, CuN, benzene) to form **II-27** in 61% yield. **II-27** was then subjected to hydrogenation (1. RhCl(PPh₃)₃, H₂, benzene) and oxidation (2. *m*CPBA, DCM) to form the sulfoxide **II-28**, which was finally eliminated (3. toluene, reflux) to yield *trans*-solamin (**II-7**) in 25% overall yield over three steps.



cleaved using HCl in methanol (MeOH), and the alkynyl intermediate **II-25** underwent Pd-catalyzed cross-coupling with γ -lactone **II-26** (prepared in 10 steps from propargyl alcohol) to provide compound **II-27**. The final route towards *trans*-solamin followed the same procedure outlined by the Sinha group (Section 2.5.1.1), yielding *trans*-solamin (**II-7**) in 3 additional steps.

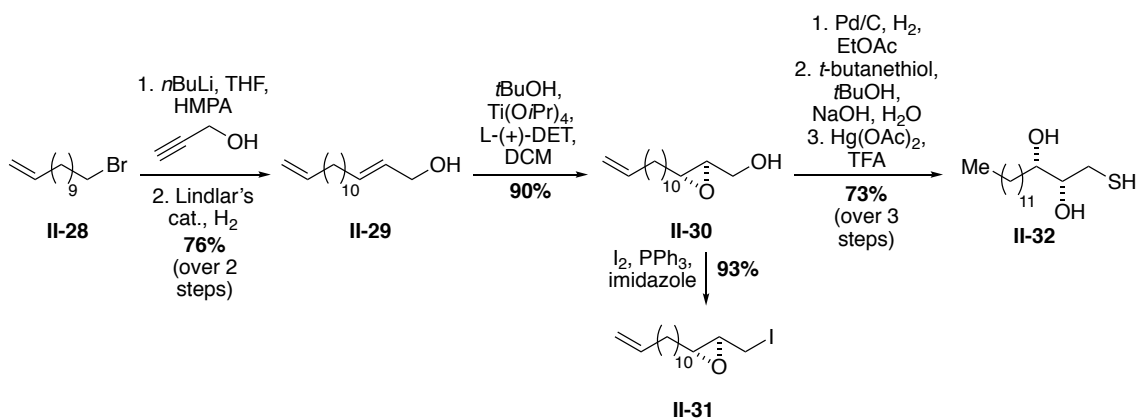
2.5.1.3 Total synthesis of *trans*-solamin by Trost, et al.

Trost and coworkers published a total synthesis towards “(+)-solamin” (later confirmed as *trans*-solamin) in 1994, featuring a convergent Ramberg–Backlund olefination between two intermediate halves to construct the main backbone of *trans*-solamin (Scheme 2.4).¹¹ Additionally, Trost’s method incorporated an unprecedented butenolide annulation for installation of the γ -lactone moiety, a transformation that has since become standard across the literature as an efficient end-game towards all solamin stereoisomers.^{27, 28} A divergent synthesis of the two olefination coupling partners began from 12-bromo-1-dodecene **II-28**, prepared in two steps from commercially available 11-bromo-1-undecanol (Scheme 2.4a). Compound **II-28** was converted into an alkynyl intermediate and reduced to yield precursor **II-29**, which underwent Sharpless asymmetric epoxidation to form key intermediate **II-30**. Epoxide **II-30** was used to access both Ramberg–Backlund olefination partners using a divergent method. Towards intermediate **II-31**, hydroxyepoxide **II-30** was converted into iodoepoxide **II-31** under Appel conditions. Alternatively, hydroxyepoxide **II-30** was reduced, then subjected to a Payne rearrangement and thiolate substitution to yield intermediate **II-32**. A Ramberg–Backlund olefination between the coupling partners **II-32** and **II-31** yielded 1,4-oxathiane intermediate **II-33**, which was then oxidized and subjected to *in situ* chlorination-rearrangement of the resultant sulfone to yield dihydrofuran intermediate **II-34** (Scheme 2.4b). Ruthenium-catalyzed butenolide annulation

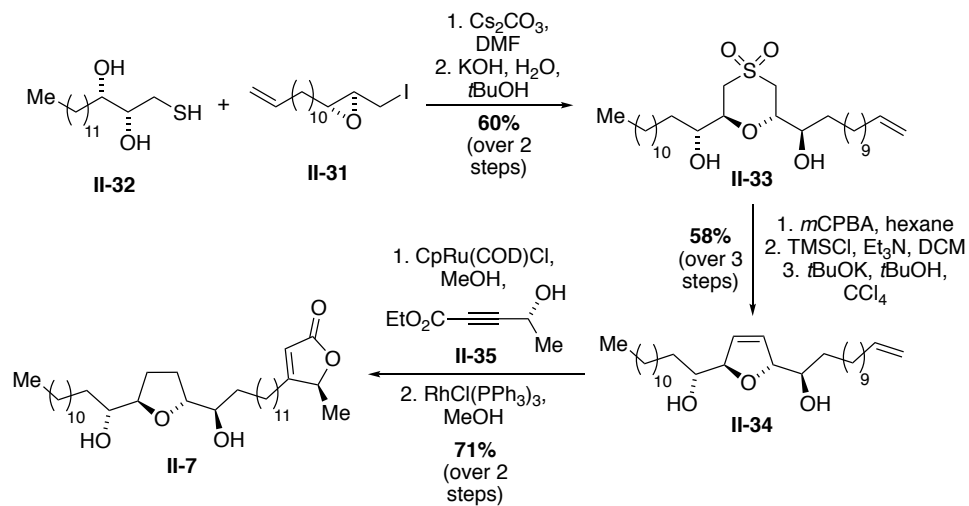
between compound **II-34** and alkyne **II-35** installed the requisite γ -lactone moiety, and a final hydrogenation using Wilkinson's catalyst provided *trans*-solamin (**II-7**).

Scheme 2.4 Total synthesis of *trans*-solamin by Trost, et al.

a. Divergent synthesis of intermediates **II-31** and **II-32**.



b. Total synthesis of *trans*-solamin.

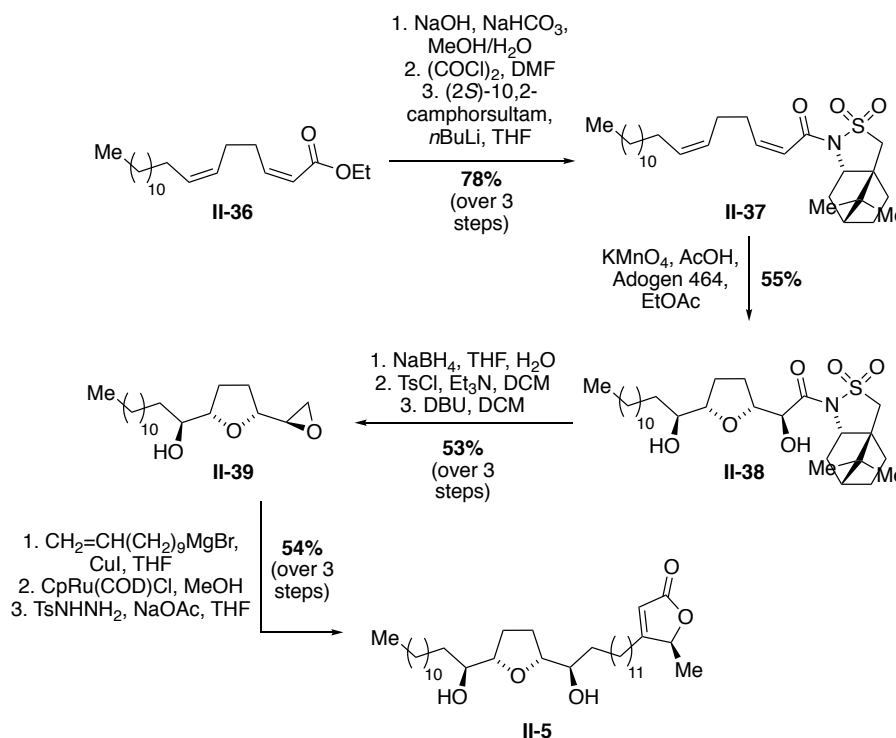


2.5.2 Total syntheses of *cis*-solamin A and B.

2.5.2.1 Total synthesis of *cis*-solamin A by Brown, et al.

In 2002, Brown and coworkers accessed “*cis*-solamin” (in fact, *cis*-solamin A) via a key permanganate-promoted oxidative cyclization of a 1,5-diene precursor (Scheme 2.5).²⁹ Conversion of 1,5-diene **II-36** (prepared in three steps from commercially available aldehyde) into the oxidative cyclization precursor **II-37** began with base-mediated hydrolysis of the ethyl ester, followed by acid chloride formation and reaction with lithiated camphorsultam to form compound **II-37**. Oxidative cyclization proceeded cleanly using KMnO_4 under phase-transfer conditions, providing the stereodefined THF core **II-38**. This cyclization product was subsequently converted into epoxide **II-39** following reductive removal of the auxiliary, and a final series involving a copper-catalyzed Grignard reaction, Trost’s ruthenium catalyzed butenolide annulation, and double bond reduction with Wilkinson’s catalyst provided *cis*-solamin A (**II-5**).

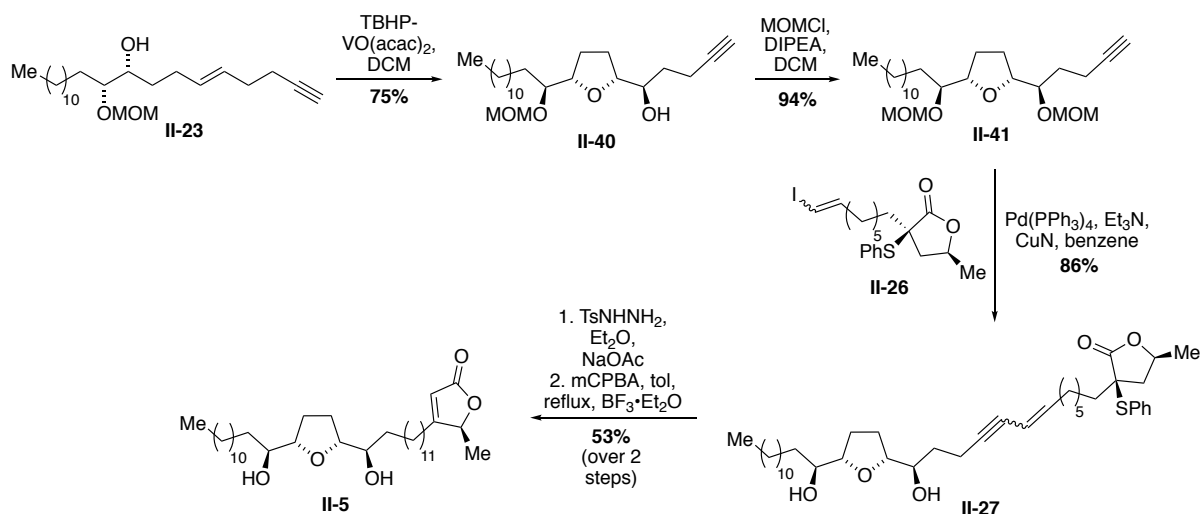
Scheme 2.5 Total synthesis of *cis*-solamin A by Brown, et al.



2.5.2.2 Total synthesis of *cis*-solamin A by Makabe, et al.

In 2004, Makabe and coworkers published a total synthesis of “*cis*-solamin” (in fact, *cis*-solamin A) via a VO(acac)₂ catalytic diastereoselective epoxidation of alcohol **II-23**, followed by spontaneous cyclization to access key THF intermediate **II-40** (Scheme 2.6).^{16, 30} Their synthetic strategy branched from their work towards *trans*-solamin published in 1994 (see Section 2.5.1.2), beginning from (*Z*)-bis-homoallylic alcohol **II-23** which was accessed in three steps from enantiopure muricatacin.²⁵ Treating alcohol **II-23** with 5 mol% VO(acac)₂ in dichloromethane (DCM) initiated the diastereoselective epoxidation/cyclization cascade, affording stereodefined THF intermediate **II-40** in 75% yield. MOM-protection of the free alcohol was followed by palladium-catalyzed cross-coupling with γ -lactone **II-26** (prepared in 10 steps from propargyl alcohol) to provide compound **II-27**. The final route towards *cis*-solamin A followed a similar procedure outlined by the Sinha group (Section 2.5.1.1), yielding *cis*-solamin A (**II-5**) in an additional two steps.

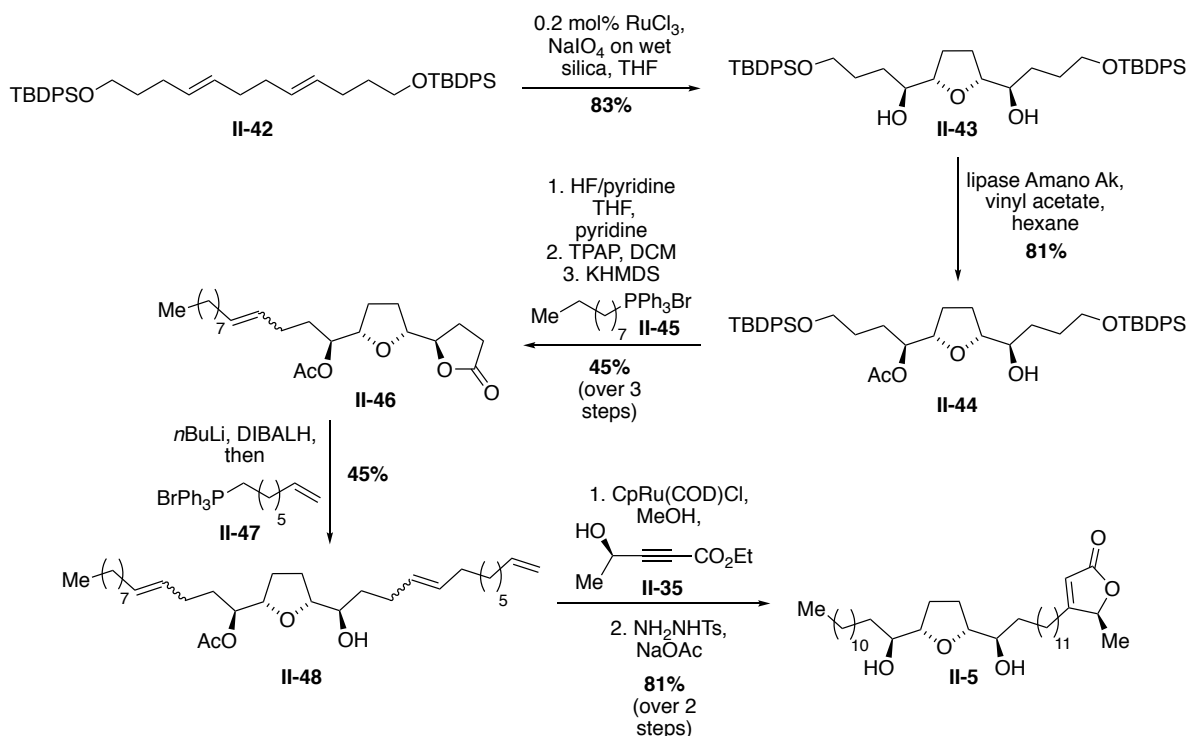
Scheme 2.6 Total synthesis of *cis*-solamin A by Makabe, et al.



2.5.2.3 Total synthesis of *cis*-solamin A by Stark, et al.

Stark and coworkers published the total synthesis of “*cis*-solamin” (here, *cis*-solamin A) in 2006 via a diastereoselective ruthenium tetroxide-catalyzed oxidative cyclization reaction (Scheme 2.7).^{31, 32} Cyclization precursor **II-42** was accessed in four steps beginning from commercially available (*E, E, E*)-1,5,9-cyclododecatriene. Treating linear precursor **II-42** with 0.2 mol % RuCl₃ as a precatalyst for *in situ* generation of ruthenium tetroxide produced cyclized *meso*-diol **II-43** in 83% yield. This stereoselective cyclization proceeded via a double *syn* specific [3+2] cycloaddition, with a conformationally constrained second intramolecular addition process providing THF intermediate **II-43**. Enzymatic desymmetrization of *meso*-diol **II-43** using lipase Amano AK provided tetraol **II-44**, which was subjected to fluoride-induced silyl deprotection and a subsequent one-pot tetrapropylammonium perruthenate (TPAP)-oxidation/Wittig olefination sequence to yield lactone **II-45**. To complete the synthesis, lactone **II-45** was reduced with

Scheme 2.7 Total synthesis of *cis*-solamin A by Stark, et al.



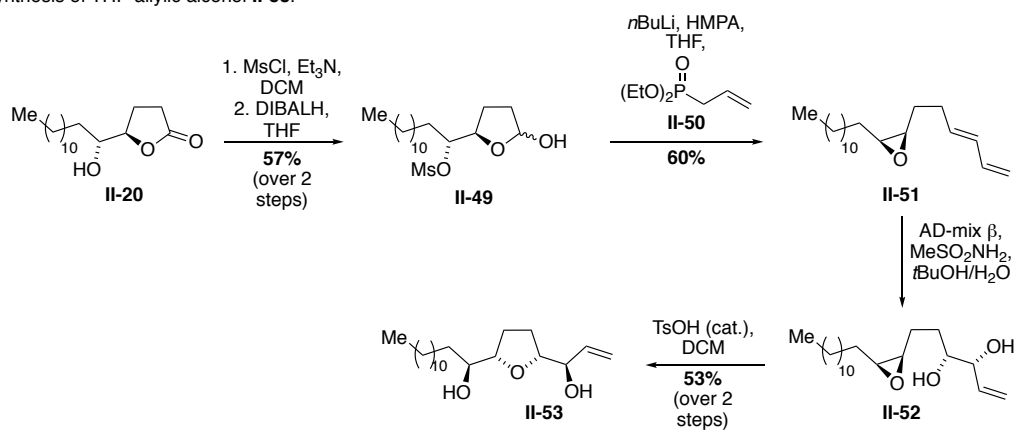
DIBAL, subjected to a second Wittig addition, treated with Trost's butenolide annulation conditions, and finally reduced with diimide to access *cis*-solamin A (**II-5**).

2.5.2.4 Total synthesis of *cis*-solamin A and *cis*-solamin B by Akaji, et al.

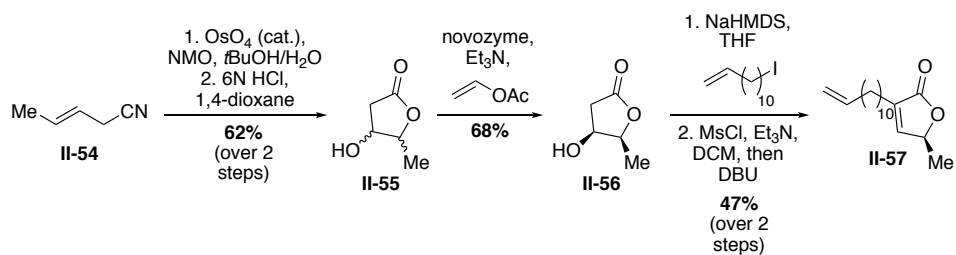
In 2010, the Akaji group published a total synthesis towards both *cis*-solamin A and B that featured a Sharpless asymmetric dihydroxylation to access the THF core, and an olefin cross-metathesis between the THF-allylic alcohol **II-53** and γ -lactone moiety **II-57** (Scheme 2.8). Synthesis began with enantiopure muricatacin (**II-20**), which was subjected to mesylation and DIBAL reduction to provide hemiacetal **II-49** (Scheme 2.8a). Horner–Wadsworth–Emmons olefination and epoxidation with the lithium salt of diethyl allylphosphonate yielded *epoxy-(E)*-diene **II-51**, which was subjected to Sharpless asymmetric hydroxylation and subsequently treated with catalytic *p*-toluenesulfonic acid (*p*TsOH) to access THF-allylic alcohol **II-53**. Preparation of the cross-metathesis partner commenced with 3-pentenenitrile (**II-54**), which was dihydroxylated with OsO₄ followed by acid-mediated lactonization to yield racemic lactone **II-55** (Scheme 2.5b). Lipase-mediated kinetic transesterification provided enantiopure lactone **II-56**, which underwent alkylation with alkyl iodide followed by mesylation/elimination to yield γ -lactone **II-57**. Olefin cross-metathesis between THF **II-53** and γ -lactone **II-57** with Grubbs II catalyst formed precursor **II-58**, and a final diimide-mediated olefin reduction produced *cis*-solamin A (**II-5**). Scheme 2.8c shows the route towards *cis*-solamin A, while *cis*-solamin B was accessed beginning from the opposite enantiomer of muricatacin.³³

Scheme 2.8 Total synthesis of *cis*-solamin A and B by Akaji, et al.

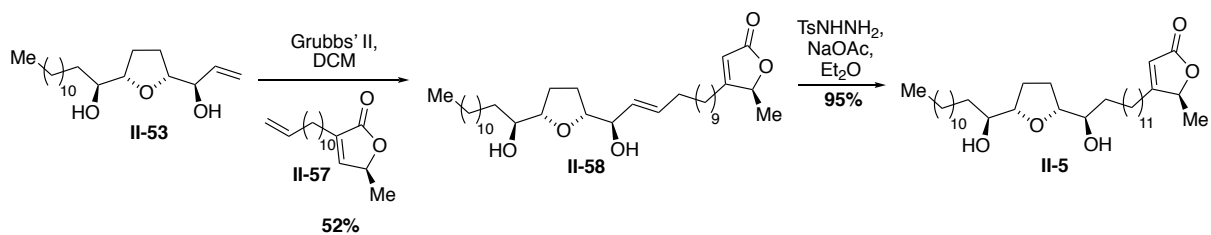
a. Synthesis of THF-allylic alcohol **II-53**.



b. Synthesis of γ -lactone **II-57**.



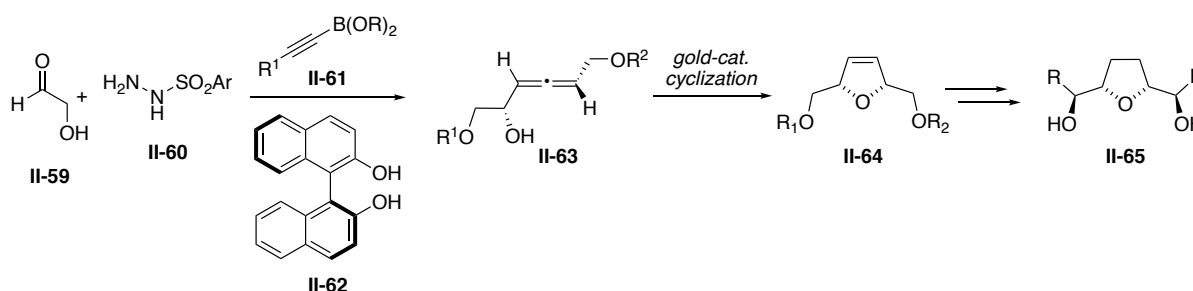
c. Synthesis of *cis*-solamin A.



2.6 This work: Application of a “traceless” Petasis reaction for solamin total synthesis.

Our strategy to access the solamin stereoisomers approaches the construction of the key mono-THF core via a novel application of a “traceless” Petasis reaction, previously developed in collaboration between the Thomson and Schaus groups.¹⁷⁻²⁰ In the remaining sections, this methodology will first be introduced, followed by a discussion of its application to solamin total synthesis. Our general strategy utilizes the traceless Petasis reaction to provide access to a chiral allenol intermediate **II-63** that, upon gold-catalyzed cyclization, forms a stereodefined 2,5-dihydrofuran solamin precursor **II-64** (Scheme 2.9). A detailed explanation of the methodological work towards the key traceless Petasis transformation follows in Section 2.6.1.

Scheme 2.9 General path towards THF-core from chiral allenol.



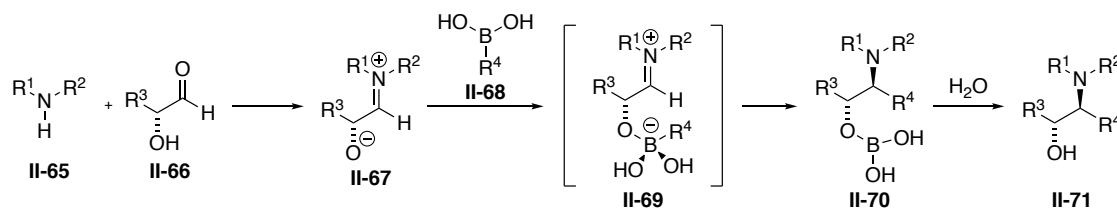
2.6.1 Petasis borono–Mannich reaction.

Development of the traceless Petasis reaction stemmed from an understanding of the Petasis borono–Mannich reaction, established in 1993 by Petasis and coworkers.³⁴ In the multicomponent Petasis borono–Mannich reaction, substituted amines are accessed via a combination of a primary (1°) or secondary (2°) amine, an aldehyde, and a boronic acid (Scheme 2.10a).³⁴ Mechanistically, an imine or iminium ion (**II-67**) forms following aldehyde condensation with a 1° or 2° amine (**II-65**), respectively. The C–N double bond then reacts with a boronic acid

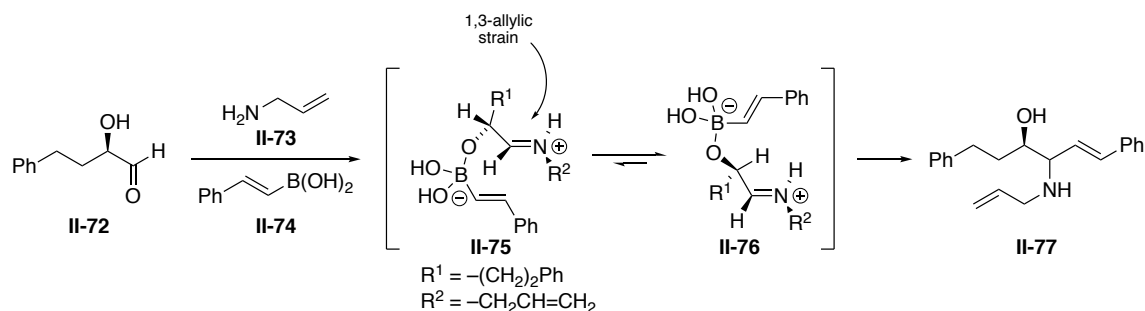
(**II-68**), proceeding through a tetrahedral boronate salt intermediate – termed the “ate” species (**II-69**). The formation and stability of this “ate” intermediate is promoted by coordination between an adjacent hydroxyl group on the imine/iminium cation. Stereocontrol arises from the geometrical constraints of the “ate” complex. For example, in reports by Pyne and coworkers using vinyl boronic acids (**II-74**),^{35, 36} the diastereocontrol arose from the (*E*) “ate”-complex (**II-76**) conformation where A1,3 strain was minimized (Scheme **2.10b**).³⁷ Enantioselective variations of the Petasis borono–Mannich reaction have since been optimized, with asymmetric induction controlled by chiral amine starting materials,^{34, 38-44} enantiopure or enantioenriched boronic esters,^{45, 46} or chiral ligands that complex with the boronic ester to form diastereomeric transition states.⁴⁷⁻⁵⁰

Scheme 2.10 Petasis borono-Mannich reaction development and stereocontrol.

a. Petasis borono-Mannich reaction.



b. Stereochemical control of chiral “ate” species.

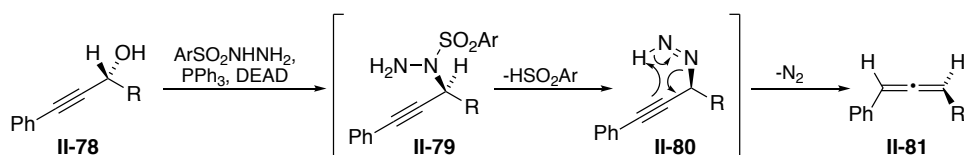


2.6.2 “Traceless” Petasis reaction inspired by Myer’s allene synthesis.

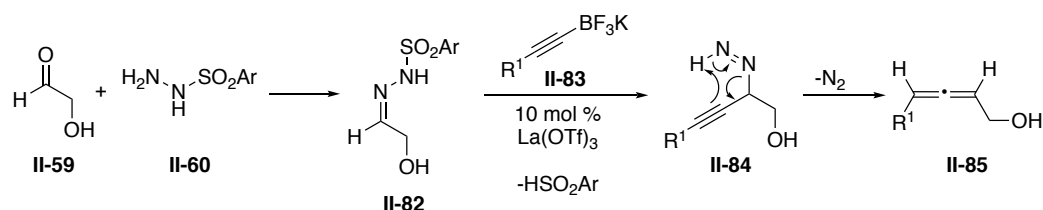
In 2012, Thomson and coworkers published a modification of the original Petasis borono–Mannich reaction, termed a “traceless” Petasis reaction.²⁰ In this work, a sulfonylhydrazine component (**II-60**) was used instead of the traditional 1° or 2° amine, resulting in the formation of an allenyl product **II-85** (vs. a substituted amine) (Scheme 2.11). This Petasis variant was inspired by a series of publications from the Myer’s group, in which allenes were synthesized via a retro-ene reaction of a sulfonylhydrazide intermediate **II-79** generated from a propargylic alcohol **II-78** (Scheme 2.11a).⁵¹⁻⁵⁴ In Myer’s work, the sulfonamide in an arene sulfonylhydrazine acted as the nucleophile in a Mitsunobu inversion reaction of a propargyl alcohol, forming a propargyl diazene **II-79** that underwent loss of N₂ via a sigmatropic elimination process (or, retro-ene reaction, **II-80**) to provide an allene (**II-81**). The Thomson group thus envisioned applying the Myer’s allene synthesis to the Petasis borono–Mannich reaction, utilizing an arene sulfonylhydrazide (**II-60**) and an alkynyl boronate (**II-61**) to construct a chiral allene in this traceless Petasis reaction. In initial studies towards this transformation, it was found that insertion of an alkynyl trifluoroborate salt **II-83** into a sulfonylhydrazone **II-82**, catalyzed by Lewis acid La(OTf)₃, formed a propargylic hydrazide species that then underwent subsequent fragmentation and loss of sulfinic acid to form desired propargylic diazene compound **II-84** (Scheme 2.11b). A final retro-ene decomposition of diazene **II-84** provided the desired allenol **II-85** as a 2:1 mixture of diastereomers.

Scheme 2.11 Myer's allene synthesis and traceless Petasis reaction development.

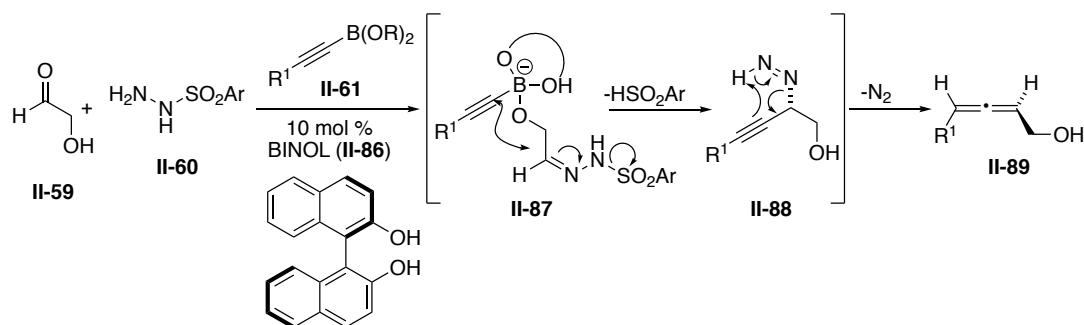
a. Myer's allene synthesis



b. $\text{La}(\text{OTf})_3$ -Catalyzed traceless Petasis reaction



c. Enantioselective traceless Petasis reaction

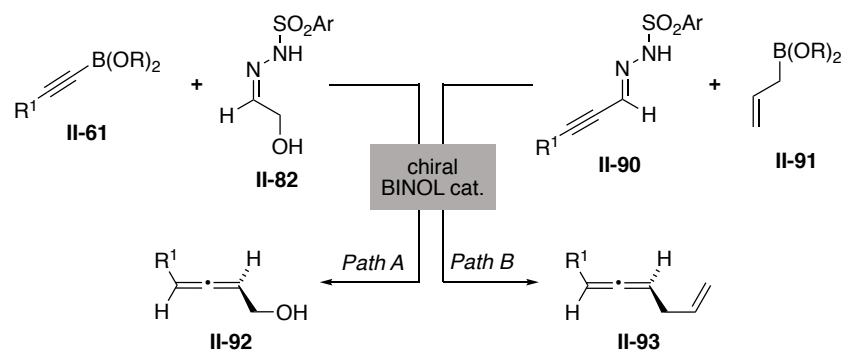


Aiming to improve upon asymmetric control, subsequent work by the Thomson and Schaus labs targeted an enantioselective traceless Petasis reaction that leveraged the known propensity for chiral diols to catalyze regular Petasis reactions with high levels of asymmetric induction.^{18, 19, 47, 49, 50} Here, a chiral 1,1'-bi-2-naphthol (BINOL, **II-86**) catalyst was used to hold the chiral “ate” species (**II-87**) in a desired conformation upon ligand exchange between the BINOL and the boronate, with high levels of enantioinduction (Scheme **2.11c**).¹⁷⁻²⁰ The stereochemistry of the

BINOL catalyst (either (*R*) or (*S*) enantiomers) determined the axial stereochemistry at the allene (**II-89**).

Furthermore, as show in Scheme 2.12, it was found that the enantioselective traceless Petasis reaction could occur either using an alkynyl boronate and aldehyde (**II-61** and **II-82**, Path A) or with an alkynyl aldehyde and an allyl boronate (**II-90** and **II-91**, Path B). In both cases, the retro-ene rearrangement of the “ate” species occurred with complete chirality transfer, forming the desired enantioenriched allene. This methodology was successful for a wide range of substrates en route to enantio- and diastereomerically pure allenols,^{18, 19} and we thus aimed to apply this enantioselective allenol synthesis towards the total synthesis of the solamin stereoisomers.

Scheme 2.12 Possible disconnections for the traceless Petasis reaction.

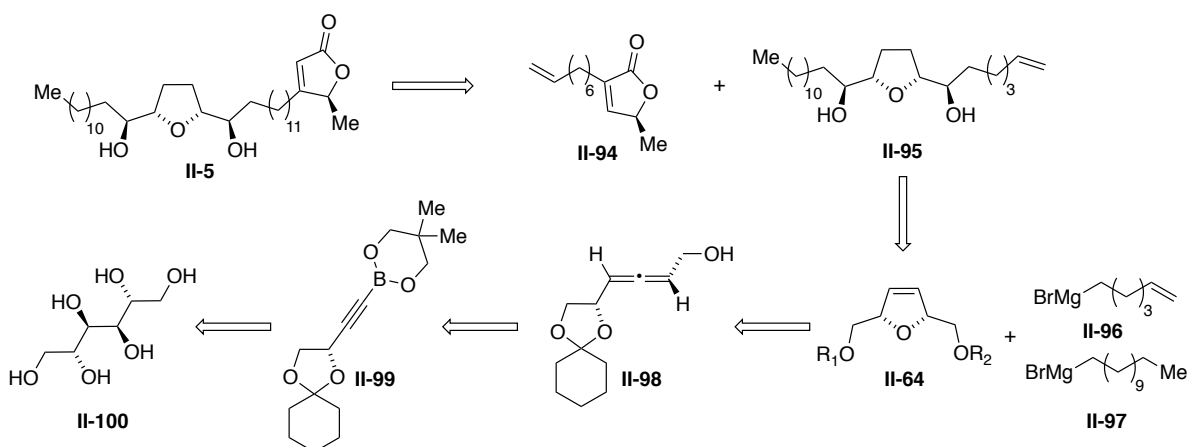


2.7 Synthesis of the solamin stereoisomers.

2.7.1 Retrosynthesis.

Our retrosynthetic approach to synthesizing the solamin stereoisomers is outlined in Scheme 2.13, with the target in this case being *cis*-solamin A (**II-5**). However, our synthetic strategy offers a stereodivergent path that can be leveraged to access all solamin stereoisomers depending on the chirality of the starting materials (see Section 2.7.2). We envisioned accessing *cis*-solamin A (**II-5**) via a Grubbs II-catalyzed cross metathesis between THF **II-95** and lactone **II-94**, inspired by the late-stage work outlined in Akaji's 2010 total synthesis (Section 2.5.2.4). The aliphatic side chains on THF **II-95** would be introduced via chelate-controlled Grignard addition of compounds **II-96** and **II-97** into disparately protected alcohol groups in compound **II-64**. 2,5-Dihydrofuran **II-64** would be constructed following a gold-catalyzed intramolecular cyclization of key chiral allenol **II-98**. To access this stereodefined allenol **II-98**, we planned to apply the aforementioned traceless Petasis reaction.¹⁷⁻²⁰ Disconnection of chiral allenol **II-98** led to alkynyl boronate species **II-99**, which was accessed from readily available D-mannitol (**II-100**) starting material.

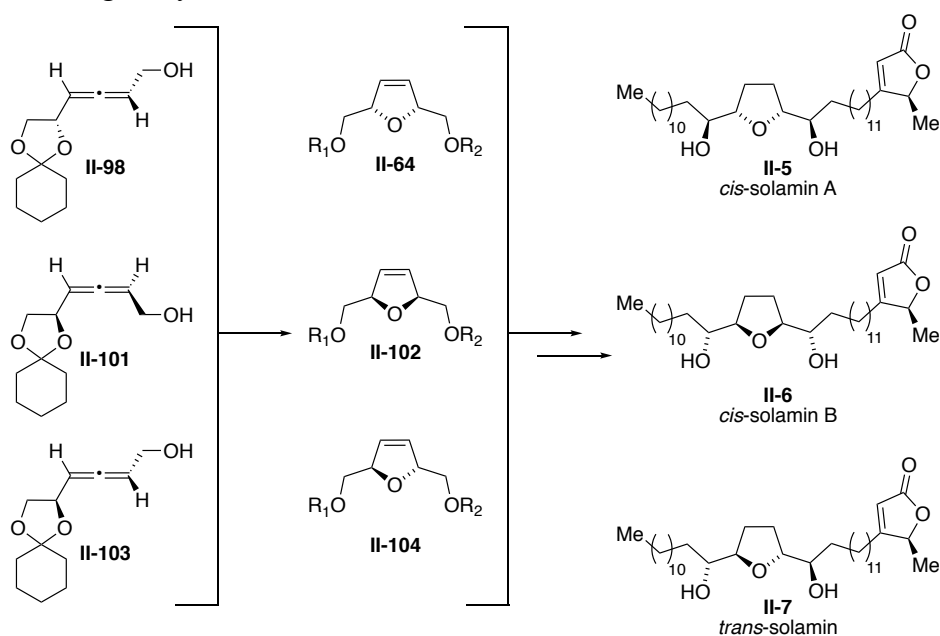
Scheme 2.13 Retrosynthesis towards *cis*-solamin A.



2.7.2 Stereodivergent method to access the solamin stereoisomers.

As shown in the retrosynthesis (Scheme 2.13), our strategy to access the stereodefined THF core of the solamin NP family utilized a gold-catalyzed cyclization of a key chiral allenol intermediate, derived from the multicomponent traceless Petasis reaction. Complete axis-to-center chirality transfer would provide the stereodefined 2,5-dihydrofuran compound **II-64**. As discussed in Section 2.6.2, the axial chirality of the allene was expected to arise from the stereochemistry of the selected BINOL catalyst, with (*R*) or (*S*) BINOL enantiomers providing either an (*R*) (**II-101**) or (*S*) (**II-98**, **II-103**) allene, respectively. Likewise, using enantiopure starting materials to construct the alkynyl boronate (here, either L- or D-mannitol) would install either an (*R*) or (*S*) stereocenter in allenol intermediates **II-98**, **II-101**, and **II-103**. This route thus offered a modular, stereodivergent method towards a chiral allenol intermediate and the desired THF core – matching enantiopure BINOLs with different enantioenriched starting materials would result in access to all the stereoisomers of solamin (Scheme 2.14) (See Appendix 2 for a detailed schematic). As mentioned, initial work targeted *cis*-solamin A given the relative availability of D-mannitol.

Scheme 2.14 Divergent synthesis of the solamin stereoisomers.

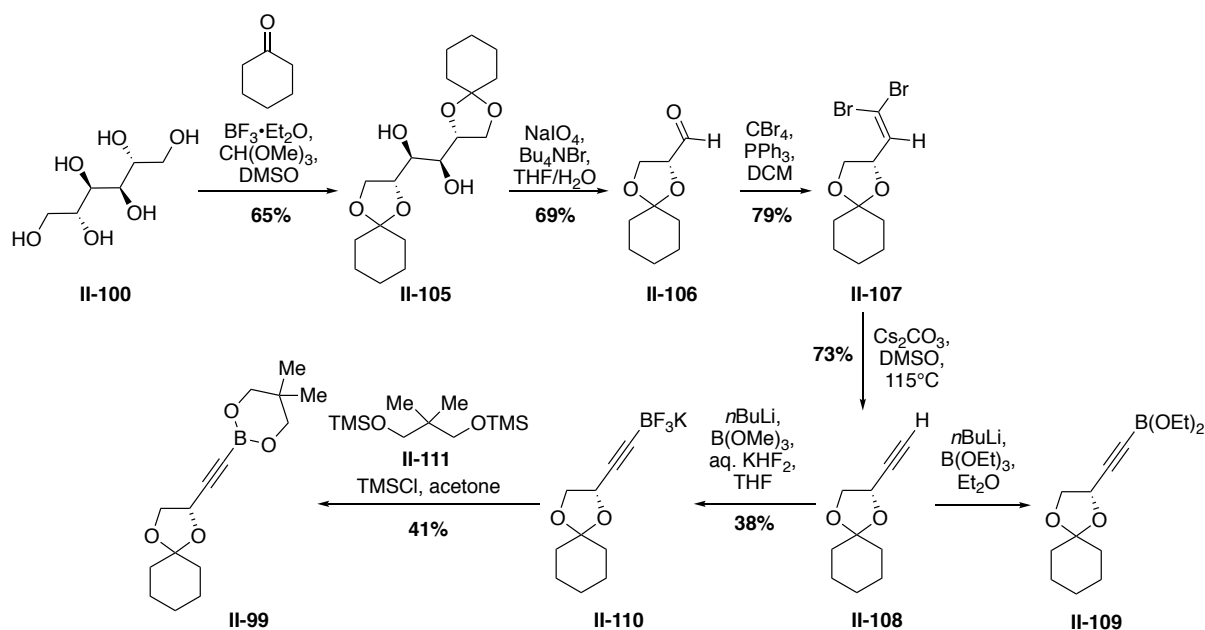


2.7.3 Enantioselective traceless Petasis reaction with D-mannitol-derived alkynyl boronates.

2.7.3.1 Synthesis of D-mannitol-derived alkynyl boronates.

Initial exploration of the proposed traceless Petasis reaction focused on utilizing an alkynyl boronate and aldehyde (Path A, Section 2.6.2, Scheme 2.12) in order to form the desired allenol. A series of alkynyl boronates, were explored, first focusing on those derived from D-mannitol. Treating D-mannitol (**II-100**) with trimethyl orthoformate and cyclohexanone in the presence of $\text{BF}_3 \cdot \text{Et}_2\text{O}$ formed cyclohexylidene acetal **II-105**. It should be noted that the choice of acetal protecting group was critical, with a less-bulky dimethyl acetal protecting group resulting in overall product degradation during subsequent transformations. Oxidative cleavage of cyclohexylidene acetal **II-105** with NaIO_4 provided unstable aldehyde **II-106**, which was immediately converted into alkyne **II-108** via a two-step modified Corey-Fuch's transformation⁵⁵ that proceeded through dibromo-alkene intermediate **II-107**.

Scheme 2.15 Synthesis of D-mannitol-derived alkynyl boronates.



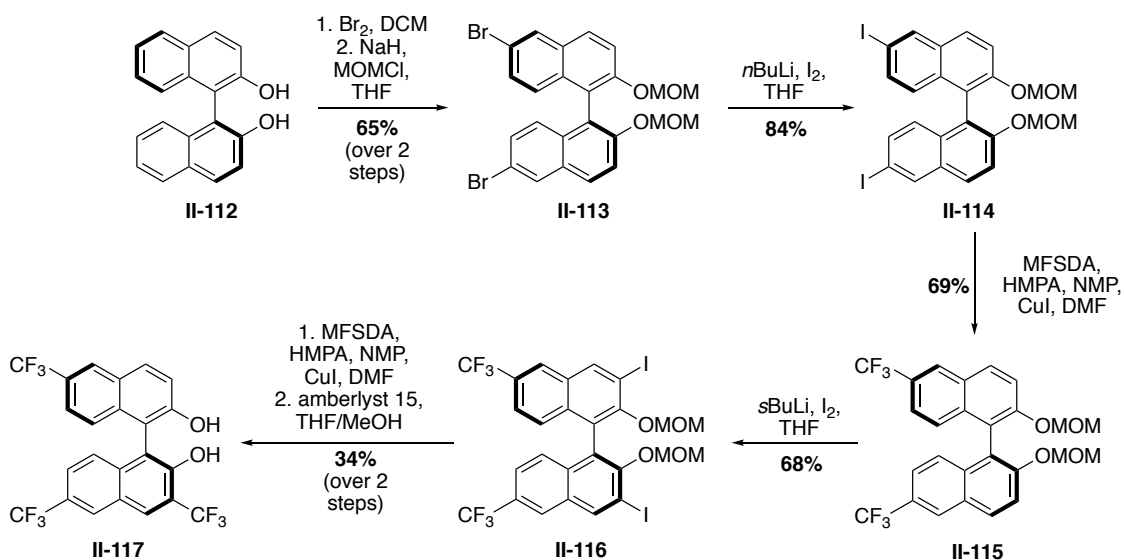
En route to diethyl boronate **II-109**, alkynyl intermediate **II-108** was treated with *n*-butyllithium (*n*BuLi) and triethylborate B(OEt)₃, forming a highly unstable alkynyl boronate **II-109**. Alkynyl boronate **II-109** was immediately siphoned into a Petasis reaction (see Section 2.7.3.3, Scheme 2.17) under air-free conditions. Alkynyl intermediate **II-108** was also used to prepare cyclic alkynyl boronate **II-99**, by first forming the alkynyl trifluoroborate salt **II-110** using KHF₂ as a mild source of fluoride anion. Trifluoroborate salt **II-110** was subsequently converted into the desired cyclic boronate **II-99** via treatment with trimethylsilyl chloride (TMSCl) and TMS-protected 1,3-propanediol **II-111**. Cyclic boronate **II-99** was likewise taken forward to the Petasis transformation crude, due to the tendency for this alkynyl boronate to undergo protodeborylation on silica gel. Efforts towards the subsequent traceless Petasis transformation using both acetal-based alkynyl boronates (**II-109** and **II-99**) will be described in Section 2.7.3.3.

2.7.3.2 Synthesis of (CF₃)₄-BINOL.

Previous methodological studies indicated that glycoaldehyde dimer (**II-119**), 2-nitrobenzenesulfonylhydrazide (NBSH) (**II-118**), and (*S*)-(CF₃)₄-BINOL are optimal substrates for the traceless Petasis reaction towards *cis*-solamin A (Section 2.7.3.3, Scheme 2.17).¹⁸ (*S*)-(CF₃)₄-BINOL was prepared by Thomson Lab undergraduate Wan Cheng Phua, following a modified procedure originally published by the Ishitani group⁵⁶ and optimized by Dr. Abdallah Diagne, a former graduate student in the Thomson lab. The synthesis of (*S*)-(CF₃)₄-BINOL began with an electrophilic aromatic bromination at the 6,6'-position of (*S*)-BINOL (**II-112**) to access compound **II-113**. Protection of the diol as methoxymethyl (MOM) ether groups was accomplished via treatment with MOMCl, followed by lithium halogen exchange with molecular iodine, which afforded compound **II-114**. Trifluoromethylation at the 6,6'-position was accomplished by treating compound **II-114** with methyl fluorosulfonyl difluoroacetate

(MFSDA),⁵⁷ yielding (CF₃)₂-BINOL intermediate **II-115**. Treating compound **II-115** with *sec*-butyllithium (*s*BuLi) and molecular iodine provided intermediate **II-116**, although typically as an inseparable mixture of mono- and diiodinated products. Again, MFSDA was used as a trifluoromethyl source, although in this instance only a single trifluoromethylation was accomplished, resulting in (CF₃)₃-BINOL derivative. Nonetheless, the (CF₃)₃-BINOL derivative intermediate was taken forward to a final acid-mediated MOM deprotection,⁵⁸ to form compound **II-117** as the final catalyst. We anticipated that the electronic difference between the targeted (CF₃)₄-BINOL and the accessed (CF₃)₃-BINOL would be nominal, and thus carried this catalyst forward towards the enantioselective Petasis reaction.

Scheme 2.16 Synthesis of (*S*)-(CF₃)₃-BINOL

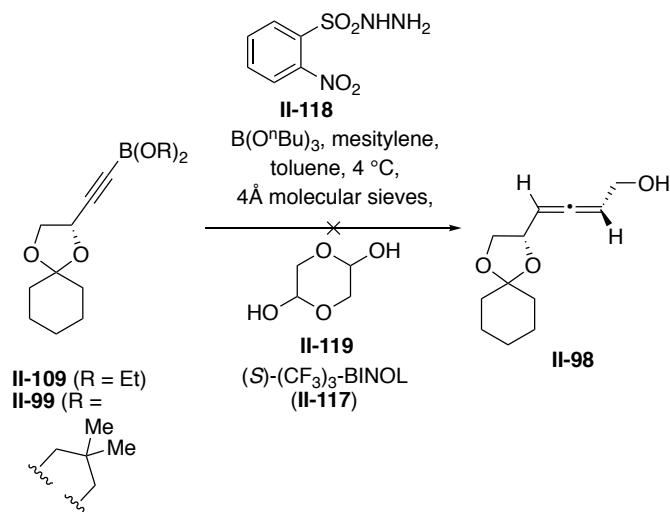


2.7.3.3 Traceless Petasis reaction with mannitol-derived alkynyl boronates.

The traceless Petasis reaction was carried forward according to Scheme 2.17, using either cyclic alkynyl boronate **II-99** or diethyl alkynyl boronate **II-109**. This reaction proved to be very moisture sensitive, and thus extra precautions were taken including rigorous distillation of all

solvents and reagents as well as addition of oven-dried powdered molecular sieves into the reaction mixture. Formation of the sulfonylhydrazone was allowed to proceed for 2 hours prior to addition of the alkynyl boronate species. Unfortunately, no allenyl product formation was observed in both alkynyl boronate cases, with exclusively protodeborylated alkyne **II-108** recovered from the reaction. We hypothesized that under this set of conditions, ligand exchange between the BINOL catalyst and the boronate was unsuccessful, meaning that formation of the chiral “ate” and the subsequent allene-forming retro-ene reaction were not occurring. A survey of the methodological substrate scope for this transformation¹⁸ led us to postulate that the alkynyl diol scaffold was interfering with the stability of the boronate overall, and we thus searched for alternative alkynyl boronate substrates to successfully access the traceless Petasis product.

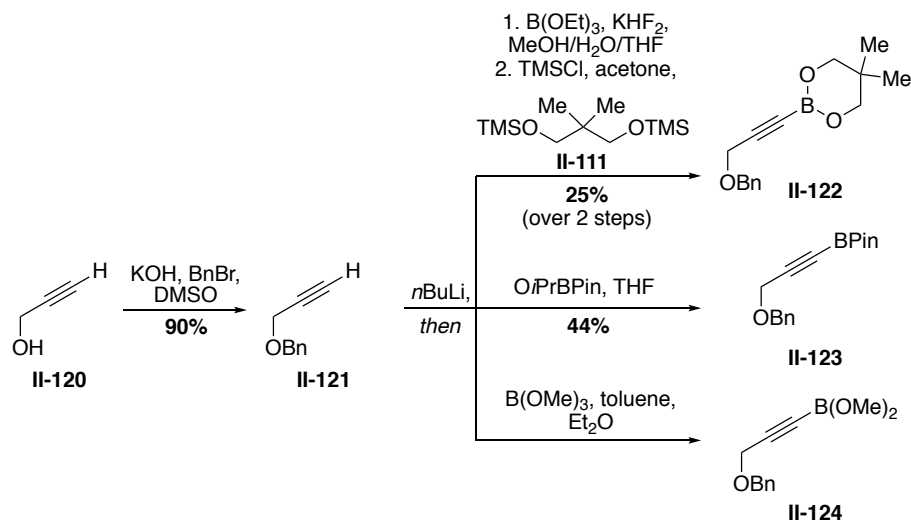
Scheme 2.17 Enantioselective traceless Petasis reaction with mannitol-derived alkynyl boronates.



2.7.4 Enantioselective traceless Petasis reaction with *O*-benzyl alkynyl boronates.

2.7.4.1 Synthesis of *O*-benzyl alkynyl boronates.

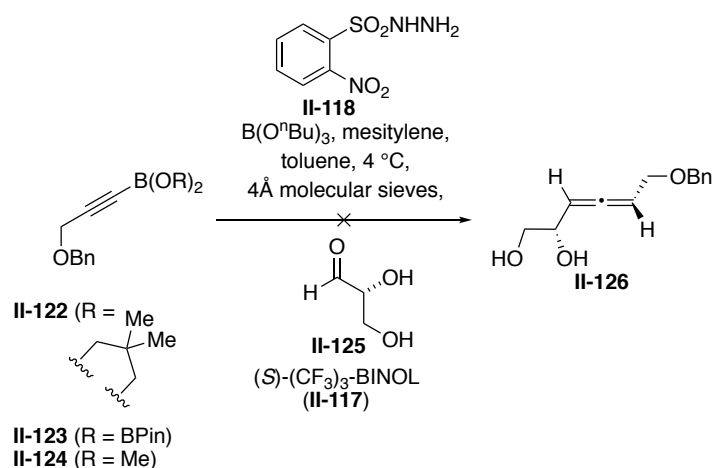
To circumvent the apparent challenge inherent to the diol based-alkynyl boronate system, we modified the Petasis reaction substrates to instead incorporate commercially available D-glyceraldehyde (**II-125**) and an *O*-benzyl alkynyl boronate. A series of alkynyl boronates were prepared and tested in the Petasis reaction, with the hopes that the simplified alkynyl substrate would experience enough longevity to undergo ligand exchange with the catalyst and form the chiral allenol in an enantiopure fashion (Scheme **2.18**). *O*-Benzyl alkyne **II-121** was prepared beginning from commercially available propargyl alcohol (**II-120**), which was treated with KOH and benzyl bromide to afford compound **II-121**. Dimethyl boronate **II-124** was accessed by treating alkyne **II-121** with *n*BuLi and trimethylborate B(OMe)₃, and it was immediately subjected to Petasis conditions with no further purification due to instability. To access bis(pinacolato)diboron (BPin) alkyne **II-123**, intermediate **II-121** was again treated with *n*BuLi followed by 2-isopropoxy-4,4,5-tetramethyl-1,3,2-dioxaborolane (*O**i*PrBPin) to afford the desired alkynyl boronate **II-123**. Finally, to access cyclic alkynyl boronate **II-122**, alkynyl intermediate **II-121** was first converted into trifluoroborate salt (**SII-1**) via treatment with *n*BuLi and KHF₂, and it was subsequently treated with protected 1,3-diol **II-111** and TMSCl, forming cyclic boronate **II-122** that was carried forward with no further purification due to instability.

Scheme 2.18 Synthesis of *O*-benzyl alkynyl boronates.

2.7.4.2 Traceless Petasis reaction with *O*-benzyl alkynyl boronates.

Both NBSH (**II-118**) and $(\text{CF}_3)_3\text{-BINOL}$ (**II-117**) were again used for this reaction. Unfortunately, no allenol products were observed in any cases using the three *O*-benzyl alkynyl boronates prepared (**II-122–II-124**), and similar to the D-mannitol derived alkynyl boronates, recovered products were typically protodeborylated alkynes (Scheme 2.19). In an optimal system, the alkynyl boronate would be stable enough to survive protodeborylation, yet labile enough to undergo ligand exchange with the BINOL catalyst. Given the apparent inherent challenges with this class of alkynyl boronates in the traceless Petasis reaction, we instead turned our attention to the alternate pathway for the traceless Petasis reaction, Path **B** (see Section 2.6.2, Scheme 2.12), which featured an alkynyl aldehyde and allyl boronate.

Scheme 2.19 Enantioselective traceless Petasis reaction with *O*-alkynyl boronates.

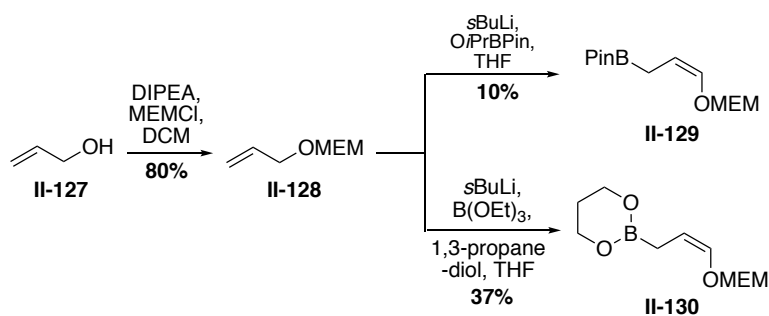


2.7.5 Enantioselective traceless Petasis reaction with allyl boronates.

2.7.5.1 Synthesis of allyl boronates for traceless Petasis reaction Path B.

Alternate pathway **B** is shown in Scheme 2.12. Here, an alkynyl hydrazone, prepared from an alkynyl aldehyde, undergoes nucleophilic attack from an allyl boronate in order to form the key chiral “ate” species. A set of allyl boronates were synthesized as shown in Scheme 2.20 in order to assess the feasibility of this route towards a chiral allenol.⁵⁹⁻⁶⁴

Scheme 2.20 Synthesis of allyl boronates.



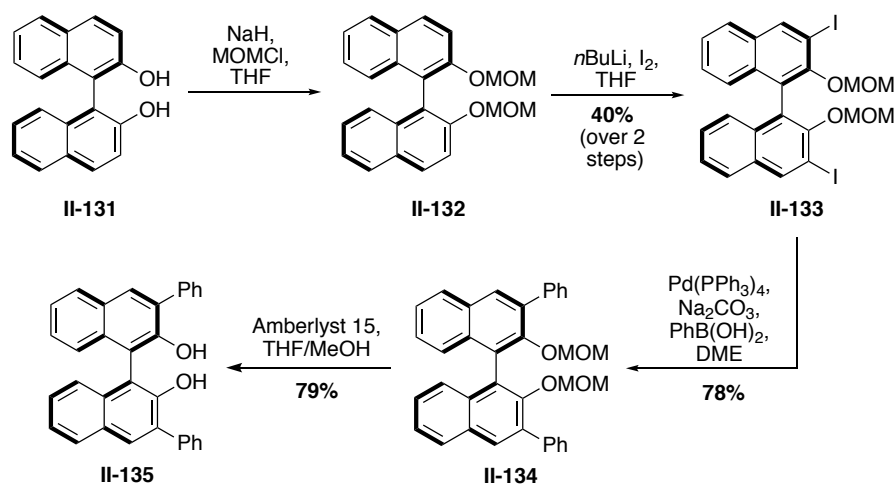
Towards allyl boronate **II-129**, allyl alcohol was treated with Hunig's base and 2-methoxyethoxymethyl chloride (MEMCl) to form allyl MEM-ether **II-128**. A final treatment with *s*BuLi and *O**i*PrBPi*n* provided boronate **II-129**, which was purified via short silica plug to avoid degradation. Low yield (10%) was due to product loss during attempts to optimize purification via distillation under high vacuum, column chromatography, recrystallization, etc. Allyl MEM-ether **II-128** was also used to access allyl boronate **II-130**, by treating with *s*BuLi and subsequent quenching of the lithiate with B(OEt)₃ and 1,3-propanediol. Purification via a short silica plug provided boronate **II-130** in 37% yield, and this material was immediately taken forward to avoid further degradation. Both of these allyl MEM-ether boronates were accessed as (*Z*) conformers due to favorable lithiate coordination with the oxygen holding the alkene in a *cis* geometry. Attempts to first access the BF₃K salt of the allyl MEM-ether species followed by subsequent conversion towards either desired boronate were unsuccessful.

2.7.5.2 Synthesis of (*R*)-(Ph)₂-BINOL.

Previously published methodological studies indicated that the allylation traceless Petasis pathway required a (Ph)₂-BINOL (**II-135**) catalyst (as opposed to the (CF₃)₄-BINOL used in alkynylation), which was synthesized by undergraduate in the Thomson lab, Wan Cheng Phua.¹⁸ The (*R*)-(Ph)₂-BINOL derivative was already in preparation for a related research aim, and thus despite our initial target being *cis*-solamin (requiring an (*S*)-BINOL catalyst), (*R*)-(Ph)₂-BINOL was used as a model catalyst determine the feasibility of the enantioselective allylation reaction. (*R*)-(Ph)₂-BINOL was synthesized beginning from (*R*)-BINOL (**II-131**), which was protected as a MOM-ether upon treatment with NaH and MOMCl to form compound **II-132** (Scheme 2.21). Subjecting intermediate **II-132** to *n*BuLi and molecular iodide formed diiodo-product **II-133**,

which then underwent a Suzuki coupling with phenyl boronic acid to yield compound **II-134**. A final acid-mediated MOM-deprotection afforded (*R*)-(Ph)₂-BINOL (**II-135**).

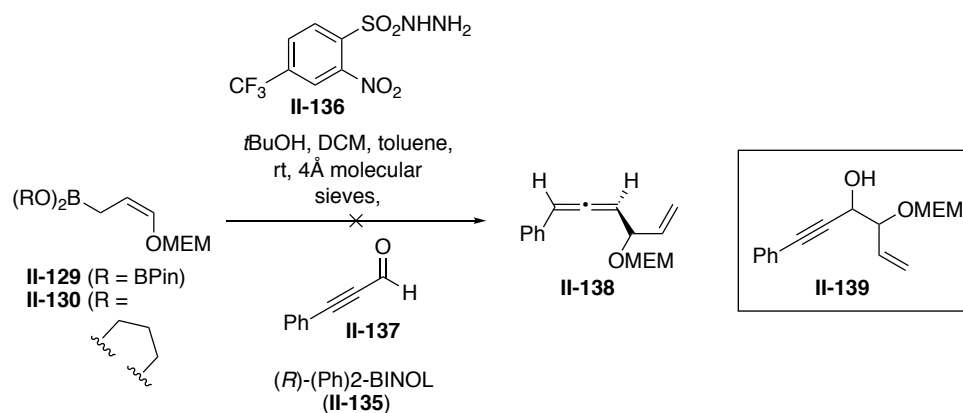
Scheme 2.21 Synthesis of (*R*)-(Ph)₂-BINOL.



2.7.5.3 Traceless Petasis reaction with allyl boronates.

For proof-of-concept allylation Petasis reactions (Path **B**), phenylpropargyl aldehyde was employed as a model system for alkynyl aldehyde **II-90** shown in Scheme 2.12. In Petasis reactions with both allyl MEM-ether boronates **II-129** and **II-130**, no allene formation was observed. However, the allylated aldehyde product **II-139** was observed and isolated, indicating that the boronates successfully inserted into trace amounts of phenylpropargyl aldehyde **II-137** starting material present in the reaction mixture (Scheme 2.22). The propensity for these allyl MEM-ether boronates to react with the aldehyde starting material despite the overwhelming presence of the sulfonylhydrazone indicated a potential electronic mismatch between hydrazone and allyl boronate. The less electrophilic hydrazone, relative to the aldehyde, was a poor reaction partner for the MEM-ether boronate, which additionally appeared to have decreased nucleophilicity due to the MEM-ether protecting group.

Scheme 2.22 Enantioselective traceless Petasis reaction with allyl boronates.



2.8 Modified route towards allenol intermediate.

2.8.1 Lewis-acid catalyzed traceless Petasis reaction towards diastereomeric allenols.

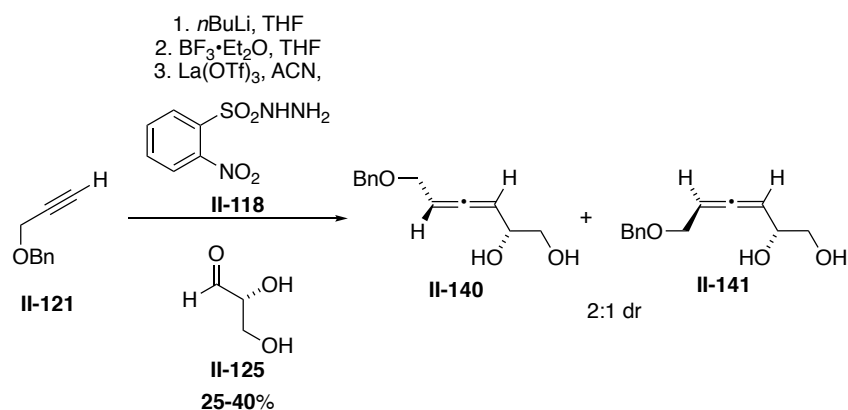
Given the challenges surrounding the aforementioned enantioselective traceless Petasis reactions, we turned our attention to an earlier method of allene synthesis published by the Thomson group wherein allenes were synthesized using achiral Lewis acid catalysis (see Section 2.6.2, Scheme 2.11b). Although this meant sacrificing the enantioselectivity of this transformation, we ultimately hoped to access a separable mixture of diastereomeric allenol products that could be taken forward separately to complete the total synthesis of solamin stereoisomers. To this end, alkynyl trifluoroborate substrates were prepared to undergo the nonselective, La(OTf)₃-catalyzed traceless Petasis reaction variant.

2.8.1.1 Synthesis of an alkynyl trifluoroborate salt and La(OTf)₃-cat. Petasis reaction.

A one-pot method was developed to convert *O*-benzyl alkyne II-121 into the La(OTf)₃-cat. Petasis reaction precursor by treating with *n*BuLi, followed by BF₃•Et₂O for the *in situ* formation

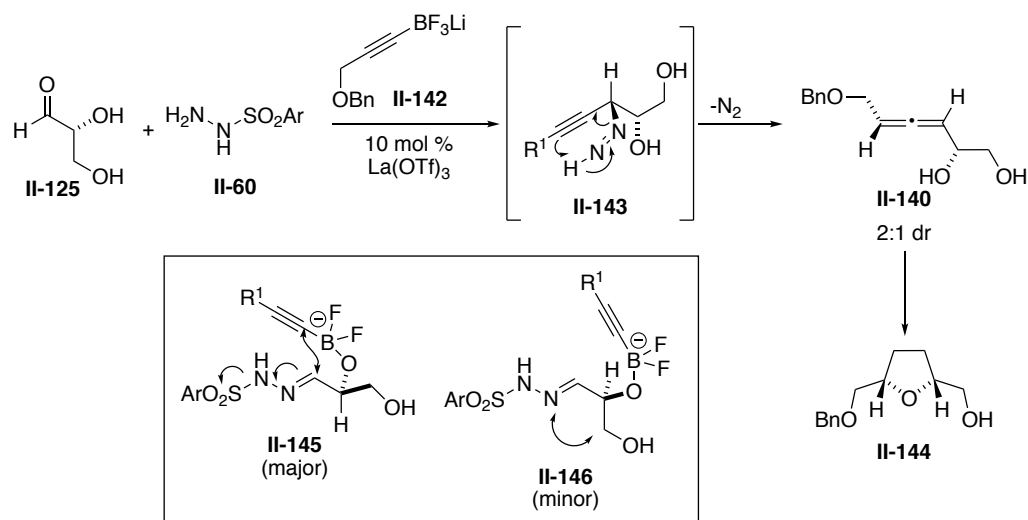
of an alkynyl BF_3Li salt (Scheme 2.23). This unstable intermediate was then cannulated directly into the Petasis reaction flask containing the sulfonylhydrazone and $\text{La}(\text{OTf})_3$ catalyst. With this method, low-yielding multi-step transformations towards the BF_3K salt were avoided, and the use of glass-etching aqueous KHF_2 was also circumvented. The one-pot Petasis procedure reliably produced allenols **II-140** and **II-141** in 25–40% yield, which matched yield observations for single-step Petasis transformations using isolated BF_3K salts. Instability of the transient BF_3Li intermediate at temperatures above $-78\text{ }^\circ\text{C}$ most likely contributed to the low yield. This Petasis transformation provided diastereomeric allenol products **II-140** and **II-141** in a 2:1 ratio, and this pair of diastereomers were chromatographically inseparable at this stage. Although this method of allenol synthesis lacked enantio- or diastereoselectivity at this step, the production of two diastereomeric allenes provided the potential for a divergent synthesis of two different solamin stereoisomers arising from a single transformation. Determination of the relative stereochemistry, and thus the anticipated solamin stereoisomer accessed from the major diastereomer, will be discussed in Future Directions, Section 2.9.1.

Scheme 2.23 One-pot synthesis of diastereomeric allenols.

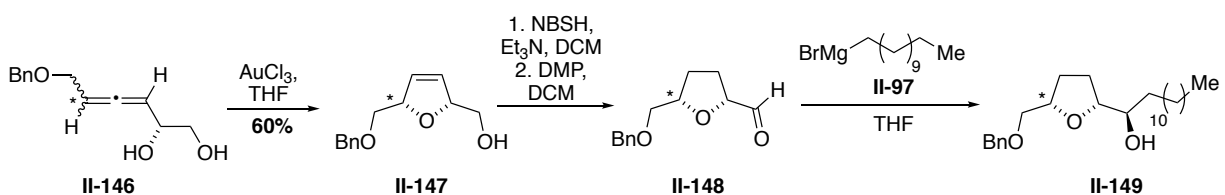


2.8.1.2 Beyond the traceless Petasis reaction: Synthesis of the solamin stereoisomers.

The diastereomic mixture of allenols **II-140** and **II-141** was carried forward to the critical Au(III)-catalyzed cyclization reaction, which proceeded in good yield to form a 2:1 mixture of separable diastereomers (Scheme 2.25). At this point, ¹H NMR spectral overlap between the two key dihydrofuran protons precluded the use of nuclear Overhauser effect (NOE) experiments to determine the relative configurations of major and minor products. However, relative stereochemistry of the major versus minor diastereomer can be hypothesized based on a stereochemical model for this Petasis reaction published by Mundal, Thomson and coworkers (Scheme 2.24).²⁰ Given the tendency for the chiral “ate” intermediate to minimize A1,2-strain, the major product formed is most likely allenol **II-140** which leads to the *syn* dihydrofuran ring, **II-144**. It is anticipated that NOE will be possible once the dihydrofuran diastereomers have been elaborated on structurally to provide a less symmetrical compound with more discriminant ¹H NMR spectral features. Because of the C₂ symmetry in dihydrofuran intermediate **II-144**, either *cis*-solamin A or B may be accessed depending on the order of oxidation and side arm additions. Initial experiments proceeded towards putative *cis*-solamin B via the major dihydrofuran diastereomer, although in future work *cis*-solamin A can be easily accessed from the same intermediate **II-144**.

Scheme 2.24 Stereochemical model of La(OTf)₃-cat. traceless Petasis reaction.

Diimide-mediate reduction of the gold-catalyzed cyclization product, dihydrofuran **II-147**, to the THF intermediate (**SII-3**) was achieved in 90% yield, and subsequent oxidation of the free alcohol with Dess-Martin periodinane (DMP) yielded aldehyde **II-148**, which was purified on silica and taken forward with minor impurities resulting from residual DMP. Grignard addition of commercially available **II-97** provided compound **II-149** (observed by MS), although the small scale of this test reaction made purification unfeasible. Future directions Section 2.9.1 outlines the final steps towards *cis*-solamin B.

Scheme 2.25 Synthesis of THF intermediate **II-149**. Asterisk denotes putative stereochemistry.

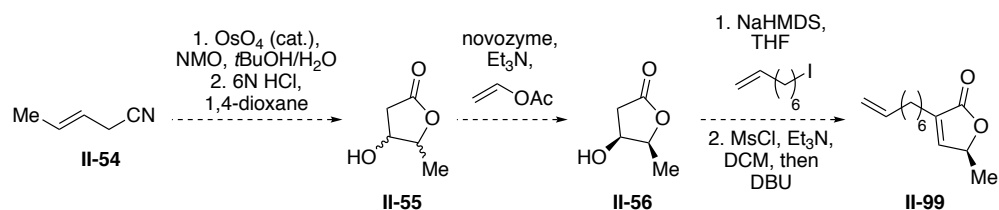
2.9 Future directions.

2.9.1 Route towards completing the total synthesis of the solamin stereoisomers.

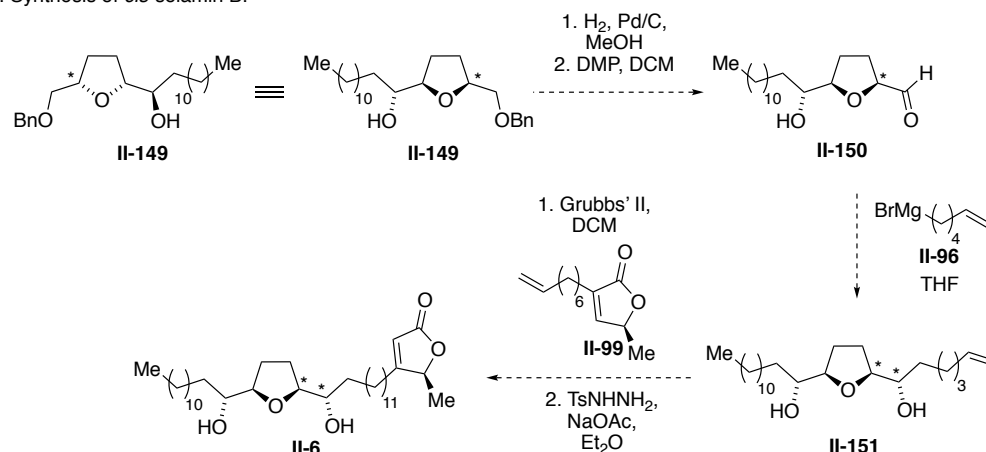
The final route towards *cis*-solamin B is outlined in Scheme 2.26. Deprotection of the benzyl ether group, followed by DMP oxidation will provide aldehyde **II-150**, which will then be subjected to chelate-controlled Grignard addition of hex-5-enyl magnesium bromide (prepared from 6-bromo-1-hexene) (Scheme 2.26b). Intermediate **II-151** will undergo cross-coupling with lactone **II-99**, prepared in five steps as shown in Scheme 2.26 and as described in Section 2.5.4.2. A final diimide-mediated reduction of the olefin will yield the solamin stereoisomer, putatively assigned as *cis*-solamin B (**II-6**). NOE analysis of the key dihydrofuran/THF ring protons will provide definitive assignment of the major vs. minor diastereomers obtained earlier in the synthesis from the La(OTf)₃-catalyzed Petasis reaction discussed in Section 2.8.1.2.

Scheme 2.26 Final route towards *cis*-solamin B. Asterisk denotes putative stereochemistry.

a. Synthesis of γ -lactone **II-99**.



b. Synthesis of *cis*-solamin B.



2.10 Conclusions.

This chapter has discussed the application of a traceless Petasis reaction towards the total synthesis of the solamin stereoisomers. This approach provides access to the stereocomplex THF core of the solamin NPs via gold-catalyzed cyclization of an unprecedented chiral allenol intermediate. Efforts towards an enantioselective traceless Petasis reaction to access the desired allenol scaffold have been outlined, as well as an alternate, non-asymmetric, La(OTf)₃-catalyzed Petasis variation that utilizes a one-pot procedure to convert a BF₃Li salt into a diastereomeric mixture of the desired allenols. Future directions (Section 2.9.1) outlines final steps to access the desired compound, completing this methodological application toward the total synthesis of the solamin stereoisomers.

2.11 Experimental Section.

2.11.1 General information.

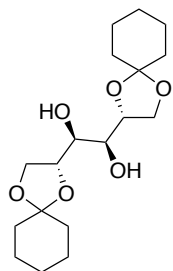
All reactions were carried out under nitrogen atmosphere in flame-dried glassware unless otherwise stated. Anhydrous solvents (DCM, DMF, acetonitrile, methanol, THF) were purified by passage through a bed of activated alumina. Reagents were purified prior to use unless otherwise stated following the guidelines of Armarego and Chai.⁶⁵ Flash column chromatography was performed manually using EM Reagent silica gel F60, 40-63 μm (230-400 mesh) or automatically using a CombiFlash instrument and ISCO prepacked columns. Analytical thin-layer chromatography (TLC) was performed using Merck Silica Gel 60 Å F-254 precoated plates (0.25 mm thickness) or EM Reagent 0.25mm silica gel 60-F plates. Visualization was achieved using UV light, ninhydrin stain or ceric ammonium molybdate. NMR experiments were carried out on a Bruker Avance III 500 MHz spectrometer (500 MHz for ¹H, 126 MHz for ¹³C) equipped with a

DCH CryoProbe, and are reported in ppm using solvent as an internal standard (CDCl_3 at 7.26 ppm except where noted). Data are reported as s = singlet, d = doublet, t = triplet, q = quartet, m = multiplet, b = broad; coupling constant(s) in Hz; integration. Optical rotation was determined using a Rudolph Research Analytical Autopol IV, Series #82239 with either a 10 cm or 5 cm pathlength cell at the sodium D line. High resolution mass spectra were collected on a Thermo Q-Exactive orbitrap mass spectrometer in ESI mode. Diamond ATR infrared spectra were obtained on a ThermoNicolet iS10 FT-IR spectrometer. Germanium ATR infrared spectra were recorded using a Bruker Tensor 37.

2.11.2 Synthesis of boronates for enantioselective *Petasis* reactions.

2.11.2.1 Synthesis of *D*-Mannitol derived alkynyl boronates.

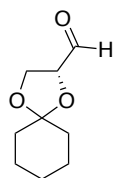
Compound II-105.



Trimethyl orthoformate (6.01 mL, 54.89 mmol, 1.0 eq) and cyclohexanone (17.05 mL, 164.68 mmol, 3.0 eq) were stirred neat at rt for 20 min. The reaction was then diluted with DMSO (22 mL) and *D*-mannitol (**II-100**) (10.0 g, 54.89 mmol, 1.0 eq) and freshly distilled $\text{BF}_3 \cdot \text{Et}_2\text{O}$ (0.677 mL, 5.50 mmol, 0.1 eq) were added and the reaction was stirred at rt overnight. The reaction was quenched with 50 mL sat. NaCl and extracted 3x with Et_2O . The organic layers were combined, dried over Na_2SO_4 , filtered, and concentrated to a clear oil. The clear oil was triturated with hexanes and concentrated under reduced pressure 3x until it yielded a white solid, which was then recrystallized using 2:1 hex/ Et_2O to yield **II-105** as a white crystalline solid (12.30 g, 65%). $^1\text{H NMR}$ (400 MHz, Chloroform-*d*) δ 4.21 (q, $J = 6.3$ Hz, 1H), 4.12 (dd, $J = 8.6, 6.3$ Hz, 1H), 3.96 (dd, $J = 8.6, 5.7$ Hz, 1H), 3.75 (t, $J = 6.3$ Hz, 1H), 2.63 – 2.59 (m, 1H), 1.65 – 1.54 (m, 8H), 1.40 (m, 2H). $^{13}\text{C NMR}$ (126 MHz, CDCl_3) δ 110.18, 71.62,

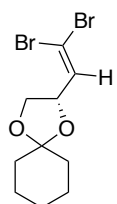
66.59, 36.57, 34.82, 25.24, 24.19, 23.93. **LRMS** (M+Na) Calc'd: 365.43. Found: 365.20. **IR** (Diamond ATR): 3409, 2934, 1772, 1617, 1163, 926 cm^{-1} .

Compound II-106.



NaIO_4 (2.99 g, 14.0 mmol, 2.4 eq) was suspended in 12 mL H_2O and stirred at rt. Meanwhile, compound **II-105** (2.00 g, 5.84 mmol, 1.0 eq) and $n\text{Bu}_4\text{Br}$ (377.2 mg, 1.17 mmol, 0.2 eq) were stirred in THF (20 mL), and this was cannulated into the NaIO_4 mixture and stirred at rt overnight. The crude mixture was filtered over celite (Et_2O), diluted with H_2O , and extracted 3x with Et_2O , then dried over Na_2SO_4 , filtered, and concentrated under reduced pressure to yield **II-106** as a light yellow oil that was carried forward with no further purification (3.26 g, 68%). Product degradation occurred within 1 week. **$^1\text{H NMR}$** (400 MHz, Chloroform-*d*) δ 9.72 (s, 1H), 4.38 (ddd, $J = 7.2, 4.6, 1.9$ Hz, 1H), 4.19 – 4.14 (m, 1H), 4.10 (dt, $J = 8.8, 4.8$ Hz, 1H), 1.68 – 1.58 (m, 10H). **$^{13}\text{C NMR}$** (126 MHz, CDCl_3) δ 202.28, 112.10, 79.72, 65.43, 36.04, 34.81, 25.14, 24.07, 23.95. **LRMS** (M+Na) Calc'd: 193.23. Found: 193.02. **IR** (Diamond ATR): 2904, 1760, 1684, 1462, 1119 cm^{-1} .

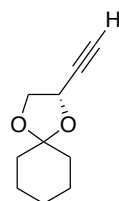
Compound II-107.



PPh_3 (30.02 g, 114.4 mmol, 4 eq) was stirred in DCM (110 mL) and cooled to 0 $^\circ\text{C}$. CBr_4 (18.98 g, 57.22 mmol, 2 eq) was added slowly over 15 minutes at 0 $^\circ\text{C}$. The reaction mixture was stirred at room temperature for 30 minutes, then cooled back down to 0 $^\circ\text{C}$. Meanwhile, compound **II-106** (4.87g, 28.6 mmol, 1.0 eq) was suspended in DCM (20 mL) at 0 $^\circ\text{C}$, and this mixture was cannulated into the reaction flask. The reaction mixture was allowed to come to rt and stirred for an additional 2 hrs. The reaction was cooled to 0 $^\circ\text{C}$ and hexanes (100 mL) was added, and the mixture was stirred for an additional hour at 0 $^\circ\text{C}$. The mixture was then filtered over celite (hex) and concentrated to yield a crude white solid that was

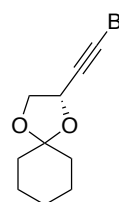
purified by on silica gel (20% hexanes/DCM) to yield **II-107** as a yellow oil (7.37 g, 79% over 2 steps). ¹H NMR (500 MHz, Chloroform-*d*) δ 6.53 (dd, *J* = 7.7, 1.7 Hz, 1H), 4.73 (td, *J* = 7.9, 7.1, 5.5 Hz, 1H), 4.18 (ddd, *J* = 8.3, 6.2, 1.7 Hz, 1H), 3.68 (ddd, *J* = 8.3, 6.4, 1.7 Hz, 1H), 1.78 – 1.06 (m, 10H).

Compound II-108.



Compound **II-107** (1.62 g, 4.74 mmol, 1.0 eq) was stirred in DMSO (46 mL) at rt. Cs₂CO₃ (3.86 g, 11.85 mmol, 2.5 eq) was added, and the reaction mixture was lowered into an oil bath pre-heated to 115 °C and stirred overnight with a reflux condenser. The reaction was cooled to rt, then quenched slowly with 1M HCl at 0 °C. The aqueous layer was then extracted 3x with Et₂O, and the combined organic layers were dried over Na₂SO₄, filtered, and concentrated under reduced pressure. The crude product was purified on silica gel (5% EtOAc/hexane) to afford compound **II-108** as a yellow oil (575.2 mg, 73%). ¹H NMR (400 MHz, Chloroform-*d*) δ 4.71 (td, *J* = 6.3, 2.1 Hz, 1H), 4.16 (dd, *J* = 8.0, 6.4 Hz, 1H), 3.94 (dd, *J* = 8.0, 6.2 Hz, 1H), 2.48 (d, *J* = 2.1 Hz, 1H), 1.75 – 1.38 (m, 10H). ¹³C NMR (126 MHz, CDCl₃) δ 135.83, 111.36, 81.79, 73.90, 69.69, 65.05, 35.80, 35.54, 25.18, 24.02. LRMS (M+ACN+Na) Calc'd: 230.22. Found: 230.17. IR (Diamond ATR): 2863, 2342, 1740, 1559, 1363, 1161, 924 cm⁻¹.

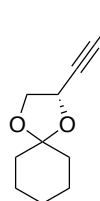
Compound II-109.



Compound **II-108** (100 mg, 0.602 mmol, 1.0 eq) was stirred in Et₂O (1 mL) at -78 °C. *n*BuLi (2.5 M in hex, 0.240 mL, 0.602 mmol, 1.0 eq) was added dropwise, and the mixture was stirred at -78 °C for 1 hr. Meanwhile, B(OEt)₃ (0.102 mL, 0.602 mmol, 1.0 eq) was stirred in Et₂O (1 mL) at -78 °C. B(OEt)₃ was cannulated into the reaction flask, and the mixture was stirred at -78 °C for 2 hrs. Anhydrous HCl (2 M in Et₂O, 0.301 mL, 0.602 mmol, 1.0 eq) was added and the reaction was raised from the dewar and allowed to come

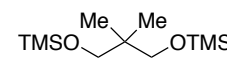
to rt over 1 hr, during which a fine white solid precipitated out. Using dry Et₂O and an air-free setup, the mixture was cannulated over celite and rinse (Et₂O), and the filtrate was evaporated using an N₂ stream to ~5 mL. Dry toluene (1 mL) was added, and the product was cannulated directly into the next reaction flask with no further purification.

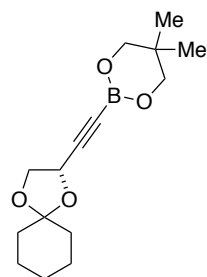
Compound II-110.



Compound **II-108** (500 mg, 3.01 mmol, 1.0 eq) was suspended in THF (9.2 mL) and stirred at -78 °C. *n*BuLi (2.5 M in hex, 1.44 mL, 3.61 mmol, 1.2 eq) was added dropwise over 10 min, and the reaction was stirred at -78 °C for 1 hr. B(OMe)₃ (0.671 mL, 6.02 mmol, 2.0 eq) was added quickly at -78 °C, and the mixture was stirred at -78 °C for 10 min and then raised out of the dewar and allowed to warm to rt over 2 hrs. The reaction mixture was cooled to 0 °C and dry MeOH (3 mL) was added, followed by aq. KHF₂ (2.4 M, 1.88 g, 24.08 mmol, 8.0 eq) via drop funnel. The biphasic mixture was stirred at 0 °C for 15 min, then removed from the ice bath and stirred at rt for 1 hr. Solvent was evaporated under reduced pressure, and the crude material was left under high vacuum overnight. The crude white solid was suspended in 25 mL acetone and spun rapidly on a rotovap at atmospheric pressure with the water bath warmed to 45 °C. The mixture was filtered over celite (acetone), the filtrate was collected, and the residue left in the round bottom was subjected to the acetone/rinse process twice more to isolate the product. The filtrates were combined and concentrated to ~30 mL, to which 10 mL Et₂O were added to crash out a crystalline white solid. The mixture was filtered over celite (Et₂O), and the product was collected and dried under high vacuum to yield **II-110** as a light brown flaky solid (310.2 mg, 38%). ¹H NMR (500 MHz, Methanol-*d*₄) δ 4.69 – 4.59 (m, 1H), 4.08 (dd, *J* = 7.8, 6.2 Hz, 1H), 3.78 (t, *J* = 7.5 Hz, 1H), 1.82 – 1.22 (m, 10H).

Compound II-111.

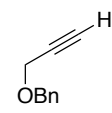

 Neopentyl glycol (3.00 g, 28.80 mmol, 1.0 eq) was stirred in DCM (120 mL) at 0 °C. Freshly distilled Et₃N (12.04 mL, 86.40 mmol, 3.0 eq) was added quickly to the reaction at 0 °C, followed by the dropwise addition of freshly distilled TMSCl (9.14 mL, 72.01 mmol, 2.5 eq) at 0 °C over ~10min. The reaction was brought to rt and stirred for 1 hr, and the mixture was then quenched with sat. NH₄Cl and stirred an additional 5 min. The crude mixture was filtered over celite (DCM) then transferred to a separatory funnel, and the organic layer was washed with sat. NaCl, dried over Na₂SO₄, filtered, and concentrated under reduced pressure. The concentrated layers were then re-suspended in Et₂O and filtered again over celite, then dried over Na₂SO₄ and concentrated to give compound **II-111** as a light yellow oil (5.26 g, 73%). ¹H NMR (400 MHz, Chloroform-*d*) δ 3.28 (s, 4H), 0.79 (s, 6H), 0.08 (s, 18H). ¹³C NMR (126 MHz, CDCl₃) δ 68.02, 37.28, 21.47, -0.37. LRMS (M+Na) Calc'd: 271.51. Found: 271.08. IR (Diamond ATR): 3307, 3029, 2928, 1787, 1661, 1219 cm⁻¹.

Compound II-99.

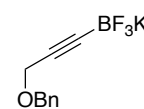
Compound **II-108** (274.8 mg, 1.01 mmol, 1.0 eq) was suspended in freshly distilled acetone (2 mL) and was stirred at rt. Compound **II-111** was suspended in acetone (1 mL), and the mixture was cannulated into the reaction flask quickly followed immediately by the addition of neat TMSCl (0.272 mL, 2.02 mmol, 2.0 eq). The reaction was stirred at rt for 24 hrs, and it was then filtered over neutral alumina (hex). The filtrate was concentrated to yield **II-99** as a dark brown oil, which was stored in toluene as a 1 M solution (115.2 mg, 41%). ¹H NMR (500 MHz, Chloroform-*d*) δ 4.72 (dd, *J* = 7.1, 5.8 Hz, 1H), 4.14 (q, *J* = 6.7 Hz, 1H), 4.03 – 3.90 (m, 1H), 3.71 – 3.60 (m, 4H), 1.91 – 1.53 (m, 10H), 1.48 (s, 3H), 1.37 (s, 3H).

2.11.2.2 Synthesis of *O*-Benzyl alkynyl boronates.

Compound II-121.

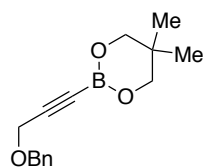
 Propargyl alcohol (1.04 mL, 17.8 mmol, 1.0 eq) and KOH (3.00 g, 53.5 mmol, 3.0 eq) were stirred in DMSO (14.5 mL) at 0 °C for 10 min. BnBr (2.12 mL, 17.8 mmol, 1.0 eq) was added at 0 °C, and the reaction mixture was raised out of the ice bath and allowed to come to rt over 3 hrs. The mixture was diluted with H₂O and extracted 3x with Et₂O, and organic layers were combined and washed with H₂O and sat. NaCl, then dried over Na₂SO₄, filtered, and concentrated under reduced pressure. The crude material was purified on silica gel (5% EtOAc/hex) to yield **II-121** as a clear oil (2.34 g, 90%). **¹H NMR** (500 MHz, Chloroform-d) δ 7.42 – 7.27 (m, 5H), 4.62 (s, 2H), 4.18 (d, J = 2.4 Hz, 2H), 2.47 (t, J = 2.4 Hz, 1H).

Compound SII-1.

 Compound **II-121** (1.00g, 6.85 mmol, 1.0 eq) was suspended in THF (24 mL) and stirred at -78 °C. *n*BuLi (1.99 M in hex, 3.45 mL, 6.85 mmol, 1.0 eq) was added dropwise, and the reaction was stirred at -78 °C for 1 hr. B(OEt)₃ (1.75 mL, 10.28 mmol, 1.5 eq) was added at -78 °C, and the reaction was stirred at -78 °C for 10 min and then raised out of the dewar and allowed to come to rt over 1 hr. The reaction mixture was cooled to 0 °C and dry MeOH (7 mL) was added, followed by aq. KHF₂ (2.4 M, 3.21 g, 41.1 mmol, 6.0 eq) via drop funnel. The biphasic mixture was stirred at 0 °C for 15 min, then removed from the ice bath and stirred at rt for 1 hr. Solvent was evaporated under reduced pressure, and the crude material was left under high vacuum overnight. The crude white solid was suspended in 60 mL acetone and spun rapidly on a rotovap at atmospheric pressure with the water bath warmed to 45 °C. The mixture was filtered over celite (acetone), the filtrate was collected, and the residue left in the round bottom was subjected to the acetone/rinse process twice more to isolate the product. The filtrates were

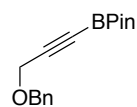
combined and concentrated to ~60 mL, to which 150 mL Et₂O were added to crash out a crystalline white solid. The mixture was filtered over celite (Et₂O), and the product was collected and dried under high vacuum to yield **SII-1** as a light brown flaky solid (445.7 mg, 26%). ¹H NMR (500 MHz, DMSO-*d*₆) δ 7.45 – 7.09 (m, 5H), 4.48 (s, 2H), 4.01 (q, *J* = 1.6 Hz, 2H).

Compound II-122.



Compound **SII-1** (225.8 mg, 0.896 mmol, 1.0 eq) was suspended in freshly distilled acetone (1 mL) and stirred at rt. Meanwhile, compound **II-111** (222.7 mg, 0.896 mmol, 1.0 eq) was stirred in freshly distilled acetone (1 mL) at rt. It was then cannulated into the reaction flask quickly, immediately followed by neat TMSCl (0.241 mL, 1.792 mmol, 2.0 eq), and the mixture was stirred at rt for 24 hrs. The reaction mixture was filtered over neutral alumina (hex), and the filtrate was concentrated to yield crude **II-122** as a dark orange oil that was stored as a 1M solution in toluene (220.9 mg, 96%). ¹H NMR (500 MHz, DMSO-*d*₆) δ 7.42 – 7.11 (m, 5H), 4.53 (d, *J* = 16.7 Hz, 2H), 4.22 (d, *J* = 1.4 Hz, 2H), 3.61 (s, 2H), 3.14 (s, 2H), 0.90 (s, 3H), 0.75 (s, 3H). ¹³C NMR (126 MHz, DMSO) δ 137.62, 128.30, 127.70, 127.66, 71.59, 70.83, 67.35, 57.25, 39.52, 37.03, 31.25, 21.47, 21.08.

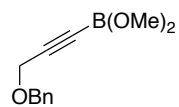
Compound II-123.



Compound **II-121** (250 mg, 1.71 mmol, 1.0 eq) was stirred in THF (4.3 mL) at -78 °C. *n*BuLi (1.99 M, 0.860 mL, 1.71 mmol, 1.0 eq) was added dropwise, and the mixture was stirred at -78 °C for 1 hr. *O**i*PrBPin (0.290 mL, 1.42 mmol, 0.83 eq) was suspended in THF (3.6 mL) at stirred at -78 °C, and this was then cannulated into the reaction mixture and stirred for 2 hrs at -78 °C. The reaction was quenched with anhydrous HCl (1.0 M in Et₂O, 1.50 mL, 1.50 mmol, 0.88 eq), and the mixture was raised out of the dewar and allowed to come to rt over 1 hr. The crude reaction mixture was concentrated and purified on silica gel (50%

Et₂O/pentane) to yield **II-123** as a brown oil (205.9 mg, 44%). ¹H NMR (500 MHz, Chloroform-*d*) δ 7.42 – 7.27 (m, 5H), 4.61 (s, 2H), 4.22 (s, 2H), 1.29 (s, 12H).

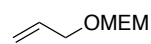
Compound II-124.



Compound **II-121** (50.0 mg, 0.342 mmol, 1.0 eq) was stirred in Et₂O (1 mL) at -78 °C. *n*BuLi (1.93 M, 0.213 mL, 0.410 mmol, 1.2 eq) was added dropwise at -78 °C, and the mixture was stirred at -78 °C for 1 hr. Freshly distilled B(OMe)₃ was added neat and the mixture was stirred at -78 °C for 2 hrs, and anhydrous HCl (1.0 M in Et₂O, 0.205 mL, 0.410 mmol, 1.2 eq) was then added and the reaction was raised out of the dewar and allowed to come to rt over 1 hr. Using dry toluene and an air-free setup, the mixture was cannulated over celite and rinse (toluene), and the filtrate was suspended as a 1 M solution in toluene that was immediately cannulated into the next reaction with no further purification.

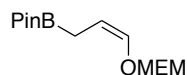
2.11.2.3 Synthesis of MEM-ether allyl boronates.

Compound II-128.



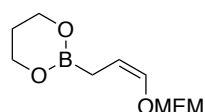
Freshly distilled allyl alcohol (2.50 mL, 36.8 mmol, 1.0 eq) was suspended in DCM (44 mL) and stirred at 0 °C. Freshly distilled DIPEA (8.97 mL, 51.5 mmol, 1.4 eq) and MEMCl (4.20 mL, 36.8 mmol, 1.0 eq) were added, and the reaction was allowed to come to rt overnight. The reaction mixture was quenched with H₂O and extracted 3x with DCM, and the organic layers were combined and washed with sat. NaCl, then dried over Na₂SO₄, filtered, and concentrated under reduced pressure. The crude pink oil was purified on silica gel (1% MeOH/DCM) to yield **II-128** as a light yellow oil (4.30 g, 80%). ¹H NMR (500 MHz, Chloroform-*d*) δ 5.92 (ddt, *J* = 17.3, 10.8, 5.6 Hz, 1H), 5.30 (dq, *J* = 17.2, 1.7 Hz, 1H), 5.18 (dq, *J* = 10.4, 1.5 Hz, 1H), 4.75 (s, 2H), 4.09 (dt, *J* = 5.6, 1.5 Hz, 2H), 3.76 – 3.66 (m, 2H), 3.63 – 3.53 (m, 2H), 3.40 (s, 3H).

Compound II-129.



Compound **II-128** (600.0 mg, 4.104 mmol, 1.0 eq) was suspended in THF (4 mL) and stirred at $-78\text{ }^{\circ}\text{C}$. *s*BuLi (1.13 M, 3.63 mL, 4.104 mmol, 1.0 eq) was added dropwise and the mixture was stirred at $-78\text{ }^{\circ}\text{C}$ for 30 min. *O**i*PrBPin (1.00 mL, 4.925 mmol, 1.2 eq) was added neat, and the reaction was allowed to come to rt in the dewar overnight. The reaction was quenched with sat. NH_4Cl (4 mL) and H_2O (6 mL) at $0\text{ }^{\circ}\text{C}$ and it was allowed to stir at rt for 1 hr. The mixture was extracted 3x with Et_2O , dried over Na_2SO_4 , filtered, and concentrated. Volatile starting materials were removed by heating the mixture to $90\text{ }^{\circ}\text{C}$ at 20 torr, and the crude material was then purified on silica gel (50% Et_2O /pentanes) to yield **II-128** as a clear oil (91.2 mg, 10%). $^1\text{H NMR}$ (499 MHz, Chloroform-*d*) δ 6.16 (dt, $J = 6.5, 1.6\text{ Hz}$, 1H), 4.89 (d, $J = 1.1\text{ Hz}$, 2H), 4.60 (dt, $J = 8.5, 6.9\text{ Hz}$, 1H), 3.73 (ddd, $J = 6.2, 3.1, 1.2\text{ Hz}$, 2H), 3.62 – 3.50 (m, 2H), 3.40 (s, 3H), 1.68 (d, $J = 7.8\text{ Hz}$, 2H), 1.25 (d, $J = 1.2\text{ Hz}$, 13H).

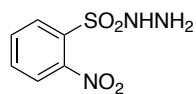
Compound **II-130**.



Compound **II-128** (100.0 mg, 0.684 mmol, 1.0 eq) was suspended in THF (2 mL) and stirred at $-78\text{ }^{\circ}\text{C}$. *s*BuLi (0.772 M in cyclohexane, 0.886 mL, 0.684 mmol, 1.0 eq) was added dropwise, and the mixture was stirred at $-78\text{ }^{\circ}\text{C}$ for 1 hr. $\text{B}(\text{OEt})_3$ (0.174 mL, 1.03 mmol, 1.5 eq) was added neat and the reaction was stirred at $-78\text{ }^{\circ}\text{C}$ for 10 min, and it was then raised out of the dewar and allowed to come to rt. The mixture was brought to $0\text{ }^{\circ}\text{C}$, and 1,3-propanediol (0.0736 mL, 1.026 mmol, 1.5 eq) was added. The reaction was then raised out of the ice bath and allowed to come to rt over 1.5 hrs, and it was then concentrated under reduced pressure. Crude material was purified on silica gel (5% MeOH/DCM), yielding **II-130** as a light yellow oil (57.6 mg, 37%). $^1\text{H NMR}$ (500 MHz, Chloroform-*d*) δ 6.14 (ddq, $J = 6.1, 3.9, 1.9\text{ Hz}$, 1H), 5.71 (ddd, $J = 17.6, 10.4, 7.7\text{ Hz}$, 1H), 5.30 (s, 2H), 4.89 (t, $J = 1.6\text{ Hz}$, 2H), 3.75 – 3.69 (m, 2H), 3.56 (m, 2H), 3.39 (s, 3H), 1.30 – 1.11 (m, 6H).

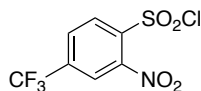
2.11.3 Synthesis of sulfonyl hydrazides.

Compound II-118.



2-Nitrobenzene sulfonyl chloride (5.00 g, 22.56 mmol, 1.0 eq) was stirred in THF (12.5 mL) at -30 °C. $\text{N}_2\text{H}_4 \cdot \text{H}_2\text{O}$ (2.74 mL, 56.40 mmol, 2.5 eq) was added dropwise, and the mixture was stirred at -30 °C for 30 min. EtOAc (50 mL) was then added, and the mixture was washed 5x with ice cold 10% NaCl. Organic layers were combined and dried over Na_2SO_4 , filtered, and concentrated under reduced pressure. The concentrated organic layer was added dropwise to hexanes (225 mL) stirring at rt to precipitate the product. The solid was collected by filtration over a frit (no celite), washed 2x with hexanes, and dried under high vacuum overnight to yield **II-118** as a white fluffy solid (3.32 g, 68%). The vial was stored wrapped in foil, and product degradation occurred after ~ 2 weeks (despite apparent stability by ^1H NMR). ^1H NMR (500 MHz, Chloroform-*d*) δ 8.30 – 8.11 (m, 1H), 8.01 – 7.86 (m, 1H), 7.86 – 7.76 (m, 2H), 6.49 (s, 1H), 3.82 (s, 2H).

Compound II-136.

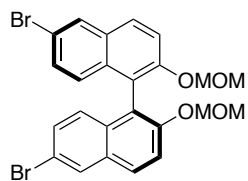


Compound **II-136** was synthesized according to the same procedure for compound **II-118**, beginning from 2-nitro-4-(trifluoromethyl)benzenesulfonyl chloride (500 mg, 1.73 mmol, 1.0 eq) to yield **II-136** as a white fluffy solid (319.0 mg, 65%). ^1H NMR (500 MHz, Acetonitrile-*d*₃) δ 8.31 – 8.24 (m, 1H), 8.24 – 8.21 (m, 1H), 8.13 (ddt, $J = 8.2, 1.8, 0.7$ Hz, 1H), 7.11 (s, 1H), 4.06 (s, 2H).

2.11.4 Synthesis BINOL catalysts for enantioselective Petasis reaction.

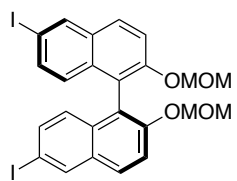
2.11.4.1 Synthesis of (*S*)-(CF₃)₃-BINOL.

Compound II-113.



(*S*)-1,1'-Bi(2-naphthol) (5.00 g, 17.5 mmol, 1.0 eq) was suspended in DCM (100 mL) stirred at -78°C . A solution of bromine (2.70 mL, 52.4 mmol, 3.0 eq) in DCM (25 mL) was added to the reaction flask dropwise over 30 minutes at -78°C . The reaction mixture was then raised from the dewar and allowed to come to rt over 2 hrs. The mixture was quenched with sat. aq. NaHSO_3 (50 mL), diluted with H_2O , and the organic layer was separated and washed with sat. NaCl , then dried over Na_2SO_4 , filtered, and concentrated under reduced pressure. The crude material was dissolved in DCM and triturated with hexanes to afford a white solid, which was taken forward with no further purification. NaH (60% dispersion in mineral oil, 2.00 g, 52.4 mmol, 3.0 eq) was suspended in THF (75 mL) and stirred at 0°C . To this suspension, a solution of (*S*)-6,6'-dibromo-2,2'-dihydroxy-1,1'-binaphthalene (assumed quantitative from previous reaction, 17.5 mmol) in THF (50 mL) was added dropwise. The mixture was stirred at 0°C for 2 hrs, then MOMCl (2.90 mL, 38.4 mmol, 2.0 eq) was added dropwise, and the reaction was allowed to come to rt overnight. The mixture was diluted with sat. NH_4Cl (50 mL) and extracted 3x with DCM. The combined organic layers were concentrated, and then triturated with hexanes to afford **II-113** as a light yellow solid (6.02 g, 65% over 2 steps). $^1\text{H NMR}$ (500 MHz, Chloroform-*d*) δ 8.03 (d, $J = 2.1$ Hz, 2H), 7.89 – 7.82 (m, 2H), 7.59 (d, $J = 9.1$ Hz, 2H), 7.29 (dd, $J = 9.0, 2.0$ Hz, 2H), 5.09 (d, $J = 6.9$ Hz, 2H), 4.98 (d, $J = 6.8$ Hz, 2H), 3.16 (s, 6H). All spectroscopic data matches literature data.^{18, 19, 56}

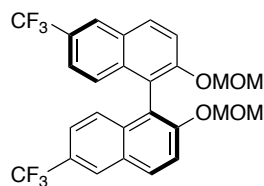
Compound II-114.



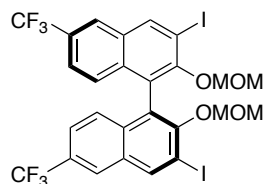
Compound **II-113** (6.00 g, 11.3 mmol, 1.0 eq) was suspended in THF (80 mL) and stirred at -78°C . $n\text{BuLi}$ (1.37 M, 24.75 mL, 33.9 mmol, 3.0 eq) was added dropwise at -78°C , and the mixture was stirred at -78°C for 2 hrs. A solution of iodine (8.63 g, 33.9 mmol, 3.0 eq) suspended in THF (18 mL), and was cannulated into the

reaction flask at $-78\text{ }^{\circ}\text{C}$ dropwise. The mixture was allowed to come to rt in the dewar and stirred overnight. The reaction mixture was quenched with sat. Na_2SO_3 (70 mL) and extracted 2x with Et_2O . The combined organic layers were washed with sat. NH_4Cl , NaCl , dried over Na_2SO_4 , filtered, and concentrated under reduced pressure. The crude material was purified on silica gel (10% EtOAc /hexanes) to yield **II-114** as a light yellow fluffy solid (3.79 g, 54%). $^1\text{H NMR}$ (500 MHz, $\text{Chloroform-}d$) δ 8.26 (d, $J = 1.7\text{ Hz}$, 2H), 7.89 – 7.79 (m, 2H), 7.57 (d, $J = 9.1\text{ Hz}$, 2H), 7.44 (dd, $J = 8.9, 1.8\text{ Hz}$, 2H), 6.83 (d, $J = 9.0\text{ Hz}$, 2H), 5.08 (d, $J = 6.9\text{ Hz}$, 1H), 4.98 (d, $J = 6.9\text{ Hz}$, 2H), 3.16 (s, 6H). All spectroscopic data matches literature data.^{18, 19, 56}

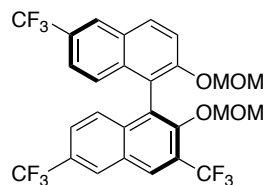
Compound II-115.



CuI (3.70 g, 19.4 mmol, 6.0 eq) was suspended in DMF (10 mL) with freshly distilled HMPA (3.4 mL, 19.4 mmol, 6.0 eq), and the mixture was stirred at rt for 10 min. Then, a solution of compound **II-114** (2.00 g, 3.2 mmol, 1.0 eq) in DMF (3 mL) was cannulated into the reaction mixture, and it was heated to $70\text{ }^{\circ}\text{C}$ with a reflux condenser. MFSDA (2.45 mL, 19.4 mmol, 6.0 eq) was added neat. The reaction mixture was stirred at $70\text{ }^{\circ}\text{C}$ for 24 hrs, and it was then filtered over celite (DCM). The filtrate was transferred to a separating funnel and washed 2x with sat. NaCl , then 0.1 M aq. HCl , dried over Na_2SO_4 , filtered, and concentrated under reduced pressure. Starting material consumption was monitored by NMR, and the crude material was resubjected to the above conditions if necessary. The crude material was purified on silica gel (30% EtOAc /hexanes) to yield **II-115** as a viscous yellow oil (1.66 g, quant.). $^1\text{H NMR}$ (500 MHz, $\text{Chloroform-}d$) δ 8.23 – 8.17 (m, 2H), 8.07 (d, $J = 9.1\text{ Hz}$, 2H), 7.70 (d, $J = 9.1\text{ Hz}$, 2H), 7.39 (dd, $J = 9.0, 1.9\text{ Hz}$, 2H), 7.20 (dq, $J = 8.9, 0.8\text{ Hz}$, 2H), 5.13 (d, $J = 7.0\text{ Hz}$, 2H), 5.04 (d, $J = 7.0\text{ Hz}$, 2H), 3.18 (s, 6H). All spectroscopic data matches literature data.^{18, 19, 56}

Compound II-116.

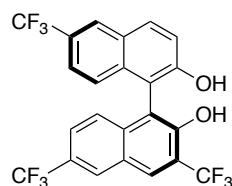
Compound **II-115** (1.00 g, 1.96 mmol, 1.0 eq) was suspended in THF (7 mL) and stirred at -78 °C. *s*BuLi (1.08 M in cyclohexane, 11.0 mL, 11.8 mmol, 6.0 eq) was added dropwise at -78 °C, and the mixture was stirred at -78 °C for 1 hr. A solution of iodine (2.98 g, 11.8 mmol, 6.0 eq) dissolved in THF (15 mL) and stirred at -78 °C, and it was then cannulated into to the flask. The reaction was allowed to come to rt in the dewar overnight. The reaction mixture was quenched with H₂O (35 mL) and sat. Na₂S₂O₃ (35 mL) and extracted 3x with Et₂O. The combined organic layers were dried over Na₂SO₄, filtered, and concentrated under reduced pressure. The crude **II-116** was taken directly on to the next step, but it would be recommended to purify by column chromatography (5% EtOAc/hexanes) in future iterations. ¹H NMR (500 MHz, Chloroform-*d*) δ 8.65 (d, *J* = 14.2 Hz, 2H), 8.15 – 8.06 (m, 2H), 7.45 (dddd, *J* = 16.8, 12.6, 8.9, 1.9 Hz, 4H), 4.85 – 4.81 (m, 2H), 4.80 – 4.77 (m, 2H), 3.74 (s, 6H). All spectroscopic data matches literature data.^{18, 19, 56}

Compound SII-2.

CuI (1.50 g, 7.9 mmol, 6.0 eq) was suspended in DMF (2 mL) with freshly distilled HMPA (1.4 mL, 7.9 mmol, 6.0 eq) and stirred at rt for 10 min. Then, a solution of compound **II-116** (assumed quantitative from previous reaction, 1.33 mmol, 1.0 eq) in DMF (8 mL) was cannulated into the reaction mixture, and it was heated to 80 °C with a reflux condenser attached. MFSDA (1.00 mL, 7.9 mmol, 6.0 eq) was neat, and the mixture was stirred at 80 °C for 24 hrs. The reaction mixture was filtered over a pad of celite (DCM), and the filtrate was transferred to a separatory funnel and diluted with 0.1M aq. HCl. The aqueous layer was extracted 2x with DCM, and the combined organic layers were washed with sat. NaHCO₃, sat. NaCl, then dried over Na₂SO₄, filtered, and concentrated under

reduced pressure. The crude brown oil was purified on silica gel (100% DCM) to give **SII-2** as a yellow oil (263 mg, 36% over 2 steps). **¹H NMR** (500 MHz, Chloroform-*d*) δ 8.45 (s, 1H), 8.37 – 8.30 (m, 1H), 8.26 – 8.22 (m, 1H), 8.15 (d, *J* = 9.3 Hz, 1H), 7.76 (d, *J* = 9.1 Hz, 1H), 7.56 (dd, *J* = 9.0, 2.0 Hz, 1H), 7.49 (dd, *J* = 9.1, 1.9 Hz, 1H), 7.35 (d, *J* = 8.7 Hz, 1H), 7.27 – 7.23 (m, 1H), 5.18 (d, *J* = 2.0 Hz, 2H), 4.70 (d, *J* = 5.2 Hz, 1H), 4.64 (d, *J* = 5.2 Hz, 1H), 3.30 (s, 3H), 2.85 (s, 3H). All spectroscopic data matches literature data.^{18, 19, 56}

Compound II-117.

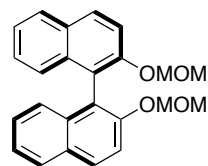


Compound **SII-2** (263 mg, 0.41 mmol, 1.0 eq) and Amberlyst 15 resin (250 mg) were stirred in a 1:1 mixture of THF/MeOH THF (8 mL). The mixture

was heated to 60 °C with a reflux condenser and stirred overnight. The resin was removed by filtration over cotton, and the filtrate was concentrated under reduced pressure. The crude material was purified on silica gel (100% DCM) to give **II-117** as a light yellow oil (100 mg, 50%). **¹H NMR** (500 MHz, Chloroform-*d*) δ 8.42 (s, 1H), 8.28 (d, *J* = 1.8 Hz, 1H), 8.20 (d, *J* = 1.7 Hz, 1H), 8.09 (d, *J* = 9.0 Hz, 1H), 7.55 (dd, *J* = 8.9, 1.8 Hz, 1H), 7.51 – 7.44 (m, 2H), 7.21 (d, *J* = 8.9 Hz, 1H), 7.17 – 7.12 (m, 1H). All spectroscopic data matches literature data.^{18, 19, 56}

2.11.4.2 Synthesis of (*R*)-Ph₂-BINOL for enantioselective *Petasis* reaction.

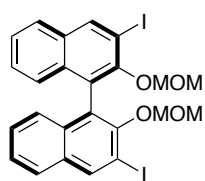
Compound II-132.



NaH (60% dispersion in mineral oil, 0.62 g, 15.4 mmol, 2.2 eq) was suspended in THF (60 mL) and stirred at 0 °C. To this, a solution of (*R*)-1,1'-bi(2-naphthol) (2.00 g, 7.0 mmol, 1.0 eq) in THF (10 mL) was added dropwise. The mixture was stirred at 0 °C for 2 hrs, then MOMCl (1.20 mL, 15.4 mmol, 2.2 eq) was added dropwise and the reaction was allowed to warm to rt overnight. The reaction was quenched with sat. NH₄Cl (15 mL) and extracted 3x with DCM. The combined organic layers were washed with sat. NaCl, dried

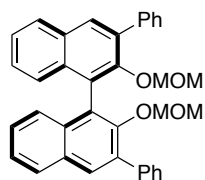
over Na₂SO₄, filtered, and concentrated under reduced pressure to yield **II-132** as a white solid (2.62 g, quant). ¹H NMR (499 MHz, Chloroform-*d*) δ 7.95 (d, *J* = 9.0 Hz, 2H), 7.87 (d, *J* = 8.2 Hz, 2H), 7.58 (d, *J* = 9.0 Hz, 2H), 7.34 (ddd, *J* = 8.1, 6.8, 1.2 Hz, 2H), 7.22 (ddd, *J* = 8.0, 6.9, 1.2 Hz, 2H), 7.15 (d, *J* = 8.5 Hz, 2H), 5.08 (d, *J* = 6.8 Hz, 2H), 4.98 (d, *J* = 6.8 Hz, 2H), 3.15 (d, *J* = 0.8 Hz, 6H). All spectroscopic data matches literature data.^{18, 19, 56}

Compound II-133.



Compound **II-132** (2.62 g, 7.0 mmol, 1.0 eq) was suspended in THF (52 mL) and stirred at -78 °C. *n*BuLi (2.21 M in hex, 9.50 mL, 21.0 mmol, 3.0 eq) was added dropwise at -78 °C, and the reaction was stirred at -78 °C for 30 min, then raised to 0 °C and stirred for an additional 2 hrs. The reaction was cooled to -78 °C, and neat iodine (5.32 g, 21.0 mmol, 3.0 eq) was added in one portion. The mixture was stirred at rt for 2 hrs, at which point the reaction was quenched with sat. Na₂S₂O₃ (75 mL). The aqueous layer was extracted 3x with EtOAc, and the combined organic layers were washed with sat. NaCl, dried over Na₂SO₄, filtered, and concentrated. The crude material was purified on silica gel (40% EtOAc/hexanes) and recrystallized from DCM/hexanes to give **II-133** as a yellow solid (1.76 g, 40%). ¹H NMR (499 MHz, Chloroform-*d*) δ 8.54 (s, 2H), 7.85 – 7.68 (m, 2H), 7.42 (ddd, *J* = 8.2, 6.8, 1.2 Hz, 2H), 7.30 (ddd, *J* = 8.2, 6.8, 1.3 Hz, 2H), 7.17 (dq, *J* = 8.6, 0.9 Hz, 2H), 4.81 (d, *J* = 5.7 Hz, 2H), 4.69 (d, *J* = 5.6 Hz, 2H), 2.60 (d, *J* = 1.1 Hz, 6H). All spectroscopic data matches literature data.^{18, 19, 56}

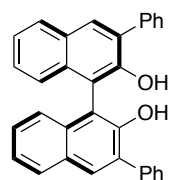
Compound II-134.



Compound **II-133** (0.50 g, 0.8 mmol, 1.0 eq) was dissolved in freshly distilled DME (5.25 mL). Pd(PPh₃)₄ (0.10 g, 0.08 mmol, 0.1 eq) was added, followed by phenylboronic acid (0.34 g, 2.8 mmol, 3.5 eq) and 2M Na₂CO₃ (2.00 mL). The

reaction mixture was heated to reflux and stirred overnight, then filtered over celite (DCM). The filtrate concentrated under reduced pressure, and the residue was dissolved in DCM and washed with sat. NH_4Cl . The aqueous layer was then extracted 2x with DCM, and the combined organic layers were washed with H_2O , sat. NaCl , then dried over Na_2SO_4 , filtered, and concentrated under reduced pressure. The crude material was purified on silica gel (15% Et_2O /hexanes) and recrystallized from DCM/hexanes to give **II-134** as a light purple oil (0.33 g, 78%). $^1\text{H NMR}$ (499 MHz, Chloroform-*d*) δ 7.95 (s, 2H), 7.89 (d, $J = 8.2$ Hz, 2H), 7.79 – 7.73 (m, 4H), 7.47 (t, $J = 7.7$ Hz, 4H), 7.42 (ddd, $J = 8.1, 5.6, 2.4$ Hz, 2H), 7.40 – 7.35 (m, 2H), 7.30 – 7.28 (m, 4H), 4.41 (d, $J = 5.8$ Hz, 2H), 4.37 (d, $J = 5.8$ Hz, 2H), 2.35 (s, 6H). All spectroscopic data matches literature data.^{18, 19, 56}

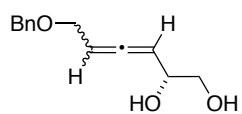
Compound II-135.



Compound **II-134** (0.33 g, 0.6 mmol, 1.0 eq) and Amberlyst 15 resin (310 mg) were stirred in a 1:1 mixture of THF/MeOH THF (10 mL). The mixture was heated to 60 °C with a reflux condenser and stirred overnight. The crude material was purified on silica gel (20% EtOAc/hexanes) and recrystallized from DCM/hexanes to give **II-135** as a light yellow solid (0.22 g, 79%). $^1\text{H NMR}$ (499 MHz, Chloroform-*d*) δ 8.02 (s, 2H), 7.95 – 7.89 (m, 2H), 7.77 – 7.70 (m, 4H), 7.49 (dd, $J = 8.4, 6.9$ Hz, 4H), 7.44 – 7.37 (m, 4H), 7.32 (ddd, $J = 8.1, 6.7, 1.3$ Hz, 2H), 7.23 (d, $J = 8.4$ Hz, 2H). All spectroscopic data matches literature data.^{18, 19, 56}

2.11.5 Synthesis of $\text{La}(\text{OTf})_3$ -derived allenols and advanced *cis*-solamin *B* intermediates.

Compound II-146.



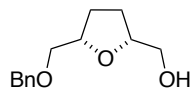
Compound **II-121** (1.95 g, 13.32 mmol, 1.5 eq) was stirred in THF (45 mL) at -78 °C. $n\text{BuLi}$ (2.5 M, 6.39 mL, 15.98 mmol, 1.8 eq) was added dropwise, and the reaction was stirred at -78 °C for 45 minutes. $\text{BF}_3 \cdot \text{Et}_2\text{O}$ (2.41 mL, 19.54 mmol, 2.2 eq)

was added neat at $-78\text{ }^{\circ}\text{C}$, and the mixture was stirred for 10 min and was then transferred to a dewar at $-30\text{ }^{\circ}\text{C}$ and stirred for 1 hr. Meanwhile, compound **II-118** (1.93 g, 8.88 mmol, 1.0 eq), D-glyceraldehyde (800.0 mg, 8.88 mmol, 1.0 eq), $\text{La}(\text{OTf})_3$ (67.0 mg, 0.888 mmol, 0.1 eq) and powdered 4 \AA molecular sieves were stirred in freshly distilled ACN (45 mL) – this mixture was allowed to stir for at least 2 hrs to form the hydrazone intermediate. The $\text{BF}_3\cdot\text{Et}_2\text{O}$ mixture was cannulated into the hydrazone reaction flask, and the reaction was stirred at rt overnight. The mixture was quenched with 0.5 M NaOH (50 mL) and was allowed to stir for 2 hrs, and it was then extracted 3x with Et_2O , dried over Na_2SO_4 , filtered, and concentrated. The crude product was purified on silica gel (5% MeOH/DCM) to yield **II-146** as a brown oil (586.8 mg, 30%). $^1\text{H NMR}$ (500 MHz, Chloroform-*d*) δ 7.40 – 7.27 (m, 5H), 5.50 (pd, $J = 6.3, 2.6$ Hz, 1H), 5.38 (dt, $J = 14.4, 5.6, 2.7$ Hz, 1H), 4.56 (s, 2H), 4.32 – 4.23 (m, 1H), 4.13 – 4.00 (m, 2H), 3.77 – 3.46 (m, 2H). $^{13}\text{C NMR}$ (126 MHz, CDCl_3 , mix of diastereomers) δ 203.84, 203.55, 137.85, 137.77, 128.61, 128.03, 127.99, 93.94, 93.65, 92.20, 91.85, 77.17, 72.55, 72.45, 69.93, 69.75, 67.37, 67.25, 66.30, 65.90.

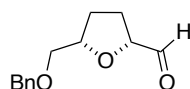
Compound II-147.



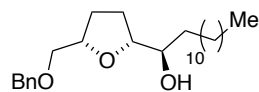
AuCl_3 (3.1 mg, 0.0102 mmol, 0.03 eq) was stirred in THF (1 mL) at rt. Compound **II-146** (74.6 mg, 0.339 mmol, 1.0 eq) was suspended in THF (2.5 mL), and the mixture was cannulated into the reaction flask and stirred at rt for 3 hrs. The crude mixture of diastereomers was concentrated under reduced pressure, and purified on silica gel (3% MeOH/DCM) to yield compound **II-147** as a brown oil (44.6 mg, 60%). $^1\text{H NMR}$ (500 MHz, Chloroform-*d*) δ 7.38 – 7.27 (m, 5H), 5.87 (dtd, $J = 7.8, 6.2, 1.6$ Hz, 2H), 5.02 – 4.89 (m, 2H), 4.66 – 4.46 (m, 2H), 3.89 (dt, $J = 12.0, 1.5$ Hz, 1H), 3.77 (dd, $J = 10.4, 2.9$ Hz, 1H), 3.64 (ddd, $J = 11.8, 9.5, 2.2$ Hz, 1H), 3.55 (td, $J = 10.4, 2.0$ Hz, 2H). $^{13}\text{C NMR}$ (126 MHz, CDCl_3) δ 137.34, 128.95, 128.89, 128.63, 128.09, 128.06, 87.57, 85.40, 77.16, 73.62, 71.68, 64.75.

Compound SII-3.

Compound **II-147** (52.2 mg, 0.237 mmol, 1.0 eq) was suspended in DCM (2 mL) and stirred at rt. Freshly distilled Et₃N (3.30 mL, 23.7 mmol, 100 eq) and compound **II-118** (1.03 g, 4.74 mmol, 20 eq) were added, and the mixture was stirred at rt overnight. Starting material consumption was monitored by TLC, with a second addition of fresh NBSH if the reaction had not proceeded to completion. The reaction mixture was diluted with Et₂O and NaHCO₃, and extracted 3x with Et₂O. The organic layers were combined and diluted with pentanes, then dried over Na₂SO₄, filtered, and concentrated. The crude material was purified on silica gel (5% MeOH/DCM) to yield **SII-3** as a brown oil (47.3 mg, 90%). ¹H NMR (500 MHz, Chloroform-*d*) δ 7.39 – 7.27 (m, 5H), 4.58 (d, *J* = 3.5 Hz, 2H), 4.20 – 4.06 (m, 2H), 3.81 – 3.76 (m, 1H), 3.62 (dd, *J* = 10.0, 3.6 Hz, 1H), 3.47 (dd, *J* = 10.0, 4.6 Hz, 2H), 1.99 – 1.82 (m, 4H).

Compound II-148.

DMP (180.5 mg, 0.426 mmol, 2.0 eq) was suspended in DCM (1 mL) and stirred at 0 °C. Compound **SII-3** (47.3 mg, 0.213 mmol, 1.0 eq) was suspended in DCM (1 mL), and the mixture was cannulated into the reaction flask and stirred for 2 hrs at rt. The crude reaction mixture was diluted with hexanes and filtered over celite (DCM), and the filtrate was concentrated under reduced pressure. The crude material was purified on silica gel (5% MeOH/DCM) to yield **II-148**, which was taken forward to the next step despite residual DMP-related impurities.

Compound II-149.

Dodecyl magnesium bromide (1.0 M in Et₂O, 0.426 mL, 0.426 mmol, 2.0 eq) was suspended in THF (0.5 mL) at -20 °C. In a separate flask, compound **II-148** (46.8 mg, 0.213 mmol, 1.0 eq) was suspended in THF (0.5 mL) at -20 °C, and this mixture

was cannulated into the Grignard reaction flask and stirred at -20 °C for 2 hrs. The mixture was slowly quenched with sat. NH_4Cl , and it was allowed to stir for 30 min at rt and was then extracted 3x with Et_2O , dried over Na_2SO_4 , filtered, and concentrated under reduced pressure. The crude product was purified on silica gel (5% MeOH/DCM) to yield **II-149** with minor impurities.

Chapter 3

Total Synthesis of Tambromycin Enabled by Indole C–H Functionalization

**Portions of this chapter are reproduced in part
with permission from *Organic Letters*:**

Miley, G.^[†], Rote, J.^[†], Silverman, R., Kelleher, N., Thomson, R. *Org. Lett.* **2018**, *20*, 2369-2373.

^[†] denotes equal contribution

3 Chapter 3

3.1 Introduction

Natural products (NPs) have served as sources of structurally variable and biologically potent drugs and pharmaceutical leads for decades.¹ An estimated two-thirds of drugs currently on the market are identified as NP-derived, and the continued discovery of novel NPs is crucial to furthering the development of biologically potent chemical scaffolds.^{1, 2} However, traditional screening techniques for NP discovery often result merely in rediscovery of robustly expressed NPs, leading to a lack of novel NP-derived drug leads. To continue supporting a pipeline of natural NP-based drug molecules, a more targeted discovery approach, namely metabologenomics, is needed to access NPs with yet-unobserved structure and function.^{1, 3-12}

This chapter will discuss the metabologenomics-driven discovery and subsequent total synthesis of a novel peptide NP, tambromycin. The unique structural characteristics and biological activity of tambromycin highlights the success of the metabologenomics platform for targeted natural product discovery. The total synthesis highlights the application of C–H functionalization, as well as stereocontrolled amination, en route to accessing this complex peptide-derived NP. Future directions, including structure–activity relationship studies and proteomics-driven target identification for tambromycin, will also be addressed.

3.1.1 Metabologenomic-driven discovery of novel NPs.

Microbially-produced small molecule NPs are a significant source of bioactive and medicinal compounds. For example, classes of bacteria such as the actinomycetes are prolific producers of diverse, medicinally-relevant NPs such as erythromycin, doxorubicin, and the actinomycins.¹³ Traditional microbial-NP discovery methods rely on growth, fractionation, and

screening bacterial extracts for biological activity. The success rate of such methods for novel compound identification, however, has diminished significantly in recent years, with fewer NP-based drugs moving through the pharmaceutical pipeline. A key limitation of these traditional screening techniques is the rediscovery of abundantly expressed metabolites, obscuring the detection of novel, medicinally-valuable compounds.¹⁴ Indeed, as metabolite-encoding biosynthetic gene clusters (BGCs) become easier to detect via low-cost genome sequencing, a disparity is growing between the number of known bacterial BGCs and the current number of discovered metabolites that may have medicinal value.¹⁴

To overcome the challenge of NP rediscovery, a targeted method of metabolite detection was developed by the Kelleher and Metcalf labs that combines bacterial genome sequencing and gene cluster prediction with mass spectrometry (MS)-based metabolomics. This platform, termed “metabologenomics,” uses large-scale correlation between BGC genomic sequences and metabolomics liquid chromatography (LC)-MS data to ultimately provide a score indicating the likelihood of association between a particular metabolite and gene cluster.¹⁴⁻¹⁶ This technique facilitates targeted metabolite discovery in two ways: (1) a unique mass fragment or m/z value can be traced back to its biosynthetic origin, and (2) a promising family of BGCs can be probed for interesting metabolite output. Because both the biosynthetic pathway (including substrate selectivity) and metabolite m/z information are embedded in metabologenomics, structural identification of these bacterially-produced compounds can be rapidly hypothesized. This method of novel NP discovery has led to the isolation of many actinomycete-produced compounds, including the peptide NP tambromycin (**III-1**).

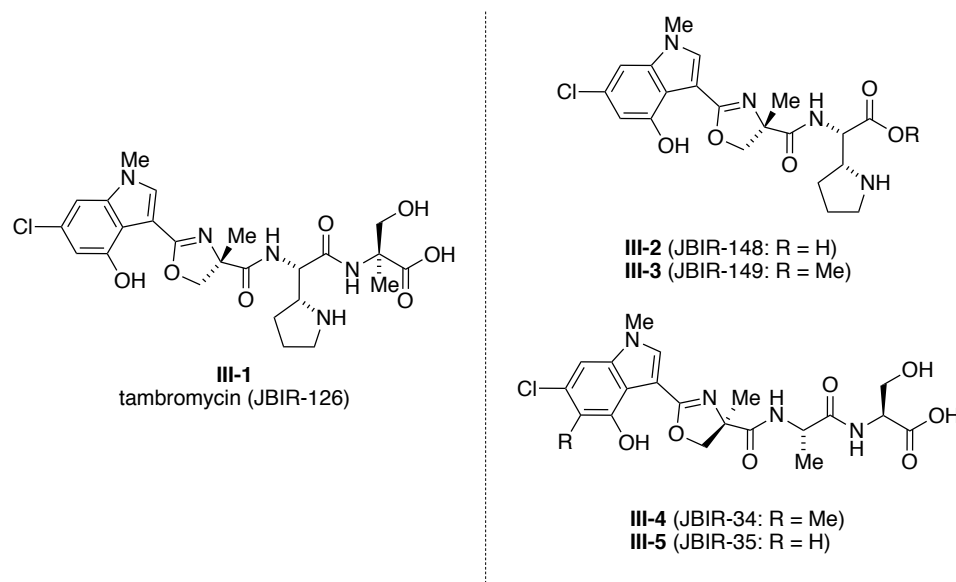
3.2 Tambromycin – Discovery, structural elucidation, and biosynthesis.

3.2.1 Discovery of tambromycin via metagenomics.

The discovery of tambromycin began with analysis of both the genetic content and metabolite data for 178 actinomycete strains¹⁴ The genome of each strain was analyzed and categorized into BGC families, with 11,422 NP BGCs identified across five different gene cluster families.¹⁴ Quantitative LC-MS of the strain library revealed 2,520 individual metabolites with masses ranging from 250.074 to 4538.881 Da.¹⁴ Correlation across gene cluster family/metabolite data revealed that the tambromycin ion, with a m/z of 536.190, was expressed by 7 out of 9 strains that each encoded the same BGC, representing a family of megaenzymes known as non-ribosomal peptide synthetase (NRPS). Tambromycin was subsequently isolated from the fermentation broth of *Streptomyces* strain F-4474 using a solid phase resin and purified via semipreparative reverse-phase HPLC.¹⁴

3.2.2 Tambromycin structural elucidation and related compounds.

Using high-accuracy mass spectrometry, the molecular formula for tambromycin was determined to be C₂₄H₃₀N₅O₇Cl. A combination of NMR studies (¹H, ¹³C, HMBC, TOCSY, NOESY, COSY) were used to identify the structure of naturally isolated tambromycin (**III-1**), shown in Figure 3.1. Both HMBC and tandem MS were employed to definitively assign the sequence of the peptide chain. The peptide scaffold is characterized by four nonproteinogenic amino acids (AAs) – a tryptophan-derived substituted indole, an oxazoline moiety arising from the dehydrogenative cyclization of α -methyl-serine, a lysine-derived pyrrolidine residue (termed tambroline, two-amino-beta-homoproline), and a terminal α -methyl-serine residue.¹⁴

Figure 3.1 Structure of tambromycin and related compounds.

Results of all structural elucidation studies were convergent with reports published concurrently by Izumikawa, et al. that outlined the independent discovery and characterization of an identical compound, JBIR-126 (**III-1**), isolated from *Streptomyces* sp. NBRC111228.¹⁷ Interestingly, JBIR-126 was isolated in conjunction with several other peptide NP derivatives (JBIR-148 **III-2**, JBIR-149 **III-3**, JBIR-34 **III-4**, JBIR-35 **III-5**) (Figure 3.1).^{17, 18} JBIR-126 (hereafter referred to as tambromycin) is the most structurally complex of this family of compounds – JBIR-148 and -149 are tripeptide derivatives lacking the terminal α -methyl-serine residue, while JBIR-34 and -35 do not incorporate the tambroline moiety. In biological assays against cancerous B- and T-cell lines, tambromycin exhibited modest inhibitory activity at 37 μ M, while JBIR-148 and -149 showed a 29 and 37% inhibition rate at 50 μ M, respectively.^{14, 17} In contrast, JBIR-34 and -35 exhibited no inhibition of cell growth, even at concentrations up to 2.5mM.¹⁸ Thus, compounds that incorporate the novel tambroline residue (i.e. tambromycin, JBIR-148, JBIR-149) exhibit moderate inhibition activity against B- and T-cell lines, while those lacking

this unique residue (JBIR-34, JBIR-35) show no cytotoxicity. This trend suggests that the tambroline residue may exert a uniquely cytotoxic influence on this peptide NP structure. This observation that will be discussed in further detail in Section 3.4.2. With the structure of tambromycin fully elucidated, the exact mechanism of biosynthesis was examined to understand how each AA residue was selected, modified, and loaded onto the NP structure.

3.2.3 Determining the biosynthetic pathway of tambromycin.

3.2.3.1 NRPS-produced NPs.

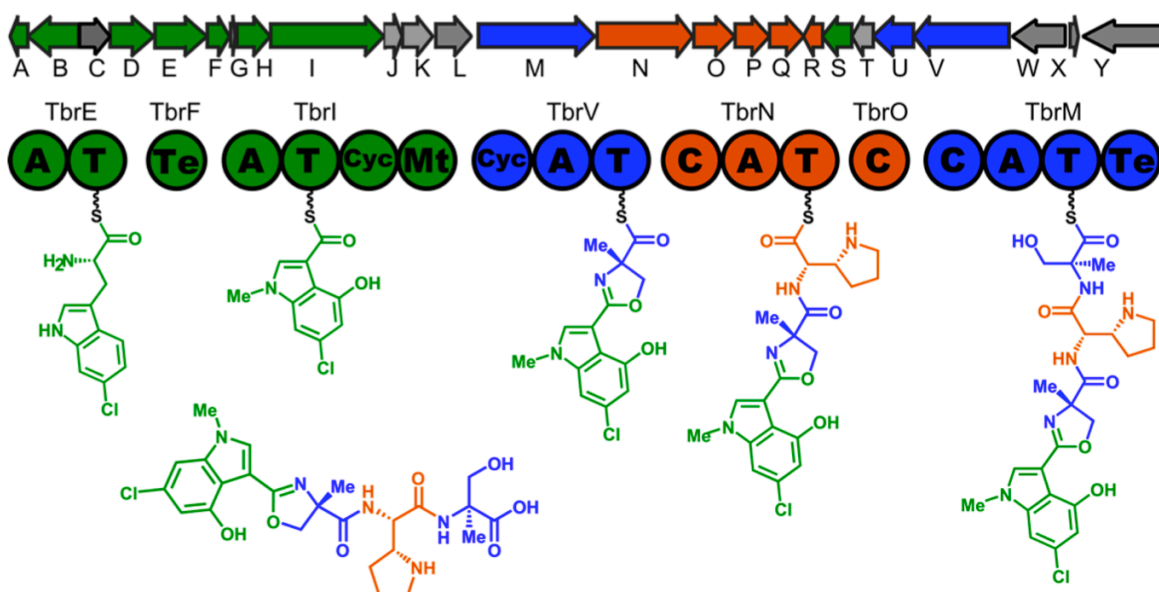
The m/z fragments of tambromycin were correlated to a BGC belonging to an NRPS, a class of enzymes that biosynthesize NPs using modular architectures of repeating catalytic domains to condense a peptide together in a growing assembly-line.¹⁹⁻²¹ The core NRPS structure consists of (1) an adenylation domain that is responsible for AA selection and activation (2) a condensation domain that forms peptide bond between adjacent residues (3) an epimerization domain and (4) a thioesterase domain that cleaves the assembled NP from the NRPS machinery.¹⁹⁻²¹ Taken together, these modules biosynthesize an NP whose structure can be confirmed via analysis of both the NRPS domain architecture and of the adenylation domain selectivity.¹⁹

3.2.3.2 NRPS assembly of tambromycin – Incorporation of four nonproteinogenic AAs.

Figure 3.2 depicts the domain substructures for each of the main NRPS carrier proteins involved in tambromycin biosynthesis. The tambromycin BGC encodes five A-domain containing NRPS proteins: TbrE, TbrI, TbrM, TbrN, and TbrV.¹⁴ TbrE activates and loads tryptophan, which then undergoes modification mediated by tryptophan halogenase and tryptophan oxygenase to produce the substituted indole. Once modified, the tryptophan derivative is released and converted into the indole acid, which is then loaded onto TbrI via a second A-domain. Following *N*-

methylation, TbrV selects for the first α -methyl-serine residue, and this undergoes a dehydrative cyclization to form an oxazoline residue. TbrN then incorporates the tambroline residue via a lysine cyclization (confirmed via stable isotope labeling studies, see Section 3.3.3.2),¹⁴ although it is yet unknown whether TbrN loads tambroline before or after the cyclization event. The final protein, TbrM, loads the terminal α -methyl-serine residue and cleaves the mature peptide from the NRPS via a TE domain.¹⁴

Figure 3.2 Biosynthetic pathway for tambromycin.

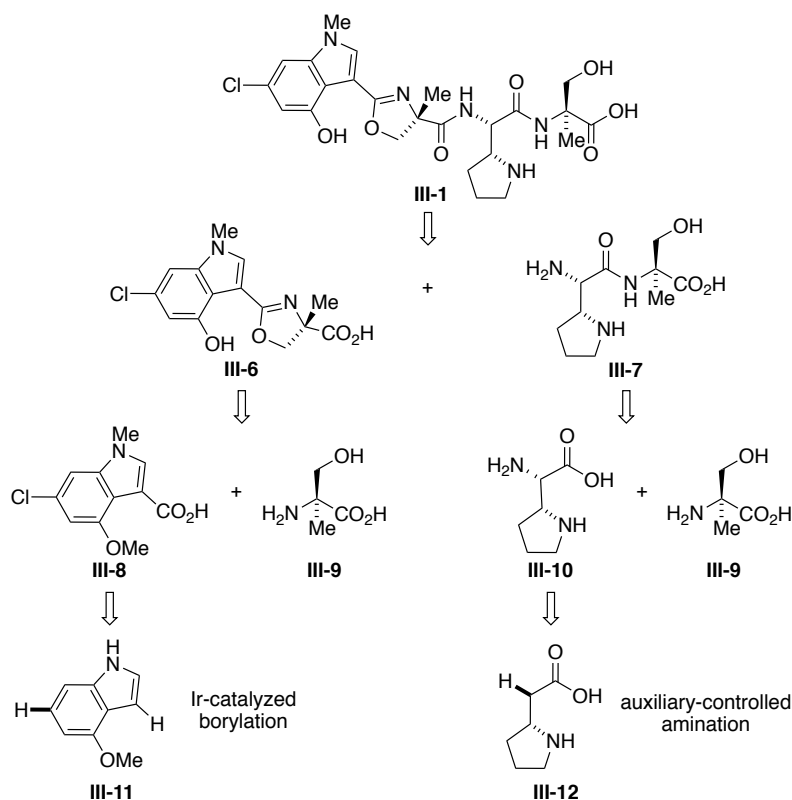


3.3 Total synthesis of tambromycin.

3.3.1 Retrosynthesis

The combination of its unique structure, unusual biosynthesis and preliminary biological results made tambromycin an attractive target for total synthesis. The following work was carried out in collaboration with Dr. Galen Miley, a former graduate student in the Kelleher and Silverman labs. Retrosynthetic analysis of tambromycin (**III-1**) led to disconnection of the central amide bond linking the oxazoline subunit **III-6** to the tambroline terminus **III-7** (Scheme 3.1). Further disconnection of these fragments led to functionalized indole acid **III-8**, two α -methylserine residues (**III-9**) and tambroline (**III-10**). The key challenges were accessing an efficient route to the 1,3,4,6-substituted indole **III-8**, and establishing a stereoselective route to tambroline (**III-10**). The indole-oxazoline and the tambroline- α -methylserine dipeptides are discussed in detail below.

Scheme 3.1 Retrosynthetic analysis of tambromycin.



3.3.2 Accessing the indole-oxazoline fragment of tambromycin.

3.3.2.1 Tambromycin indole substitution and connectivity: Related NP structures.

The tryptophan-derived indole fragment **III-6** of tambromycin exhibits a rare pattern of substitution as compared with other peptide NPs across the literature. To our knowledge, the only compounds exhibiting both the 4,6-substitution pattern on the indole arene *and* the C3-connectivity of an oxazoline moiety are tambromycin and its family members JBIR-148, -149, and -35 (**III-2**, **-3**, **-4**). However, the halogenation and hydroxylation pattern of the indole ring system of tambromycin is reminiscent of those found within breitfussin B (**III-13**),²² aspido-stomide G (**III-14**)²³ and inducamide C (**III-15**) (Figure 3.3).²⁴ Breitfussin B also incorporates a C3-substituent on its indole core, albeit a more highly oxidized oxazole moiety.

Despite this exact substitution pattern appearing in few NPs to date, the biological relevance of this type of halogenated core has been established in many other available therapeutics.^{25, 26} Examples include anticancer compounds such as the β -lactone salinosporamide A^{26, 27} and the indolocarbazole rebeccamycin (**III-16**),^{26, 28} as well as antibiotic compounds such as vancomycin,^{26, 29, 30} chlortetracycline (**III-17**),^{25, 26} and pyrrolnitrin (**III-18**) (Figure 3.3).^{25, 31} In fact, multiple studies have confirmed a direct correlation between the presence of chlorine substituents and biological activity – vancomycin requires two chlorines to maintain antibacterial activity,^{26, 32} and deschloro rebeccamycin loses all antibacterial activity.^{26, 33} The indole core of tambromycin therefore potentially offers both biological relevance (via the chlorine substituent) and a novel substitution scaffold (via the 4-,6-substitution pattern).

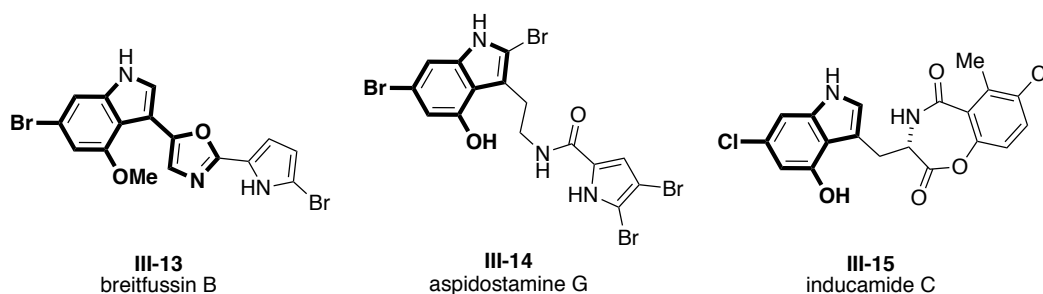
The 4-methyloxazoline monomer attached to the indole at C3 is another rare structural feature, as most secondary metabolites incorporate 5-methyl oxazole or oxazolines – parabactin,

vibriobactin (**III-19**), and siphonazole (**III-20**) are among many NP drugs with the 5-methyl motif (Figure 3.3).³⁴⁻³⁸ The reason for this disparity in 4-methyl versus 5-methyl oxazolines is a result of their biogenesis: 5-methyl oxazolines arise from the cyclization of threonine,^{39, 40} while the 4-methyl counterparts result from a cyclization of a non-proteinogenic AA, α -L-methyl-serine.^{14, 17,}

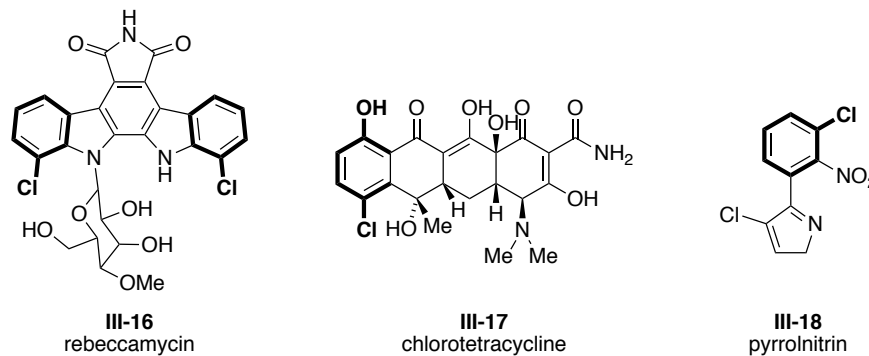
18, 34

Figure 3.3 Natural products structurally related to the indole-oxazoline core.

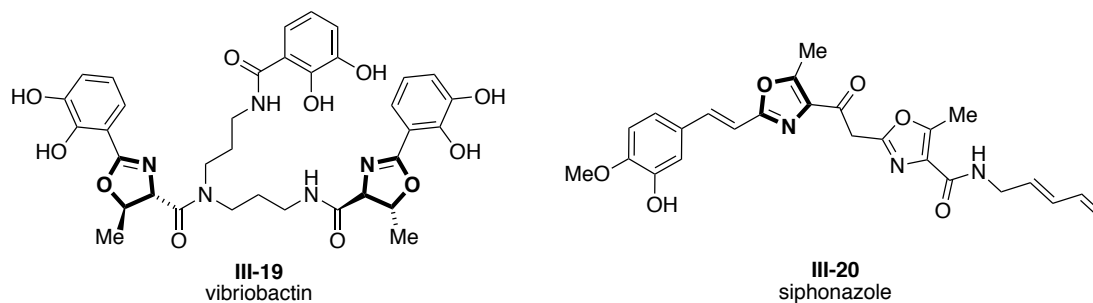
a. Indole natural products with 4,6-substitution pattern.



b. Halogenated cores of bioactive natural products.



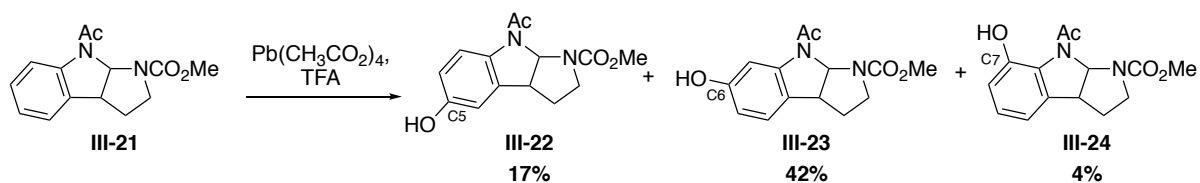
c. Oxazoline-containing natural products.



3.3.2.2 Synthetic strategy to access the 1,3,4,6-substituted indole fragment of tambromycin.

The unique 4-hydroxy-6-chloro substitution pattern on tambromycin presented a distinct challenge for total synthesis – in particular, selectively functionalizing the C6–H bond of the tryptophan system was anticipated to be a major hurdle, as it is well known that the indole reacts preferentially at the C2,⁴¹⁻⁴³ C3,⁴¹⁻⁴³ and C7⁴⁴⁻⁴⁷ positions. Indeed, the C6 position is one of the most difficult positions to functionalize on an indole, with electrophilic aromatic substitution or *ortho*-metalation reactions proceeding regioselectively at the C6 position only in cases where an electron-withdrawing group (EWG) is present at N1 or C3.⁴⁸ To target the C6-chlorinated indole motif of tambromycin, *de novo* methods for indole ring construction were first considered in order to pre-install the requisite 4-hydroxy-6-chloro pattern (including Leimgruber-Batcho, Reissart, Sugawara, Gassman, Fischer, Japp-Klingemann, and Buchwald indole syntheses).⁴⁹ However, gaining access to our desired indole scaffold required reasonably complex starting materials that would ultimately be incompatible with *de novo* ring construction, due to complicating regioselectivity considerations.

Scheme 3.2 Hino, et al. route to regioisomeric mixture of substituted indole products.

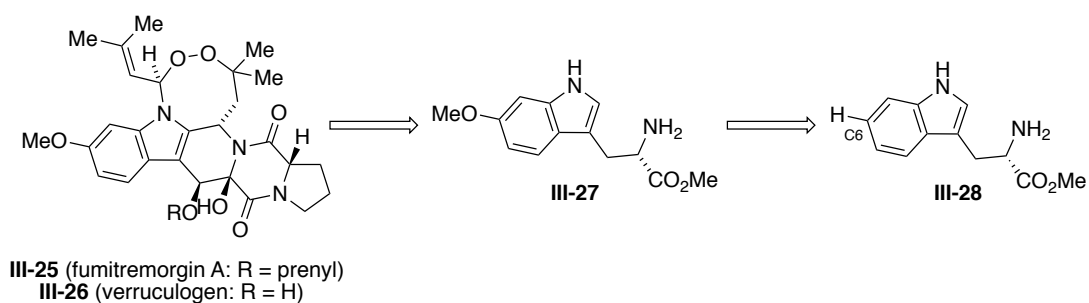


Instead, a direct method of indole C6-functionalization was considered – a route that, if successful, would offer a more elegant and straightforward approach towards tryptophan derivatization versus indole-ring construction methods. A literature survey revealed very few instances of regioselective C6-functionalization. In 1984, Hino et al. published a method for

tryptophan hydroxylation via lead tetraacetate oxidation that resulted in a complex mixture of regioisomers at the C5, C6, and C7 positions (Scheme 3.2).⁵⁰ Although aiming to access C5-hydroxylated tryptophan derivatives in their work, the Hino group discovered that treatment with $\text{Pb}(\text{CH}_3\text{CO})_4$ in trifluoroacetic acid (TFA), followed by methoxy protection using methyl iodide (MeI) and K_2CO_3 in acetone provided a separable mixture of C5 (**III-22**), C6 (**III-23**), and C7 (**III-24**) regioisomers in 17%, 42% and 4% respectively.⁵⁰ The successful formation of a C6-derivative in this work indicated the feasibility of accessing a C6 indole adduct with some level of regiocontrol.

In 2015, the Baran group published the first known route towards regioselective indole C6-hydroxylation via ligand-controlled C–H borylation, en route to the NPs verruculogen (**III-26**) and fumitremorgin (**III-25**) (Scheme 3.3).⁴⁸ In order to introduce their methoxy-protected hydroxyl precursors directly onto the indole core, the Baran group utilized a method of indole C–H functionalization developed by Movassaghi et al. in 2014.⁴⁷

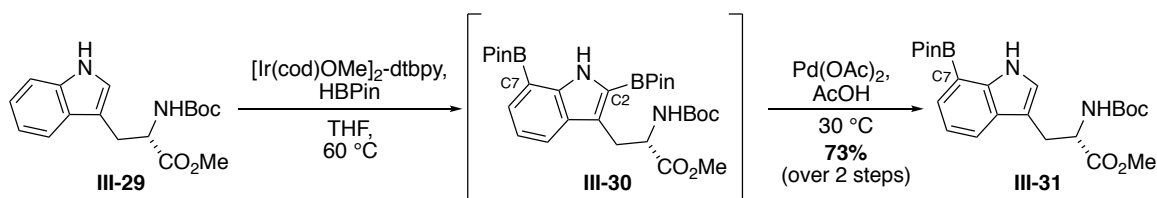
Scheme 3.3 Retrosynthesis by Baran, et al. to access fumitremorgin A and verruculogen.



In their work, the Movassaghi group accomplished regioselective C7-indole substitution via iridium-catalyzed C–H activation/pinacol borylation (Scheme 3.4).^{44, 45, 47, 51, 52} They exploited the known propensity for five-membered heterocycles to readily undergo C2 protodeborylation

to develop a sequence of diboration/protodeborylation that effectively introduced a pinacol borane group to the C7-indole position only.⁴⁷ Iridium-catalyzed borylation with $[\text{Ir}(\text{cod})\text{OMe}]_2 \cdot \text{dtbpy}$ and 4,4,5,5-tetramethyl-1,3,2-dioxaborolane (HPBin) of a C3-substituted indole proceeded first at C2 and then at C7, and following an acidic work-up, this diborated indole **III-30** underwent *ipso*-protonation, rearomatization, and cleavage of the C2 boron-carbon bond to afford 7-boronindole **III-31**.⁴⁷

Scheme 3.4 Movassaghi, et al. route to C7-substituted indoles via Ir-cat. borylation.

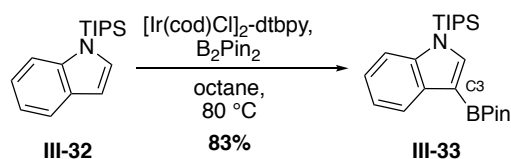


In the Baran group's application of this Ir-cat. C–H borylation methodology, an emphasis was placed on developing an even more direct route towards indole regioselectivity, with a particular focus on the C6–H bond. Although the Movassaghi group relied on C2 protodeborylation to access their C7 product, they noted that their Ir-cat. indole borylations could proceed selectively at the C7-position if the more reactive C2-position is either substituted, or disfavored via a directing and/or protecting group on the indole.⁴⁷ In particular, large silane protecting groups at the N1-indole position could direct Ir-cat. C–H activation away from adjacent indole carbons via steric bulk.^{41, 53} In 2002, Miyaura, et al. discovered that when exposed to $[\text{Ir}(\text{cod})\text{Cl}]_2 \cdot \text{dtbpy}$ and bis(pinacolato)diboron (B_2Pin_2), *N*-triisopropyl silane (TIPS) indole (**III-32**) underwent regioselective borylation only at C3 – the large TIPS protecting group effectively blocked the reactive C2 and C7 positions from undergoing C–H activation (Scheme 3.5).⁴¹ Likewise, in 2014 the Jia group discovered that treating *N*-TIPS protected C3-substituted indole

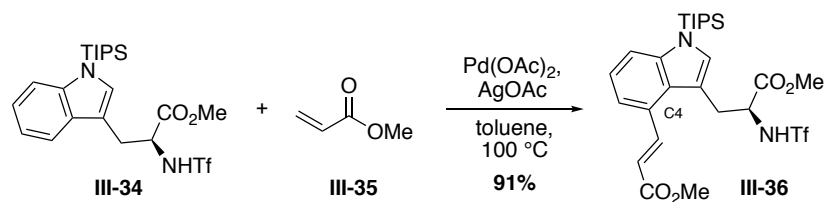
III-34 with palladium(II) acetate ($\text{Pd}(\text{OAc})_2$) and silver acetate (AgOAc) promoted regioselective C4-olefination, again avoiding any C2- or C7-substituted products due to the sterically demanding *N*-TIPS group (Scheme 3.5).⁵³

Scheme 3.5 Indole functionalization directed by *N*-TIPS protecting group.

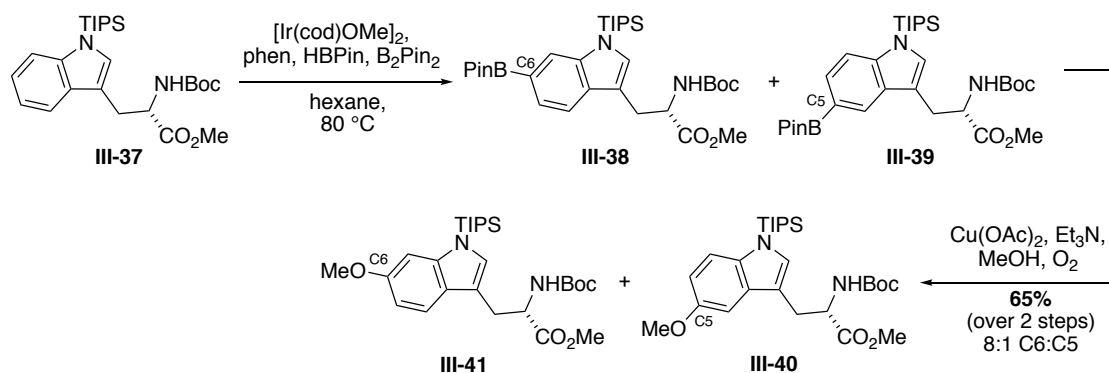
a. Miyaura route to C3-borylation



b. Jia route to C4-olefination



Thus, in accessing a C6-substituted indole, the Baran group applied the Movassaghi and Miyaura/Jia methods of C–H functionalization/borylation directed by an *N*-silane protected indole. They postulated that the *N*-TIPS group would block the C2- and C7-positions from activation, and that by using a C3-substituted indole starting material, the next most reactive and available C–H bond for activation would be the C6 position.⁴⁸ Indeed, treating their substituted indole starting material with $[\text{Ir}(\text{cod})\text{OMe}]_2$, 1,10-phenanthroline (1,10-Phen), HBPIn and B_2Pin_2 afforded the desired product in a 77% yield, with an 8:1 mixture of C6:C5 regioisomers (**III-38**, **III-39**) (Scheme 3.6).⁴⁸

Scheme 3.6 Baran, et al. route towards regioselective indole C6-functionalization.

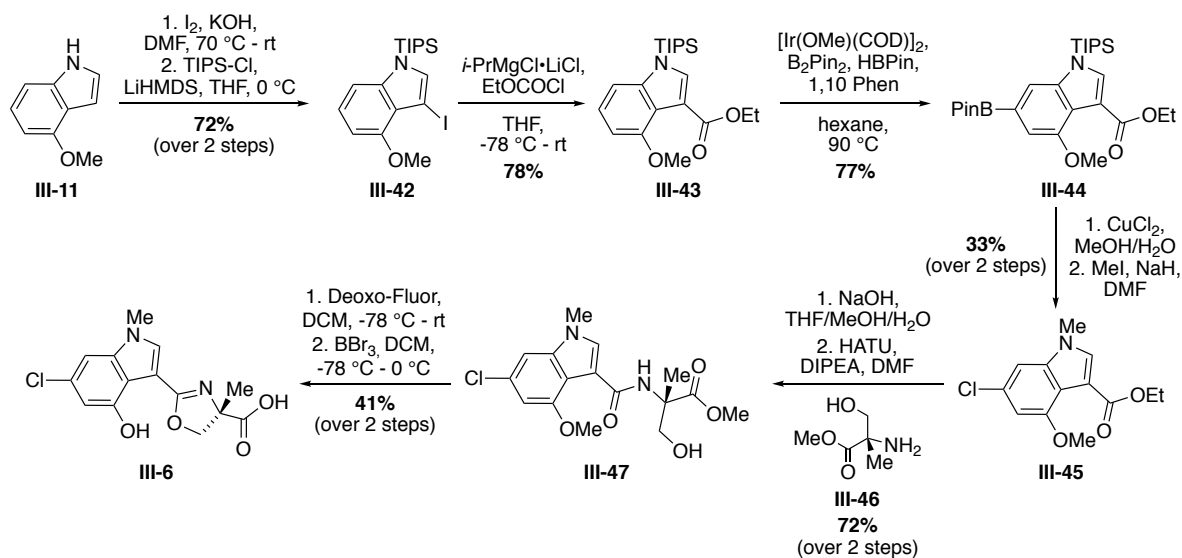
This C6-BPin intermediate immediately underwent Chan-Lam coupling with methanol to afford the final C6-methoxy indole **III-40**. The Baran group's method of regioselective C6-borylation for tryptophan motifs can be readily applied in the pursuit of many synthetic targets; with an indole based-system tuned to install a reactive boronate handle at the C6-position, a wide range of deborylation transformations are available. Additionally, their exploration of substrates showed the reaction to be quite general for a host of indoles and carbazoles. We thus postulated indole **III-11** should be an excellent substrate for applying the Baran lab's borylation chemistry, with an expectation that our 4-methoxy indole starting material would further direct borylation to the desired C6 position.

3.3.2.3 Synthesis of tambromycin indole-oxazoline fragment III-6.

Synthesis towards the indole-oxazoline fragment **III-6** was carried out by Dr. Galen Miley, beginning with a regioselective substrate-controlled iodination of 4-methoxyindole (**III-11**) with molecular iodine (Scheme 3.7). The intermediate 3-iodoindole proved unstable and was therefore converted directly to the chromatographically stable TIPS derivative **III-42** upon treatment with TIPSCl (72% over two steps). Magnesium-halogen exchange using isopropylmagnesium chloride

lithium chloride complex (*i*-PrMgCl•LiCl) under Knochel's conditions^{54, 55} and subsequent quenching of the intermediate Grignard reagent with ethyl chloroformate delivered 3-carboxy intermediate **III-43** in 78% yield, setting the stage for the crucial Ir-catalyzed transformation.⁵⁶ Treating with the conditions outlined by Baran and coworkers, full consumption of our starting material **III-43** was observed within 2 hours using 5 mol% of [Ir(OMe)(COD)]₂ to deliver the desired boronate **III-44** as a single regioisomer. The enhanced preference for borylation at C6 over C5 in our system can be explained by the added steric hindrance around the C5 C–H bond, due to the C4-methoxy substituent present on our substrate. This reaction proved to be highly efficient and scalable, as the product was delivered in 77% yield on a 4.85 g scale, providing sufficient flux of material for our synthesis while highlighting the power of modern methods for complex C–H functionalization.⁵⁷

Scheme 3.7 Our synthesis of indole-oxazoline fragment **III-6**.



While the borylation step was straightforward, conversion of the boronate group in **III-44** to the requisite chlorine substituent proved to be more problematic. Exposure of **III-44** to copper(II) chloride in a 1:1 mixture of methanol (MeOH) and water at 90 °C led to successful chlorination⁵⁸ but was complicated by isolation issues resulting from partial hydrolysis of the TIPS group and formation of a purple copper–indole complex that was observed to develop as the reaction progressed. Initial attempts to liberate the desired product from the reaction mixture using aqueous acid or base washes led to poor isolated yields of the major product. Viewing the partial hydrolysis of the TIPS group as an opportunity to streamline the synthesis, we optimized the timing of the reaction to ensure complete silyl cleavage prior to work-up. Subsequent rigorous extraction of the reaction mixture with a 0.1 M ethylenediaminetetraacetic acid (EDTA) solution allowed the effective removal of copper salts and ultimately enabled the chlorinated indole **III-S1** to be isolated on a 2 g scale. *N*-Methylation with MeI and NaH provided indole **III-45** in 33% yield over two steps. Base-mediated hydrolysis of the ethyl ester within **III-45** delivered the first of the desired building-blocks, indole **III-S2**. The coupling of the indole carboxylic acid to α -L-methyl-serine methyl ester (**III-46**) was next explored, as a prelude to installing the necessary oxazoline group. We desired to elicit this amide bond formation without the need to first protect the free primary alcohol within **III-46**, and to this end a number of reagents and conditions were investigated to find those favoring amide formation over the undesired esterification. Ultimately, it was found that using 1-hydroxy-7-azabenzotriazole (HATU) with sonication cleanly produced linear dipeptide **III-47** in excellent yield (72% over two steps) with no observed formation of the corresponding ester.⁵⁹ Initial attempts at forming the oxazoline ring **III-S3** focused on first mesylating the α -L-methyl-serine residue, but cyclization of this intermediate proved inefficient. Instead, it was found that exposure of **III-47** to [bis(2-methoxyethyl)amino]sulfur trifluoride (Deoxo-Fluor) directly

generated desired the desired oxazoline **III-S3** in a single step.⁶⁰ Finally, treating **III-S3** with rigorously redistilled boron tribromide induced concomitant cleavage of both the methoxy ether and methyl ester to cleanly deliver key fragment **III-6** in 41% yield over two steps.

3.3.3 Accessing the tambroline fragment of tambromycin.

3.3.3.1 Tambroline biosynthesis and related modified lysine-containing NPs.

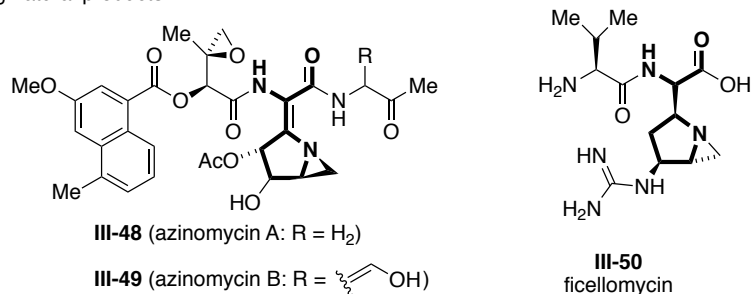
To our knowledge, tambromycin and its derivative compounds, JBIR-148 and -149, are the only NPs known to incorporate the unique lysine-derived tambroline residue. The closest examples of this type of pyrrolidine residue incorporated into NPs are seen in azinomycin A (**III-48**), B (**III-49**), and ficellomycin (**III-50**), three structurally related genotoxic molecules that contain the azabicyclo-modified pyrrolidine residue (Figure 3.4).⁶¹ Comparison between the hypothesized biosynthetic pathways of tambroline and azinomycin B reveal highly similar acyl-CoA dehydrogenase (ACAD) genes encoded in the BGCs for both NPs, hinting that these pyrrolidine moieties may be of similar biosynthetic origin, i.e. a dehydrogenative lysine cyclization.¹⁴ However, the azinomycin A/B BGC contains a second pair of ACAD proteins, ultimately suggesting that the linear biosynthetic precursor for this compound is in fact an extended acetyl-glutamate residue as opposed to a lysine monomer.⁶²

There are, however, are a handful of NPs that incorporate modified lysine residues into their structures. Given the reactive nature of the primary amino-side chain of lysine, this residue can be involved in intramolecular cyclization reactions to increase NP structural complexity. For example, lysine residues in compounds like streptide (**III-51**)^{63, 64, 65} and darobactin (**III-52**)^{66, 65} cross-link with distant, unactivated tryptophan residues following activation by radical *S*-adenosylmethionine (SAM) enzymes (Figure 3.4). The macrocyclic compounds formed via the

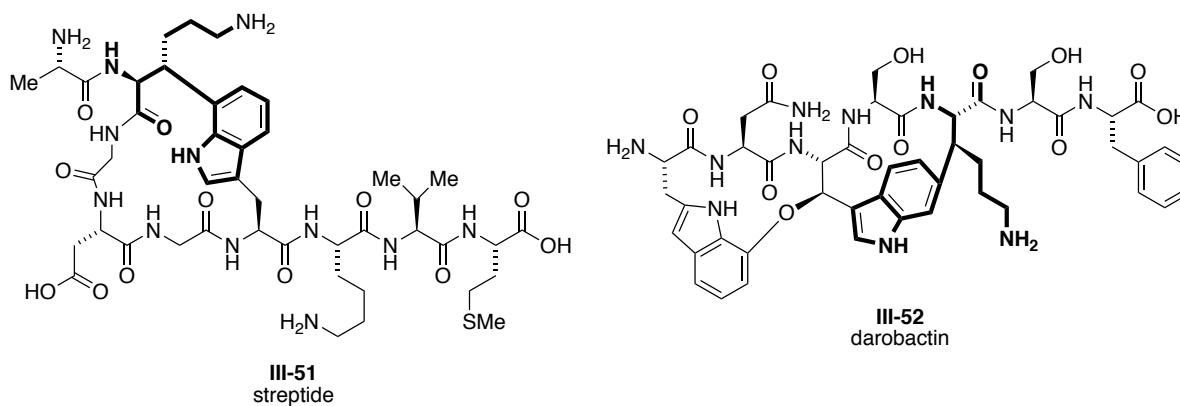
C3-Lys and C7-Trp connectivity are hypothesized to have increased antibacterial activity, as their cyclized structures are more highly resistant to protease breakdown.

Figure 3.4 Modified lysine-containing NPs.

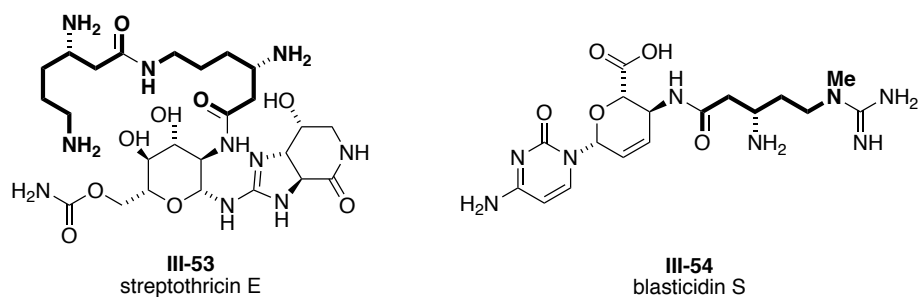
a. Pyrrolidine-containing natural products



b. Cross-linked Lys/Trp natural products



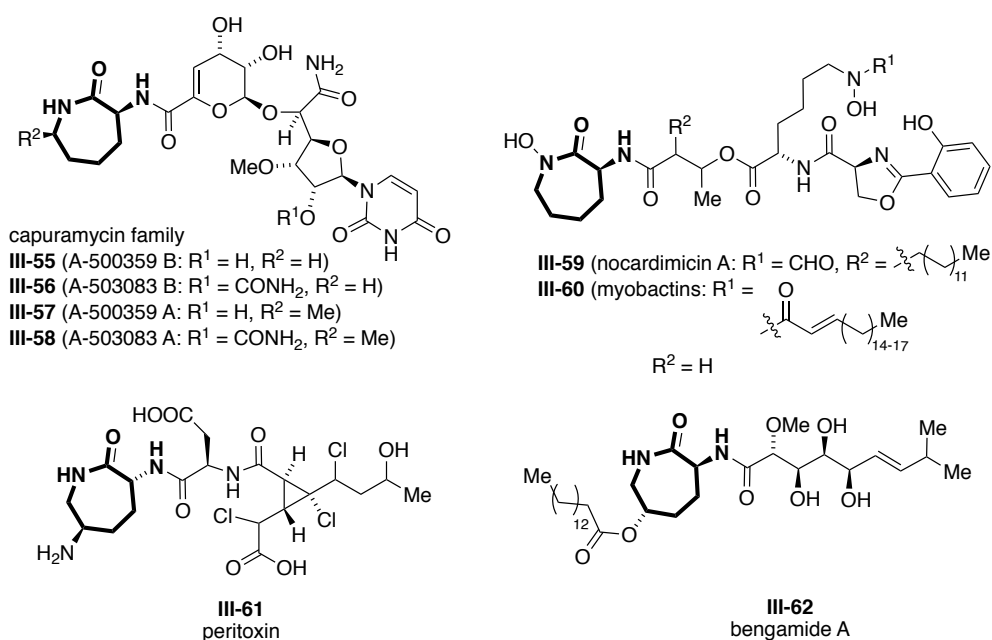
c. Homolysine-containing natural products



A variety of NPs incorporate the nonproteinogenic homolysine, or β -lysine, residue. β -AAs contribute structural diversity and characteristic architectures beyond those observed for traditional α -AA residues, thus endowing unique biological activity to NPs that incorporate this type of monomer. Compounds like the streptothricins (**III-53**),⁶⁷ blasticidin S (**III-54**),⁶⁸ lysinomycin,⁶⁹ and myomycin⁶⁹ are all characterized by a non-acylated β -amino lysine, a characteristic feature of water-soluble, basic antibiotic compounds (Figure 3.4).

A range of NPs contain a modified lysine residue called aminocaprolactam, or L- α -amino- ϵ -caprolactam (L-ACL). This seven-membered cyclized lysine derivative has been identified in the capuramycin-type antibiotics (**III-55**, **-56**, **-57**, **-58**),⁷⁰ as well as bengamide A (**III-62**),⁷¹ caprolactin A, peritoxin A (D-ACL) (**III-61**), circinatin (D-ACL),⁷² and the nocardimicin (**III-59**)⁷³ and myobactin (**III-60**) siderophores (Figure 3.5).⁷⁴ An investigation of capuramycin biosynthesis revealed that L-ACL is formed via an NRPS promoted lactamization of L-lysine.⁷⁴ The bioactivity of these molecules include anti-cancer, -tuberculosis, and -fungal applications.

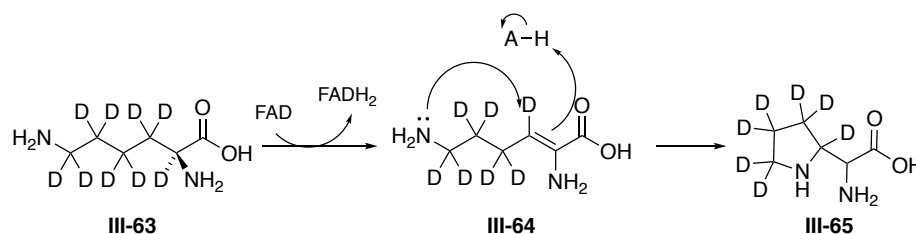
Figure 3.5 Aminocaprolactam-containing NPs.



3.3.3.2 Tambroline biosynthesis and stereochemical assignment.

Although postulated to arise from a lysine precursor, the biosynthetic pathway of the tambroline residue was fully investigated by Thomson and Kelleher, et al. in 2016 using stable isotope feeding experiments (Scheme 3.8).¹⁴ These studies confirmed that tambroline's characteristic 5-membered pyrrolidine ring is most likely biosynthesized via a dehydrogenative lysine cyclization.¹⁴ During isotope feeding experiments, 7 out of 9 deuterons from lysine-*d*₆ were incorporated into the tambroline structure (**III-85**), while all six carbons from a ¹³C₆-labelled lysine were identified in the tambroline residue.¹⁴ These studies indicated that one proton from each of the α- and β-positions of lysine must be removed during tambromycin biosynthesis, ruling out any biosynthetic pathway that would involve the complete oxidation of the lysine β-position.

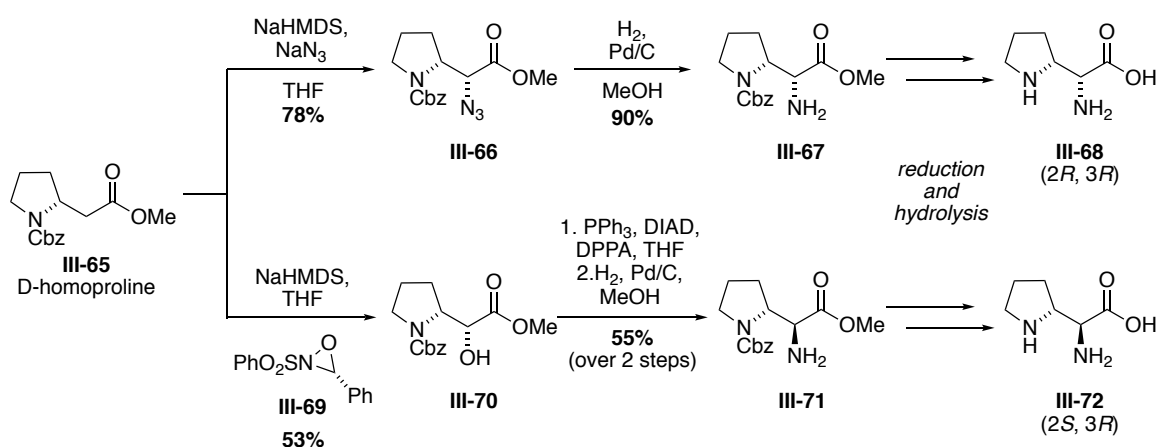
Scheme 3.8 Stable isotope feeding experiment to determine tambroline biosynthetic precursor.



To assign absolute stereochemical designations for the tambroline residue, diastereomeric standards were synthesized and analyzed using Marfey's derivatization. A more detailed discussion of theory and general analytical details of Marfey's analysis can be found in Appendix 1. Graduate student Ryan McClure, from the Thomson and Kelleher labs, prepared synthetic standards of tambroline according to a procedure outlined by Hanessian, et al.,⁷⁵ from either L- or D-proline (Scheme 3.9).¹⁴ This route relied on a substrate-controlled reaction of *N*-benzyloxycarbonyl (Cbz)-D- and L-homoproline methyl ester (**III-65**) to install the α-amino group.

Direct amination of *N*-Cbz-D- and L-homoproline methyl ester via treatment with sodium bis(trimethylsilyl)amide (NaHMDS) and NaN₃, followed by hydrogenative azide reduction, yielded the (*R*, *S*) and (*S*, *R*) stereoisomers. Alternatively, the (*R*, *R*) and (*S*, *S*) isomers were accessed via Davis oxaziridine-mediated hydroxylation of either *N*-Cbz-D- or L-homoproline methyl ester, followed by Mitsunobu inversion using diphenylphosphoryl azide.¹⁴

Scheme 3.9 Synthesis of stereodefined tambroline isomers.

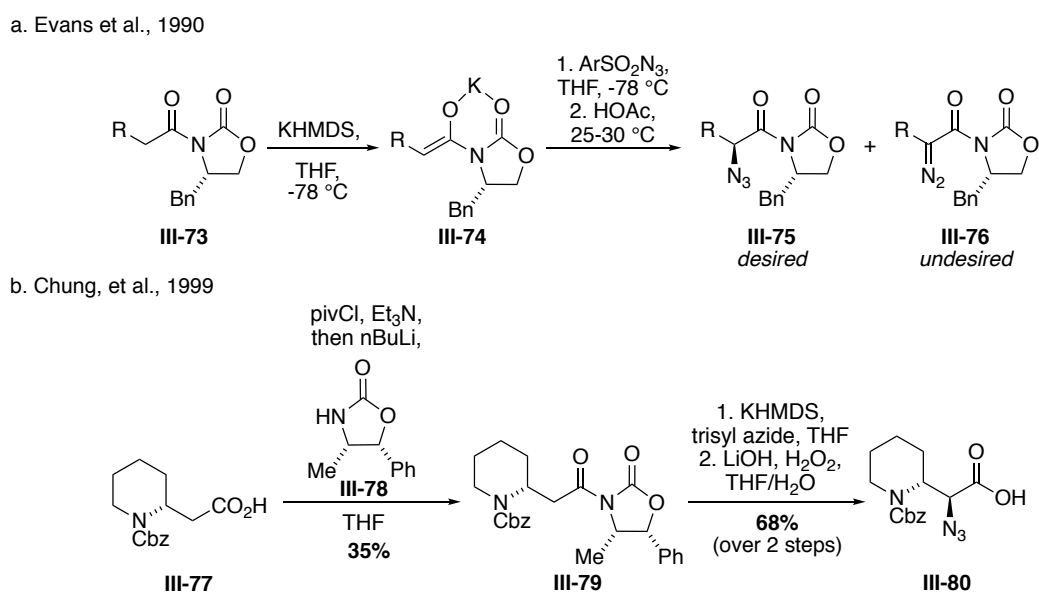


Marfey's analysis with all four diastereomeric standards (*S*, *S*), (*R*, *R*), (*S*, *R*), and (*R*, *S*) revealed a match between the naturally isolated tambroline residue and the (*S*, *R*) stereochemical standard (III-72) (Appendix 2). Unfortunately, this isomer was one that required the Mitsunobu inversion method, which we viewed as somewhat inefficient in terms of completing a planned total synthesis of tambroline. Instead, we devised a more efficient strategy to allow for direct introduction of the desired stereochemical relationship, inspired by electrophilic azidation methods developed by Evans, et al.^{76, 77} and applied to similar systems by Chung, et al.⁷⁸

3.3.3.3 Direct electrophilic azidation to access tambroline stereochemistry.

Our route towards the tambroline monomer was inspired by a method published in 1999 by Chung, et al (Scheme 3.10).⁷⁸ In this work, the Chung group stereospecifically functionalized an *N*-Cbz protected piperidine ring **III-77** at the α -carbon using a method of direct electrophilic azidation developed by the Evans group (Scheme 3.10).^{76, 77} Their method for the asymmetric synthesis of α -AAs utilized α -azido carboximides as versatile α -AA synthons that could be readily converted into their corresponding α -AAs under reductive conditions.^{76, 77} Previous studies by the Evans group established the use of oxazolidinone-derived carboximides **III-73** for the construction of enantiomerically pure compounds, with carboximide enolates exhibiting good diastereoselectivity in asymmetric enolate alkylation,⁷⁹ acylation,⁸⁰ hydroxylation,⁸¹ and aldol addition reactions.⁸²⁻⁸⁴ Thus, Evans et al. envisioned using these structures in combination with α -aminating reagents, namely electrophilic arylsulfonyl N_3 sources, to access α - N_3 carboxylic acids that upon treatment with reductive conditions would reveal the desired α -AA derivatives.^{76, 77}

Scheme 3.10 Stereospecific synthesis of α - N_3 carboxylic acids.



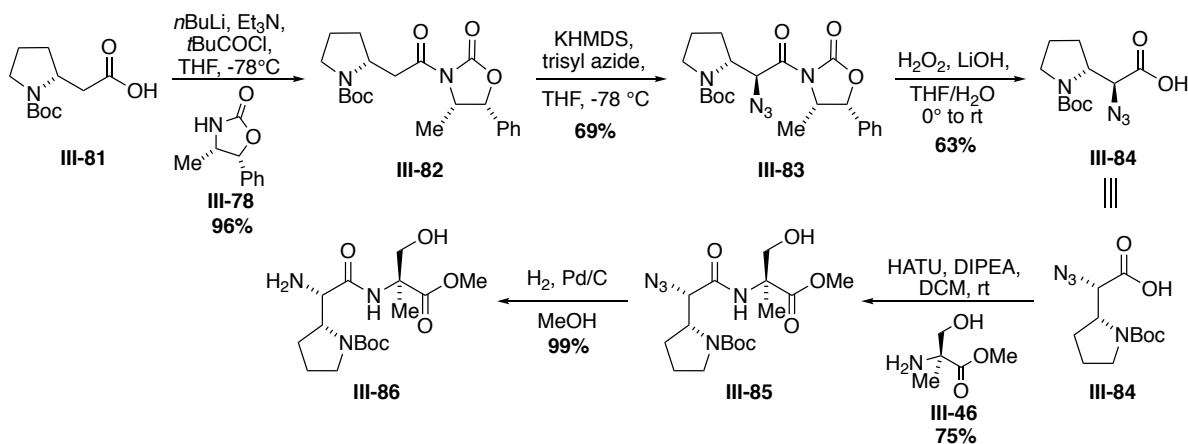
Indeed, direct azidation of the carboximide enolate **III-73**, shown in Scheme **3.10**, using with triisopropylbenzenesulfonyl azide (trisyl azide), potassium hexamethyldisilazane (KHMDs), and acetic acid was found to provide access to the desired α -azido carboximide **III-75** with >20:1 diastereoselectivity.⁷⁶ Reactions of enolates with arylsulfonyl azides are known to provide several different types of products depending on the course of fragmentation of the intermediate adduct, potentially forming either the net diazo transfer product (**III-76**) or the N₃ transfer product (**III-75**). A methodological study of this azidation reaction by the Evans group revealed that the transformation is extremely sensitive to metal enolate structure, N₃ transfer reagent, and quench reagent.^{76, 77} Using a more electropositive enolate counterion (e.g. Li \ll Na < K) and a more electron-rich and sterically demanding arylsulfonyl N₃ source (e.g. *p*-nitrobenzylsulfonyl N₃ < tosyl N₃ < trisyl N₃), azide transfer products are favored over diazo transfer.⁷⁷ Acetic acid as a quench reagent was found to be most effective in promoting breakdown of the primary addition adduct towards the azide product.⁷⁷ The Chung group was able to successfully apply this electrophilic azidation methodology to their piperidine derived substrate, accessing the α -azido carboximide product **III-80** in >20:1 d.r., with subsequent reduction to their desired α -amino group.⁷⁸ We thus envisioned that a similar strategy of α -amination could be applied to an *N*-*tert*-butyl dicarbonate (Boc) pyrrolidine residue, to provide an α -azido carboximide precursor to our desired homoproline residue. Stereoselectivity driven by the chiral Evans oxazolidinone was predicted to provide the desired stereochemical relationship for the tambroline residue.

3.3.3.4 Synthesis of tambroline dipeptide fragment III-86.

Our synthesis began with commercially available *N*-Boc-homoproline (**III-81**), which was converted into the requisite carboximide **III-82** following treatment with *n*-butyllithium (*n*BuLi)

and Evans oxazolidinone **III-78** (Scheme 3.11). We were pleased to find that under carefully optimized conditions using KHMDS in conjunction with trisyl azide, imide **III-83** was produced in 69% yield and as a single stereoisomer.^{76, 85} This reaction proceeded with variable yields that were extremely scale dependent – aberrant breakdown of the primary addition adduct would often give either the diazo product, or a trapped trisyl-bound intermediate. However, with the α -azido intermediate in hand, the chiral auxiliary was removed cleanly and without any epimerization using lithium hydrogen peroxide to afford free acid **III-84**.⁸⁶ Completion of tambroline dipeptide fragment **III-86** (a protected derivative of **III-7** in Scheme 3.1) was accomplished by HATU-mediated amide bond coupling to α -L-methyl-serine methyl ester (**III-46**), followed by mild azide reduction using Pd/C and hydrogen (75% yield over two steps).

Scheme 3.11 Our synthesis of tambroline dipeptide **III-86**.

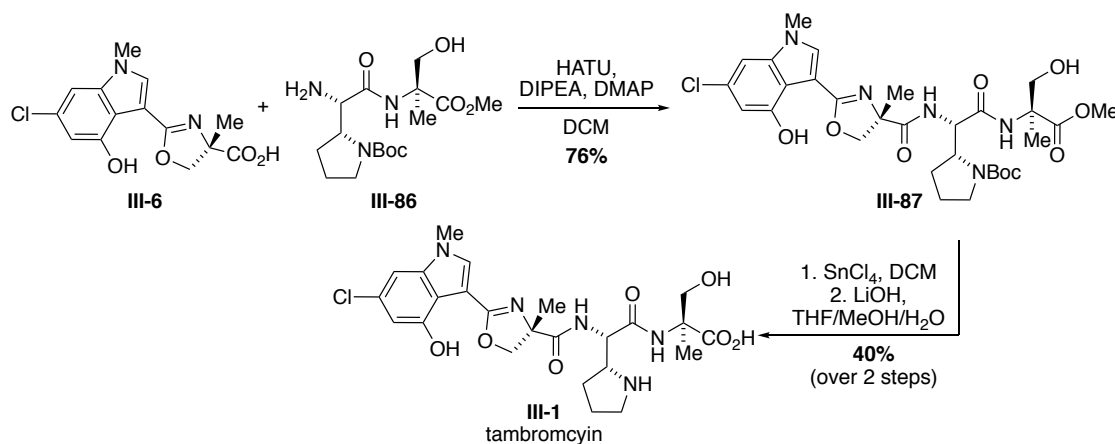


3.3.4 Final steps towards tambromycin total synthesis.

With the two key dipeptide fragments **III-6** and **III-86** in hand, the complete framework of tambromycin was accessed by another HATU-mediated amide coupling reaction that delivered differentially protected derivative **III-87** in 76% yield (Scheme 3.12). It was necessary to subject the tambroline dipeptide to this coupling reaction with the pyrrolidine still *N*-Boc protected, in

order to avoid any unwanted cross-coupling products at the secondary amine. However, removal of the pyrrolidine *N*-Boc group presented itself as a late-stage obstacle because of the acid sensitivity of the oxazoline ring within **III-87**, which was readily hydrolyzed to a linear peptide when exposed to standard conditions for Boc group removal (e.g., TFA or HCl). Ultimately, it was found that careful treatment of **III-87** with anhydrous tin(IV) chloride in dichloromethane for 10 minutes removed the Boc group cleanly and in high yield (**III-S4**).^{87, 88} Finally, the C-terminal methyl ester of **III-S4** was cleaved using LiOH to deliver tambromycin (**III-1**), which was isolated in 40% yield over two steps after purification using reverse phase C18 flash chromatography.

Scheme 3.12 Final coupling and deprotection for tambromycin total synthesis.



A comparison of the spectral properties of synthetic material to the published spectra of natural isolates was initially hampered by an observed pH dependence in the organization and shift of the resonances. In both reported spectra of isolated, natural tambromycin a strong formic acid peak is present.^{14, 17} We postulated that the observed incongruity between our initial spectra and the published work resulted from a difference in protonation state. Indeed, upon the addition of a small amount of formic acid, the collected NMR spectra shifted to tightly align with that of the natural material (see Appendix 2 for a tabulated comparison of chemical shifts). Analysis of the synthetic material by high resolution tandem mass spectrometry, infrared spectroscopy, and optical rotation further supported the identity of the sample, thereby establishing the completion of the total synthesis. Overall, tambromycin (**III-1**) was accessed in 13 steps (longest linear sequence) from 4-methoxy indole (**III-11**) with a combined yield of 1.3%.

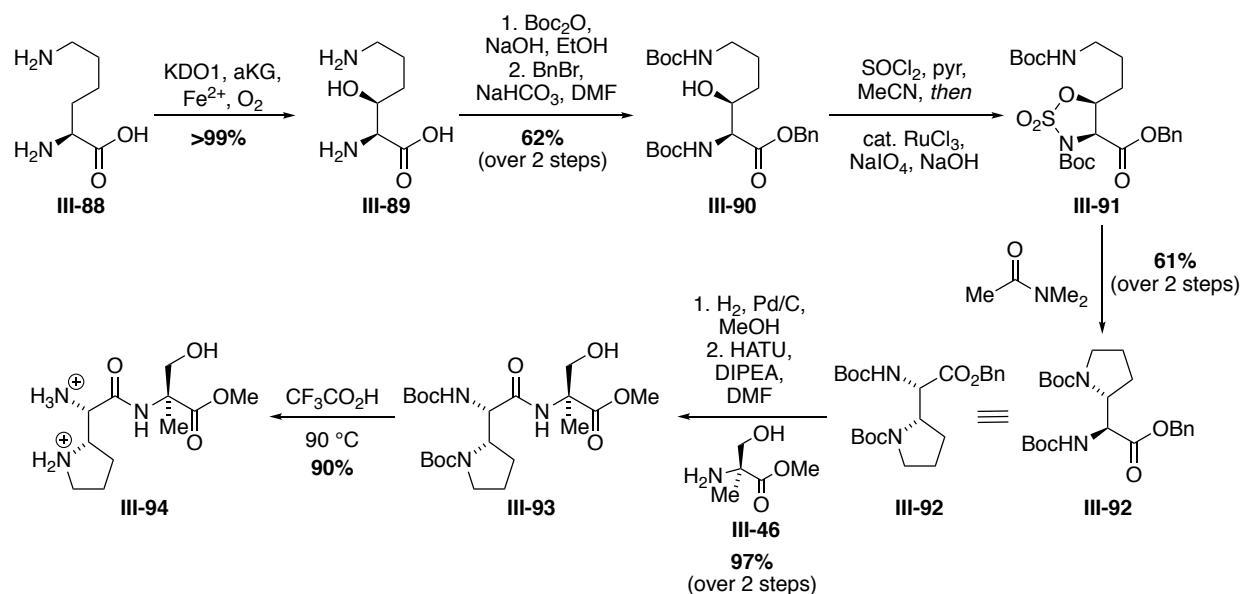
3.4 Conclusions and outlooks

3.4.1 Biosynthetic-inspired total synthesis of tambromycin by Renata and coworkers.

In 2018, both our synthetic route to access tambromycin,⁸⁹ as well as a complementary total synthesis of tambromycin by Renata, et al.⁹⁰ were published concurrently. While the Renata lab applied the same Baran-inspired iridium catalyzed C–H borylation method to elaborate the indole core, their work diverges from ours in the synthesis of the tambroline residue. Instead of the chiral auxiliary-directed electrophilic azidation method employed in our work, the Renata lab focused on a biomimetic, enzymatic construction of the tambroline residue from a linear lysine precursor (Scheme **3.13**).⁹⁰ Using hydroxylase KDO1, a member of the iron- and α -ketoglutarate-dependent dioxygenase superfamily (Fe/ α KG), a hydroxyl group was regio- and stereoselectively installed at the C3 position of free L-lysine (**III-88**) to form intermediate **III-89**.⁹⁰ Subsequent

activation of the alcohol and stereoinvertive, intramolecular displacement via the ϵ -amino group provided the pyrrolidine residue **III-92**.⁹⁰ This work thus presents an alternate route towards the total synthesis of tambromycin, relying on a fundamental understanding of the biosynthetic origin of this complex NP.

Scheme 3.13 Renata, et al. route towards tambroline dipeptide.

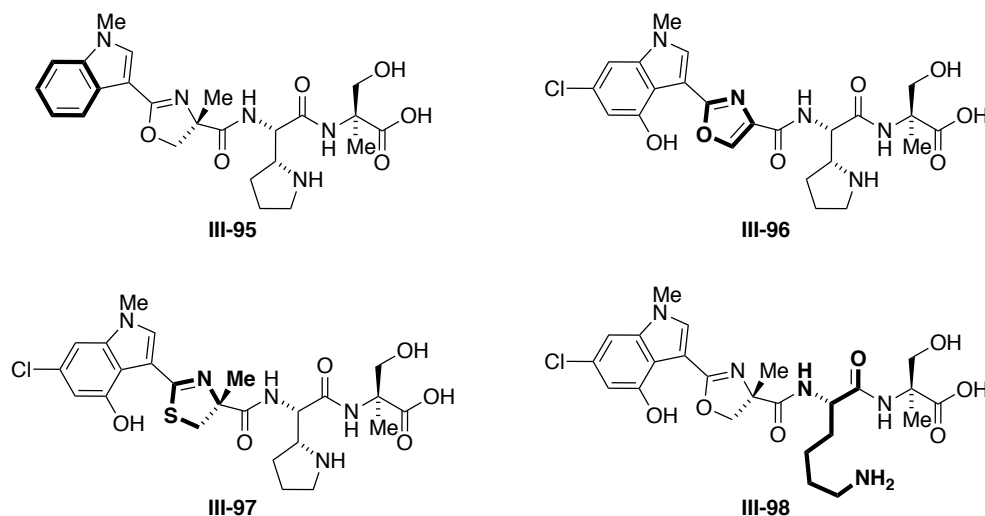


3.4.2 Future directions.

Our synthetic route towards tambromycin has enabled us to now approach a variety of projects aiming to probe both the molecule's biological activity and its mechanism of action. As mentioned in Section 3.2.2, tambromycin was initially found to have bioactivity against B- and T-cell lines at an inhibitory concentration of 37 μ M. In order to improve this bioactivity, we aim to synthesize a suite of tambromycin derivatives for structure–activity–relationship (SAR) studies, in order to deduce (1) which residues contribute to the overall biological activity, and (2) what

modifications can be made in order to increase its inhibitory action. Potential SAR analogues may incorporate different substitution patterns on the indole core (ex. **III-95**), variable oxidation states or heteroatoms about the oxazoline residue (ex. **III-96**, **III-97**), and cyclized versus uncyclized lysine monomers (ex. **III-98**) (Figure 3.6).

Figure 3.6 Proposed tambromycin SAR analogues.



Preliminary SAR studies will elucidate positions on tambromycin that are available for modification without jeopardizing the bioactivity of the compound, so that a tambromycin-based probe can be developed for proteomics-driven target identification. A tambromycin probe derivative will require both a chemical tag (for downstream analysis) and a reactive handle (for covalent enzyme attachment), given that this peptide-based NP will most likely bind an active site noncovalently.^{91, 92}

Figure 3. 7 Proposed tambromycin-based proteomics probe.

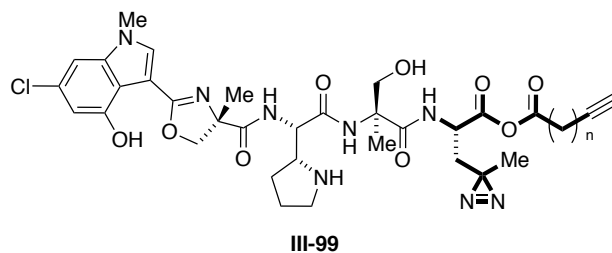


Figure 3.7 depicts a plausible example of a tambromycin-based proteomics probe (**III-99**). An alkyne tag attached to tambromycin will undergo copper(I) catalyzed azide-alkyne cycloaddition (CuAAC click chemistry) with an azide-functionalized biotin bead, thus allowing for pull-down of associated proteins via a streptavidin column.⁹¹⁻⁹³ For the reactive chemical handle, an AA-based photoaffinity labeling (PAL) group, such as photoleucine, will be installed. Because these PALs are derived from AAs, they can also be incorporated in place of a monomer in the tambromycin peptide chain.⁹⁴

3.4.3 Conclusions.

In conclusion, the metabologenomics-driven discovery and concise total synthesis of the unusual tetrapeptide NP, tambromycin (**III-1**), has been achieved. The synthetic route features a scalable, completely regioselective iridium-catalyzed C–H borylation allowing straightforward installation of the indole C6 chlorine substituent, as well as a diastereoselective amination to efficiently produce the novel AA, tambroline (**III-10**). Access to synthetic tambromycin will enable future exploration of its biological activity, mechanism of action, and enable investigations into SAR studies among the related family of peptide NPs.

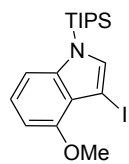
3.5 Experimental Section

3.5.1 General information.

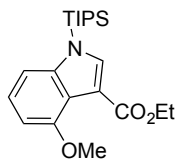
All reactions were carried out under nitrogen atmosphere in flame-dried glassware unless otherwise stated. Anhydrous solvents (DCM, DMF, acetonitrile, methanol, THF) were purified by passage through a bed of activated alumina. Reagents were purified prior to use unless otherwise stated following the guidelines of Armarego and Chai.⁹⁵ Flash column chromatography was performed manually using EM Reagent silica gel F60, 40-63 μm (230-400 mesh) or automatically using a CombiFlash instrument and ISCO prepacked columns. Analytical thin-layer chromatography (TLC) was performed using Merck Silica Gel 60 Å F-254 precoated plates (0.25 mm thickness) or EM Reagent 0.25mm silica gel 60-F plates. Visualization was achieved using UV light, ninhydrin stain or ceric ammonium molybdate. NMR experiments were carried out on a Bruker Avance III 500 MHz spectrometer (500 MHz for ^1H , 126 MHz for ^{13}C) equipped with a DCH CryoProbe, and are reported in ppm using solvent as an internal standard (CDCl_3 at 7.26 ppm except where noted). Data are reported as s = singlet, d = doublet, t = triplet, q = quartet, m = multiplet, b = broad; coupling constant(s) in Hz; integration. Optical rotation was determined using a Rudolph Research Analytical Autopol IV, Series #82239 with either a 10 cm or 5 cm pathlength cell at the sodium D line. High resolution mass spectra were collected on a Thermo Q-Exactive orbitrap mass spectrometer in ESI mode. Diamond ATR infrared spectra were obtained on a ThermoNicolet iS10 FT-IR spectrometer. Germanium ATR infrared spectra were recorded using a Bruker Tensor 37.

3.5.2 Synthesis of indole-oxazoline fragment.

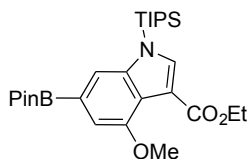
Compound III-42.



Recrystallized 4-methoxy-1*H*-indole (**III-11**) (4.50 g, 30 mmol, 1.0 eq) and DMF (45 mL) were added to a flame-dried round bottom flask and stirred at RT. KOH (4.22 g, 75 mmol, 2.5 eq) was added, and the mixture was heated to 75°C for 15 min. Upon cooling to rt, iodine (7.64 g, 30.3 mmol, 1.01 eq) in DMF (20 mL) was added dropwise and the reaction mixture stirred for 45 min. The mixture was then poured into 600 mL ice water containing 1% v/v NH₄OH and 0.2% w/v sodium metabisulfite and stirred for 20 min. A pink solid was collected by filtration and dried to give 3-iodo-4-methoxy-1*H*-indole (not shown) as a light pink powder (6.89 g, 82%). The solid degraded on silica gel and was therefore used in the next step without further purification. 3-Iodo-4-methoxy-1*H*-indole (6.50 g, 23.8 mmol, 1.0 eq) and THF (20 mL) were added to a flame-dried round bottom flask and cooled to 0°C. LiHMDS 1M in THF (26.2 mL, 26.2 mmol, 1.1 eq) was added portion-wise over 5 min with no exotherm observed. The reaction mixture was brought to rt and stirred for 20 min, after which time triisopropylsilyl chloride (5.6 mL, 26.2 mmol, 1.1 eq) was added in one portion. The reaction mixture was quenched with water and extracted with EtOAc. Combined organics were washed with sat. NaCl, dried over MgSO₄ and concentrated *in vacuo*. The crude black oil was purified by flash chromatography on silica gel (2-15% gradient DCM/hexanes) to yield indole **III-42** as a clear oil, slowly setting to a white low melting solid on extended cooling (9.28 g, 91%). ¹H NMR (500 MHz, Chloroform-*d*) δ 7.15 (s, 1H), 7.12 – 7.07 (m, 1H), 7.08 – 7.01 (m, 1H), 6.52 (d, *J* = 7.6 Hz, 1H), 3.91 (s, 3H), 1.63 (h, *J* = 7.5 Hz, 3H), 1.11 (d, *J* = 7.6 Hz, 18H). ¹³C NMR (126 MHz, Chloroform-*d*) δ 153.47, 142.21, 135.12, 122.83, 120.96, 107.39, 100.86, 55.29, 52.93, 18.07, 12.80. HRMS (M⁺) Calc'd: 429.0984. Found: 429.0960. IR (Diamond ATR): 1464, 1424, 1260, 1225, 1101 cm⁻¹.

Compound III-43.

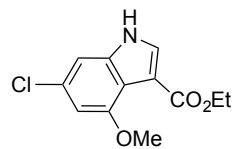
Indole **III-42** (7.50 g, 17.5 mmol, 1.0 eq) and THF (72 mL) were added to a flame-dried round bottom flask and stirred at -40°C . Isopropylmagnesium chloride•lithium chloride (1.3M in THF, 16.8 mL, 21.8 mmol, 1.25 eq) was added slowly, and the mixture was stirred at -40°C for 90 min. The reaction mixture was then cooled to -78°C , ethyl chloroformate (2.07 mL, 21.8 mmol, 1.25 eq) was added dropwise, and the mixture stirred at -78°C for 15 min. The reaction mixture was warmed to rt, and water (100 mL, containing 0.5% w/v EDTA) was added. The resulting mixture was extracted with ethyl acetate, and the combined organic layers were washed with sat. NaCl, dried over MgSO_4 and concentrated *in vacuo*. The crude viscous oil was purified by flash chromatography on silica gel (0–40% gradient EtOAc/hexanes) to give **III-43** as a clear crystal (5.1 g, 78%). ^1H NMR (500 MHz, Chloroform-*d*) δ 7.84 (s, 1H), 7.17 – 7.08 (m, 2H), 6.67 (dd, $J = 6.6, 2.0$ Hz, 1H), 4.36 (q, $J = 7.1$ Hz, 2H), 3.96 (s, 3H), 1.70 (hept, $J = 7.5$ Hz, 3H), 1.40 (t, $J = 7.1$ Hz, 3H), 1.15 (d, $J = 7.6$ Hz, 18H). ^{13}C NMR (126 MHz, Chloroform-*d*) δ 164.84, 154.16, 143.30, 137.96, 123.33, 118.21, 111.35, 107.43, 102.83, 77.28, 77.03, 76.77, 59.89, 55.67, 18.91, 18.05, 14.54, 12.96, 12.73, 12.50. **HRMS** (M+H) Calc'd: 376.2303. Found: 376.2267. **IR** (Diamond ATR): 1671, 1521, 1490, cm^{-1} .

Compound III-42.

(1,5-Cyclooctadiene)(methoxy)iridium(I) dimer (0.427 g, 0.645 mmol, 0.05 eq), 1,10-phenanthroline (0.231 g, 1.29 mmol, 0.1 eq) and anhydrous degassed hexanes (87 mL) were added to a 200 mL glass pressure vessel. After sparging briefly with argon, bis(pinacolato)diboron (13.1 g, 51.7 mmol, 4.0 eq), 4,4,5,5-tetramethyl-1,3,2-dioxaborolane (0.468 mL, 3.22 mmol, 0.25 eq) and **III-43** (4.85 g, 12.9 mmol, 1.0 eq) were added to the reaction mixture. The headspace was charged with argon (5 psi), and the

pressure vessel was sealed and placed into an oil bath preheated to 90°C. After 2 hr, the reaction mixture was cooled, poured over a 1:1 mixture of sat. NaHCO₃ and EtOAc, and stirred for 20 minutes. The biphasic mixture was filtered through a pad of celite, the organic layer was separated, and the aqueous layer was extracted with additional EtOAc. The combined organics were washed with sat. NaCl, dried over MgSO₄, and adsorbed onto celite (15 g). Using a dry load vessel, the mixture was chromatographed on silica gel (0-25% gradient EtOAc/hexanes). Titration with hexanes under sonication followed by filtration gave **III-44** as a white granular solid (4.97 g, 77%) ¹H NMR (500 MHz, Chloroform-*d*) δ 7.87 (s, 1H), 7.56 (s, 1H), 7.03 (s, 1H), 4.33 (q, *J* = 7.1 Hz, 2H), 3.98 (s, 3H), 1.70 (hept, *J* = 7.5 Hz, 3H), 1.37 (t, *J* = 7.1 Hz, 3H), 1.33 (s, 12H), 1.13 (d, *J* = 7.6 Hz, 18H). ¹³C NMR (126 MHz, Chloroform-*d*) δ 164.76, 153.52, 143.06, 139.09, 120.73, 114.64, 111.37, 107.78, 83.55, 59.89, 55.80, 24.92, 18.09, 14.53, 12.68. **HRMS** (M+H) Calc'd: 502.3155. Found: 502.3135. **IR** (Diamond ATR): 1680, 1524, 1350, 1199 cm⁻¹.

Compound III-S1.

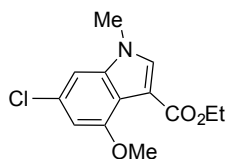


Compound **III-44** (2.00 g, 3.98 mmol, 1.0 eq) and MeOH (50 mL) were added to a flame-dried round bottom flask outfitted with a reflux condenser. Copper(II) chloride (2.04 g, 11.9 mmol, 3.0 eq) in 50 mL water was added, and the mixture was heated to 90°C for 18 hrs. The reaction mixture was concentrated *in vacuo*, diluted with 0.1 M EDTA in water, and extracted with EtOAc. The combined organic layers were washed with sat. NaCl, dried over MgSO₄, and adsorbed onto celite (5 g). Using a dry loading vessel, the mixture was chromatographed on silica gel (0-20% gradient EtOAc/hexanes) to give compound **III-S1** as a white solid (0.449 g 44%). ¹H NMR (500 MHz, Chloroform-*d*) δ 8.47 (s, 1H), 7.79 (d, *J* = 2.9 Hz, 1H), 7.01 (d, *J* = 1.6 Hz, 1H), 6.63 (d, *J* = 1.6 Hz, 1H), 4.33 (q, *J* = 7.1 Hz, 2H), 3.95 (s, 3H), 1.36 (t, *J* = 7.1 Hz, 3H). ¹³C NMR (126 MHz, Chloroform-*d*) δ 163.99, 154.48, 138.01, 130.88,

129.87, 114.03, 110.05, 104.60, 104.16, 60.10, 55.93, 14.47. **HRMS** (M+H) Calc'd: 254.0579.

Found: 254.0567. **IR**(Diamond ATR):3252, 1694, 1579, 1512, 1417, cm^{-1} .

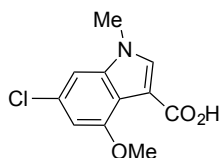
Compound III-45.



Ester **III-S1** (0.449 g, 1.77 mmol, 1.0 eq) and DMF (8 mL) were added to a flame-dried round bottom flask and stirred at rt. Sodium hydride 60% disp. (0.212 g, 5.30 mmol, 3.0 eq) was added portion-wise over 5 min, and the

reaction was stirred at rt for 30 min. Methyl iodide (0.132 mL, 2.12 mmol, 1.2 eq) in DMF (2 mL) was added, and the mixture was stirred at rt for 12 hrs. The reaction was slowly quenched with water (50 mL) and stirred for 20 min, then filtered through celite. The precipitate was washed with water, dried, and purified by flash chromatography on silica gel (0-20% EtOAc/hexanes) to obtain indole **III-45** as a white crystalline solid (356 mg 75%). ^1H NMR (500 MHz, Chloroform-*d*) δ 7.67 (s, 1H), 6.94 (d, $J = 1.6$ Hz, 1H), 6.64 (d, $J = 1.6$ Hz, 1H), 4.31 (q, $J = 7.1$ Hz, 2H), 3.95 (s, 3H), 3.73 (s, 3H), 1.36 (t, $J = 7.1$ Hz, 3H). ^{13}C NMR (126 MHz, Chloroform-*d*) δ 163.83, 154.52, 139.16, 135.42, 129.54, 114.58, 108.06, 104.00, 103.09, 59.96, 55.99, 33.67, 14.52. **HRMS** (M+H) Calc'd. 268.0735. Found: 268.0723. **IR** (Diamond ATR): 1716, 1451, 1344, 1197 cm^{-1} .

Compound III-S2.

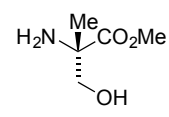


Indole **III-45** (0.300 g, 1.1 mmol, 1.0 eq), THF (10 mL), MeOH (3 mL) and 2M NaOH (10 mL) were added to a flame-dried round bottom flask. The

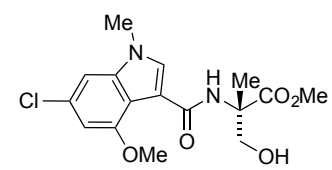
mixture was sealed and heated to 80°C for 18 hrs. The reaction mixture was then acidified with 1M HCl and concentrated *in vacuo* to give compound **III-S2** as a white powder, with no further purification required (240 mg, 89%). ^1H NMR (500 MHz, DMSO-*d*₆) δ 11.60 (s, 1H), 7.96 (s, 1H), 7.27 (s, 1H), 6.75 (s, 1H), 3.89 (s, 3H), 3.78 (s, 3H). ^{13}C NMR (126 MHz, DMSO-*d*₆) δ 164.25, 153.88, 139.26, 137.27, 128.35, 114.24, 107.68, 104.46, 103.89, 56.56, 40.59, 40.49, 40.42, 40.33,

40.25, 40.16, 40.08, 39.99, 39.83, 39.66, 39.49, 33.73. **HRMS** (M+H) Calc'd: 240.0422. Found: 240.4111. **IR** (Diamond ATR): 3206, 1703, 1523, 1358 cm^{-1} .

Compound III-46.

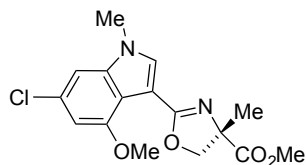

 (S)-2-Amino-3-hydroxy-2-methylpropanoic acid (**III-9**) (500 mg, 4.2 mmol, 1.0 eq) and MeOH (8 mL) were added to a flame-dried round bottom flask and stirred at 0°C. Thionyl chloride (2.0 mL, 27 mmol, 6.45 eq) was added, and the reaction was heated at reflux for 48 hrs. The mixture was concentrated *in vacuo*, and the crude product was dissolved in a 1:1 mixture of MeOH/water and applied to a Dowex 50WX8 column (3 cm ht x 1 cm dia, prepared by washing with 3 column volumes of water, MeOH, 1M HCl, and water, sequentially). Non-binding impurities were washed from the column with water and MeOH, and **III-46** was eluted with 7M ammonia in MeOH. Solvents were evaporated to give **III-46** as a clear oil that formed an off-white solid upon sitting (487 mg, 87%). All characterization data matched that reported previously in the literature.⁹⁶

Compound III-47.

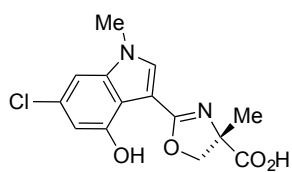

 Compound **III-S2** (50 mg, 0.21 mmol, 1.0 eq) and amine-free DMF (2 mL) were added to a flame-dried round bottom flask and stirred at rt. 1-[Bis(dimethylamino) methylene]-1H-1,2,3-triazolo[4,5-b]pyridinium 3-oxide hexafluorophosphate (HATU, 87 mg, 0.23 mmol, 1.1 eq) and N,N-diisopropylamine (109 μL , 0.630 mmol, 3.0 eq) were added at rt, and a thick precipitate formed after 10 min. Compound **III-46** (42 mg, 0.25 mmol, 1.2 eq) was then added neat and the mixture was sonicated for 10 min, then stirred at rt for 12 hrs. The reaction mixture was diluted with water and carefully acidified with conc. HCl to break any formed gel, and the mixture was extracted with EtOAc. Organic layers were dried over MgSO_4 and concentrated *in vacuo*. The crude product was purified by flash

chromatography on silica gel (0-100% EtOAc/DCM) to give **III-47** as a white amorphous solid (60 mg 81%). ^1H NMR (500 MHz, Chloroform-*d*) δ 9.23 (s, 1H), 7.81 (s, 1H), 6.98 (d, $J = 1.6$ Hz, 1H), 6.65 (d, $J = 1.7$ Hz, 1H), 4.20 – 4.06 (m, 2H), 4.03 (s, 3H), 3.79 (s, 3H), 3.71 (s, 3H), 1.61 (s, 3H). ^{13}C NMR (126 MHz, Chloroform-*d*) δ 173.89, 164.37, 152.33, 139.31, 136.28, 128.93, 112.66, 111.17, 104.31, 103.42, 67.53, 62.10, 55.97, 52.75, 33.64, 20.95. **HRMS** (M+H) Calc'd: 355.1055. Found: 355.1033. $[\alpha]_D^{24} + 11.3$ (*c* 0.08, MeOH). **IR** (Diamond ATR): 3308, 1741, 1605, 1548, 1451 cm^{-1} .

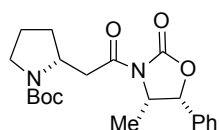
Compound III-S3.



Compound **III-47** (42 mg, 0.12 mmol, 1.0 eq) and DCM (2 mL) were added to a flame-dried round bottom flask and stirred at -78°C . Deoxofluor (27 μL , 0.15 mmol, 1.25 eq) was added in one portion, and the yellow mixture was stirred at -78°C for 10 min, then warmed to rt and stirred for 1 hr. The reaction mixture was quenched with MeOH (1 mL) and adsorbed onto celite (1 g) *in vacuo*. Using a dry loading vessel, the crude product was purified by flash chromatography on silica gel (0–30% gradient THF/DCM) to give **III-S3** as a white foam (27 mg, 68%) ^1H NMR (500 MHz, Acetonitrile-*d*₃) δ 7.79 (s, 1H), 7.18 (d, $J = 1.4$ Hz, 1H), 6.77 (d, $J = 1.5$ Hz, 1H), 4.87 (dd, $J = 8.9, 1.0$ Hz, 1H), 4.33 (dd, $J = 8.9, 1.0$ Hz, 1H), 3.94 (s, 3H), 3.79 (s, 3H), 3.78 (s, 3H), 1.62 (s, 3H). ^{13}C NMR (126 MHz, Acetonitrile-*d*₃) δ 173.41, 163.89, 154.10, 139.68, 135.85, 129.90, 114.46, 104.66, 104.53, 101.38, 77.03, 72.64, 56.46, 52.99, 33.98, 24.04. **HRMS** (M+H) Calc'd: 337.0950. Found: 337.0947. $[\alpha]_D^{24} + 47.5$ (*c* 0.08, MeOH). **IR**(Diamond ATR):1725, 1636, 1455, 1292, 1051 cm^{-1} .

Compound III-6.

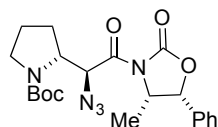
Compound **III-S3** (25 mg, 0.075 mmol, 1.0 eq) and DCM (2 mL) were added to a flame-dried round bottom flask and stirred at -78°C . BBr_3 (9.3 μL , 0.098 mmol, 1.33 eq, distilled twice to remove all traces of orange color) was added, and the mixture was stirred at -78°C for 30 min, then warmed to 0°C with continued stirring for 3 hr. Excess BBr_3 was quenched by the dropwise addition of a 1:3 water/MeCN mixture at 0°C . The organics were removed *in vacuo*, and the pH was adjusted to 9 with 2M NaOH. The aqueous solution was applied to a Dowex 1X2 column (3 cm ht x 1 cm dia, prepared by washing with 3 column volumes of water, MeOH, 1M NaOH, and water, sequentially). Non-binding impurities were washed from the column with water, and **III-6** was eluted with 0.05 M HCl followed by MeOH. Solvents were evaporated and the white solid was titrated with EtOAc, to give **7** as a white powder (14 mg, 61%). $^1\text{H NMR}$ (500 MHz, $\text{DMSO-}d_6$) δ 13.11 (s, 1H), 7.92 (s, 1H), 7.07 (s, 1H), 6.46 (s, 1H), 4.83 (d, $J = 8.7$ Hz, 1H), 4.35 (d, $J = 8.7$ Hz, 1H), 3.77 (s, 3H), 1.53 (s, 3H). $^{13}\text{C NMR}$ (126 MHz, $\text{DMSO-}d_6$) δ 174.20, 163.81, 152.61, 139.67, 133.74, 129.66, 113.67, 107.22, 102.03, 101.36, 77.12, 72.04, 33.87, 24.67. **HRMS** $[\text{M}+\text{H}]^+$, Calc'd: 309.0637. Found: 309.0604. $[\alpha]_D^{24} - 50.0$ (c 0.08, MeOH). **IR** (Diamond ATR): 2926, 1728, 1636, 1570, 1344 cm^{-1} .

3.5.3 Synthesis of tambroline dipeptide.**Compound III-82.**

Commercially available *N*-Boc-D-beta-homoproline (**81**) (400 mg, 1.74 mmol, 1.0 eq) and THF (6 mL) were added to a flame-dried round bottom flask and stirred at -78°C . Et_3N (0.294 mL, 2.11 mmol, 1.33 eq) and pivaloyl chloride (0.224 mL, 1.82

mmol, 1.15 eq) were added, and the mixture was brought to 0°C and stirred for 1hr. Meanwhile, the Evan's auxiliary (**III-78**) ((4*S*, 5*R*)-4-methyl-5-phenyl-2-oxazolidinone) (281 mg, 1.59 mmol, 1.0 eq) was stirred in THF (5 mL) at -30° to -45°C. Triphenylmethane indicator was added, and *n*BuLi was added dropwise to the flask until a bright red color persisted. Both reaction flasks were then brought to -78°C, and the Evan's auxiliary solution was rapidly cannulated into the *N*-Boc-D-beta-homoproline flask. The mixture was stirred at -78°C for 30 min, then warmed to 0°C and partitioned between DCM and pH 7 sodium phosphate buffer. The organic layer was washed with sat. NaHCO₃ solution, half sat. NaCl solution, dried over Na₂SO₄, and concentrated *in vacuo*. The crude yellow oil was purified by flash chromatography on silica gel (40% EtOAc in hexanes), which afforded **III-82** as a clear oil that forms a white foam upon drying (590 mg, 96% yield). ¹H NMR (500 MHz, CDCl₃), mixture of rotamers, δ 7.43-7.31 (m, 5H), 5.75 (d, *J* = 6.8 Hz, 1H) 4.72 (t, *J* = 6.5, 1H), 4.40 (d, *J* = 6.7 Hz, 1H), 3.42 – 3.31 (m, 2H), 3.18 (d, *J* = 6.5, 1H), 2.18 – 2.07 (m, 1H), 1.96 – 1.84 (m, 2H), 1.76 – 1.65 (m, 1H), 1.46 (s, 9H), 0.90 (d, *J* = 6.4 Hz, 3H). ¹³C NMR (126 MHz, CDCl₃), mixture of rotamers, δ 171.17 and 171.05, 154.69 and 154.36, 153.46 and 153.13, 133.74 and 133.35, 128.81, 125.84, 79.31 and 79.24, 60.54, 55.01 and 54.86, 53.74 and 53.55, 46.50 and 46.27, 40.85 and 40.65, 31.88 and 31.40, 28.68, 23.63 and 22.99, 14.81 and 14.68. HRMS [M+H]⁺, Calc'd: 389.1998. Found 389.2066. [α]_D²⁴ = +54.0 (*c* 0.83, MeOH). IR (Germanium ATR): 2974, 1782, 1690, 1394, cm⁻¹.

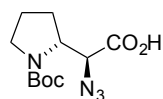
Compound III-83.



Potassium bis(trimethylsilyl)amide (0.5 M KHMDS in toluene, 4.08 mL, 1.04 mmol, 1.1 eq, titrated according to procedure by Ireland et al),⁹⁷ and THF (2 mL) were added to a flame-dried round bottom flask and stirred at -78°C. **III-82** (365 mg, 0.941 mmol, 1.0 eq) and THF (3 mL) were stirred in a separate flask and cooled to -78°C, then transferred

via cannula into the KHMDS reaction flask. The yellow solution was stirred for 30 min at -78°C to form the potassium enolate. Meanwhile, a 0.82M solution of trisyl azide in toluene (1.45 mL, 1.19 mmol, 1.26 eq) was stirred in THF (2 mL) at -78°C , and this solution was very rapidly cannulated into the potassium enolate reaction flask at -78°C . The reaction stirred for exactly 1 min, with the solution changing to bright yellow and then brown yellow over the course of the reaction. After 1 min, the reaction was immediately quenched with conc. glacial acetic acid (0.250 mL, 4.33 mmol, 4.6 eq), and the reaction flask was directly transferred to a warm water bath (25°C to 30°C) and stirred for 30 min (turning cloudy white once warmed). The mixture was then partitioned between DCM and sat. NaCl solution, and the aqueous layer was extracted with DCM. The combined organic layers were washed with sat. NaHCO_3 , dried over Na_2SO_4 , and concentrated *in vacuo*. The resulting yellow oil was purified by flash chromatography on silica gel (1% MeOH in DCM), giving **III-83** as a clear oil (267 mg, 66% yield). $^1\text{H NMR}$ (500 MHz, CDCl_3) δ 7.42 – 7.31 (m, 5H), 5.91 (d, $J = 7.1$ Hz, 1H), 4.86 (s, 1H), 4.70 (dt, $J = 13.9, 6.9$ Hz, 1H), 4.57 (d, $J = 7.9$ Hz, 1H), 3.46 (t, $J = 6.8$ Hz, 2H), 2.21 – 2.11 (m, 2H), 2.02 – 1.97 (m, 1H), 1.91 – 1.83 (m, 1H), 1.45 (s, 9H), 0.95 (d, $J = 6.7$ Hz, 3H). $^{13}\text{C NMR}$ (126 MHz, CDCl_3) δ 169.20, 155.65, 153.89, 133.52, 128.80, 125.89, 80.24, 80.08, 64.56, 58.54, 56.28, 47.74, 30.00, 28.54, 24.49, 14.96. **HRMS** $[\text{M}+\text{H}]^+$, Calc'd: 430.2012. Found 420.2088. $[\alpha]_D^{24} = +80.4$ (c 0.83, MeOH). **IR** (Germanium ATR): 2976, 2110, 1778, 1689, 1367, 1237 cm^{-1} .

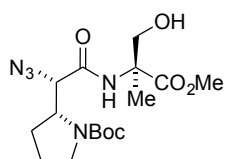
Compound III-84.



Compound **III-83** (267 mg, 0.623 mmol, 1.0 eq) and a 3:1 mixture of THF/ H_2O (12 mL) were added to a round bottom flask and stirred at 0°C . H_2O_2 30% (w/w) in H_2O (0.515 mL, 4.985 mmol, 8.0 eq) was added, followed by LiOH solid (29.8 mg, 1.25 mmol, 2.0 eq). The reaction was warmed to rt and stirred for 1 hr, then cooled to 0°C and quenched with

a 1.5N Na₂SO₃ solution in 10% excess (0.57 mL). The mixture was buffered to pH = 9-10 with sat. NaHCO₃ if needed. THF was removed *in vacuo*, and the aqueous layer was extracted with DCM to recover the Evan's auxiliary. The aqueous layer was then carefully acidified to pH = 2 using conc. HCl, and extracted with EtOAc. Combined organic layers were dried over Na₂SO₄ and concentrated *in vacuo*. The light yellow oil **III-84** was taken on with no further purification needed (129 mg, 76% yield). ¹H NMR (500 MHz, CDCl₃) δ 4.38 (br s, 1H), 4.09 (br s, 1H), 3.51 (br s, 1H), 3.43 – 3.38 (m, 1H), 2.19 – 2.11 (m, 1H), 2.06 – 1.88 (m, 2H), 1.88 – 1.80 (m, 1H), 1.48 (s, 9H). ¹³C NMR (126 MHz, CDCl₃) δ 171.89, 80.81, 63.77, 58.63, 47.41, 29.80, 28.35, 23.78, 23.59. HRMS [M-Boc+H]⁺ (major peak), Calc'd 171.1328. Found 171.0874. [M+H]⁺ (minor peak), Calc'd 271.1328. Found 271.1397. [α]_D²⁴ = +46.8 (c 0.83, MeOH). IR (Germanium ATR): 2976, 2112, 1742 – 1632, 1402, 1154 cm⁻¹.

Compound III-85.

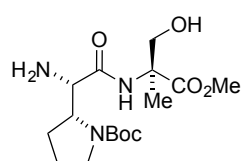


Acid **III-84** (15.7 mg, 0.058 mmol, 1.2 eq), 1-[bis(dimethylamino)methylene]-1*H*-1,2,3-triazolo[4,5-*b*]pyridinium 3-oxid hexafluorophosphate (HATU, 20.3 mg, 0.0533 mmol, 1.1 eq), and DCM (1 mL) were added to a

flame-dried round bottom flask and stirred at rt. **III-46** (6.5 mg, 0.048 mmol, 1.0 eq), freshly distilled *N,N*-diisopropylethylamine (0.042 mL, 0.242 mmol, 5.0 eq), and DCM (1 mL) were stirred in a separate flask at rt for 30 min. The solution of **III-46** was then transferred into the reaction flask via cannula and the mixture stirred for 1 hr at rt (mixture turned light yellow after 10 minutes). The mixture was concentrated *in vacuo*, diluted with EtOAc, and washed with sat. NH₄Cl, H₂O, sat. NaHCO₃, sat. NaCl, dried over Na₂SO₄, and concentrated *in vacuo*. The crude product was purified by flash chromatography on silica gel (50% EtOAc in hexanes), resulting in **III-85** as a clear oil (16.7 mg, 75% yield). ¹H NMR (500 MHz, CDCl₃) δ 7.45 (br s, 1H), 4.62 –

4.45 (m, 2H), 3.94 (s, 1H), 3.81 (s, 3H), 3.75 (t, $J = 10.7$ Hz, 1H), 3.54 – 3.48 (m, 1H), 3.39 – 3.33 (m, 1H), 2.32 – 2.24 (m, 1H), 2.03 – 1.87 (m, 2H), 1.86 – 1.77 (m, 1H), 1.55 (s, 3H), 1.41 (s, 9H). ^{13}C NMR (126 MHz, CDCl_3) δ 174.24, 168.02, 155.25, 80.84, 68.02, 64.71, 63.65, 58.51, 53.22, 48.04, 32.30, 28.61, 24.01, 19.06. HRMS $[\text{M}+\text{H}]^+$, Calc'd 386.1961. Found 386.2028. $[\alpha]_D^{24} = +31.2$ (c 0.83, MeOH). IR (Germanium ATR): 3370, 2976, 2110, 1739, 1681, 1395, cm^{-1} .

Compound III-86.

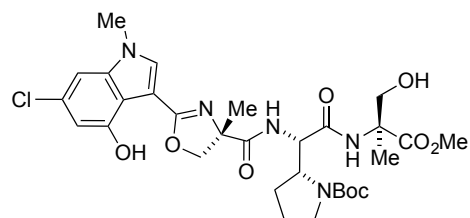


Azide **III-85** (92.4 mg, 0.240 mmol, 1.0 eq) and MeOH (2 mL) were added to a flame-dried round bottom flask and stirred at rt. To this, 10 wt % Pd/C (26.0 mg, 0.0240 mmol, 0.10 eq) was added, and the solution was stirred

under H_2 for 30 min. The reaction was then flushed with N_2 and filtered over celite. The organic layer was dried over Na_2SO_4 and concentrated *in vacuo*. The white crystalline solid **III-86** required no further purification (86.2 mg, quantitative yield). ^1H NMR (500 MHz, CDCl_3) δ 8.43 (br s, 1H), 4.54 – 4.43 (br m, 2H), 3.80 (s, 3H), 3.74 (d, $J = 11.3$ Hz, 1H), 3.59 – 3.52 (m, 1H), 3.38 – 3.22 (m, 2H), 2.15 (br s, 1H), 1.91 – 1.72 (m, 4H), 1.55 (s, 3H), 1.40 (s, 9H). ^{13}C NMR (126 MHz, CDCl_3) δ 174.62, 173.54, 155.53, 80.63, 64.95, 63.02, 59.14, 57.73, 53.00, 48.39, 31.77, 28.64, 24.13, 19.31. HRMS $[\text{M}+\text{H}]^+$, Calc'd 360.2056. Found 360.2114. $[\alpha]_D^{24} = +40.8$ (c 0.83, MeOH). IR (Germanium ATR): 3345, 2976, 1740, 1678, 1394, 1167 cm^{-1} .

3.5.4 Final coupling and deprotection.

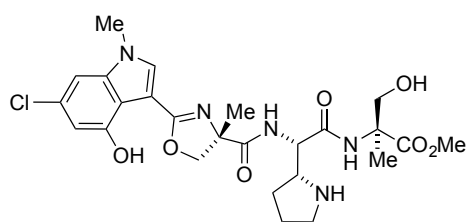
Compound III-87.



Compound **III-6** (9.8 mg, 0.032 mmol, 1.0 eq), 1-[bis(dimethylamino) methylene]-1*H*-1,2,3-triazolo[4,5-*b*]pyridinium 3-oxid hexafluorophosphate (HATU, 13.4

mg, 0.035 mmol, 1.1 eq), 4-dimethylamino pyridine (DMAP, 390.0 μg , 0.0032 mmol, 0.1 eq) and DCM (1 mL) were added to a flame-dried round bottom flask and stirred at rt for 30 min. Compound **III-86** (11.8 mg, 0.032 mmol, 1.0 eq), freshly distilled N,N-diisopropylethylamine (DIPEA, 28 μL , 0.159 mmol, 5.0 eq), and DCM (1 mL) were stirred in a separate flask at rt for 30 min. The solution containing compound **III-86** was then transferred via cannula into the reaction flask containing compound **III-6**. After stirring for 2 hr at rt, the reaction mixture was concentrated *in vacuo*, and the crude material was purified by flash chromatography on silica gel (0 – 100% EtOAc/DCM) to afford compound **III-87** as a clear oil (17.3 mg 76%). ^1H NMR (500 MHz, Chloroform-*d*) δ 12.37 (s, 1H), 7.88 (s, 1H), 7.42 (s, 1H), 7.24 (s, 1H), 7.02 (s, 1H), 6.79 (d, J = 1.7 Hz, 1H), 6.67 (d, J = 1.6 Hz, 1H), 4.81 (d, J = 8.9 Hz, 1H), 4.41 (s, 1H), 4.35 (d, J = 11.5 Hz, 1H), 4.25 (d, J = 8.8 Hz, 1H), 4.16 (s, 1H), 3.80 (d, J = 11.6 Hz, 1H), 3.77 (s, 3H), 3.72 (s, 3H), 3.31 – 3.22 (m, 1H), 3.09 (dt, J = 11.0, 6.4 Hz, 1H), 2.07 – 1.95 (m, 1H), 1.72 (s, 3H), 1.63 (dt, J = 12.9, 6.1 Hz, 2H), 1.60 – 1.53 (m, 1H), 1.51 (s, 3H), 1.22 (s, 9H). ^{13}C NMR (126 MHz, Chloroform-*d*) δ 175.73, 174.00, 169.07, 164.28, 152.63, 139.36, 131.90, 131.11, 113.72, 108.50, 100.94, 97.93, 80.85, 73.39, 64.43, 62.75, 58.59, 57.60, 52.94, 47.78, 38.64, 33.78, 30.35, 29.71, 27.97, 26.21, 23.86, 19.21. HRMS (M+H) Calc'd: 650.2587. Found: 650.2578. $[\alpha]_D^{24}$ – 27.5 (c 0.08, MeOH). IR (Diamond ATR): 2920, 2850, 1678, 1640, 1463, 1391 cm^{-1}

Compound III-S4.

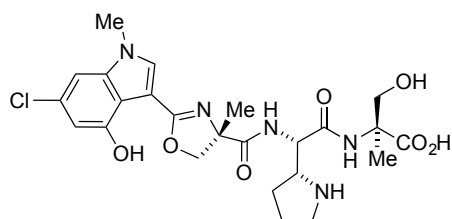


Compound **III-87** (14.3 mg, 0.022 mmol, 1.0 eq) and DCM (2 mL) were added to a flame-dried round bottom flask and stirred at rt. Fuming SnCl_4 (13 μL , 0.101 mmol, 5.0 eq) was added neat at rt, and the reaction was stirred for 15 min until all starting material was consumed.

The solution was concentrated *in vacuo*, and the crude product was purified by flash

chromatography on silica gel (0 – 100% EtOAc/DCM) to afford **III-S4** as a white film, (10.1 mg, 83%). $^1\text{H NMR}$ (500 MHz, Methanol- d_4) δ 8.07 (s, 1H), 7.12 (d, $J = 1.6$ Hz, 1H), 6.69 (d, $J = 1.6$ Hz, 1H), 5.10 (d, $J = 9.1$ Hz, 1H), 4.82 (d, $J = 6.6$ Hz, 1H), 4.67 (d, $J = 9.2$ Hz, 1H), 3.99 (dt, $J = 9.8, 6.9$ Hz, 1H), 3.88 (d, $J = 11.3$ Hz, 1H), 3.86 (s, 3H), 3.83 (d, $J = 11.2$ Hz, 1H), 3.74 (s, 3H), 3.37 (s, 2H), 2.25 (dtd, $J = 13.3, 7.3, 3.9$ Hz, 1H), 2.15 – 2.06 (m, 1H), 2.05 – 1.97 (m, 1H), 1.88 (dq, $J = 13.1, 9.0$ Hz, 1H), 1.80 (s, 3H), 1.50 (s, 3H). $^{13}\text{C NMR}$ (126 MHz, Methanol- d_4) δ 173.65, 172.89, 167.87, 166.20, 150.98, 139.99, 136.47, 130.79, 113.01, 108.01, 102.43, 99.05, 78.26, 70.78, 64.23, 61.22, 61.02, 53.59, 51.70, 45.58, 32.92, 26.82, 23.52, 23.13, 18.69. **HRMS** (M+H) Calc'd: 550.2063. Found: 550.2062. $[\alpha]_D^{24} = -42.5$ (c 0.08, MeOH). **IR**(Diamond ATR):2923, 2852, 1620, 1530, 1456 cm^{-1} .

Compound III-1 (tambromycin).



Compound **III-S4** (9.0 mg, 0.016 mmol, 1.0 eq) and THF:MeOH:H₂O (3:1:1, 1 mL) were added to a flame-dried round bottom flask and stirred at rt. Lithium hydroxide (2.0 mg, 0.082 mmol, 5.0 eq) was added at rt, and the suspension was stirred for 3 hrs. The crude mixture was evaporated to dryness, and purified by column chromatography using C18 resin (0–100% CH₃CN/H₂O, 10 steps, 1 mL each, 1g resin) to afford **III-1** (4.2 mg, 48%). For comparison to naturally isolated material, ^1H and ^{13}C NMR was conducted in 1:1 Methanol- d_4 + Chloroform- d , and 0.2 μL formic acid was added directly to the NMR tube to make the formate salt (both references isolate material containing substantial amounts of formic acid as judged by inspection of published spectra).^{14, 17} $^1\text{H NMR}$ (500 MHz, Methanol- d_4 + Chloroform- d) 7.61 (s, 1H), 6.90 (s 1H), 6.59 (s, 1H), 4.96 (d, $J = 8.7$, 1H), 4.91 (d, $J = 4.9$, 1H), 4.33 (d, $J = 8.8$, 1H), 4.08 (ddd, $J = 10.1, 7.2, 4.9$, 1H), 4.02 (d, $J = 11.1$, 1H), 3.81 (d, $J = 11.2$, 1H), 3.81 (s, 3H), 3.32 (dt, $J =$

11.2, 7.6, 1H), 3.22 (ddd $J = 11.9, 8.6, 5.6$, 1H), 2.08 (dtd, $J = 12.8, 7.4, 3.7$, 1H), 1.99 (ddt $J = 11.9, 8.0, 3.4$, 1H), 1.91 (dt, $J = 12.9, 8.0$, 1H), 1.74 (m 1H), 1.75 (s, 3H), 1.46 (s, 3H). ^{13}C NMR (126 MHz, Methanol- d_4 + Chloroform- d) 178.37, 175.51, 168.37, 165.08, 152.37, 139.97, 133.11, 131.20, 114.00, 108.15, 102.50, 101.88, 77.49, 73.88, 65.98, 63.55, 60.73, 54.01, 45.97, 33.78, 27.22, 25.39, 24.27, 19.67. **HRMS** (M+H) Calc'd: 536.1907. Found: 536.1898. $[\alpha]_{\text{D}}^{24} -70.8$ (c 0.2, MeOH). **IR** (Diamond ATR): 3311, 2936, 2830, 1616, 1456, 1344 cm^{-1} .

Chapter 1 References.

1. Burton, B. S., von Pechmann, H. , Ueber die Einwirkung von Chlorphosphor auf Acetondicarbonsäureäther. *Ber. Dtsch. Chem. Ges.* **1887**, *20*, 145-149.
2. Yu, S.; Ma, S., Allenes in Catalytic Asymmetric Synthesis and Natural Product Syntheses. *Angew. Chem. Int. Ed.* **2012**, *51* (13), 3074-3112.
3. Liu, L.; Ward, R. M.; Schomaker, J. M., Mechanistic Aspects and Synthetic Applications of Radical Additions to Allenes. *Chem. Rev.* **2019**, *119* (24), 12422-12490.
4. Ma, S., Some Typical Advances in the Synthetic Applications of Allenes. *Chem. Rev.* **2005**, *105* (7), 2829-2872.
5. Ma, S., Electrophilic Addition and Cyclization Reactions of Allenes. *Acc. Chem. Res.* **2009**, *42* (10), 1679-1688.
6. Hieda, Y.; Choshi, T.; Fujioka, H.; Hibino, S., Total Synthesis of the Neuronal Cell-Protecting Carbazole Alkaloids Carbazomadurin A and (S)-(+)-Carbazomadurin B. *Eur. J. Org. Chem.* **2013**, *2013* (32), 7391-7401.
7. Choshi, T.; Sada, T.; Fujimoto, H.; Nagayama, C.; Sugino, E.; Hibino, S., Total Syntheses of Carazostatin, Hyellazole, and Carbazoquinocins B–F. *J. Org. Chem.* **1997**, *62* (8), 2535-2543.
8. Hagiwara, H.; Choshi, T.; Fujimoto, H.; Sugino, E.; Hibino, S., A Novel Total Synthesis of Antibiotic Carbazole Alkaloid Carbazomycin G. *Tetrahedron* **2000**, *56* (32), 5807-5811.
9. Abe, T.; Ikeda, T.; Choshi, T.; Hibino, S.; Hatae, N.; Toyata, E.; Yanada, R.; Ishikura, M., Total Synthesis of Calothrixins A and B by Palladium-Catalyzed Tandem Cyclization/Cross-Coupling Reaction of Indolylborate. *Eur. J. Org. Chem.* **2012**, *2012* (26), 5018-5027.
10. Choshi, T.; Fujimoto, H.; Sugino, E.; Hibino, S., Synthesis of new tetracyclic oxazolocarbazoles as functionalized precursors to antioxidative agents, antiostatins and carbazoquinocins. *Heterocycles* **1996**, *43* (9), 1847-1854.
11. Sears, J. E.; Barker, T. J.; Boger, D. L., Total Synthesis of (-)-Vindoline and (+)-4-epi-Vindoline Based on a 1,3,4-Oxadiazole Tandem Intramolecular [4 + 2]/[3 + 2] Cycloaddition Cascade Initiated by an Allene Dienophile. *Org. Lett.* **2015**, *17* (21), 5460-5463.
12. Sasaki, Y.; Kato, D.; Boger, D. L., Asymmetric Total Synthesis of Vindorosine, Vindoline, and Key Vinblastine Analogues. *J. Am. Chem. Soc.* **2010**, *132* (38), 13533-13544.
13. Kato, D.; Sasaki, Y.; Boger, D. L., Asymmetric Total Synthesis of Vindoline. *J. Am. Chem. Soc.* **2010**, *132* (11), 3685-3687.

14. Ishikawa, H.; Elliott, G. I.; Velcicky, J.; Choi, Y.; Boger, D. L., Total Synthesis of (-)- and ent-(+)-Vindoline and Related Alkaloids. *J. Am. Chem. Soc.* **2006**, *128* (32), 10596-10612.
15. Line, N. J.; Witherspoon, B. P.; Hancock, E. N.; Brown, M. K., Synthesis of ent-[3]-Ladderanol: Development and Application of Intramolecular Chirality Transfer [2+2] Cycloadditions of Allenic Ketones and Alkenes. *J. Am. Chem. Soc.* **2017**, *139* (41), 14392-14395.
16. Xu, Y.; Conner, M. L.; Brown, M. K., Cyclobutane and Cyclobutene Synthesis: Catalytic Enantioselective [2+2] Cycloadditions. *Angew. Chem. Int. Ed.* **2015**, *54* (41), 11918-11928.
17. Conner, M. L.; Xu, Y.; Brown, M. K., Catalytic Enantioselective Allenolate-Alkene [2 + 2] Cycloadditions. *J. Am. Chem. Soc.* **2015**, *137* (10), 3482-3485.
18. Guo, R.; Witherspoon, B. P.; Brown, M. K., Evolution of a Strategy for the Enantioselective Synthesis of (-)-Cajanusine. *J. Am. Chem. Soc.* **2020**, *142* (11), 5002-5006.
19. Feldman, K. S.; Antoline, J. F., Synthesis studies on the Melodinus alkaloid meloscine. *Tetrahedron* **2013**, *69* (5), 1434-1445.
20. Ruitenbergh, K.; Kleijn, H.; Elsevier, C. J.; Meijer, J.; Vermeer, P., Palladium(O)-promoted synthesis of functionally substituted allenes by means of organozinc compounds. *Tet. Lett.* **1981**, *22* (15), 1451-1452.
21. Amatov, T.; Pohl, R.; Císařová, I.; Jahn, U., Synthesis of Bridged Diketopiperazines by Using the Persistent Radical Effect and a Formal Synthesis of Bicyclomycin. *Angew. Chem. Int. Ed.* **2015**, *54* (41), 12153-12157.
22. Herzon, S. B.; Myers, A. G., Enantioselective Synthesis of Stephacidin B. *J. Am. Chem. Soc.* **2005**, *127* (15), 5342-5344.
23. Trost, B. M.; Cramer, N.; Bernsmann, H., Concise Total Synthesis of (±)-Marcfortine B. *J. Am. Chem. Soc.* **2007**, *129* (11), 3086-3087.
24. Trost, B. M.; Bringley, D. A.; Zhang, T.; Cramer, N., Rapid Access to Spirocyclic Oxindole Alkaloids: Application of the Asymmetric Palladium-Catalyzed [3 + 2] Trimethylenemethane Cycloaddition. *J. Am. Chem. Soc.* **2013**, *135* (44), 16720-16735.
25. Crick, P. J.; Simpkins, N. S.; Highton, A., Synthesis of the Asperparaline Core by a Radical Cascade. *Org. Lett.* **2011**, *13* (24), 6472-6475.
26. Simpkins, N.; Pavlakos, I.; Male, L., Rapid access to polycyclic indolines related to the stephacidin alkaloids using a radical cascade. *Chem. Comm.* **2012**, *48* (14), 1958-1960.

27. Simpkins, N. S.; Pavlakos, I.; Weller, M. D.; Male, L., The cascade radical cyclisation approach to prenylated alkaloids: synthesis of stephacidin A and notoamide B. *Org. Biomol. Chem.* **2013**, *11* (30), 4957-4970.
28. Movassaghi, M.; Ahmad, O. K., N-Isopropylidene-N'-2-nitrobenzenesulfonyl Hydrazine, a Reagent for Reduction of Alcohols via the Corresponding Monoalkyl Diazenes. *J. Org. Chem.* **2007**, *72* (5), 1838-1841.
29. Williams, R. M.; Armstrong, R. W.; Dung, J. S., Stereocontrolled total synthesis of (+-)- and (+)-bicyclomycin: new carbon-carbon bond-forming reactions on electrophilic glycine anhydride derivatives. *J. Am. Chem. Soc.* **1984**, *106* (19), 5748-5750.
30. Williams, R. M.; Armstrong, R. W.; Dung, J. S., Stereocontrolled total synthesis of (+-)- and (+)-bicyclomycin. *J. Am. Chem. Soc.* **1985**, *107* (11), 3253-3266.
31. Lee, H.; Kang, T.; Lee, H.-Y., Total Synthesis of (±)-Waihoensene. *Angew. Chem. Int. Ed.* **2017**, *56* (28), 8254-8257.
32. Kim, Y.-J.; Yoon, Y.; Lee, H.-Y., An asymmetric total synthesis of (+)-pentalenene. *Tetrahedron* **2013**, *69* (36), 7810-7816.
33. Geum, S.; Lee, H.-Y., Total Synthesis of Panaginsene with Structural Revision. *Org. Lett.* **2014**, *16* (9), 2466-2469.
34. Kang, T.; Song, S. B.; Kim, W.-Y.; Kim, B. G.; Lee, H.-Y., Total Synthesis of (-)-Crinipellin A. *J. Am. Chem. Soc.* **2014**, *136* (29), 10274-10276.
35. DeAngelis, A.; Dmitrenko, O.; Fox, J. M., Rh-Catalyzed Intermolecular Reactions of Cyclic α -Diazocarbonyl Compounds with Selectivity over Tertiary C-H Bond Migration. *J. Am. Chem. Soc.* **2012**, *134* (26), 11035-11043.
36. McCabe, S. R.; Wipf, P., Eight-Step Enantioselective Total Synthesis of (-)-Cycloclavine. *Angew. Chem. Int. Ed.* **2017**, *56* (1), 324-327.
37. Ahlers, A.; de Haro, T.; Gabor, B.; Fürstner, A., Concise Total Synthesis of Enigmazole A. *Angew. Chem. Int. Ed.* **2016**, *55* (4), 1406-1411.
38. Buzas, A.; Istrate, F.; Gagosz, F., Gold(I)-Catalyzed Stereoselective Formation of Functionalized 2,5-Dihydrofurans. *Org. Lett.* **2006**, *8* (9), 1957-1959.
39. Jiang, Y.; Diagne, A. B.; Thomson, R. J.; Schaus, S. E., Enantioselective Synthesis of Allenes by Catalytic Traceless Petasis Reactions. *J. Am. Chem. Soc.* **2017**, *139* (5), 1998-2005.
40. Zhang, X.; Fu, C.; Yu, Y.; Ma, S., Stereoselective Iodolactonization of 4-Allenic Acids with Efficient Chirality Transfer: Development of a New Electrophilic Iodination Reagent. *Chem. Eur. J.* **2012**, *18* (42), 13501-13509.

41. Yasui, M.; Ota, R.; Tsukano, C.; Takemoto, Y., Total synthesis of avenaol. *Nat. Comm.* **2017**, *8* (1), 674.
42. Li, Y.; Dai, M., Total Syntheses of the Reported Structures of Curcusones I and J through Tandem Gold Catalysis. *Angew. Chem. Int. Ed.* **2017**, *56* (38), 11624-11627.
43. Li, Y.; Wei, M.; Dai, M., Gold catalysis-facilitated rapid synthesis of the daphnane/tigliane tricyclic core. *Tetrahedron* **2017**, *73* (29), 4172-4177.
44. Lv, C.; Tu, Q.; Gong, J.; Hao, X.; Yang, Z., Asymmetric total synthesis of (-)-perforanoid A. *Tetrahedron* **2017**, *73* (26), 3612-3621.
45. Inagaki, F.; Mukai, C., Rhodium(I)-Catalyzed Intramolecular Pauson–Khand-Type [2 + 2 + 1] Cycloaddition of Allenenes. *Org. Lett.* **2006**, *8* (6), 1217-1220.
46. Brummond, K. M.; Chen, H.; Fisher, K. D.; Kerekes, A. D.; Rickards, B.; Sill, P. C.; Geib, S. J., An Allenic Pauson–Khand-Type Reaction: A Reversal in π -Bond Selectivity and the Formation of Seven-Membered Rings. *Org. Lett.* **2002**, *4* (11), 1931-1934.
47. Osano, M.; Jhaveri, D. P.; Wipf, P., Formation of 6-Azaindoles by Intramolecular Diels–Alder Reaction of Oxazoles and Total Synthesis of Marinoquinoline A. *Org. Lett.* **2020**, *22* (6), 2215-2219.

Chapter 2 References.

1. Li, N.; Shi, Z.; Tang, Y.; Chen, J.; Li, X., Recent progress on the total synthesis of acetogenins from Annonaceae. *Beilstein J. Org. Chem.* **2008**, *4*, 48.
2. Tempesta, M. S.; Kriek, G. R.; Bates, R. B., Uvaricin, a new antitumor agent from *Uvaria accuminata* (Annonaceae). *J. Org. Chem.* **1982**, *47* (16), 3151-3153.
3. Tundis, R.; Xiao, J.; Loizzo, M. R., *Annona* species (Annonaceae): a rich source of potential antitumor agents? *Ann. NY Acad. Sci.* **2017**, *1398* (1), 30-36.
4. Abdul Wahab, S. M.; Jantan, I.; Haque, M. A.; Arshad, L., Exploring the Leaves of *Annona muricata* L. as a Source of Potential Anti-inflammatory and Anticancer Agents. *Front. Pharmacol.* **2018**, *9* (661).
5. Carmen Zafra-Polo, M.; Figadère, B.; Gallardo, T.; Tormo, J.; Cortes, D., Natural acetogenins from annonaceae, synthesis and mechanisms of action. *Phytochemistry* **1998**, *48* (7), 1087-1117.
6. Chang, F.-R.; Chen, J.-L.; Lin, C.-Y.; Chiu, H.-F.; Wu, M.-J.; Wu, Y.-C., Bioactive acetogenins from the seeds of *Annona atemoya*. *Phytochemistry* **1999**, *51* (7), 883-889.
7. Figadere, B., Syntheses of Acetogenins of Annonaceae: A New Class of Bioactive Polyketides. *Acc. Chem. Res.* **1995**, *28* (9), 359-365.
8. Hoppe, R., Scharf, H. D. , Annonaceous Acetogenins - Synthetic Approaches Towards a Novel Class of Natural Products *Synthesis* **1995**, *12*, 1447-1464.
9. Rupprecht, J. K.; Hui, Y.-H.; McLaughlin, J. L., Annonaceous Acetogenins: A Review. *J. Nat. Prod.* **1990**, *53* (2), 237-278.
10. Sinha, S. C.; Keinan, E., Total synthesis of naturally occurring acetogenins: solamin and reticulatacin. *J. Am. Chem. Soc.* **1993**, *115* (11), 4891-4892.
11. Sun, S.; Liu, J.; Sun, X.; Zhu, W.; Yang, F.; Felczak, L.; Ping Dou, Q.; Zhou, K., Novel Annonaceous acetogenins from *Graviola* (*Annona muricata*) fruits with strong anti-proliferative activity. *Tet. Lett.* **2017**, *58* (19), 1895-1899.
12. Hla Myint, S.; Cortes, D.; Laurens, A.; Hocquemiller, R.; Lebeuf, M.; Cavé, A.; Cotte, J.; Quéro, A.-M., Solamin, a cytotoxic mono-tetrahydrofuranic γ -lactone acetogenin from *Annona muricata* seeds. *Phytochemistry* **1991**, *30* (10), 3335-3338.
13. Gleye, C.; Duret, P.; Laurens, A.; Hocquemiller, R.; Cavé, A., cis-Monotetrahydrofuran Acetogenins from the Roots of *Annona muricata*. *J. Nat. Prod.* **1998**, *61* (5), 576-579.

14. Hu, Y.; Cecil, A. R. L.; Frank, X.; Gleye, C.; Figadère, B.; Brown, R. C. D., Natural cis-solamin is a mixture of two tetra-epimeric diastereoisomers: biosynthetic implications for Annonaceous acetogenins. *Org. Biomol. Chem.* **2006**, *4* (7), 1217-1219.
15. Tormo, J. R.; Gallardo, T.; Aragón, R.; Cortes, D.; Estornell, E., Specific interactions of monotetrahydrofuranic annonaceous acetogenins as inhibitors of mitochondrial complex I. *Chemico-Biol. Interact.* **1999**, *122* (3), 171-183.
16. Makabe, H.; Hattori, Y.; Kimura, Y.; Konno, H.; Abe, M.; Miyoshi, H.; Tanaka, A.; Oritani, T., Total synthesis of cis-solamin and its inhibitory action with bovine heart mitochondrial complex I. *Tetrahedron* **2004**, *60* (47), 10651-10657.
17. Diagne, A. B.; Li, S.; Perkowski, G. A.; Mrksich, M.; Thomson, R. J., SAMDI Mass Spectrometry-Enabled High-Throughput Optimization of a Traceless Petasis Reaction. *ACS Combi. Sci.* **2015**, *17* (11), 658-662.
18. Jiang, Y.; Diagne, A. B.; Thomson, R. J.; Schaus, S. E., Enantioselective Synthesis of Allenes by Catalytic Traceless Petasis Reactions. *J. Am. Chem. Soc.* **2017**, *139* (5), 1998-2005.
19. Jiang, Y.; Thomson, R. J.; Schaus, S. E., Asymmetric Traceless Petasis Borono-Mannich Reactions of Enals: Reductive Transposition of Allylic Diazenes. *Angew. Chem. Int. Ed.* **2017**, *56* (52), 16631-16635.
20. Mundal, D. A.; Lutz, K. E.; Thomson, R. J., A Direct Synthesis of Allenes by a Traceless Petasis Reaction. *J. Am. Chem. Soc.* **2012**, *134* (13), 5782-5785.
21. Kuriyama, W., Ishigami, K., Kitahara, T., Total synthesis of solamin. *Heterocycles* **1999**, *50*, 981-988.
22. Urra, F. A.; Muñoz, F.; Lovy, A.; Cárdenas, C., The Mitochondrial Complex(I)ty of Cancer. *Front. Oncol.* **2017**, *7* (118).
23. Adrian, J.; Stark, C. B. W., Total Synthesis of Muricadienin, the Putative Key Precursor in the Solamin Biosynthesis. *Org. Lett.* **2014**, *16* (22), 5886-5889.
24. Adrian, J.; Gross, L. J.; Stark, C. B. W., The direct oxidative diene cyclization and related reactions in natural product synthesis. *Beilstein J. Org. Chem.* **2016**, *12*, 2104-2123.
25. Makabe, H.; Tanaka, A.; Oritani, T., Total synthesis of solamin and reticulatacin. *J. Chem. Soc., Perkin Transactions 1* **1994**, (14), 1975-1981.
26. Makabe, H., Tanaka, A., Oritani, T., *Biosci. Biotech. Biochem.* **1993**, *57*.
27. Trost, B. M.; Shi, Z., A Concise Convergent Strategy to Acetogenins. (+)-Solamin and Analogs. *J. Am. Chem. Soc.* **1994**, *116* (16), 7459-7460.

28. Trost, B. M.; Mueller, T. J. J.; Martinez, J., Ruthenium Catalyzed Synthesis of Butenolides and Pentenolides via Contra-Electronic α -Alkylation of Hydroxyalkynoates. *J. Am. Chem. Soc.* **1995**, *117* (7), 1888-1899.
29. Cecil, A. R. L.; Brown, R. C. D., Synthesis of cis-Solamin Using a Permanganate-Mediated Oxidative Cyclization. *Org. Lett.* **2002**, *4* (21), 3715-3718.
30. Makabe, H.; Hattori, Y.; Tanaka, A.; Oritani, T., Total Synthesis of cis-Solamin. *Org. Lett.* **2002**, *4* (7), 1083-1085.
31. Göksel, H.; Stark, C. B. W., Total Synthesis of cis-Solamin: Exploiting the RuO₄-Catalyzed Oxidative Cyclization of Dienes. *Org. Lett.* **2006**, *8* (16), 3433-3436.
32. Roth, S.; Göhler, S.; Cheng, H.; Stark, C. B. W., A Highly Efficient Procedure for Ruthenium Tetroxide Catalyzed Oxidative Cyclizations of 1,5-Dienes. *Eur. J. Org. Chem.* **2005**, *2005* (19), 4109-4118.
33. Konno, H.; Makabe, H.; Hattori, Y.; Nosaka, K.; Akaji, K., Synthesis of solamin type mono-THF acetogenins using cross-metathesis. *Tetrahedron* **2010**, *66* (40), 7946-7953.
34. Petasis, N. A.; Akritopoulou, I., The boronic acid mannich reaction: A new method for the synthesis of geometrically pure allylamines. *Tet. Lett.* **1993**, *34* (4), 583-586.
35. Davis, A. S.; Pyne, S. G.; Skelton, B. W.; White, A. H., Synthesis of Putative Uniflorine A. *J. Org. Chem.* **2004**, *69* (9), 3139-3143.
36. Au, C. W. G.; Pyne, S. G., Asymmetric Synthesis of anti-1,2-Amino Alcohols via the Borono-Mannich Reaction: A Formal Synthesis of (-)-Swainsonine. *J. Org. Chem.* **2006**, *71* (18), 7097-7099.
37. Candeias, N. R.; Montalbano, F.; Cal, P. M. S. D.; Gois, P. M. P., Boronic Acids and Esters in the Petasis-Borono Mannich Multicomponent Reaction. *Chem. Rev.* **2010**, *110* (10), 6169-6193.
38. Petasis, N. A.; Goodman, A.; Zavialov, I. A., A new synthesis of α -arylglycines from aryl boronic acids. *Tetrahedron* **1997**, *53* (48), 16463-16470.
39. Petasis, N. A.; Zavialov, I. A., A New and Practical Synthesis of α -Amino Acids from Alkenyl Boronic Acids. *J. Am. Chem. Soc.* **1997**, *119* (2), 445-446.
40. Sugiura, M.; Hirano, K.; Kobayashi, S., α -Aminoallylation of Aldehydes with Ammonia: Stereoselective Synthesis of Homoallylic Primary Amines. *J. Am. Chem. Soc.* **2004**, *126* (23), 7182-7183.

41. Jiang, B.; Yang, C.-G.; Gu, X.-H., A highly stereoselective synthesis of indolyl N-substituted glycines. *Tet. Lett.* **2001**, *42* (13), 2545-2547.
42. Nanda, K. K.; Wesley Trotter, B., Diastereoselective Pétasis Mannich reactions accelerated by hexafluoroisopropanol: a pyrrolidine-derived arylglycine synthesis. *Tet. Lett.* **2005**, *46* (12), 2025-2028.
43. Harwood, L. M.; Currie, G. S.; Drew, M. G. B.; Luke, R. W. A., Asymmetry in the boronic acid Mannich reaction: diastereocontrolled addition to chiral iminium species derived from aldehydes and (S)-5-phenylmorpholin-2-one. *Chem. Comm.* **1996**, (16), 1953-1954.
44. Currie, G. S.; Drew, M. G. B.; Harwood, L. M.; Hughes, D. J.; Luke, R. W. A.; Vickers, R. J., Chirally templated boronic acid Mannich reaction in the synthesis of optically active α -amino acids. *J. Chem. Soc., Perkin Transactions 1* **2000**, (17), 2982-2990.
45. Koolmeister, T.; Södergren, M.; Scobie, M., The first example of chiral induction using homochiral boronic esters in the Pétasis reaction. *Tet. Lett.* **2002**, *43* (34), 5969-5970.
46. Southwood, T. J.; Curry, M. C.; Hutton, C. A., Factors affecting the efficiency and stereoselectivity of α -amino acid synthesis by the Pétasis reaction. *Tetrahedron* **2006**, *62* (1), 236-242.
47. Lou, S.; Schaus, S. E., Asymmetric Pétasis Reactions Catalyzed by Chiral Biphenols. *J. Am. Chem. Soc.* **2008**, *130* (22), 6922-6923.
48. Yamaoka, Y.; Miyabe, H.; Takemoto, Y., Catalytic Enantioselective Pétasis-Type Reaction of Quinolines Catalyzed by a Newly Designed Thiourea Catalyst. *J. Am. Chem. Soc.* **2007**, *129* (21), 6686-6687.
49. Bishop, J. A.; Lou, S.; Schaus, S. E., Enantioselective Addition of Boronates to Acyl Imines Catalyzed by Chiral Biphenols. *Angew. Chem. Int. Ed.* **2009**, *48* (24), 4337-4340.
50. Muncipinto, G.; Moquist, P. N.; Schreiber, S. L.; Schaus, S. E., Catalytic Diastereoselective Pétasis Reactions. *Angew. Chem. Int. Ed.* **2011**, *50* (35), 8172-8175.
51. Myers, A. G.; Finney, N. S., Direct observation and retro-ene reaction of a propargylic diazene. Stereochemical assignment of monoalkyl diazenes. *J. Am. Chem. Soc.* **1990**, *112* (26), 9641-9643.
52. Myers, A. G.; Finney, N. S.; Kuo, E. Y., Allene synthesis from 2-alkyn-1-ols. *Tet. Lett.* **1989**, *30* (42), 5747-5750.
53. Myers, A. G.; Zheng, B., New and Stereospecific Synthesis of Allenes in a Single Step from Propargylic Alcohols. *J. Am. Chem. Soc.* **1996**, *118* (18), 4492-4493.

54. Movassaghi, M.; Ahmad, O. K., N-Isopropylidene-N'-2-nitrobenzenesulfonyl Hydrazine, a Reagent for Reduction of Alcohols via the Corresponding Monoalkyl Diazenes. *J. Org. Chem.* **2007**, *72* (5), 1838-1841.
55. Zhao, M.; Kuang, C.; Yang, Q.; Cheng, X., Cs₂CO₃-mediated synthesis of terminal alkynes from 1,1-dibromo-1-alkenes. *Tet. Lett.* **2011**, *52* (9), 992-994.
56. Ishitani, H.; Ueno, M.; Kobayashi, S., Enantioselective Mannich-Type Reactions Using a Novel Chiral Zirconium Catalyst for the Synthesis of Optically Active β -Amino Acid Derivatives. *J. Am. Chem. Soc.* **2000**, *122* (34), 8180-8186.
57. Zhang, C.-P.; Chen, Q.-Y.; Guo, Y.; Xiao, J.-C.; Gu, Y.-C., Difluoromethylation and trifluoromethylation reagents derived from tetrafluoroethane β -sultone: Synthesis, reactivity and applications. *Coord. Chem. Rev.* **2014**, *261*, 28-72.
58. Mandai, H.; Fujii, K.; Yasuhara, H.; Abe, K.; Mitsudo, K.; Korenaga, T.; Suga, S., Enantioselective acyl transfer catalysis by a combination of common catalytic motifs and electrostatic interactions. *Nat. Comm.* **2016**, *7* (1), 11297.
59. Brown, H. C.; Jadhav, P. K.; Bhat, K. S., Chiral synthesis via organoboranes. 13. A highly diastereoselective and enantioselective addition of [(Z)-gamma-alkoxyallyl]diisopinocampheylboranes to aldehydes. *J. Am. Chem. Soc.* **1988**, *110* (5), 1535-1538.
60. Erb, W.; Grassot, J.-M.; Linder, D.; Neuville, L.; Zhu, J., Enantioselective Synthesis of Putative Lipiarmycin Aglycon Related to Fidaxomicin/Tiacumicin B. *Angew. Chem. Int. Ed.* **2015**, *54* (6), 1929-1932.
61. Morrison, R. J.; Hoveyda, A. H., γ -, Diastereo-, and Enantioselective Addition of MEMO-Substituted Allylboron Compounds to Aldimines Catalyzed by Organoboron-Ammonium Complexes. *Angew. Chem. Int. Ed.* **2018**, *57* (36), 11654-11661.
62. Wang, Y. D.; Kimball, G.; Prashad, A. S.; Wang, Y., Zr-Mediated hydroboration: stereoselective synthesis of vinyl boronic esters. *Tet. Lett.* **2005**, *46* (50), 8777-8780.
63. Yamamoto, Y.; Miyairi, T.; Ohmura, T.; Miyaura, N., Synthesis of Chiral Esters of (E)-3-(Silyloxy)-2-propenylboronic Acid via the Iridium-Catalyzed Isomerization of the Double Bond. *J. Org. Chem.* **1999**, *64* (1), 296-298.
64. Yin, N.; Wang, G.; Qian, M.; Negishi, E., Stereoselective Synthesis of the Side Chains of Mycolactones A and B Featuring Stepwise Double Substitutions of 1,1-Dibromo-1-alkenes. *Angew. Chem. Int. Ed.* **2006**, *45* (18), 2916-2920.
65. Armarego, W. L. F.; Chai, C. L. L., *Purification of Laboratory Chemicals*. 5 ed.; Butterworth-Heinemann: 2003.

Chapter 3 References.

1. Newman, D. J.; Cragg, G. M., Natural Products as Sources of New Drugs from 1981 to 2014. *J. Nat. Prod.* **2016**, *79* (3), 629-661.
2. Newman, D. J.; Cragg, G. M., Natural Products As Sources of New Drugs over the 30 Years from 1981 to 2010. *J. Nat. Prod.* **2012**, *75* (3), 311-335.
3. Patridge, E.; Gareiss, P.; Kinch, M. S.; Hoyer, D., An analysis of FDA-approved drugs: natural products and their derivatives. *Drug Discov. Today* **2016**, *21* (2), 204-207.
4. Pye, C. R.; Bertin, M. J.; Lokey, R. S.; Gerwick, W. H.; Linington, R. G., Retrospective analysis of natural products provides insights for future discovery trends. *PNAS* **2017**, *114* (22), 5601-5606.
5. Gomes, N. G. M.; Pereira, D. M.; Valentão, P.; Andrade, P. B., Hybrid MS/NMR methods on the prioritization of natural products: Applications in drug discovery. *J. Pharma. and Biomed. Analy.* **2017**.
6. Atanasov, A. G.; Waltenberger, B.; Pferschy-Wenzig, E.-M.; Linder, T.; Wawrosch, C.; Uhrin, P.; Temml, V.; Wang, L.; Schwaiger, S.; Heiss, E. H.; Rollinger, J. M.; Schuster, D.; Breuss, J. M.; Bochkov, V.; Mihovilovic, M. D.; Kopp, B.; Bauer, R.; Dirsch, V. M.; Stuppner, H., Discovery and resupply of pharmacologically active plant-derived natural products: A review. *Biotech. Adv.* **2015**, *33* (8), 1582-1614.
7. Gaudencio, S. P.; Pereira, F., Dereplication: racing to speed up the natural products discovery process. *Nat. Prod. Rep.* **2015**, *32* (6), 779-810.
8. Koehn, F. E.; Carter, G. T., The evolving role of natural products in drug discovery. *Nat. Rev. Drug. Discov.* **2005**, *4* (3), 206-220.
9. Kong, D. X.; Guo, M. Y.; Xiao, Z. H.; Chen, L. L.; Zhang, H. Y., Historical Variation of Structural Novelty in a Natural Product Library. *Chem. & Biodiv.* **2011**, *8* (11), 1968-1977.
10. Walsh, C. T., A chemocentric view of the natural product inventory. *Nat. Chem. Biol.* **2015**, *11* (9), 620-624.
11. Ju, K.-S.; Gao, J.; Doroghazi, J. R.; Wang, K.-K. A.; Thibodeaux, C. J.; Li, S.; Metzger, E.; Fudala, J.; Su, J.; Zhang, J. K.; Lee, J.; Cioni, J. P.; Evans, B. S.; Hirota, R.; Labeda, D. P.; van der Donk, W. A.; Metcalf, W. W., Discovery of phosphonic acid natural products by mining the genomes of 10,000 actinomycetes. *PNAS* **2015**, *112* (39), 12175-12180.
12. Baltz, R. H., Marcel Faber Roundtable: Is our antibiotic pipeline unproductive because of starvation, constipation or lack of inspiration? *J. Ind. Microbiol. Biot.* **2006**, *33* (7), 507-513.

13. Takahashi, Y.; Nakashima, T., Actinomycetes, an Inexhaustible Source of Naturally Occurring Antibiotics. *Antibiotics (Basel)* **2018**, *7* (2), 45.
14. Goering, A. W.; McClure, R. A.; Doroghazi, J. R.; Albright, J. C.; Haverland, N. A.; Zhang, Y.; Ju, K.-S.; Thomson, R. J.; Metcalf, W. W.; Kelleher, N. L., Metabologenomics: Correlation of Microbial Gene Clusters with Metabolites Drives Discovery of a Nonribosomal Peptide with an Unusual Amino Acid Monomer. *ACS Cent. Sci.* **2016**, *2* (2), 99-108.
15. Doroghazi, J. R.; Albright, J. C.; Goering, A. W.; Ju, K.-S.; Haines, R. R.; Tchalukov, K. A.; Labeda, D. P.; Kelleher, N. L.; Metcalf, W. W., A roadmap for natural product discovery based on large-scale genomics and metabolomics. *Nat Chem Biol* **2014**, *10* (11), 963-968.
16. Doroghazi, J. R.; Metcalf, W. W., Comparative genomics of actinomycetes with a focus on natural product biosynthetic genes. *BMC Genomics* **2013**, *14*, 611-611.
17. Izumikawa, M.; Kawahara, T.; Kagaya, N.; Yamamura, H.; Hayakawa, M.; Takagi, M.; Yoshida, M.; Doi, T.; Shin-ya, K., Pyrrolidine-containing peptides, JBIR-126, -148, and -149, from *Streptomyces* sp. NBRC 111228. *Tet. Lett.* **2015**, *56* (39), 5333-5336.
18. Motohashi, K.; Takagi, M.; Shin-ya, K., Tetrapeptides Possessing a Unique Skeleton, JBIR-34 and JBIR-35, Isolated from a Sponge-Derived Actinomycete, *Streptomyces* sp. Sp080513GE-23. *J. Nat. Prod.* **2010**, *73* (2), 226-228.
19. Payne, J. A. E.; Schoppet, M.; Hansen, M. H.; Cryle, M. J., Diversity of nature's assembly lines - recent discoveries in non-ribosomal peptide synthesis. *Mol. BioSyst.* **2017**, *13* (1), 9-22.
20. Felnagle, E. A.; Jackson, E. E.; Chan, Y. A.; Podevels, A. M.; Berti, A. D.; McMahon, M. D.; Thomas, M. G., Nonribosomal Peptide Synthetases Involved in the Production of Medically Relevant Natural Products. *Mol. Pharm.* **2008**, *5* (2), 191-211.
21. Martínez-Núñez, M. A.; López, V. E. L. y., Nonribosomal peptides synthetases and their applications in industry. *Sustain. Chem. Process.* **2016**, *4* (1), 13.
22. Hanssen, K. Ø.; Schuler, B.; Williams, A. J.; Demissie, T. B.; Hansen, E.; Andersen, J. H.; Svenson, J.; Blinov, K.; Repisky, M.; Mohn, F.; Meyer, G.; Svendsen, J.-S.; Ruud, K.; Elyashberg, M.; Gross, L.; Jaspars, M.; Isaksson, J., A Combined Atomic Force Microscopy and Computational Approach for the Structural Elucidation of Breitfussin A and B: Highly Modified Halogenated Dipeptides from *Thuiaria breitfussi*. *Angew. Chem. Int. Ed.* **2012**, *51* (49), 12238-12241.
23. Patiño C, L. P.; Muniain, C.; Knott, M. E.; Puricelli, L.; Palermo, J. A., Bromopyrrole Alkaloids Isolated from the Patagonian Bryozoan *Aspidostoma giganteum*. *J. Nat. Prod.* **2014**, *77* (5), 1170-1178.

24. Fu, P.; Jamison, M.; La, S.; MacMillan, J. B., Inducamides A–C, Chlorinated Alkaloids from an RNA Polymerase Mutant Strain of *Streptomyces* sp. *Org. Lett.* **2014**, *16* (21), 5656-5659.
25. Gribble, G. W., Natural Organohalogens: A New Frontier for Medicinal Agents? *J. Chem. Ed.* **2004**, *81* (10), 1441.
26. Neumann, C. S.; Fujimori, D. G.; Walsh, C. T., Halogenation Strategies In Natural Product Biosynthesis. *Chem. & Biol.* **2008**, *15* (2), 99-109.
27. Fenical, W.; Jensen, P. R., Developing a new resource for drug discovery: marine actinomycete bacteria. *Nat. Chem. Biol.* **2006**, *2* (12), 666-673.
28. Nettleton, D. E.; Doyle, T. W.; Krishnan, B.; Matsumoto, G. K.; Clardy, J., Isolation and structure of rebeccamycin - a new antitumor antibiotic from *Nocardia aerocoligenes*. *Tet. Lett.* **1985**, *26* (34), 4011-14.
29. Gribble, G. W., Naturally Occurring Organohalogen Compounds. *Acc. Chem. Res.* **1998**, *31*, 141-152.
30. Kirby, W. M. M.; Perry, D. M.; Bauer, A. W., Treatment of Staphylococcal Septicemia with Vancomycin. *N. Engl. J. Med.* **1960**, *262* (2), 49-55.
31. Arima, K.; Imanaka, H.; Kousaka, M.; Fukuta, A.; Tamura, G., Pyrrolnitrin, a New Antibiotic Substance, Produced by *Pseudomonas*. *Agric. Biol. Chem.* **1964**, *28* (8), 575-576.
32. Harris, C. M.; Kannan, R.; Kopecka, H.; Harris, T. M., The role of the chlorine substituents in the antibiotic vancomycin: preparation and characterization of mono- and didechlorovancomycin. *J. Am. Chem. Soc.* **1985**, *107* (23), 6652-6658.
33. Rodrigues Pereira, E.; Belin, L.; Sancelme, M.; Prudhomme, M.; Ollier, M.; Rapp, M.; Severe, D.; Riou, J.-F.; Fabbro, D.; Meyer, T., Structure–Activity Relationships in a Series of Substituted Indolocarbazoles: Topoisomerase I and Protein Kinase C Inhibition and Antitumoral and Antimicrobial Properties. *J. Med. Chem.* **1996**, *39* (22), 4471-4477.
34. Muliandi, A.; Katsuyama, Y.; Sone, K.; Izumikawa, M.; Moriya, T.; Hashimoto, J.; Kozono, I.; Takagi, M.; Shin-ya, K.; Ohnishi, Y., Biosynthesis of the 4-Methyloxazoline-Containing Nonribosomal Peptides, JBIR-34 and -35, in *Streptomyces* sp. Sp080513GE-23. *Chem. & Biol.* *21* (8), 923-934.
35. Ong, S. A.; Peterson, T.; Neilands, J. B., Agrobactin, a siderophore from *Agrobacterium tumefaciens*. *J. Biol. Chem.* **1979**, *254*, 1860-1865.
36. Bergeron, R. J.; Kline, S. J., Short synthesis of parabactin. *J. Am. Chem. Soc.* **1982**, *104* (16), 4489-4492.

37. Linder, J.; Blake, A. J.; Moody, C. J., Total synthesis of siphonazole and its O-methyl derivative, structurally unusual bis-oxazole natural products. *Org. Biomol. Chem.* **2008**, *6* (21), 3908-3916.
38. Griffiths, G. L.; Sigel, S. P.; Payne, S. M.; Neilands, J. B., Vibriobactin, a siderophore from *Vibrio cholerae*. *J. Biol. Chem.* **1984**, *259*, 383-385.
39. Sakakura, A.; Kondo, R.; Umemura, S.; Ishihara, K., Dehydrative cyclization of serine, threonine, and cysteine residues catalyzed by molybdenum(VI) oxo compounds. *Tetrahedron* **2009**, *65* (10), 2102-2109.
40. Sinha Roy, R.; M. Gehring, A.; C. Milne, J.; J. Belshaw, P.; T. Walsh, C., Thiazole and oxazole peptides: biosynthesis and molecular machinery. *Nat. Prod. Rep.* **1999**, *16* (2), 249-263.
41. Takagi, J.; Sato, K.; Hartwig, J. F.; Ishiyama, T.; Miyaura, N., Iridium-catalyzed C–H coupling reaction of heteroaromatic compounds with bis(pinacolato)diboron: regioselective synthesis of heteroarylboronates. *Tet. Lett.* **2002**, *43* (32), 5649-5651.
42. Kallepalli, V. A.; Shi, F.; Paul, S.; Onyeozili, E. N.; Maleczka, R. E.; Smith, M. R., Boc Groups as Protectors and Directors for Ir-Catalyzed C–H Borylation of Heterocycles. *J. Org. Chem.* **2009**, *74* (23), 9199-9201.
43. Kawamorita, S.; Ohmiya, H.; Sawamura, M., Ester-Directed Regioselective Borylation of Heteroarenes Catalyzed by a Silica-Supported Iridium Complex. *J. Org. Chem.* **2010**, *75* (11), 3855-3858.
44. Paul, S.; Chotana, G. A.; Holmes, D.; Reichle, R. C.; Maleczka, R. E.; Smith, M. R., Ir-Catalyzed Functionalization of 2-Substituted Indoles at the 7-Position: Nitrogen-Directed Aromatic Borylation. *J. Am. Chem. Soc.* **2006**, *128* (49), 15552-15553.
45. Robbins, D. W.; Boebel, T. A.; Hartwig, J. F., Iridium-Catalyzed, Silyl-Directed Borylation of Nitrogen-Containing Heterocycles. *J. Am. Chem. Soc.* **2010**, *132* (12), 4068-4069.
46. Homer, J. A.; Sperry, J., A short synthesis of the endogenous plant metabolite 7-hydroxyoxindole-3-acetic acid (7-OH-OxIAA) using simultaneous C–H borylations. *Tet. Lett.* **2014**, *55* (42), 5798-5800.
47. Loach, R. P.; Fenton, O. S.; Amaike, K.; Siegel, D. S.; Ozkal, E.; Movassaghi, M., C7-Derivatization of C3-Alkylindoles Including Tryptophans and Tryptamines. *J. Org. Chem.* **2014**, *79* (22), 11254-11263.
48. Feng, Y.; Holte, D.; Zoller, J.; Umemiya, S.; Simke, L. R.; Baran, P. S., Total Synthesis of Verruculogen and Fumitremorgin A Enabled by Ligand-Controlled C–H Borylation. *J. Am. Chem. Soc.* **2015**, *137* (32), 10160-10163.

49. Humphrey, G. R.; Kuethe, J. T., Practical Methodologies for the Synthesis of Indoles. *Chem. Rev.* **2006**, *106* (7), 2875-2911.
50. Taniguchi, M.; Anjiki, T.; Nakagawa, M.; Hino, T., Formation and Reactions of the Cyclic Tautomers of Tryptophans and Tryptamines. VII. Hydroxylation of Tryptophans and Tryptamines. *Chem. Pharm. Bull.* **1984**, *32* (7), 2544-2554.
51. Meyer, F.-M.; Liras, S.; Guzman-Perez, A.; Perreault, C.; Bian, J.; James, K., Functionalization of Aromatic Amino Acids via Direct C–H Activation: Generation of Versatile Building Blocks for Accessing Novel Peptide Space. *Org. Lett.* **2010**, *12* (17), 3870-3873.
52. Ishiyama, T.; Takagi, J.; Yonekawa, Y.; Hartwig, J. F.; Miyaura, N., Iridium-Catalyzed Direct Borylation of Five-Membered Heteroarenes by Bis(pinacolato)diboron: Regioselective, Stoichiometric, and Room Temperature Reactions. *Adv. Synth. & Catal.* **2003**, *345* (9-10), 1103-1106.
53. Liu, Q.; Li, Q.; Ma, Y.; Jia, Y., Direct Olefination at the C-4 Position of Tryptophan via C–H Activation: Application to Biomimetic Synthesis of Clavicipitic Acid. *Org. Lett.* **2013**, *15* (17), 4528-4531.
54. Knochel, P.; Dohle, W.; Gommermann, N.; Kneisel, F. F.; Kopp, F.; Korn, T.; Sapountzis, I.; Vu, V. A., Highly Functionalized Organomagnesium Reagents Prepared through Halogen–Metal Exchange. *Angew. Chem. Int. Ed.* **2003**, *42* (36), 4302-4320.
55. Pandey, S. K.; Guttormsen, Y.; Haug, B. E.; Hedberg, C.; Bayer, A., A Concise Total Synthesis of Breitfussin A and B. *Org. Lett.* **2015**, *17* (1), 122-125.
56. Yuan, C.; Liu, B., Total synthesis of natural products via iridium catalysis. *Org. Chem. Front.* **2018**, *5* (1), 106-131.
57. Gutkunst, W. R.; Baran, P. S., C-H functionalization logic in total synthesis. *Chem. Soc. Rev.* **2011**, *40* (4), 1976-1991.
58. Murphy, J. M.; Liao, X.; Hartwig, J. F., Meta Halogenation of 1,3-Disubstituted Arenes via Iridium-Catalyzed Arene Borylation. *J. Am. Chem. Soc.* **2007**, *129* (50), 15434-15435.
59. Carpino, L. A., 1-Hydroxy-7-azabenzotriazole. An efficient peptide coupling additive. *J. Am. Chem. Soc.* **1993**, *115* (10), 4397-4398.
60. Phillips, A. J.; Uto, Y.; Wipf, P.; Reno, M. J.; Williams, D. R., Synthesis of Functionalized Oxazolines and Oxazoles with DAST and Deoxo-Fluor. *Org. Lett.* **2000**, *2* (8), 1165-1168.

61. Foulke-Abel, J.; Agbo, H.; Zhang, H.; Mori, S.; Watanabe, C. M. H., Mode of action and biosynthesis of the azabicyclic-containing natural products azinomycin and ficellomycin. *Nat. Prod. Rep.* **2011**, *28* (4), 693-704.
62. Zhao, Q.; He, Q.; Ding, W.; Tang, M.; Kang, Q.; Yu, Y.; Deng, W.; Zhang, Q.; Fang, J.; Tang, G.; Liu, W., Characterization of the Azinomycin B Biosynthetic Gene Cluster Revealing a Different Iterative Type I Polyketide Synthase for Naphthoate Biosynthesis. *Chem. & Biol.* **2008**, *15* (7), 693-705.
63. Schramma, K. R.; Bushin, L. B.; Seyedsayamdost, M. R., Structure and biosynthesis of a macrocyclic peptide containing an unprecedented lysine-to-tryptophan crosslink. *Nat. Chem.* **2015**, *7* (5), 431-437.
64. Isley, N. A.; Endo, Y.; Wu, Z.-C.; Covington, B. C.; Bushin, L. B.; Seyedsayamdost, M. R.; Boger, D. L., Total Synthesis and Stereochemical Assignment of Streptide. *J. Am. Chem. Soc.* **2019**, *141* (43), 17361-17369.
65. Sengupta, S.; Mehta, G., Macrocyclization via C–H functionalization: a new paradigm in macrocycle synthesis. *Org. Biomol. Chem.* **2020**, *18* (10), 1851-1876.
66. Imai, Y.; Meyer, K.; Iinishi, A.; Favre-godal, Q.; Green, R.; Manuse, S.; Caboni, M.; Mori, M.; Niles, S.; Ghiglieri, M.; Honrao, C.; Ma, X.; Guo, J.; Makriyannis, A.; Linares-Otaya, L.; Böhringer, N.; Wuisan, Z.; Kaur, H.; Wu, R.; Lewis, K., A new antibiotic selectively kills Gram-negative pathogens. *Nature* **2019**, 576.
67. Ji, Z.; Wang, M.; Wei, S.; Zhang, J.; Wu, W., Isolation, structure elucidation and antibacterial activities of streptothricin acids. *J. Antib.* **2009**, *62* (5), 233-237.
68. Davison, J. R.; Lohith, K. M.; Wang, X.; Bobyk, K.; Mandadapu, S. R.; Lee, S.-L.; Cencic, R.; Nelson, J.; Simpkins, S.; Frank, K. M.; Pelletier, J.; Myers, C. L.; Piotrowski, J.; Smith, H. E.; Bewley, C. A., A New Natural Product Analog of Blasticidin S Reveals Cellular Uptake Facilitated by the NorA Multidrug Transporter. *Antimicrob. Agents Chemo.* **2017**, *61* (6), e02635-16.
69. Kudo, F.; Miyanaga, A.; Eguchi, T., Biosynthesis of natural products containing β -amino acids. *Nat. Prod. Rep.* **2014**, *31* (8), 1056-1073.
70. Siricilla, S.; Mitachi, K.; Wan, B.; Franzblau, S. G.; Kurosu, M., Discovery of a capuramycin analog that kills nonreplicating Mycobacterium tuberculosis and its synergistic effects with translocase I inhibitors. *J. Antib.* **2015**, *68* (4), 271-278.
71. White, K. N.; Tenney, K.; Crews, P., The Bengamides: A Mini-Review of Natural Sources, Analogues, Biological Properties, Biosynthetic Origins, and Future Prospects. *J. Nat. Prod.* **2017**, *80* (3), 740-755.

72. Macko, V.; Stimmel, M. B.; Peeters, H.; Wolpert, T. J.; Dunkle, L. D.; Acklin, W.; Banteli, R.; Jaun, B.; Arigoni, D., The structure of circinatin, a non-toxic metabolite from the plant pathogenic fungus *Periconia circinata*. *Experientia* **1990**, *46* (11), 1206-1209.
73. Ikeda, Y.; Nonaka, H.; Furumai, T.; Onaka, H.; Igarashi, Y., Nocardimicins A, B, C, D, E, and F, Siderophores with Muscarinic M3 Receptor Inhibiting Activity from *Nocardia* sp. TP-A0674. *J. Nat. Prod.* **2005**, *68* (7), 1061-1065.
74. Liu, X.; Jin, Y.; Cui, Z.; Nonaka, K.; Baba, S.; Funabashi, M.; Yang, Z.; Van Lanen, S. G., The Role of a Nonribosomal Peptide Synthetase in L-Lysine Lactamization During Capuramycin Biosynthesis. *ChemBioChem* **2016**, *17* (9), 804-810.
75. Hanessian, S., Sharma, R., The Synthesis of Bicyclic Piperazine-2-Carboxylic Acids from L-Proline. *Heterocycles* **2000**, *52* (3), 1231-1239.
76. Evans, D. A.; Britton, T. C.; Ellman, J. A.; Dorow, R. L., The asymmetric synthesis of .alpha.-amino acids. Electrophilic azidation of chiral imide enolates, a practical approach to the synthesis of (R)- and (S)-.alpha.-azido carboxylic acids. *J. Am. Chem. Soc.* **1990**, *112* (10), 4011-4030.
77. Evans, D. A.; Britton, T. C., Electrophilic azide transfer to chiral enolates. A general approach to the asymmetric synthesis of .alpha.-amino acids. *J. Am. Chem. Soc.* **1987**, *109* (22), 6881-6883.
78. Chung, H., Kim, H., Chung, K., Synthesis of optically active 2-piperidylglycine. *Heterocycles* **1999**, *51* (12), 2983-2989.
79. Evans, D. A.; Ennis, M. D.; Mathre, D. J., Asymmetric alkylation reactions of chiral imide enolates. A practical approach to the enantioselective synthesis of .alpha.-substituted carboxylic acid derivatives. *J. Am. Chem. Soc.* **1982**, *104* (6), 1737-1739.
80. Evans, D. A.; Ennis, M. D.; Le, T.; Mandel, N.; Mandel, G., Asymmetric acylation reactions of chiral imide enolates. The first direct approach to the construction of chiral .beta.-dicarbonyl synthons. *J. Am. Chem. Soc.* **1984**, *106* (4), 1154-1156.
81. Evans, D. A.; Morrissey, M. M.; Dorow, R. L., Asymmetric oxygenation of chiral imide enolates. A general approach to the synthesis of enantiomerically pure .alpha.-hydroxy carboxylic acid synthons. *J. Am. Chem. Soc.* **1985**, *107* (14), 4346-4348.
82. Evans, D. A.; Weber, A. E., Asymmetric glycine enolate aldol reactions: synthesis of cyclosporin's unusual amino acid, MeBmt. *J. Am. Chem. Soc.* **1986**, *108* (21), 6757-6761.
83. Evans, D. A.; Sjogren, E. B.; Weber, A. E.; Conn, R. E., Asymmetric synthesis of anti- β -hydroxy- α -amino acids. *Tet. Lett.* **1987**, *28* (1), 39-42.

84. Evans, D. A.; Sjogren, E. B.; Bartroli, J.; Dow, R. L., Aldol addition reactions of chiral crotonate imides. *Tet. Lett.* **1986**, 27 (41), 4957-4960.
85. Evans, D. A.; Britton, T. C.; Dorow, R. L.; Dellaria Jr, J. F., The asymmetric synthesis of α -amino and α -hydrazino acid derivatives via the stereoselective amination of chiral enolates with azodicarboxylate esters. *Tetrahedron* **1988**, 44 (17), 5525-5540.
86. Evans, D. A.; Britton, T. C.; Ellman, J. A., Contrasteric carboximide hydrolysis with lithium hydroperoxide. *Tet. Lett.* **1987**, 28 (49), 6141-6144.
87. Frank, R.; Schutkowski, M., Extremely mild reagent for Boc deprotection applicable to the synthesis of peptides with thioamide linkages. *Chem. Comm.* **1996**, (22), 2509-2510.
88. Miel, H.; Rault, S., Total deprotection of N,N'-bis(tert-butoxycarbonyl)guanidines using SnCl₄. *Tet. Lett.* **1997**, 38 (45), 7865-7866.
89. Miley, G. P.; Rote, J. C.; Silverman, R. B.; Kelleher, N. L.; Thomson, R. J., Total Synthesis of Tambromycin Enabled by Indole C–H Functionalization. *Org. Lett.* **2018**, 20 (8), 2369-2373.
90. Zhang, X.; King-Smith, E.; Renata, H., Total Synthesis of Tambromycin by Combining Chemocatalytic and Biocatalytic C–H Functionalization. *Angew. Chem. Int. Ed.* **2018**, 57 (18), 5037-5041.
91. Lehmann, J.; Wright, M. H.; Sieber, S. A., Making a Long Journey Short: Alkyne Functionalization of Natural Product Scaffolds. *Chem. Eur. J.* **2016**, 22 (14), 4666-4678.
92. Wright, M. H.; Sieber, S. A., Chemical proteomics approaches for identifying the cellular targets of natural products. *Nat. Prod. Rep.* **2016**, 33 (5), 681-708.
93. Liang, L.; Astruc, D., The copper(I)-catalyzed alkyne-azide cycloaddition (CuAAC) “click” reaction and its applications. An overview. *Coord. Chem. Rev.* **2011**, 255 (23), 2933-2945.
94. MacKinnon, A. L.; Garrison, J. L.; Hegde, R. S.; Taunton, J., Photo-Leucine Incorporation Reveals the Target of a Cyclodepsipeptide Inhibitor of Cotranslational Translocation. *J. Am. Chem. Soc.* **2007**, 129 (47), 14560-14561.
95. Armarego, W. L. F.; Chai, C. L. L., *Purification of Laboratory Chemicals*. 5 ed.; Butterworth-Heinemann: 2003.
96. Dubuisson, C.; Fukumoto, Y.; Hegedus, L. S., Synthesis of Dipeptides by the Photolytic Coupling of Chromium Aminocarbene Complexes with α -Amino Acid Esters. 2. Side Chain Functionalized and α , α -Disubstituted α -Amino Acid Esters and N-Methyl- and N-Methyl- α , α -dialkyl- α -amino Acid Esters. *J. Am. Chem. Soc.* **1995**, 117 (13), 3697-3704.

97. Ireland, R. E.; Meissner, R. S., Convenient method for the titration of amide base solutions. *J. Org. Chem.* **1991**, *56* (14), 4566-4568.

APPENDIX 1

Synthesis of Diastereomeric β -Hydroxy Phenylalanine Residues for Structural Elucidation of Faulknamycin

**Portions of this chapter are reproduced in part
from:**

Tryon, J. H., Rote, J. C., Chen, L., Robey, M., Vega, M., Phua, W. C., Ju, K., Kelleher, N., Thomson, R.J. Metabologenomics directed genome mining for cyclic-guanidino functional groups unveils a novel biosynthetic route. *In preparation*.

A1.1 Introduction

A1.1.1 Development of synthetic standards for natural product (NP) structural elucidation.

Organic synthesis has existed as one of the most powerful and reliable methods for natural product (NP) stereochemical and structural elucidation for centuries.¹ Although modern analytical techniques like NMR spectroscopy, MS, and X-ray crystallography have significantly contributed to the ease with which NPs are structurally characterized, structure misassignment is still possible due to both human error and to the interpretive nature of these analytical methods.^{1,2} Synthetic methods towards structural elucidation, on the other hand, can provide unambiguous validation of putatively assigned structures. While structure-determining total syntheses are often time-consuming and methodologically challenging, if paired with modern degradation/fragment derivatization processes, stereodefined synthesis of NP fragments can provide concrete evidence of absolute configuration. This fragment-based approach is particularly applicable to certain classes of natural products, such as peptide NPs, wherein sequencing methods can be used to deconstruct the molecule into discrete components ideal for comparison with synthetic standards.

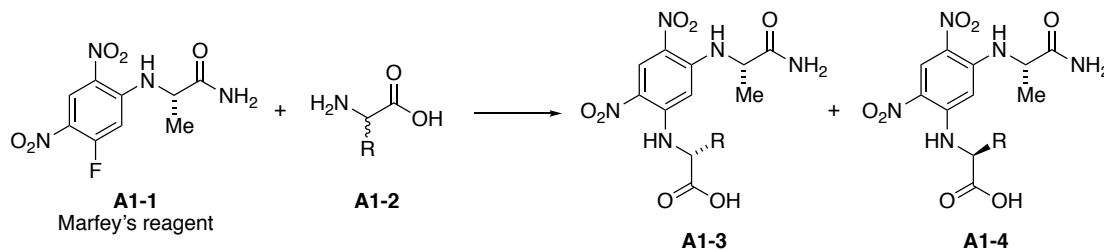
A1.1.2 Marfey's analysis for stereochemical assignment of amino acid residues.

Synthetic derivatization methods for absolute stereochemical determination are frequently applied to peptide NPs, structures that are universally assembled via amide bond condensation of discrete amino acid (AA) residues. Given the sensitivity of this bond towards fragmentation, peptide NPs are well-suited towards MS-based sequencing, wherein chemical hydrolysis/ionization techniques are used to deconstruct the peptide and provide mass-fragment data that corresponds to each constituent AA monomer. However, proteinogenic amino acids that are condensed onto peptide natural products exhibit chirality at the α -carbon, resulting in a level of stereocomplexity that MS fragmentation data alone cannot assign. Modern derivatization

methods have thus been developed in order to determine the absolute stereochemistry of each amino acid monomer incorporated into a peptide NP. These techniques rely on LC-MS, used in conjunction with chemical degradation/derivatization and enantiopure standards, to elucidate the chirality of a single residue. LC-MS retention times of stereodefined standards are compared against the retention time of a naturally occurring target residue; a match between standard and unknown informs the fragment's correct stereochemical assignment. Additionally, pre-column chiral derivatization reagents can be utilized to form diastereomeric mixtures of amino acids, with subsequent separation on an achiral column providing an even higher level of resolution and separation between standards/target compounds (versus direct methods of enantiomeric separation via chiral chromatography).

The most widely used pre-column chiral derivatizing reagent is 1-fluoro-2,4-dinitrophenyl-5-L-alanine (FDNP-L-Ala-NH₂), or Marfey's reagent (**A1-1**).^{3,4} Marfey first published the use of this novel chiral derivatizing reagent in 1984, where it was used to separate a mixture of five pairs of DL-AAs by HPLC.⁵ Marfey's reagent is derived from 1,5-difluoro-2,4-dinitrobenzene (DNFNB, or Sanger's reagent), with nucleophilic substitution of a single fluorine introducing an L- or D-alanine residue to the aromatic ring. The remaining fluorine can undergo nucleophilic attack via a primary amine from an AA, forming diastereomers with different physio-chemical properties ideal for achiral column separation (Scheme **A1.1**).

Scheme A1.1 Chiral derivatizing reagent FDNP-L-Ala-NH₂, or Marfey's reagent.

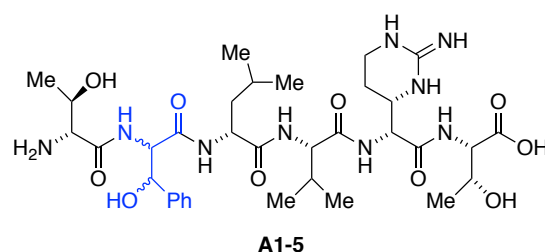


In Marfey's analysis, a peptide NP undergoes hydrolysis at each amide bond, and the mixture is treated with the chiral derivatizing reagent to form Marfey's-bound diastereomers. LC-MS analysis provides retention times for each individual monomer – matching the retention time of a target AA against a Marfey's-bound standard allows a definitive stereochemical assignment of the target residue. Although straightforward when applied to proteinogenic amino acids (where enantiomeric standards are available commercially), Marfey's analysis of non-proteinogenic or functionalized AAs often requires synthetic routes to access stereodefined standards.

A1.2 Faulknamicin discovery and structural assignment of non-proteinogenic AAs.

A novel peptide-derived natural product, faulknamicin (Fau, **A1-5**), was discovered by graduate student, Hudson Tryon from the Kelleher and Thomson labs in 2020 using the correlative metabologenomics platform discussed in Chapter 3. The preliminary structural sequence of faulknamicin was established using LC-MS/MS, and this was subsequently confirmed by probing its biogenesis using genomic information (Figure **A1.1**).

Figure A1.1 Peptide NP faulknamicin with unknown β -PheOH stereochemistry.



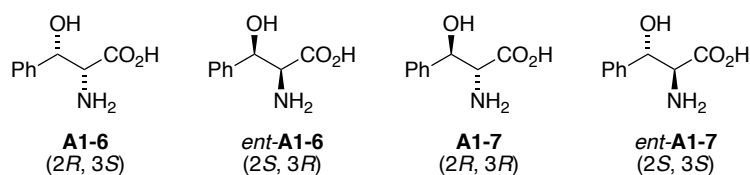
Incorporated into faulknamicin's structure are two non-proteinogenic amino acid residues, capreomycin and β -hydroxy-phenylalanine (β -PheOH). To determine the absolute stereochemistry at both these and the remaining proteinogenic residues (leucine, threonine, valine), Marfey's analysis was employed. Stereoisomers of Thr, Leu, and Val were obtained commercially,

while those of capreomycin were accessed semi-synthetically via hydrolysis of the natural products capreomycin and chymostatin. Stereoisomeric standards of β -PheOH residues, however, are not commercially available and thus required a synthetic method to ultimately access each stereoisomer for subsequent Marfey's analysis of the natural structure.

A1.3 Diastereoselective synthesis of β -PheOH stereoisomers.

β -PheOH is an unnatural amino acid residue with two stereogenic centers at the α - and β -carbons, resulting in a set of four diastereomers – ($2R$, $3S$) (**A1-6**), ($2S$, $3R$) (*ent*-**A1-6**), ($2R$, $3R$) (**A1-7**), and ($2S$, $3S$) (*ent*-**A1-7**) (Figure A1.2)

Figure A1.2 β -PheOH stereoisomers.

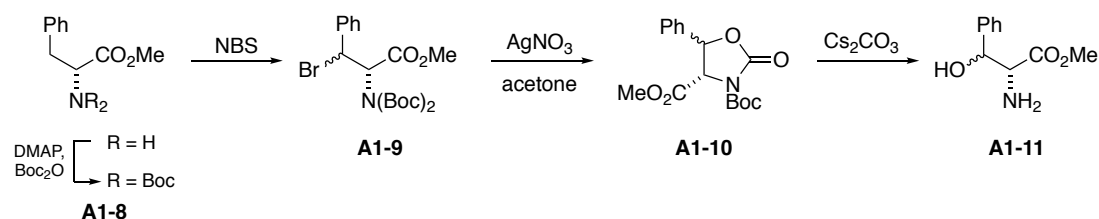


In order to stereoselectively access all four isomers of β -PheOH, we explored a variety of synthetic methods including radical-mediated *N*-bromosuccinimide (NBS) bromination of α -amino acids⁶ and Schöllkopf chiral auxiliary-mediated benzaldehyde condensation (Scheme A1.2).^{7, 8} However, each of these methods proved unreliable both in scale-up efforts and in purification/separation of diastereomeric mixtures. Instead, a route towards the four stereoisomers of β -PheOH was developed following a series of protocols published by Davies, et al., in which chiral (camphorylsulfonyl)oxaziridines (CSOs) are employed for a diastereoselective

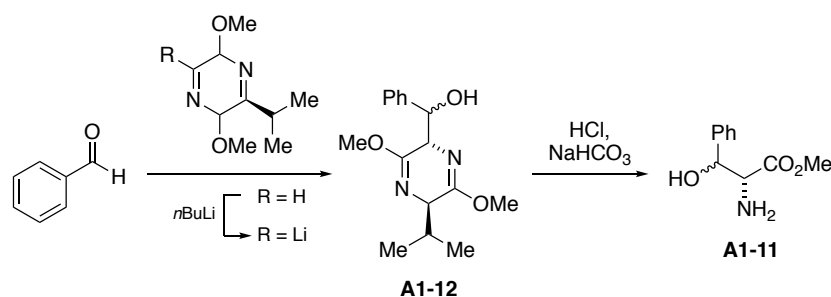
aminohydroxylation, with the subsequent α -hydroxy- β -aminoesters giving rise to the desired β -PheOH diastereomers in a divergent fashion.⁹⁻¹²

Scheme A1.2 Routes explored for synthesis of β -PheOH standards

a. NBS-mediated bromination of amino acids



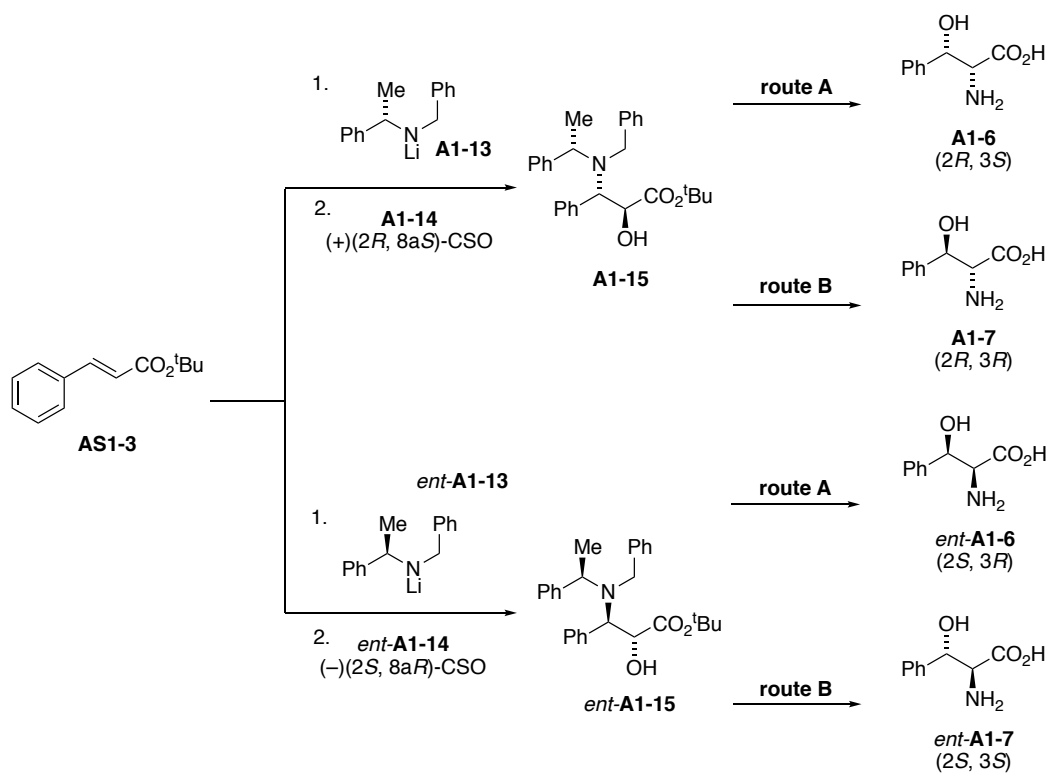
b. Schöllkopf derivitization of benzaldehyde



A1.3.1 Synthesis of β -PheOH isomers via stereoselective aminohydroxylation.

A modified version of a method developed by Davies, et al. was used to access all four diastereomers of β -PheOH (Scheme A1.3). This method relies on the affinity of (*E*)- α,β -unsaturated ester substrates to undergo conjugate addition. It features the conjugate addition of a homochiral lithium (*R*)- or (*S*)-*N*-benzyl-(α -methylbenzyl)amide to a conjugate acceptor, *tert*-butyl cinnamate, followed by a diastereoselective aminohydroxylation mediated by chiral CSOs.^{10, 11, 13} Enantiomeric α -hydroxy- β -aminoesters are then taken forward in two divergent pathways – either: **A**) proceeding through a *trans*-aziridine intermediate/rearrangement to access the (2*S*, 3*R*) and (2*R*, 3*S*) β -PheOH enantiomers or **B**) proceeding through an amino group migration via an aziridinium intermediate to access the (2*S*, 3*S*) and (2*R*, 3*R*) enantiomers.

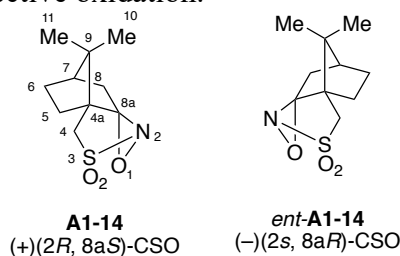
Scheme A1.3 Representative route towards all four β -PheOH stereoisomers.



A1.3.1.1 Synthesis of diastereomerically pure CSOs.

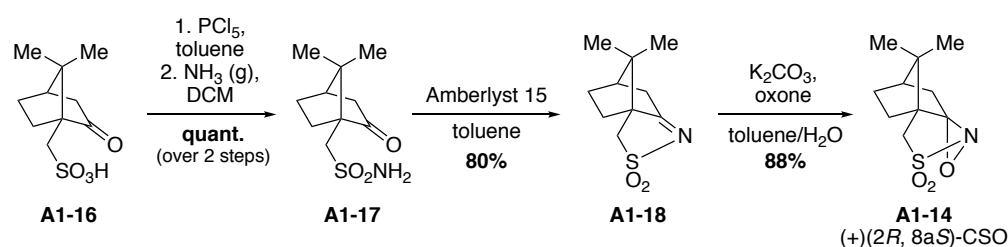
Reagent controlled asymmetric oxidation of prochiral alkenes, sulfides, and enolates can be accomplished via the use of diastereomerically pure *N*-sulfonyloxaziridines. These optically active oxidizing reagents offer high levels of asymmetric induction and applicability to challenging substrates (particularly achiral enolates), in comparison with other stereoselective oxidizing methods such as chiral organometallic peroxides or the Sharpless reagent.⁹ CSOs (Figure A1.3) afford notably high levels of enantioselectivity (50-95% ee), provide high yields regardless of the counterion present, and enantiomers reliably promote the opposite sense of asymmetric induction.⁹

Figure A1.3 CSOs for stereoselective oxidation.



CSOs (+)-(2*R*, 8*aS*) (**A1-14**) and (-)-(2*S*, 8*aR*) (*ent*-**A1-14**) were synthesized according to the following procedure published by Davis, et al (Scheme **A1.4**).⁹ Towards (+)-(2*R*, 8*aS*), the route began with (+)-(1*S*)-camphorsulfonic acid (**A1-16**), which was converted into the sulfonyl chloride derivative using PCl₅. Treatment with ammonia gas (prepared *in situ* via dropwise addition of conc. NH₄OH to NaOH solid)¹⁴ provided sulfonyl amide **A1-17**, which upon exposure to Amberlyst 15 ion-exchange resin underwent an intramolecular imine condensation to form camphorsulfonimine **A1-18**. Treating compound **A1-18** with potassium peroxymonosulfate (Oxone) in a biphasic mixture of toluene/H₂O buffered to pH = 9 with K₂CO₃ provided a stereoselective oxidation to yield the CSO **A1-14**.

Scheme A1.4 Synthesis of (+)(2*R*, 8*aS*)-CSO.

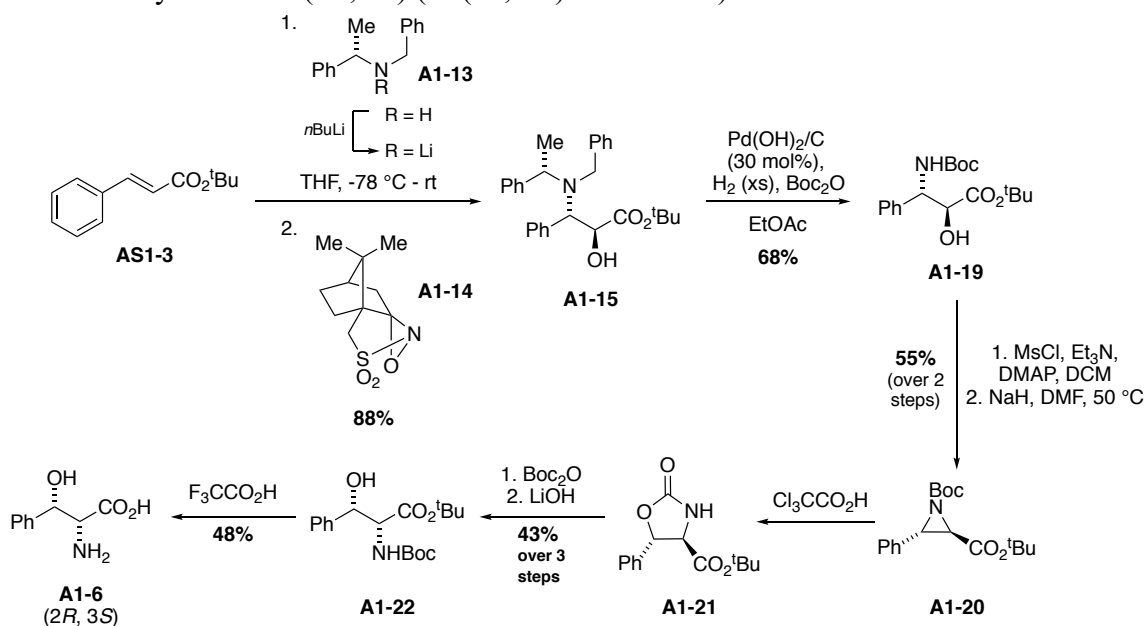


Notably, this reaction was extremely sensitive to the freshness of the Oxone, and it occasionally required a second addition of Oxone after siphoning off the first Oxone-containing aqueous layer. Scheme **A.4** outlines the synthesis towards (+)-(2*R*, 8*aS*), while following the same route beginning with the opposite enantiomer of camphorsulfonic acid **A1-16** provides (-)-(2*S*, 8*aR*).

A1.3.1.2 Synthesis of (2*R*, 3*S*) β -PheOH via route A.

Scheme A1.5 outlines route A towards the (2*R*, 3*S*) diastereomer A1-6. *tert*-Butyl cinnamate (AS1-3) was first prepared via a Horner–Wadsworth–Emmons reaction between benzaldehyde and phosphonate AS1-2. *tert*-Butyl cinnamate (AS1-3) was then added to a solution of lithium (*R*)- or (*S*)-*N*-benzyl-(α -methylbenzyl)amide (A1-13) to form the conjugate addition products with high diastereoselectivity (>95%).¹¹ Stereoselectivity matched previous models that describe the selectivity of lithium amides towards α,β -unsaturated esters relative to the known configuration of the α -methylbenzyl stereocenter.¹⁵ *In situ* oxidation of the conjugate addition intermediate lithium (*Z*)- β -amino enolates with (+)(2*R*, 8*aS*)-CSO (A1-14) gave α -hydroxy- β -aminoester A1-15 as a single diastereomer (>99:1 dr).

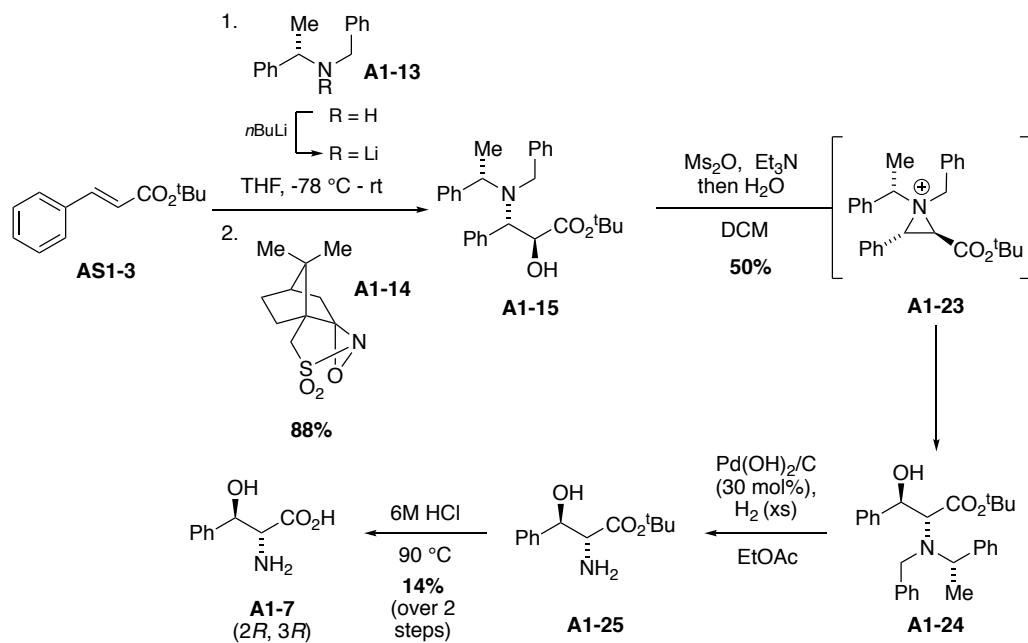
Scheme A1.5 Synthesis of (2*R*, 3*S*) (or (2*S*, 3*R*) enantiomer) via route A.



Hydrogenolysis of the (α -methylbenzyl)amide moiety in the presence of di-*tert*-butyl dicarbonate (Boc₂O) provided intermediate A1-19. Notably, this reaction requires a high-pressure hydrogen source (60psi) and a specialized catalyst, Pearlman's catalyst (Pd(OH)₂/C) in

order to afford the debenzylated product. Intermediate **A1-19** was subjected to *O*-mesylation and was then treated with NaH to form *N*-Boc protected *trans*-aziridine **A1-20**. Employing Cl₃CCO₂H for an acid-promoted rearrangement provided oxazolidin-2-one **A1-21** with retention of stereochemistry at the C(3) position. This proceeded via an S_N1-type ring-opening of the aziridine that generates a benzylic carbonium ion, which then undergoes a rapid intramolecular ring formation with the carbamate to ultimately form the oxazolidinone ring with concomitant loss of the *tert*-butyl group. Literature precedent indicated that direct hydrolysis of oxazolidinone **A1-21** would result in epimerization at the β-carbon, providing an 80:20 diastereomeric mixture of products.¹¹ To circumvent epimerization, an *N*-Boc group was reintroduced to oxazolidinone **A1-21**, and the ring was subsequently hydrolyzed using LiOH furnishing precursor **A1-22** with a 98:2 dr. A final acid-mediated deprotection of the *N*-Boc group using F₃CCO₂H afforded the final (*2R*, *3S*) β-PheOH (**A1-6**). Following this identical procedure using aminoester starting material *ent*-**A1-15** afforded the enantiomeric (*2S*, *3R*) residue.

Scheme A1.6 Synthesis of (2*R*, 3*R*) (or (2*S*, 3*S*) enantiomer) via route **B**.



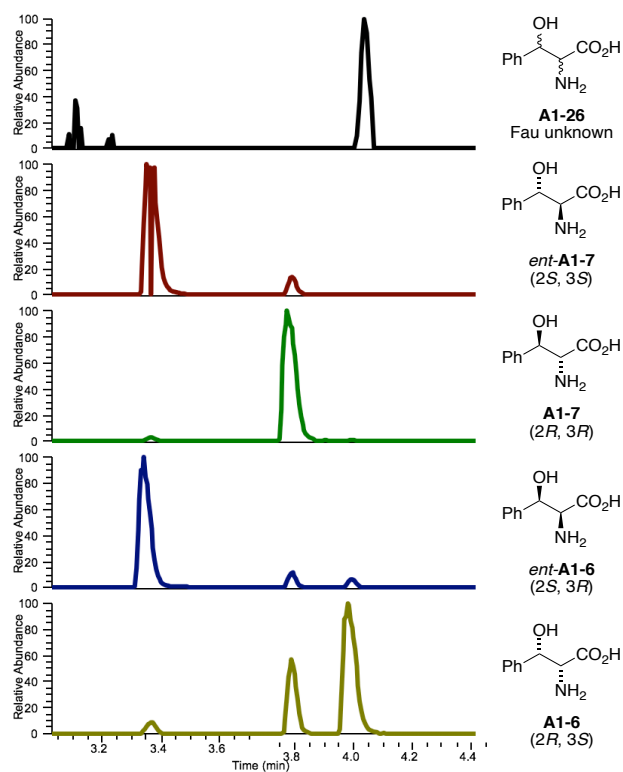
A1.3.1.3 Synthesis of (2*R*, 3*S*) β -hydroxy-phenylalanine via route **B**.

Route **B** towards the (2*R*, 3*R*) diastereomer **A1-7** is shown in Scheme **A1.6**, again beginning from α -hydroxy- β -aminoester **A1-15**. Activation of the hydroxyl group with methanesulfonyl chloride (MsCl) promoted migration of the amino group to the C(2) position, proceeding via intermediate aziridinium species **A1-23**. Regioselective ring opening provided precursor **A1-24**. This process provided overall stereochemical inversion – at C(2) during the aziridinium intermediate formation, and at C(3) during the ring opening. The rearranged α -hydroxy- β -aminoester **A1-24** was then subjected to hydrogenolysis (following the same high pressure conditions outlined above), furnishing compound **A1-25**, which then underwent a final *tert*-butyl ester hydrolysis to afford the (2*R*, 3*R*) diastereomer **A1-7**. Again, following this identical procedure using aminoester starting material *ent*-**A1-15** afforded the enantiomeric (2*S*, 3*S*) residue.

A1.4 Marfey's analysis of faulknamycin using β -PheOH synthetic standards.

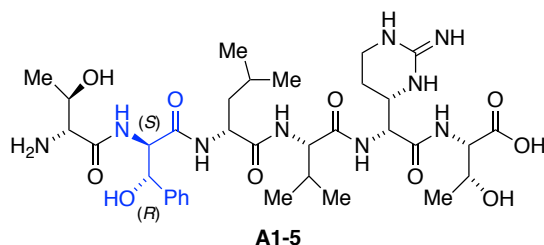
With all four β -PheOH standards in hand, Marfey's analysis was performed by graduate student Hudson Tryon in order to identify a stereochemical match for the naturally occurring residue in faulknamycin. Naturally isolated faulknamycin was subjected to vacuum hydrolysis, and the fragmented NP was subsequently treated with Marfey's reagent. Based on mass fragmentation data, an LC-MS retention time was identified for the Marfey's bound β -PheOH residue. Likewise, the four synthetic standards were converted into Marfey's bound derivatives and analyzed via LC-MS using an optimized method that provided the highest level of separation and resolution for these substrates. Retention times for the faulknamycin unknown residue and the four prepared diastereomeric standards are shown in Figure A1.4.

Figure A1.4 LC-MS traces of Marfey's analysis for diastereomeric standards and Fau unknown (provided by Hudson Tryon)



Compounds *ent*-**A1-7** ((2*S*, 3*S*)) and *ent*-**A1-6** ((2*S*, 3*R*)) exhibited extremely similar retention times, albeit with enough resolution to verify that these compounds were in fact diastereomers and not stereochemically identical. The similar retention times between these two residues may be due to their common incorporation of the 2*S* stereocenter – this correlates to the natural L configuration of phenylalanine, and it is most likely exerting a stronger inductive effect in the Marfey's construct resulting in similar physio-chemical properties for compounds *ent*-**A1-7** and *ent*-**A1-6**. Despite this, both compounds can be ruled out as a stereochemical match, as their retention times are significantly earlier than the natural Fau unknown.

Figure A1.5 Final structural assignment for faulknamycin.



The LC-MS trace shows that compound **A1-7** ((2*R*, 3*R*)) is a single diastereomer with no epimerization, and similarly, that this residue does not align with the unknown Fau residue and therefore is not a stereochemical match. Compound **A1-6** ((2*R*, 3*S*)), although displaying minor incorporation of diastereomer (2*R*, 3*R*) (**A1-7**), accurately matches the retention time observed for the naturally occurring Fau residue. Collectively, the LC-MS data obtained from this Marfey's analysis means that the β -PheOH residue in naturally occurring faulknamycin can unambiguously be assigned as (2*R*, 3*S*) (Figure **A1.5**).

A1.5 Experimental Section

A1.5.1 General information.

All reactions were carried out under nitrogen atmosphere in flame-dried glassware unless otherwise stated. Anhydrous solvents were purified by passage through a bed of activated alumina. Reagents were purified prior to use unless otherwise stated following the guidelines of Armarego and Chai.¹⁶ Flash column chromatography was performed manually using EM Reagent silica gel F60, 40-63 μm (230-400 mesh). Analytical thin-layer chromatography (TLC) was performed using Merck Silica Gel 60 Å F-254 precoated plates (0.25 mm thickness) or EM Reagent 0.25mm silica gel 60-F plates. Visualization was achieved using UV light, ninhydrin stain or ceric ammonium molybdate. NMR experiments were carried out on a Bruker Avance III 500 MHz spectrometer (500 MHz for ^1H , 126 MHz for ^{13}C) equipped with a DCH CryoProbe, and are reported in ppm using solvent as an internal standard (CDCl_3 at 7.26 ppm except where noted). Data are reported as s = singlet, d = doublet, t = triplet, q = quartet, m = multiplet, br = broad; coupling constant(s) in Hz; integration. Optical rotation was determined using a Rudolph Research Analytical Autopol IV, Series #82239 with either a 10 cm or 5 cm pathlength cell at the sodium D line. High resolution mass spectra were collected on a Thermo Q-Exactive orbitrap mass spectrometer in ESI mode. Germanium ATR infrared spectra were recorded using a Bruker Tensor 37 FT-IR spectrometer.

A1.5.2 Reported spectra for β -hydroxyphenylalanine standards.

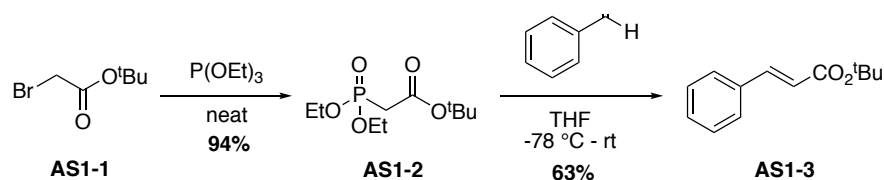
Synthetic routes towards all four diastereomers of β -hydroxyphenylalanine were adapted from procedures published by Davies, et al.^{11,12} Spectroscopic data for all intermediate compounds towards (2*S*, 3*R*) (*ent*-**A1-6**) and (2*S*, 3*S*) (*ent*-**A1-7**) matched published data. As expected, spectroscopic data for all intermediates towards (2*R*, 3*S*) (**A1-6**) and (2*R*, 3*R*) (**A1-7**) data matched their respective enantiomeric spectra. Reported protocols therefore focus on (2*R*, 3*S*) (**A1-6**) and

(2*R*, 3*R*) (**A1-7**), given both the lack of reported data for these isomers and the observed match between the (2*R*, 3*S*)- β -PheOH standard and faulknamycin. Beginning with the opposite enantiomers of *N*-benzyl-1-phenylethylamine (*ent*-**A1-13**) and CSO (*ent*-**A1-14**) provided the opposite pair of diastereomers (Scheme **A.3**).

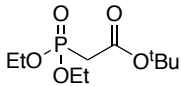
A1.5.3 Synthesis of (2*R*, 3*S*) and (2*R*, 3*R*) β -PheOH standard.

A1.5.3.1 Preparation of *t*-Bu-cinnamate starting material.

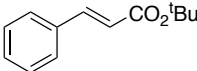
Scheme SA. 1 *tert*-Butyl cinnamate synthesis.



Compound AS1-2.

 *tert*-Butyl bromoacetate (5.00 mL, 33.9 mmol, 1 eq) and P(OEt)₃ (5.81 mL, 33.9 mmol, 1 eq) were stirred neat at 50 °C with a reflux condenser for 2 hrs. The reaction was cooled to rt, concentrated under reduced pressure to remove volatile sm, and was pumped down on under high vac overnight to yield **AS1-2** as a clear liquid (8.05 g, 94%). ¹H NMR (400 MHz, Chloroform-*d*) δ 4.17 (m, 4H), 2.88 (d, *J* = 21.4 Hz, 2H), 1.47 (s, 9H), 1.35 (t, *J* = 7.0 Hz, 6H). All spectroscopic data matches literature data for **AS1-2**.¹⁷

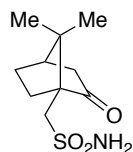
Compound AS1-3.

 **AS1-2** (2.00 g, 7.90 mmol, 1 eq) was stirred in THF (45 mL) at -78 °C. *n*BuLi (2.5M in hex, 3.64 mL, 7.90 mmol, 1 eq) was added at -78 °C and the reaction was stirred at -78 °C for 30 min. Meanwhile, benzaldehyde (740 μ L, 7.27 mmol, 0.92 eq) was suspended in THF (5 mL) and stirred at -78 °C. Benzaldehyde was cannulated into the reaction

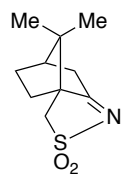
flask at -78°C , and the reaction was raised out of the dewar and allowed to come to rt. It was then cooled to -78°C and quenched with sat. NH_4Cl (10 mL), extracted 3x with DCM, dried over Na_2SO_4 , filtered, and concentrated under reduced pressure. The crude yellow oil was run through a silica plug (DCM) and concentrated under reduced pressure (not under high vac due to volatility) to yield **AS1-3** as a light yellow oil (1.01 g, 63%). $^1\text{H NMR}$ (400 MHz, Chloroform-*d*) δ 7.59 (d, $J=15.9$ Hz, 1H), 7.51 (m, 2H), 7.37 (m, 3H), 6.37 (d, $J=15.9$, 1H). All spectroscopic data matches literature data for **AS1-3**.¹⁰

A1.5.3.2 Preparation of (+)-(2R, 8aS)-CSO.

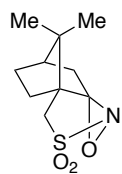
Compound A1-17.



(1S)-(+)-10-Camphorsulfonic acid (10.0 g, 43.1 mmol, 1 eq) was stirred in toluene (290 mL) and 0°C . PCl_5 (14.3 g, 68.9 mmol, 1.6 eq) was added and the reaction was stirred at 0°C for 1 hr, and it was then warmed to rt and stirred for 3 hrs. The reaction mixture was transferred to a separatory funnel and washed with sat. NaCl , dried over Na_2SO_4 , filtered, and concentrated under reduced pressure. The crude material was then suspended in DCM (145 mL), and NH_3 (g) was bubbled through the reaction mixture for 1 hr (NH_3 (g) prepared *in situ* via dropwise addition of conc. NH_4OH to NaOH solid). The reaction changed from a homogenous brown mixture to a cloudy white solution within 15 min of NH_3 exposure. Upon completion, the reaction was diluted with DCM, washed 1x with H_2O , dried over Na_2SO_4 , filtered, and concentrated under reduced pressure to yield **A1-17** as a fine white solid (9.95 g, quant. over 2 steps). $^1\text{H NMR}$ (400 MHz, Chloroform-*d*) δ 5.33 (br s, 2H, NH_2), 3.47 (d, $J=15.1$ Hz, 1H), 3.13 (d, $J=15.1$ Hz, 1H), 2.57 – 1.30 (m, 7H), 1.01 (s, 3H), 0.93 (s, 3H). All spectroscopic data matches literature data for **A1-17**.⁹

Compound A1-18.

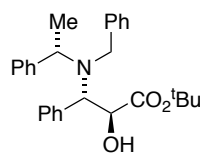
Compound **A1-17** (9.95 g, 43.1 mmol, 1 eq) and Amberlyst 15 (2.29 g) were suspended in toluene (250 mL). The reaction flask was outfitted with a dean-stark trap and reflux condenser, and it was stirred at reflux for 3 hrs. The reaction was cooled to rt, and DCM (100 mL) were added while the mixture was still warm. The mixture was filtered over cotton to remove the Amberlyst, and the crude product was concentrated under reduced pressure. No further purification was necessary, yielding **A1-18** as a fine white solid (6.40 g, 80%). ¹H NMR (400 MHz, Chloroform-*d*) δ 3.20 (d, *J* = 13.3 Hz, 1H), 2.99 (d, *J* = 13.3 Hz, 1H), 2.87 – 1.38 (m, 7H), 1.11 (s, 3H), 0.90 (s, 3H). All spectroscopic data matches literature data for **A1-18**.⁹

Compound A1-14.

Compound **A1-18** (6.40 g, 30.0 mmol, 1 eq) was suspended in toluene (150 mL) and stirred at rt. K₂CO₃ (37.1 g, 270.4 mmol, 9 eq) in H₂O (100 mL) was added to the reaction mixture. Oxone (36.5 g, 240.3 mmol, 8 eq) was likewise suspended in H₂O (120 mL) and added to the reaction slowly via drop funnel. The biphasic mixture was stirred overnight. An aliquot of the organic layer was tested via HNMR for reaction conversion, and if sm remained, the aqueous layer was cannulated off and a second portion of aq. K₂CO₃/oxone was added and the reaction was stirred at rt overnight. The reaction mixture was then transferred to a separatory funnel and diluted with H₂O. The toluene layer was removed and the aqueous layer was washed 2x with toluene. The combined organic layers were washed with sat. Na₂SO₃, NaCl, dried over Na₂SO₄, filtered, and concentrated under reduced pressure to yield **A1-14** as a fine white solid (5.93 g, 86%). ¹H NMR (400 MHz, Chloroform-*d*) δ 3.27 (d, *J* = 13.9 Hz, 1H), 3.10 (d, *J* = 14.0 Hz, 1H), 2.69 – 1.36 (m, 7H), 1.18 (s, 3H), 1.03 (s, 3H). All spectroscopic data matches literature data for **A1-14**.⁹

A1.5.3.3 Synthesis of (2*R*, 3*S*) β -hydroxy-phenylalanine.

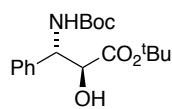
Compound A1-15.



(*S*)-*N*-Benzyl-1-phenylethylamine (**A1-13**) (0.730 mL, 3.49 mmol, 1.6 eq) was stirred in THF (8 mL) at -78°C ; *n*BuLi (2.5M in hex, 1.40 mL, 3.49 mmol, 1.6 eq) was added to reaction at -78°C and the reaction was stirred for 30 minutes.

Meanwhile, *t*Bu-cinnamate (**AS1-3**) (445 mg, 2.18 mmol, 1.0 eq, prepared from benzaldehyde¹⁰) was stirred in THF (3 mL) at -78°C . The *t*Bu-cinnamate mixture was cannulated into reaction flask at -78°C , and the reaction was stirred for 2 hrs at -78°C . (+)(2*R*, 8*aS*)-CSO (**A1-14**) (800 mg, 3.49 mmol, 1.6 eq) was then added neat and portionwise at -78°C , and the reaction was allowed to slowly come to room temp in dewar overnight. Sat. NH_4Cl was added and the reaction was let to stir for 5 minutes, and was then diluted with DCM and 10% citric acid solution and washed 3x with DCM. Organic layers were combined and washed with sat NaHCO_3 , NaCl , dried with Na_2SO_4 , filtered, and concentrated. The crude orange oil was purified via column chromatography (dry load in 40% hex in DCM), yielding **A1-15** a light yellow oil (829.7mg, 88%). $^1\text{H NMR}$ (400 MHz, Chloroform-*d*) δ 7.49 – 7.45 (m, 4H), 7.36 – 7.16 (m, 11H), 4.38 (q, $J = 3.3$ Hz, 1H), 4.20 (m, 2H), 4.11 (d, $J = 14.5$ Hz, 1H), 3.83 (d, $J = 14.5$ Hz, 1H), 2.75 (d, $J = 4.5$ Hz, 1H), 1.53 (s, 3H), 1.19 (s, 9H). All spectroscopic data matched literature data for *ent*-**1-15**.¹²

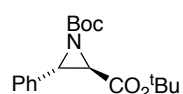
Compound A1-19.



Compound **A1-15** (133 mg, 0.310 mmol, 1 eq) was stirred in freshly distilled EtOAc (3 mL) in a glass pressure vessel with Teflon screw top. 20 wt% $\text{Pd}(\text{OH})_2/\text{C}$ (20 mol%, 65.3 mg, 0.093 mmol, 0.3 eq) and Boc_2O (111.7 mg, 0.512 mmol, 1.65 eq) were added to the vessel, and the reaction mixture was degassed three times on high vacuum. The Swage-Lock vessel was then fitted to a pressurized hydrogen line, and the reaction was stirred 16 hrs at a

pressure of 60 psi. The crude reaction mixture was filtered over celite (EtOAc), dried over Na₂SO₄, and concentrated under reduced pressure. The crude yellow oil was purified on silica gel (20% EtOAc in hex) to give **A1-19** a light yellow oil (77.2 mg, 89%). ¹H NMR (400 MHz, Chloroform-*d*) δ 7.22 – 7.36 (m, 5H), 5.63 (d, *J* = 8.7 Hz, 1H), 5.06 (d, *J* = 8.7 Hz, 1H), 4.48 (m, 1H), 1.43 (s, 9H), 1.36 (s, 9H). All spectroscopic data matched literature data for *ent*-**A1-19**.¹¹

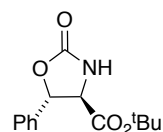
Compound A1-20.



Compound **A1-19** (35.2 mg, 0.085 mmol, 1 eq) was stirred in DMF (1.7 mL) at rt.

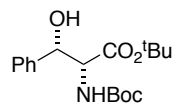
NaH (60 % dispersion in mineral oil, 4.07 mg, 0.102 mmol, 1.2 eq) was then added and the reaction was heated to 50°C and stirred with a reflux condenser for 3 hrs. The reaction mixture was cooled to rt, diluted with Et₂O and washed 4x with H₂O, then dried over Na₂SO₄, filtered, and concentrated under reduced pressure. The crude material was purified on silica gel (100% DCM) to afford compound **A1-20** as a clear oil (23.6 mg, 87%). ¹H NMR (400 MHz, Chloroform-*d*) δ 7.28 – 7.35 (m, 5H), 3.73 (d, *J* = 2.6 Hz, 1H), 3.00 (d, *J* = 2.6 Hz, 1H), 1.51 (s, 9H), 1.47 (s, 9H). All spectroscopic data matched literature data for *ent*-**A1-20**.¹⁸

Compound A1-21.

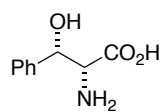


Compound **A1-20** (183 mg, 0.573 mmol, 1 eq) was stirred in DCM (6 mL) at rt.

Cl₃CCO₂H (750 mg, 4.58 mmol, 8 eq) was then added and the reaction was stirred at rt 16 hrs. The reaction was diluted with sat. NaHCO₃, and the aq layer was extracted 3x with DCM. The organic layers were combined, dried over Na₂SO₄, filtered, and concentrated under reduced pressure to give **A1-21**. ¹H NMR (400 MHz, Chloroform-*d*) δ 7.35 – 7.43 (m, 5H), 5.61 (d, *J* = 5.3 Hz, 1H), 4.15 (d, *J* = 5.3 Hz, 1H), 1.53 (s, 9H). All crude spectroscopic data matched literature data for *ent*-**A1-20**,¹⁸ and crude product was used directly in the next reaction.

Compound A1-22.

Crude compound **A1-21** (assume quant.) was stirred in THF (8 mL), and Et₃N (0.160 mL, 5.15 mmol, 2 eq), Boc₂O (575 mg, 2.64 mmol, 4.6 eq), and cat. DMAP (3.5 mg, 0.029 mmol, 0.05 eq) were added. The reaction was stirred at rt for 16 hr, concentrated, diluted with DCM, and the organic layer was extracted with sat. NaHCO₃, then dried over Na₂SO₄. All crude spectroscopic data matched literature data,¹¹ and crude product was carried forward. Crude material (assume quant.) was suspended in 1,4-dioxane (14 mL). LiOH solution (2.0M in H₂O, 0.14 g, 5.73 mmol, 10 eq) was added, and the mixture was stirred at rt for 4 hrs. Mixture was diluted with CHCl₃, dried over Na₂SO₄, and concentrated. The crude product was purified via column chromatography (15% EtOAc/hex), and it was then recrystallized using hot 8% EtOAc in hex followed by rapid cooling to yield the pure compound **A1-22** as a light yellow oil (90 mg, 46% over 3 steps). ¹H NMR (400 MHz, Chloroform-*d*) δ 7.27 – 7.47 (m, 5H), 5.33 (d, *J* = 4.7 Hz, 1H), 4.49 (d, *J* = 4.7 Hz, 1H), 1.30 (s, 9H), 1.27 (s, 9H). All spectroscopic data matched literature data for *ent*-**A1-22**.¹⁸

Compound A1-6.

Compound **A1-22** (90.0 mg, 0.267 mmol, 1 eq) was suspended in a 4:1 mixture of DCM/TFA (9 mL) and was stirred at rt for 2 hrs. The reaction mixture was then concentrated, resuspended in 6M HCl (4.5 mL), and the mixture was stirred at rt for 1.5 hrs. The reaction was diluted with DCM and concentrated, and the resulting residue was diluted with H₂O and extracted 2x with CHCl₃, then dried over Na₂SO₄ and concentrated under reduced pressure. The crude material was purified via ion exchange chromatography using a Dowex-50WX8 resin (7N NH₃ in MeOH solution as the mobile phase). Ion exchange yielded **A1-6** as a white solid (23.4 mg, 48%). ¹H NMR (500 MHz, D₂O) δ 7.50 – 7.40 (m, 5H), 5.30 (d, *J* = 4.4 Hz, 1H), 3.92 (d, *J* =

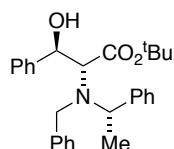
4.4 Hz, 1H). ^{13}C NMR (126MHz, D_2O) δ 171.94, 139.00, 128.82, 128.44, 125.73, 71.19, 60.77.

HRMS (M+H) Calc'd: 182.0739. Found: 182.0812. $[\alpha]_D^{24} + 49.4$ (c 0.208, MeOH). **IR**

(Diamond ATR): 3103, 2972, 2838, 1740, 1639, 1198, 838 cm^{-1} .

A1.5.3.4 Synthesis of (2R, 3R) β -hydroxy-phenylalanine.

Compound A1-24.



Compound **A1-15** (100 mg, 0.232 mmol, 1eq) was stirred in DCM (2 mL) at 0°C ;

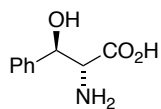
mesylsulfonic anhydride (121.1 mg, 0.696 mmol, 3 eq) and Et_3N (145.5 μL , 1.04 mmol, 4.5 eq) were then added, and the reaction was brought to rt and allowed to stir for 45 min.

H_2O (125.3 μL , 6.96 mmol, 30 eq) was then added, and the reaction was stirred at rt for 16 hrs.

The reaction mixture was diluted with H_2O and extracted 3x with DCM. The organic layers were then combined and washed with 2M HCl, NaHCO_3 , and half sat. NaCl then dried over Na_2SO_4 , filtered, and concentrated. The crude, dark orange oil was purified via column chromatography

(1% MeOH/DCM), yielding **A1-24** as a light yellow oil (49.2mg, 50%). ^1H NMR (400 MHz, Chloroform-*d*) δ 7.39 – 6.86 (m, 15H), 4.92 (dd, $J = 8.0, 4.7$ Hz, 1H), 4.19 (d, $J = 14.2$ Hz, 1H), 4.01 (q, $J = 6.9$ Hz, 1H), 3.94 (d, $J = 14.2$ Hz, 1H), 3.60 (d, $J = 8.0$ Hz, 1H), 2.59 (br s, 1H), 1.58 (s, 9H), 1.39 (d, $J = 6.9$ Hz, 3H). All spectroscopic data matched literature data for *ent*-**A1-24**.¹²

Compound A1-7.



Compound **A1-24** (125.6 mg, 0.291 mmol, 1 eq) was suspended in MeOH (1.5 mL)

with $\text{Pd}(\text{OH})_2/\text{C}$ (20 mol%, 102.2 mg, 0.146 mmol, 0.50 eq) in a glass pressure vessel with Teflon screw top, and the mixture was degassed 3 times on high vacuum. The Swage-Lock vessel was then fitted to a pressurized hydrogen line, and the reaction was stirred 16 hrs at a pressure of 60psi. The crude reaction mixture was filtered over celite and concentrated to yield a light yellow oil that was taken on crude. The reduced crude intermediate was then suspended in

6M HCl (6 mL), heated to 90°C w/reflux condenser, and left to stir for 16hrs. The reaction mixture was cooled to rt, concentrated, and purified via ion exchange chromatography using a Dowex-50WX8 resin (7N NH₃ in MeOH solution as the mobile phase). Ion exchange yielded **A1-7** as a white solid (9.1mg, 14% over 2 steps). **¹H NMR** (500 MHz, D₂O) δ 7.49 – 7.37 (m, 5H), 5.36 (d, *J* = 4.2 Hz, 1H), 4.09 (d, *J* = 4.2 Hz, 1H). **¹³C NMR** (126MHz, D₂O) δ 171.31, 136.89, 128.80, 128.76, 126.30, 71.21, 60.46. **HRMS** (M+H) Calc'd: 182.0739. Found: 182.0810. [α]_D²⁴ + 9.4 (*c* 0.379, MeOH). **IR** (Diamond ATR): 3176, 2892, 2880, 1788, 1693, 1134, 828 cm⁻¹.

APPENDIX 2

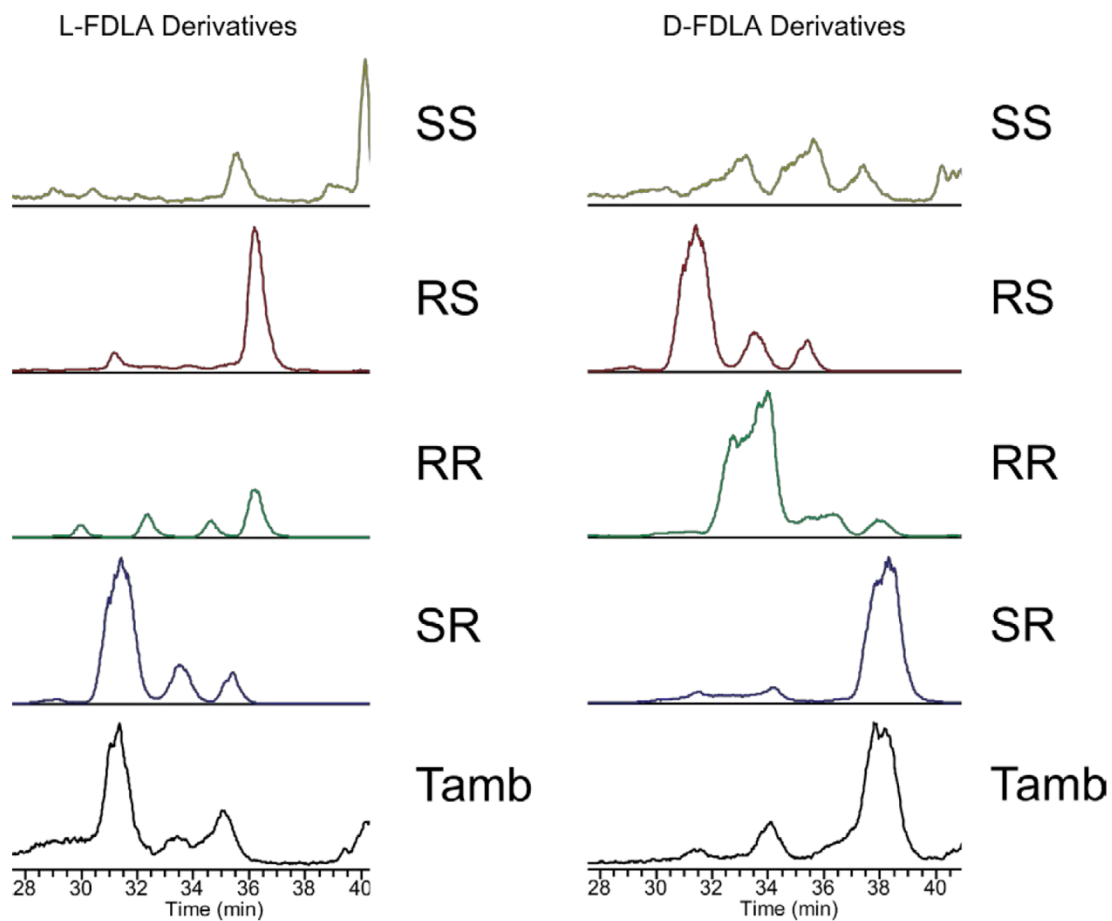
Supplementary Data

A2.1 Supplementary Data.**A2.1.1 NMR comparison of tambromycin III-1 to isolated natural material.**

¹³ C NMR			¹ H NMR		
Literature ¹	Synthetic Material	Diff.	Literature ¹	Synthetic Material	Diff.
177.5	178.36	0.86	7.61 (s) 1H	7.61 (s) 1H	0
175.7	175.51	0.19	6.89 (s) 1H	6.90 (s) 1H	0.01
168.1	168.37	0.27	6.57 (s) 1H	6.59 (s) 1H	0.02
165.2	165.08	0.12	4.96 (d, <i>J</i> = 8.8) 1H	4.96 (d, <i>J</i> = 8.7) 1H	0
152.3	152.37	0.07	4.93 (d, <i>J</i> = 4.7) 1H	4.91 (d, <i>J</i> = 4.9) 1H	0.02
140.1	139.96	0.14	4.31 (d, <i>J</i> = 8.8) 1H	4.33 (d, <i>J</i> = 8.8) 1H	0.02
133.4	133.11	0.29	4.09 (ddd, <i>J</i> = 11.5, 7.1, 4.7) 1H	4.08 (ddd, <i>J</i> = 10.1, 7.2, 4.9) 1H	0.01
131.3	131.2	0.1	3.96 (d, <i>J</i> = 11.0) 1H	4.02 (d, <i>J</i> = 11.1) 1H	0.06
114.1	114	0.1	3.82 (d, <i>J</i> = 11.1) 1H	3.81 (d, <i>J</i> = 11.2) 1H	0.01
108.2	108.14	0.06	3.82 (s) 3H	3.81 (s) 3H	0.01
102.5	102.5	0	3.27 (m) 2H	3.32 (dt, <i>J</i> = 11.2, 7.6) 1H	N/A
102.1	101.88	0.22		3.22 (ddd, <i>J</i> = 11.9, 8.6, 5.6) 1H	N/A
77.4	77.49	0.09	2.1 (m) 1H	2.08 (dtd, <i>J</i> = 12.8, 7.4, 3.7) 1H	0.02
73.9	73.88	0.02	2.0 (m) 1H	1.99 (ddt, <i>J</i> = 11.9, 8.0, 3.4) 1H	0.01
65.7	65.98	0.28	1.93 (m) 1H	1.91 (dt, <i>J</i> = 12.9, 8.0) 1H	0.02
63.3	63.54	0.24	1.74 (m) 1H	1.74 (m) 1H	0
61.4	60.73	0.67	1.71 (s) 3H	1.75 (s) 3H	0.04
53.5	54.01	0.51	1.46 (s) 3H	1.46 (s) 3H	0
46.0	45.97	0.03			
33.9	33.77	0.13			
27.1	27.22	0.12			
25.4	25.39	0.01			
24.3	24.26	0.04			
19.8	19.67	0.13			

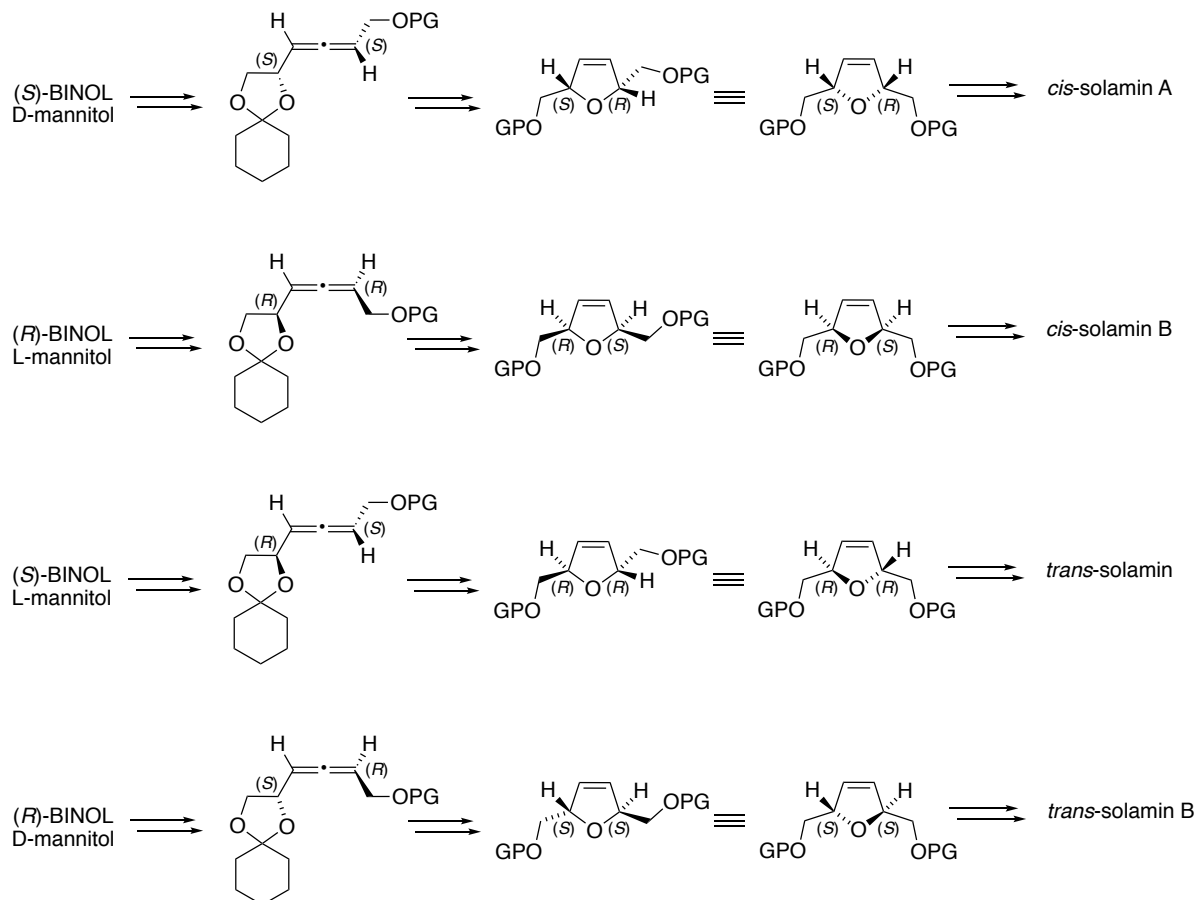
A2.1.2 Marfey's analysis of tambroline stereoisomers.

Figure A2.1 Marfey's analysis for tambroline diastereomers. Both L- and D-Marfey's reagent analyzed.¹



A2.1.3 Stereodivergent route to the solamin stereoisomers.

Scheme A2.1 Stereodivergent pathway to all solamin stereoisomers. PG = protecting group.



Appendix 1 References.

1. Maier, M. E., Structural revisions of natural products by total synthesis. *Nat. Prod. Rep.* **2009**, *26* (9), 1105-1124.
2. Nicolaou, K. C.; Snyder, S. A., Chasing Molecules That Were Never There: Misassigned Natural Products and the Role of Chemical Synthesis in Modern Structure Elucidation. *Angew. Chem. Int. Ed.* **2005**, *44* (7), 1012-1044.
3. B'Hymer, C.; Montes-Bayon, M.; Caruso, J. A., Marfey's reagent: Past, present, and future uses of 1-fluoro-2,4-dinitrophenyl-5-L-alanine amide. *J. Sep. Sci.* **2003**, *26* (1-2), 7-19.
4. Marfey, P., Determination of D-amino acids. II. Use of a bifunctional reagent, 1,5-difluoro-2,4-dinitrobenzene. *Carlsberg Res. Comm.* **1984**, *49* (6), 591.
5. Bhushan, R.; Brückner, H., Use of Marfey's reagent and analogs for chiral amino acid analysis: Assessment and applications to natural products and biological systems. *J. Chromatog. B* **2011**, *879* (29), 3148-3161.
6. Crich, D.; Banerjee, A., Expedient Synthesis of threo- β -Hydroxy- α -amino Acid Derivatives: Phenylalanine, Tyrosine, Histidine, and Tryptophan. *J. Org. Chem.* **2006**, *71* (18), 7106-7109.
7. Schöllkopf, U.; Groth, U.; Deng, C., Enantioselective Syntheses of (R)-Amino Acids Using L-Valine as Chiral Agent. *Angew. Chem. Int. Ed.* **1981**, *20* (9), 798-799.
8. Sugiyama, H.; Shioiri, T.; Yokokawa, F., Syntheses of four unusual amino acids, constituents of cyclomarin A. *Tet. Lett.* **2002**, *43* (19), 3489-3492.
9. Davis, F. A.; Towson, J. C.; Weismiller, M. C.; Lal, S.; Carroll, P. J., Chemistry of oxaziridines. 11. (Camphorylsulfonyl)oxaziridine: synthesis and properties. *J. Am. Chem. Soc.* **1988**, *110* (25), 8477-8482.
10. Davies, S. G.; Mulvaney, A. W.; Russell, A. J.; Smith, A. D., Parallel synthesis of homochiral β -amino acids. *Tet. Asymm.* **2007**, *18* (13), 1554-1566.
11. Davies, S. G.; Fletcher, A. M.; Frost, A. B.; Lee, J. A.; Roberts, P. M.; Thomson, J. E., Trading N and O: asymmetric syntheses of β -hydroxy- α -amino acids via α -hydroxy- β -amino esters. *Tetrahedron* **2013**, *69* (42), 8885-8898.
12. Davies, S. G.; Fletcher, A. M.; Frost, A. B.; Roberts, P. M.; Thomson, J. E., Trading N and O. Part 2: Exploiting aziridinium intermediates for the synthesis of β -hydroxy- α -amino acids. *Tetrahedron* **2014**, *70* (35), 5849-5862.
13. Davies, S. G.; Walters, I. A. S., Asymmetric synthesis of anti- α -alkyl- β -amino acids. *J. Chem. Soc., Perkin Transactions 1* **1994**, *9*, 1129-1139.

14. Vandewalle, M.; Van der Eycken, J.; Oppolzer, W.; Vullioud, C., Iridoids : enantioselective synthesis of loganin via an asymmetric diels-alder reaction. *Tetrahedron* **1986**, 42 (14), 4035-4043.
15. Keirs, D.; Moffat, D.; Overton, K.; Tomanek, R., Asymmetric syntheses of the naturally occurring β -amino acids, β -lysine, β -leucine and β -phenyl- β -alanine via nitronc cycloaddition. *J. Chem. Soc., Perkin Transactions 1* **1991**, (5), 1041-1051.
16. Armarego, W. L. F.; Chai, C. L. L., *Purification of Laboratory Chemicals*. 5 ed.; Butterworth-Heinemann: 2003.
17. Davies, S. G.; Fletcher, A. M.; Roberts, P. M.; Smith, A. D., Asymmetric synthesis of Sedum alkaloids via lithium amide conjugate addition. *Tetrahedron* **2009**, 65 (49), 10192-10213.
18. Bull, S. D.; Davies, S. G.; Moss, W. O., Practical synthesis of Schöllkopf's bis-lactim ether chiral auxiliary: (3S)-3,6-dihydro-2,5-dimethoxy-3-isopropyl-pyrazine. *Tet. Asymm.* **1998**, 9 (2), 321-327.

Appendix 2 References.

1. Goering, A. W.; McClure, R. A.; Doroghazi, J. R.; Albright, J. C.; Haverland, N. A.; Zhang, Y.; Ju, K.-S.; Thomson, R. J.; Metcalf, W. W.; Kelleher, N. L., Metabologenomics: Correlation of Microbial Gene Clusters with Metabolites Drives Discovery of a Nonribosomal Peptide with an Unusual Amino Acid Monomer. *ACS Cent. Sci.* **2016**, 2 (2), 99-108.